Light-dependent regulation of photosynthesis genes in *Dinoroseobacter shibae*

Von der Fakultät für Lebenswissenschaften

der Technischen Universität Carolo-Wilhelmina zu Braunschweig

zur Erlangung des Grades einer

Doktorin der Naturwissenschaften

(Dr. rer. nat.)

genehmigte

D i s s e r t a t i o n

von Miriam Becker
aus Ostercappeln

1. Referent: Professor Dr. Dieter Jahn
2. Referent: apl. Professor Dr. Michael Hust
eingereicht am: 09.07.2021
mündliche Prüfung (Disputation) am: 05.10.2021

Druckjahr 2021

Vorveröffentlichungen der Dissertation

Teilergebnisse aus dieser Arbeit wurden mit Genehmigung der Fakultät für Lebenswissenschaften, vertreten durch den Mentor der Arbeit, in folgenden Beiträgen vorab veröffentlicht:

Tagungsbeiträge

Becker, M.; Härtig, E. and Jahn, D.

Function of the light-oxygen-voltage (LOV) histidine kinase Dshi_1135 in regulation of bacteriochlorophyll *a* biosynthesis in *Dinoroseobacter shibae*. Gordon Research Conference "Photosensory Receptors and Signal Transduction", Lucca (Barga), Italy (2018).

Posterbeiträge

Becker, M.; Heyber, S.; Härtig, E. and Jahn, D.

The role of the light-oxygen-voltage (LOV)-histidine kinase Dshi_1135 for regulation of the bacteriochlorophyll *a* biosynthesis in *Dinoroseobacter shibae*. VAAM Jahrestagung, Würzburg (2017).

Becker, M.; Härtig, E. and Jahn, D.

Function of the light-oxygen-voltage (LOV) histidine kinase Dshi_1135 in regulation of bacteriochlorophyll *a* biosynthesis in *Dinoroseobacter shibae*. Gordon Research Conference "Photosensory Receptors and Signal Transduction", Lucca (Barga), Italy (2018).

Becker, M.; Härtig, E. and Jahn, D.

Characterization of the LOV (light-oxygen-voltage) histidine kinase Dshi_1135 and its role in the light-dependent regulation of bacteriochlorophyll *a* biosynthesis in *Dinoroseobacter shibae*. VAAM Jahrestagung, Wolfsburg (2018).

Becker, M.; Härtig, E. and Jahn, D.

Towards a regulatory network – light-dependent biosynthesis of bacteriochlorophyll *a* in *Dinoroseobacter shibae*. VAAM Jahrestagung, Mainz (2019).

Becker, M.; Pucelik, S.; Jahn, D. and Härtig, E.

A novel light-oxygen-voltage histidine kinase is involved in light-dependent regulation of bacteriochlorophyll *a* biosynthesis in *Dinoroseobacter shibae*. Marine Microbiota, Oldenburg (2019).

Meinen Eltern

In den Wissenschaften ist viel Gewisses, sobald man sich von den Ausnahmen nicht irre machen läßt und die Probleme zu ehren weiß.

Johann Wolfgang von Goethe

Table of Contents

Abbreviations

°C	degree Celsius
%	percent
µCi	microcurie
µg	microgram
µl	microliter
µm	micrometer
µM	micromole
A	ampere
AAP	aerobic anoxygenic phototrophic
ADP	adenosine diphosphate
ALA	5-aminolevulinic acid
Amp	Ampicillin
APS	ammonium persulfate
ATP	adenosine triphosphate
AU	absorption units
BCIP	5-bromo-4-chloro-3-indolyl phosphate
bp	base pairs
BSA	bovine serum albumin
Ci	Curie
Cml	Chloramphenicol
CV	column volumes
Da	Dalton
dATP	deoxyadenosine triphosphate
dH_2O	deionized water
DMF	dimethylformamide
DMSO	dimethyl sulfoxide
DNA	deoxyribonucleic acid
DNase	deoxyribonuclease
dNTP	deoxynucleotide triphosphate
DOM	dissolved organic matter
DPOR	dark-operative PChlide oxidoreductase

dsDNA	double-stranded DNA
DTT	dithiothreitol
dTTP	deoxythymidine triphosphate
EDTA	ethylenediaminetetraacetic acid
et al.	*et alteri* (and others)
FMN	flavin mononucleotide
FPLC	fast liquid protein chromatography
g	earth gravity
g	gram
Gm	Gentamicin
GPC	gel permeation chromatography
GSH	glutathione
GST	glutathione S-transferase
h	hours
HGT	horizontal gene transfer
HK	histidine kinase
hMB	half-concentrated Marine Broth
IPTG	isopropyl-β-D-galactopyranoside
Kan	Kanamycin
kDa	kilo Dalton
L	liter
LB	Lysogeny Broth
LED	light-emitting diode
LIC	ligation indepedent cloning
LOV	Light-Oxygen-Voltage
LPOR	light-dependent PChlide oxidoreductase
M	molar
m	milli
mA	milli ampere
MB	Marine Broth
MCS	multiple cloning site
mg	milligram
min	minutes

ml	milliliter
mM	millimolar
mm	millimeter
MPE	Mg-Proto IX monomethylester
M_r	relative molecular mass
MWCO	molecular weight cut off
NBT	nitrotetrazolium blue
nm	nanometer
OD	optical density
ONPG	2-nitrophenyl-β-D-galactopyranosid
p.s.i.	pounds per square inch
PAGE	polyacrylamide gel electrophoresis
PBG	porphobilinogen
PBS	phosphate buffered saline
PChlide	3,8-divinyl protochlorophyllide *a*
PCR	polymerase chain reaction
pH	negative decadic logarithm of the H+ concentration in a solution
pmol	picomole
POR	PChlide oxidoreductase
Proto IX	protoporphyrin IX
PVDF	polyvinylidene difluoride
RNA	ribonucleic acid
RNase	ribonuclease
rpm	rounds per minute
RR	response regulator
SAM	S-adenosyl-L-methionine
SDS	sodium dodecyl sulfate
sec	seconds
SWM	salt water medium
TAE	Tris-acetate-EDTA
TE	Tris-EDTA
TEMED	N,N,N',N',-tetramethyl ethylene diamine
Tris	tris(hydroxymethyl)aminomethane

TRX	thioredoxin
U	units
UV	ultraviolet
UV/Vis	ultraviolet and visible spectrum of light
V	volt
v/v	volume per volume
w/v	weight per volume
λ	wavelength

1 Introduction

1.1 The Marine Habitat

Commonly, the Earth is often referred to as the blue planet. More than 70 % of its surface is covered with water, which strongly reflects blue light in particular. As a result, the Earth appears to us in a vivid blue from space. The oceans hold about 98 % of the water resources and are accounted for 90 % of the habitable space on Earth and therefore build the world's largest ecosystem. This ecosystem includes near coastal regions like salt marshes, seagrass meadows, mudflats, mangroves or coral reefs and also offshore areas as the surface ocean, pelagic ocean waters, the deep sea or the sea floor. At first sight the ocean appears to be a rather hostile and rough environment, but in fact it is home to a vast variety of highly adapted marine life and has the greatest abundance of life. Only 5 % of the oceans are explored so far and scientists predict that about 91 % of marine species are not classified yet. Besides the obvious representatives of marine life like fish, sharks or marine mammals, it is mainly microorganisms that colonize the oceans and are accounted for most of the marine biomass.

Studies showed that the upper 200 m of the ocean contain about $3.6 \cdot 10^{28}$ cells ($5 \cdot 10^{5}$ cells/ml), deep sea waters contain about $6.5 \cdot 10^{28}$ cells ($5 \cdot 10^{4}$ cells/ml) (Whitman *et al.,* 1998). These worldwide distributed populations of marine microorganisms form the basis of the marine food web and are the engines that drive various biogeochemical cycles in the oceans, like the carbon, nitrogen, phosphorus or sulphur cycle (Falkowski *et al.,* 2008). About $2.9 \cdot 10^{27}$ microorganisms in the upper 200 m of the ocean are believed to be autotrophs (Whitman *et al.,* 1998), and are therefore primary producers like for example phytoplankton. Phytoplankton are unicellular organisms capable of photosynthesis. It is assumed that phytoplankton fixes roughly 44 % of the total carbon per year through this process (Jardillier *et al.,* 2010) and contributes 50-75 % of the oxygen to the Earth's atmosphere and is therefore indirectly involved in climate control.

Thus, the world's oceans and the contained marine microorganisms make a major contribution to the life on Earth and from an environmental perspective it is mandatory to understand their physiology and ecology.

1.2 Marine Roseobacter Group

The microbial community in the oceans forms the marine microbiome but however, in the past only little attention has been paid to it. This was partly due to the fact that many of these organisms could not be cultured under laboratory conditions and where therefore simply overseen in marine samples. Through the development of modern molecular biological techniques like DNA sequencing it became evident, that there is actually a huge variety of bacteria and other microorganisms present in marine waters. Today there are rapidly growing databases available that contain fully sequenced genomes and 16S rRNA sequences from different marine microorganisms and habitats. With that also the knowledge about the bacteria that are present in the oceans has been expanded.

One of the most extensively studied groups of marine bacteria is the Roseobacter group. It was mentioned first in 1991 by the Japanese scientist Tsuneo Shiba and he described the first two members *Roseobacter litoralis* and *Roseobacter denitrificans* as pink-pigmented and bacteriochlorophyll *a* (Bchl *a*) containing strains (Shiba, 1991). Initially Roseobacters were assumed to be a monophyletic group and therefore defined as Roseobacter clade. New comprehensive phylogenetic analysis and analysis of the affiliation of the Roseobacter members led to a renaming to Roseobacter group (Simon *et al.,* 2017). This lineage shows >89 % identity on 16S rRNA level and represents a physiologically heterogeneous and abundant group of α-Proteobacteria that comprises up to 25 % of microbial communities in the marine environment (Buchan *et al.,* 2005; Wagner-Döbler & Biebl, 2006). Roseobacters can be found in all major marine habitats, but dominantly in coastal zones and the polar regions and also often in association with marine eukaryotes like algae, corals, sponges, squid, seagrass or dinoflagellates (Weidner *et al.,* 2000; Brinkmeyer *et al.,* 2003; Webster *et al.,* 2004; Taylor *et al.,* 2004; Wagner-Döbler & Biebl, 2006). Another characteristic of the Roseobacter group members are their relatively large genomes with an average size of 4.4 Mb (Buchan *et al.,* 2005). Furthermore, they can carry up to 12 plasmids per cell (Pradella *et al.,* 2010). Those plasmids often contain genes for important metabolic and ecological functions, like photosynthesis, flagella formation, biosynthesis of antibiotic tropodithietic acid or biofilm formation (Petersen *et al.,* 2013). Various strains possess a large and unique gene pool for carbon and energy obtaining mechanisms and therefore Roseobacters are often called ecological generalists, as they are able to adapt to numerous marine habitats

and environmental conditions. Most of the Roseobacter members are heterotrophs but some, however, are able to use additional energy generating mechanisms, e.g. aerobic anoxygenic photosynthesis, carbon monoxide oxidation, sulfur transformations, aromatic compound degradation, nitrate respiration or DMSP degradation (Buchan *et al.,* 2005; Wagner-Döbler & Biebl, 2006; Brinkhoff *et al.,* 2008). The question remains how such great genetic variability evolved and it is assumed today, that both horizontal gene transfer (HGT) and homologous recombination were the driving forces (Newton *et al.,* 2010). Especially HGT might have been of major importance for the adaptation of Roseobacters to their ecological niche, as they show a high distribution of extrachromosomal elements. Plasmids carrying advantageous properties were probably maintained and others were lost again (Petersen *et al.,* 2012). Today there is even evidence for conjugative plasmid transfer across biogeographical and phylogenetic barriers in the family of Rhodobacteraceae, clarifying the importance of HGT for the evolution of the Roseobacter group (Petersen & Wagner-Döbler, 2017).

Due to the great number of energy generating mechanisms, the Roseobacter group is responsible for processing a large number of relevant carbon, nitrogen and sulphur compounds, which is supported by metaproteomic data (Christie-Oleza & Armengaud, 2015) and thus, it plays an important role in driving global biogeochemical cycles in the oceans.

1.2.1 Type Strain *Dinoroseobacter shibae* DFL12^T - Model Organism of the Roseobacter Group

Type strain *Dinoroseobacter shibae* DFL12^T (DSM 16493^T = NCIMB 14021^T) was first isolated from the benthic dinoflagellate *Prorocentrum lima* and named after Professor Tsuneo Shiba, who was the first to describe marine aerobic anoxygenic phototrophic bacteria (Biebl *et al.,* 2005; Shiba *et al.,* 1979).

D. shibae is a Gram-negative bacterium shaped as cocci or ovoid rods with a single polar or subpolar attached flagellum (Figure 1a). On agar plates it grows in smooth and convex colonies with entire margins and appears in a typical deep red pigmentation, caused by the photoactive carotenoid spheroidenone (Figure 1b). Liquid cultures that are grown in the dark show the same pigmentation phenotype but however, cells grown under high light conditions are faintly beige (Biebl *et al.,* 2005).

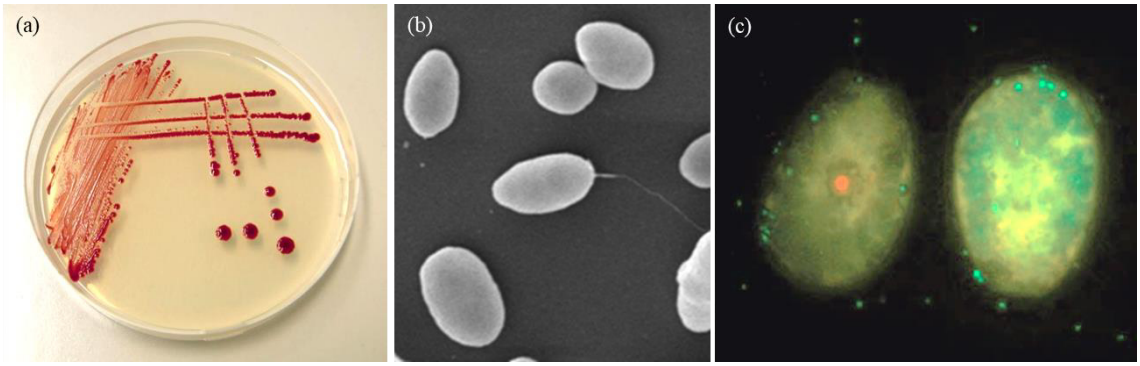

Figure 1: Macroscopic and microscopic morphology of *D. shibae*
(a) Agar plate of aerobically grown *D. shibae* cells with characteristic pink pigmentation (Wozniczka, DSMZ, Braunschweig, Germany).
(b) Transmission electron microscopic image of oval rod shaped *D. shibae* cells with a monotrichous flagellum (Manfred Rohde, HZI, Braunschweig, Germany).
(c) Catalyzed reporter deposition fluorescent in situ hybridization (CARD-FISH) experiments show attached *D. shibae* cells (green dots) to the dinoflagellate *P. lima* (Wagner-Döbler *et al.,* 2010).

D. shibae preferably grows in a temperature range from 15 °C to 38 °C and pH levels between 6.5 and 8.8. The organism is strictly salt-dependent and requires between 1-7 % salinity for optimal growth and is auxotrophic for biotin, nicotinic acid and 4-aminobenzoic acid (Biebl *et al.,* 2005). Like most Roseobacter species, *D. shibae* is able to utilize a broad spectrum of organic substances such as acetate, succinate, fumarate, lactate, citrate, glutamate, pyruvate, fructose and glycerol as carbon source (Biebl *et al.,* 2005).

Several closely related strains to *D. shibae* DFL12^T were found in association with different dinoflagellates and marine microalgae, like *Alexandrium ostenfeldii*, *Protoceratium reticulatum* or *Isochrysis galbana* (Allgaier *et al.,* 2003; Wagner-Döbler *et al.,* 2010). A physical interaction of host cells and bacteria was proposed and later verified by catalyzed reporter deposition (CARD) FISH experiments, using a coculture of *P. lima* and *D. shibae* DFL12^T (Figure 1c). It was assumed that this interaction is not host specific and that *D. shibae* is able to form a symbiotic relationship with different algal species. Basis of this symbiosis is most likely an exchange of micronutrients that is beneficial for both sides (Wagner-Döbler *et al.,* 2010). In coculture experiments with *D. shibae* DFL12^T and the dinoflagellate *Prorocentrum minimum* in culture medium lacking the vitamins B_1 and B_{12}, it was demonstrated that the bacteria can stimulate the growth of *P. minimum* by providing these vitamins. On the other hand, *D. shibae* uses the photosynthetic products of *P. minimum* as carbon source for its own metabolism (Wagner-Döbler *et al.,* 2010). In long-term experiments, however, it was found that this mutualistic relationship in coculture breaks after 21 days and is followed by a

pathogenic phase, where the bacteria kill their algal host (Wang & Tomasch *et al.,* 2014). This behavior and the underlying mechanism are not fully understood, but it was found that the killing effect of *D. shibae* on *P. minimum* is dependent on cell density and a so far unknown factor, which is encoded on the 191 kb plasmid of *D. shibae*, the so called "killer plasmid". In experiments with a *D. shibae* mutant strain, lacking the respective plasmid, the bacteria were no longer able to kill off the *P. minimum* cells after the critical time point of 21 days (Wang *et al.,* 2015).

The genome of *D. shibae* DFL12^T was fully sequenced at the Joint Genome Institute (JGI) (Wagner-Döbler *et al.,* 2010). It was shown that the genome consists of a circular chromosome and five additional circular plasmids (pDS191, pDS153, pDS126, pDS82 and pDS76). Similar to other Roseobacter genomes, the whole genome of *D. shibae* has a size of 4.4 Mbp comprising 4198 protein-coding genes. About one quarter of these gene products have a till now unknown function. Notable is the large number of genes that enable the adaptation to a broad spectrum of environmental conditions. For example, genes for carbon monoxide oxidation, aromatic compound degradation, sulphur oxidation, denitrification, nitrate assimilation, type IV secretion, dimethylsulfoniopropionate and aerobic anoxygenic photosynthesis were identified. Furthermore, a large set of different transposases and integrases was found. Together with the type IV secretion systems, which enable the exchange of genetic material *via* conjugation, this could be the explanation for the high genetic variability of *D. shibae* (Wagner-Döbler *et al.,* 2010).

D. shibae is able to generate its energy through various mechanisms. Preferred is aerobic respiration with oxygen as the terminal electron acceptor. In the absence of oxygen, *D. shibae* can, for example, ferment arginine to maintain metabolism. (Wagner-Döbler *et al.,* 2010). In addition, various alternative electron acceptors such as nitrate, nitrite or DMSO can be used. The complete denitrification pathway and the DMSO reductase were found in the genome (Wagner-Döbler *et al.,* 2010; Laass *et al.,* 2014). It was also shown that the four regulators FnrL, DnrD, DnrF and DnrE form a fine-tuned regulatory network and are required for the switch from aerobic to anaerobic growth of *D. shibae* (Ebert *et al.,* 2017). In addition to aerobic and anaerobic respiration and fermentation, *D. shibae* is also able to perform aerobic anoxygenic photosynthesis to generate ATP. All required components for this pathway, with a few exceptions, are located together in the photosynthetic gene cluster (PGC) (Tomasch *et al.,* 2011).

1.3 Aerobic Anoxygenic Photosynthesis

Photosynthesis is a complex metabolic process and one of the most important biochemical reactions on Earth. It utilizes solar energy and H_2O to convert inorganic carbon dioxide into glucose and molecular oxygen, which form the basis for (almost) all life on Earth. Origin and evolution of photosynthesis are still not fully understood. It is assumed that a mechanistically simpler anoxygenic variant of bacterial origin is the precursor of oxygenic photosynthesis, which was first performed by cyanobacteria about 2.7 billion years ago (Xiong & Bauer, 2002; Xiong *et al.,* 2000; Blankenship, 2010). This event led to the rise of the molecular oxygen concentration in the Earth's atmosphere and is coupled to the development of complex multicellular organisms with an efficient aerobic metabolism. Today, oxygenic photosynthesis is dominating and mainly performed by green land plants and marine microorganisms. But also anoxygenic photosynthesis still exists and is exclusively performed by prokaryotes, using bacteriochlorophyll (Bchl) as light harvesting pigment. For a long time, it was believed that phototrophic growth of these bacteria only occurred under strict anaerobic conditions and that the metabolism switches to heterotrophy in the presence of oxygen for two reasons. First, because aerobic respiration is energetically more favorable than photosynthesis and second, because the combination of photoactive pigments, light and oxygen promotes the formation of toxic reactive oxygen species (ROS), that could cause serious cell damage.

About 40 years ago, Shiba and colleagues made an important discovery and described the first strictly aerobic bacteria that contained Bchl *a* (Shiba *et al.,* 1979). This finding changed the statement that bacteria exclusively perform anaerobic anoxic photosynthesis and that instead it could also occur under oxidizing conditions. It might be that aerobic photosynthesis in bacteria forms an evolutionary intermediate stage between bacteria performing photosynthesis anaerobically and strict heterotrophic bacteria. The structure of the photosynthetic apparatus, the light harvesting complex I and the reaction center, as well as the electron transfer does not differ between anaerobic and aerobic photosynthetic bacteria (Yurkov & Beatty, 1998). The conversion from light into chemical energy is enabled by a cyclic electron transport chain (Figure 2).

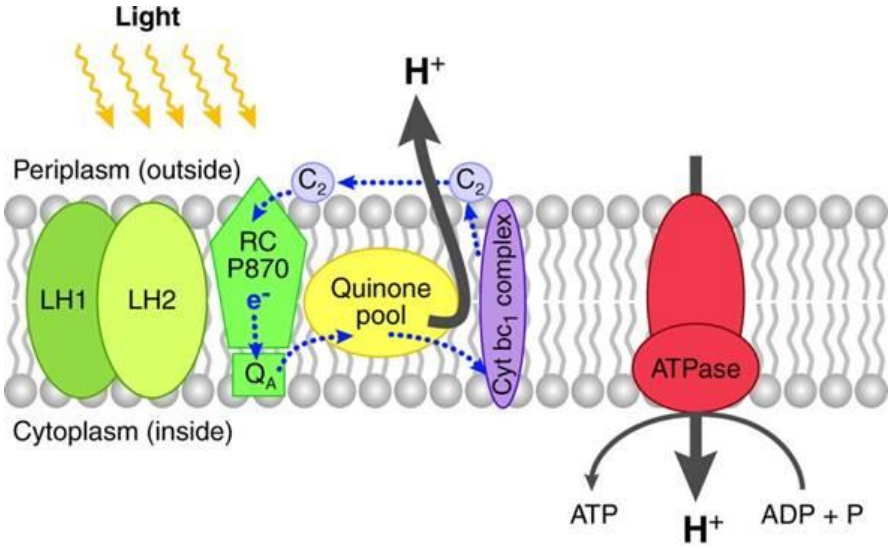

Figure 2: Mechanism of anaerobic photosynthesis
Light energy is harvested by the light harvesting (LH) complexes 1 and 2, which leads to a cyclic electron flow from the reaction center P870 (RC P870) *via* Q_A, the quinone pool, the cytrochrome bc_1 complex and the cytochrome c_2 (C_2) back to RC P870 (Wagner-Döbler & Biebl, 2006).

The light harvesting complexes consisting of Bchl *a*, carotenoids and the antenna complexes absorb the photons, which leads to the transformation of the reaction center P870 into a strong electron donor. First, the electrons flow into the quinone pool *via* a primary electron acceptor Q_A and are then further transferred to the cytochrome bc_1 complex. Using cytochrome c_2, the electrons are transferred back to the reaction center P870 and the cycle can restart by taking up photons again. This electron transport allows establishment of a proton gradient along the cell membrane, resulting in the phosphorylation of ADP to ATP by the membrane associated ATPase complex, (Wagner-Döbler & Biebl, 2006).

1.3.1 Aerobic Anoxygenic Phototrophic Bacteria

Since their discovery in the late 1970's, aerobic anoxygenic phototrophic (AAP) bacteria were extensively studied and many new species were described. AAP bacteria are not only common in the marine habitat, but also in other aquatic environments like inland freshwater or saline lakes (Koblížek, 2015; Gich & Overmann, 2006; Fuerst *et al.,* 1993; Shiba *et al.,* 1991; Csotonyi *et al.,* 2008). Some species were even isolated from more exceptional places such as Antarctic sea ice, biofilms, soil or acidic mine drainage (Koh *et al.,* 2011; Hirose *et al.,* 2012; Csotonyi *et al.,* 2010; Yurkov & Csotonyi, 2009). However, the majority of AAP bacteria have been ubiquitously found in eutrophic marine waters. There they are accounted to be the third most numerous

group of phototrophic bacteria and also potentially form a significant part of the heterotrophic bacterial community (Yurkov & Beatty, 1998; Koblížek, 2015; Kolber *et al.,* 2001).

The report of the widespread occurrence of Bchl *a* containing AAP bacteria led to more extensive investigations regarding their distribution and abundance in several sampling expeditions. The number of AAP bacteria found varied depending on the investigated area and ranged from 1.66 % to 11 % in the North East Pacific (Kolber *et al.,* 2001; Schwalbach & Fuhrman, 2005), 24 % in the South Pacific Ocean (Lami *et al.,* 2007) and 10 % in the Mid Atlantic Bight (Cottrell *et al.,* 2006). Often a correlation between Bchl *a* and chlorophyll concentration was observed, indicating a close relationship between AAP bacteria and autotrophic microorganisms and the dependency of AAP bacteria abundance on organic substrates (Jiao *et al.,* 2007).

Bchl *a* was identified as the only Bchl present in AAP bacteria, but however, they synthesize a broad spectrum of different carotenoids. Their composition varies among different species, giving them an individual phenotype ranging from bright yellow to red and brown (Yurkov & Beatty, 1998; Yurkov & Csotonyi, 2009). These carotenoids serve two purposes. First, they serve as auxiliary pigments in addition to Bchl *a*, (Yurkov & Beatty, 1998) and second, they are used for protection against ROS. As AAP bacteria perform photosynthesis under oxic conditions, there is a risk that the combination of oxygen, Bchl *a* and light will produce toxic singlet oxygen. Due to their conjugated double bonds, carotenoids can filter high-energy radiation and quench singlet oxygen. In addition, AAP bacteria protect themselves against ROS formation by only synthesizing Bchl *a* in the dark. Even low light intensities already have an inhibitory effect on Bchl *a* biosynthesis. Furthermore, AAP bacteria have been shown to produce at least ten times less Bchl *a* than bacteria performing anaerobic photosynthesis and have a significant excess of protective carotenoids (Beatty, 2002; Yurkov & Csotonyi, 2009; Koblížek, 2015).

Most AAP bacteria are strict aerobes, but exceptions have been found that are able to use alternative electron acceptors for anaerobic respiration (Yurkov & Beatty, 1998; Shiba, 1991; Biebl *et al.,* 2005; Wagner-Döbler & Biebl, 2006). They are not capable of a photoautotrophic lifestyle, but live photoheterotrophic. As the name suggests, photoheterotrophic bacteria are able to generate part of their energy from sunlight. A crucial difference to photoautotrophic organisms, however, is on the one hand the

missing enzyme ribulose-1,5-bisphosphate carboxylase/oxygenase, preventing the fixation of carbon dioxide *via* the Calvin cycle (Yurkov & Beatty, 1998). On the other hand, the redox potential of Bchl *a* is not sufficient to split water during photosynthesis to obtain electrons. As a consequence, no molecular oxygen is produced, which is why this type of photosynthesis is called anoxygenic. Due to the missing carbon fixation, AAP bacteria do not count as primary producers. However, since they play an important role in the recycling of dissolved organic matter (DOM), they are considered secondary producers in the ocean (Koblížek, 2015). It is assumed that AAP bacteria depend on heterotrophy for about 80 %, thus the energy generated by photosynthesis only contributes a small percentage (Yurkov & Csotonyi, 2009). But this little extra energy is sufficient to maintain the metabolism of these bacteria over a longer starvation period and reduces the requirement to respire organic matter (Kirchman & Hanson, 2013). This gives AAP bacteria a clear advantage over strictly heterotrophic organisms in oligotrophic surface waters (Koblížek, 2015; Martínez-García & Pinhassi, 2019).

Although much has been discovered about the lifestyle of AAP bacteria, their ecological role is not yet fully understood. They are a highly active part of the microbial community and were found to be relevant for the recycling of organic and inorganic carbon (Kolber *et al.,* 2001). It is assumed that between 2-5 % of photosynthetic electron transport in the upper ocean is due to AAP bacteria (Kolber *et al.,* 2000). Furthermore, they play a key role, together with photoautotrophic microorganisms, in the light-controlled carbon and redox cycle. Jiao and colleagues hypothesized that AAP bacteria may even be critical for a marine region to rather be a sink than a source of atmospheric carbon dioxide. If the energy that is obtained by AAP bacteria *via* photosynthesis would otherwise be generated by heterotrophic respiration, the carbon dioxide output from the ocean would rise, which would have a negative effect on the nutrient supply in the euphotic zone and on Earth's climate (Jiao *et al.,* 2010). Thus, the ecological relevance of AAP bacteria should be further investigated.

1.4 Bacteriochlorophyll *a* Biosynthesis

Tetrapyrroles are a family of complex chemical compounds that typically consist of four pyrrole or pyrrole-like rings that are either linear or cyclically linked with each other. These pyrroles are 5-atom ring systems that each contain four carbon atoms and one nitrogen atom. One key feature of cyclic tetrapyrroles, also called porphyrins, is their

ability to chelate different metal ions, such as iron, magnesium, cobalt or nickel. The porphyrin ring structure represents an aromatic compound containing a total of 26 π-electrons, making it a highly conjugated system. Depending on the degree of conjugation and the inserted central metal ion, tetrapyrroles exhibit different absorption properties in the visible spectrum of light and thus appear in different colors. Due to this property, tetrapyrroles are often referred to as the "pigments of life" (Battersby, 2000).

Modified tetrapyrroles are involved in a wide variety of fundamental biochemical processes, for example in catalysis of metabolic pathways, respiration or photosynthesis. Additionally, they often serve as cofactors or prosthetic groups in enzymatic reactions or as regulators for protein activity and mediate the response to different signals, like nutrient concentration, oxygen level or light (Bryant *et al.,* 2020; Yin & Bauer, 2013). The probably best-known members of the tetrapyrrole family are heme, cobalamin (vitamin B_{12}) and (bacterio)chlorophyll. The heme molecule contains iron as chelated metal ion and is the key component of hemoglobin, which is responsible for oxygen and carbon dioxide transport during respiration and also known as the red blood pigment. Cobalamin chelates cobalt as central ion and is involved in catalysis of methyl transfer reactions and radical based rearrangements (Banerjee & Ragsdale, 2003; Layer *et al.,* 2010). Chlorophylls and Bchls are magnesium chelating pigments that are responsible for the green color of plant leaves, algae and some bacteria. Most importantly, they allow light harvesting during photosynthesis (Bollivar, 2006).

From a chemical point of view, all (bacterio)chlorophylls are derivatives of the same parent molecule porphyrin. They share the isocyclic pentanone ring V, a propionic ester at the C17 atom and a central magnesium ion (Senge & Smith, 1995). Besides that, alterations in the rings, side chains and the degree of reduction lead to a high diversity of (bacterio)chlorophyll molecules, which all show different absorption behavior (Chen, 2014). At least 12 different types of (bacterio)chlorophylls are known to be present in bacteria (Chew & Bryant, 2007b), where Bchl *a* and Bchl *b* are the most common ones (Senge & Smith, 1995). Generally, Bchls show a higher diversity in their esterifying alcohol, compared to chlorophylls. This is mostly due to the modification of the basic Bchl structure by enzymes that are involved in the late steps of Bchl biosynthesis (Senge & Smith, 1995; Chew & Bryant, 2007b).

All tetrapyrroles share the same chemical backbone and to a certain point a common biosynthetic pathway and are all derived from the same precursor molecule 5-aminolevulinic acid (ALA). Formation of ALA can occur *via* two different pathways. The Shemin or C4 pathway was first discovered and described by Shemin and Russell and occurs in most eukaryotes (apart from plants) and α-Proteobacteria (Shemin & Russell, 1953). Here, the enzyme ALA synthase (HemA/T) catalyzes the condensation of succinyl coenzyme A and glycine, resulting in ALA. In the alternative C5 pathway, which is present in plants, algae, bacteria (except α-Proteobacteria) and archaea, ALA is produced from glutamate (Beale & Castelfranco, 1973). Later is was found that glutamate is converted in two enzymatic steps *via* glutamyl tRNA and glutamate semialdehyde into ALA. (Huang *et al.,* 1984; Jahn *et al.,* 1992; Jahn *et al.,* 2006; Bryant *et al.,* 2020). In the next step two ALA molecules are condensed by porphobilinogen synthase/ 5-ALA dehydratase, resulting in the pyrrole porphobilinogen (PBG) (Warren *et al.,* 1998). Four PBG molecules are then assembled to hydroxymethylbilane by PBG deaminase (HemC) and next the intermediate is catalyzed to uroporphyrinogen III by uroporphyrinogen III synthase (HemD). The formation of uroporphyrinogen III represents the first branch point in tetrapyrrole biosynthesis. From here, the pathway can either be directed towards the generation of heme d_1, siroheme, coenzyme F_{430} or vitamin B_{12}, or towards the protoporphyrin IX (Proto IX) branch, which results in either heme or (bacterio)chlorophyll, respectively (Senge & Smith, 1995; Willows & Kriegel, 2009).

First step of the Proto IX pathway is the conversion of uroporphyrinogen III into coproporphyrinogen III by decarboxylation through the *hemE* encoded enzyme uroporphyrinogen III decarboxylase. Oxidative decarboxylation by coproporphyrinogen III oxidase (HemF) of coproporphyrinogen III leads to the formation of the tetrapyrrole protoporphyrinogen IX, which is finally converted into Proto IX *via* a six-electron oxidation by protoporphyrinogen IX oxidase (HemG/Y) (Boynton *et al.,* 2009; Möbius *et al.,* 2010; Heinemann *et al.,* 2008). The biosynthetic pathway of Proto IX downwards to Bchl *a* is illustrated in Figure 3.

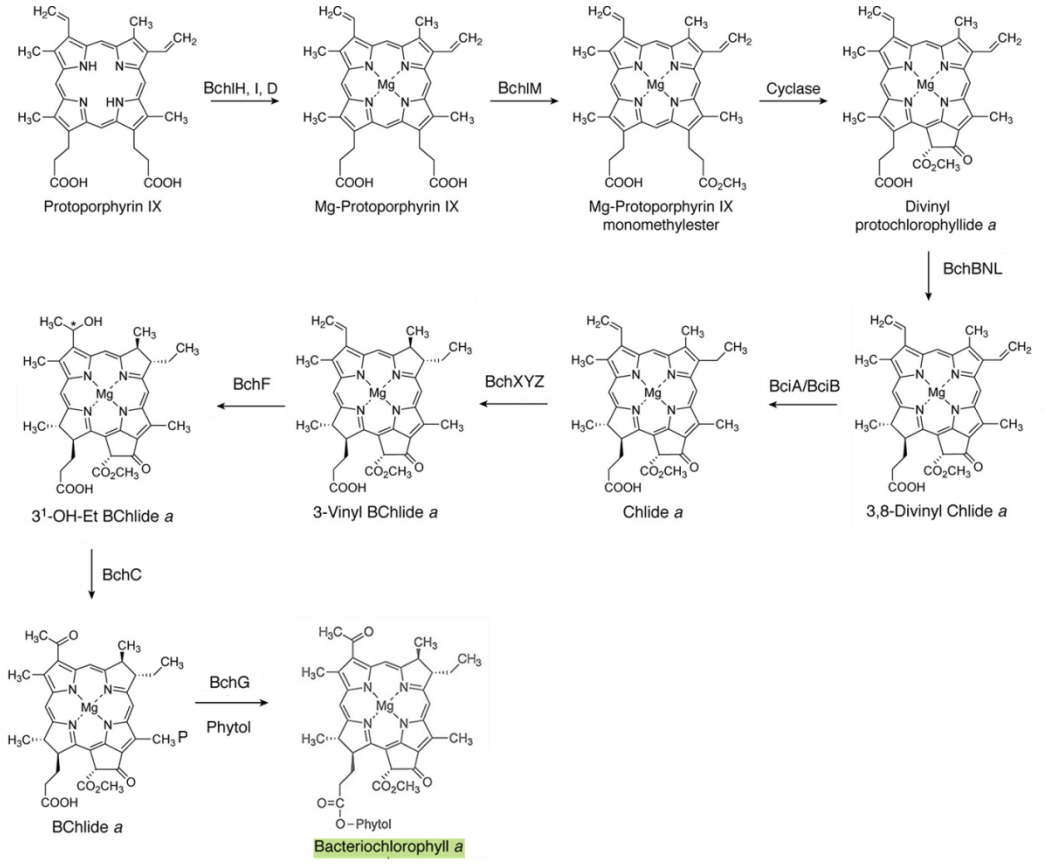

Figure 3: The biosynthesis of bacteriochlorophyll *a* from protoporphyrin IX
In the first step magnesium is inserted into the protoporphyrin IX framework by magnesium chelatase BchHID, resulting in Mg-protoporphyrin IX. Esterification of the intermediate's propionate side chain with a methyl group by BchM in a SAM-dependent manner, leads to the formation of Mg-protoporphyrin IX monomethylester. Next, the cyclase forms ring E of 3,8-divinyl protochlorophyllide *a*. Reduction of the C17=C18 double bond by BchBNL causes the generation of 3,8-divinyl Chlide *a*. BciA and BciB reduce the C8-vinyl group of the B ring to an ethyl group to form Chlide *a*. Reduction of the C7=C8 double bond of ring B is catalyzed by BchXYZ, resulting in 3-vinyl BChlide *a*. This intermediate serves as substrate for BchF to form 3^1-OH-Et BChlide *a*, BchC subsequently oxidizes the 3-hydroxyethyl group to a 3-acyl group, resulting in BChlide *a*. Geranylgeraniol is esterified to the C17 propionate chain of ring D by BchG. In parallel geranylgeraniol is reduced by BchP to a phytol group, finally resulting in the formation of Bchl *a*. (Bryant *et al.,* 2020, modified)

Depending on the inserted metal ion at this point of the biosynthetic pathway, either heme or (bacterio)chlorophyll is synthesized. Insertion of ferrous iron (Fe^{2+}) by the ferrochelatase HemH results in heme biosynthesis, whereas magnesium chelatase BchHID catalyzes the insertion of magnesium (Mg^{2+}) into the tetrapyrrole framework, pushing the pathway towards (bacterio)chlorophyll generation. Mg^{2+} is incorporated into Proto IX in an ATP-dependent step, resulting in Mg-Proto IX (Willows, 2003; Chew & Bryant, 2007b). Next, the attached propionate side chain to ring C is esterified with a methyl group by S-adenosyl-L-methionine (SAM) Mg-Proto IX methyl transferase BchM, using SAM as a methyl donor. The methylated propionate side chain on ring C of the product Mg-Proto IX monomethylester (MPE) is now used to form the

isocyclic ring E. This formation is catalyzed by the Mg-Proto IX monomethylester (oxidative) cyclase, yielding in 3,8-divinyl protochlorophyllide *a* (PChlide *a*). It has been found that two different enzymes are capable to catalyze this cyclase reaction. First, the oxygen-dependent cyclase AcsF, that incorporates molecular oxygen into the E ring and second, the oxygen-independent cyclase BchE, that is able to use oxygen from water for incorporation into ring E (Walker *et al.,* 1989; Porra *et al.,* 1996; Willows, 2003). PChlide formation is followed by the reduction of the C17=C18 double bond of ring D by PChlide oxidoreductase (POR), whereby 3,8-divinyl chlorophyllide a (Chlide *a*) is produced. Again, interestingly two different and also unrelated enzymes have been found to catalyze this reaction step. The light-dependent POR (LPOR) catalyzes the reduction of the double bond as the name suggests exclusively in the presence of light. However, the dark-operative POR (DPOR) is an enzyme consisting of three subunits (BchLNB) and does not require light for activity. The produced 3,8-divinyl Chlide *a* serves as a substrate for divinyl reductases, which reduce the C8-vinyl group of the B ring to an ethyl group and causing the formation of Chlide *a*. This reduction step is not fully understood to date and it is suggested, that this step could also occur prior to PChlide formation. A variety of divinyl reductases have been found in different organisms and some early reports assumed that the BchJ protein in *Rhodobacter capsulatus* catalyzes this step (Suzuki & Bauer, 1995) but however, this did not seem to be the case for homologous proteins in related organisms (Chew & Bryant, 2007a). The BciA and BciB proteins in different bacterial species, as well as their homologues in higher plants, show divinyl reductase activity and therefore might be involved in this step of the (bacterio)chlorophyll pathway (Bryant *et al.,* 2020).

Compared to chlorophylls, Bchls possess a reduced B ring and differ in the attached substituent on ring A. Reduction of the C7=C8 double bond, which yields in 3-vinyl bacteriochlorophyllide *a* (BChlide *a*), of ring B is catalyzed by the Chlide oxidoreductase (COR), consisting of the three subunits BchXYZ. Interestingly the COR enzyme also shows divinyl reductase activity and might be involved in the reduction of 3,8-divinyl Chlide *a* to Chlide *a*. The 3-vinyl BChlide *a* hydratase, encoded by *bchF*, mediates the hydroxylation of the 3-vinyl group of ring A, causing the formation of 3-hydroxyl (3HE)-BChlide *a*, and the 3-hydroxyethyl-BChlide *a* dehydratase (BchC) subsequently oxidizes the 3-hydroxyethyl group to a 3-acyl group, resulting in BChlide *a*. In the final steps BChlide *a* is esterified with a geranylgeraniol on the C17

propionate side chain of the D ring by the bacteriochlorophyll synthase (BchG), then the geranylgeraniol is reduced by the geranylgeranyl reductase (BchP) to a phytol group, resulting in the formation of Bchl *a* (Willows & Kriegel, 2009; Bryant *et al.,* 2020).

1.4.1 The Photosynthetic Gene Cluster in Anoxygenic Phototrophic Bacteria

In past studies both, anaerobic and aerobic anoxygenic phototrophic bacteria, were extensively studied regarding their genetic predisposition of performing photosynthesis. In the mid 1970's Yen and Marrs found, that the genes for Bchl and carotenoid biosynthesis in the purple non-sulfur bacterium *R. capsulatus* are clustered together in a relatively small region on the chromosome. They considered that such gene arrangement could be a benefit for the simultaneous transcription of those genes and enables a faster response to regulatory stimuli that either initiate or repress the biosynthesis of photopigments (Yen & Marrs, 1976). Six years later Taylor *et al*. described the alignment of a restriction map of a 46 kb gene fragment of the *R. capsulatus* chromosome with the genetic map of the photosynthesis region of the chromosome by a marker rescue method. As a result they determined the position of several genes that are involved in Bchl, carotenoid and reaction center biosynthesis on the 46 kb fragment (Taylor *et al.,* 1983). Therefore, they were the first ones to describe the presence of a gene region that is known today as the PGC. Investigations of the related organism *Rhodobacter sphaeroides* regarding the arrangement of its photosynthesis genes led to the assumption, that there might be a similar clustering of those genes in the genome. Also, by restriction mapping, Coomber and Hunter analysed different photosynthetic mutants of *R. sphaeroides* and assembled the first map of its 45 kb large PGC (Coomber & Hunter, 1989).

Today it is known that the organization of photosynthesis genes in the PGC is highly conserved within the photosynthetic active Proteobacteria. All studied PGCs have an average size of 35-50 kb, which corresponds to roughly 1 % of the genome, and contain about 40 different genes coding for enzymes involved in Bchl (*bch*) and carotenoid (*crt*) biosynthesis, in assembly of the reaction center and light harvesting complex I (*puf, puh*) and in regulation of the photosynthesis machinery (Nagashima & Nagashima, 2013; Zheng *et al.,* 2011; Liu *et al.,* 2019). Only the light harvesting complex II, encoded by the *puc* operon, which is not present in all photo(hetero)trophic bacteria, is located separately elsewhere in the genome (Liotenberg *et al.,* 2008). Zheng *et al*. analysed the arrangement of diverse PGCs in AAP bacteria and found that a basic set of

27 genes is present in all investigated species. Most of those genes can be assigned to the Bchl *a* biosynthesis pathway (Zheng *et al.,* 2011). Also the amino acid sequences of most Bch enzymes are highly conserved between different AAP bacteria with up to 60 % (Nagashima & Nagashima, 2013). Interestingly, a high variability was found for the *crt* genes in all investigated AAP bacteria (Zheng *et al.,* 2011; Nagashima & Nagashima, 2013). Bchl *a* is the major chlorophyll used in AAP bacteria, which explains the conservation of *bch* genes. In comparison, the carotenoid composition varies considerably among AAP bacteria (Yurkov & Beatty, 1998) and hence the *crt* genes present. Usually, the order of genes and operons within the PGC is well conserved but can differ between the three subclasses of Proteobacteria (Liotenberg *et al.,* 2008).

The organization of genes belonging to the same metabolic pathway in a common cluster or an operon, as here in the case of the PGC, is often observed in the genomes of bacteria. This enables the simultaneous expression of genes and thus fast adaptation to, for example, changing environmental conditions. AAP bacteria also live in a habitat with constant changes, such as fluctuating oxygen concentrations or light intensities. The rapid adaptation through coexpression of the photosynthesis genes protects the cells from damage caused by free tetrapyrroles or ROS, for example (Liotenberg *et al.,* 2008).

1.4.1.1 Evolution of the Photosynthetic Gene Cluster

The evolution of photosynthesis and the PGC in bacteria has long been disputed. Two possible scenarios have been repeatedly investigated and discussed in recent years. A common phototrophic ancestor, from which other species have evolved and that have lost their photosynthesis genes over time, could be an explanation for the heterogeneous occurrence of photo(hetero)trophic species within the Rhodobacteraceae family (Koblížek *et al.,* 2013; Nowicka & Kruk, 2016). The second hypothesis is that different heterotrophic species have independently gained photosynthetic genes *via* HGT and have thus became photo(hetero)trophs (Koblížek *et al.,* 2013). The first scenario was initially ruled out by Koblížek *et al*. by performing G+C profiling of 22 species of the Roseobacter group. They compared the G+C content of the PGCs and the chromosomes and found no big differences, which they would have expected to be the case, if the PGC was of different origin and acquired *via* HGT. Consequently, a common origin of the PGC in all Rhodobacteraceae was concluded (Koblížek *et al.,* 2013).

However, in the past there were already sound indications that photosynthesis genes could be transferred *via* HGT between species. The complete PGC of *R. litoralis* and *Sulfitobacter guttiformis*, both members of the Roseobacter group, was found localized on a plasmid (Kalhoefer *et al.,* 2011; Petersen *et al.,* 2012). The investigation of 105 Rhodobacteraceae genome sequences revealed additional four plasmid-located PGCs (Brinkmann *et al.,* 2018). From the core genome present in all 105 species, a phylogenomic tree of Rhodobacteraceae was assembled. In addition, a PGC tree was created using 33 PGC marker genes. A comparison of these trees showed that they are not congruent and thus a strictly vertical evolution of anoxygenic photosynthesis and a common origin of the PGC can be excluded. Furthermore, the data revealed that not only single photosynthesis genes were transferred *via* HGT, but also whole operons or superoperons of the PGC *via* so-called horizontal operon transfer (Brinkmann *et al.,* 2018). To date, it is assumed that about 20 % of all known Roseobacter PGCs are located outside the chromosome (Liu *et al.,* 2019).

Both initially mentioned hypotheses can be well combined to explain the scattered distribution of AAP bacteria and their PGC within the phylum of Proteobacteria. A combination of loss of photosynthesis genes, HGT and horizontal operon transfer seems to be the most plausible explanation (Brinkmann *et al.,* 2018; Liu *et al.,* 2019).

1.4.1.2 Regulation of the Photosynthetic Gene Cluster

The regulation of photosynthesis and the PGC in anaerobic and aerobic anoxygenic phototrophic bacteria is a rather complex process and occurs on different levels. This is particularly necessary to protect the bacteria from cell damage by, for example, ROS or toxic amounts of free tetrapyrroles and intermediates of tetrapyrrole biosynthesis (Yin & Bauer, 2013). Furthermore, a constant uncontrolled synthesis of the photosynthetic apparatus under unfavorable conditions, where no photosynthesis can or should occur, would waste valuable energy reserves of the organism.

Since all known tetrapyrroles are synthesized from the same precursor molecule ALA, a feedback regulation is necessary to ensure that all end products are available in the cell in the required amounts but also not in excess. The product of one branch can directly or indirectly influence the synthesis of the other ones. In the case of Bchl *a* biosynthesis it is for instance known, that both heme and cobalamin serve as cofactors for regulator proteins of the PGC (Han *et al.,* 2007; Yin *et al.,* 2012; Vermeulen & Bauer, 2015). Additionally, *in vivo* experiments in *R. capsulatus* demonstrated that the activity of the

anaerobic cyclase BchE is dependent on cobalamin (Gough *et al.,* 2000). The enzyme CobZ on the other hand, involved in cobalamin biosynthesis, binds heme as cofactor, making cobalamin biosynthesis heme dependent (McGoldrick *et al.,* 2005).

Most of the research regarding the regulation of photosynthesis genes was performed in the two purple non-sulfur bacteria *R. capsulatus* and *R. sphaeroides*. In both organisms it was found that the global regulators FNR and RegA/RegB (*R. capsulatus*) or PrrA/PrrB (*R. sphaeroides*) are involved in oxygen- or redox-dependent regulation of Bchl synthesis (Yin & Bauer, 2013). *Escherichia coli* FNR is a well-studied transcriptional regulator, required for the switch between aerobic and anaerobic metabolism (Sawers *et al.,* 1988; Spiro, 1994). In the two Rhodobacter species FNR also mediates the response to redox changes. Since these bacteria perform photosynthesis exclusively under (semi) anaerobic conditions, redox control is important. During early Bchl biosynthesis, FNR acts as an anaerobic activator of several *hem* genes (Smart *et al.,* 2004). Also, the RegAB/PrrAB two-component system can sense changes in oxygen tension. The redox signal is detected by the sensor kinase RegB/PrrB, which causes its autophosphorylation and the subsequent phosphotransfer to the response regulator (RR) RegA/PrrA. It was shown that the RR phosphorylation can increase the DNA binding affinity up to 16-fold (Elsen *et al.,* 2004). Described targets of the RegAB/PrrAB regulator system are for example *puh*, *puc*, *puf* and *bchC* operons (Elsen *et al.,* 2004).

There are several additional transcription factors that only specifically regulate the tetrapyrrole or Bchl biosynthesis. Such a DNA-binding transcription factor is PpsR from *R. sphaeroides* (the homologue in *R. capsulatus* is termed CrtJ; for reasons of simplicity, only called PpsR in the following), which is well characterized and known as a master regulator of photosynthesis genes. In all purple bacteria in which PpsR is present, the corresponding *ppsR* gene was located within the PGC (Elsen *et al.,* 2005). It is a tetrameric protein, that binds a heme cofactor and acts as a redox-regulated repressor (Masuda *et al.,* 2002; Yin *et al.,* 2012). This family of regulators does not seem to be conserved, since amino acid sequence alignments of known PpsR proteins only showed a poor identity, ranging from 26-54 % (Elsen *et al.,* 2005). In contrast, the architecture of the PpsR protein is generally conserved among different species. It consists of three domains: the C-terminus possesses a helix-turn-helix DNA-binding motif, the protein center contains two Per-Arnt-Sim (PAS) domains for proper

conformation and repressor activity and the N-terminus shows no similarity to any known protein domain known to date and has thus an unknown function (Gomelsky *et al.,* 2000; Elsen *et al.,* 2005). Binding of the heme cofactor changes the binding affinity to target promoter regions and induces the transcription of PpsR regulated genes (Yin *et al.,* 2012). Under aerobic conditions PpsR represses the transcription of several photosynthesis genes or whole operons within the PGC, like the *bch*, *crt* and *puc* operon and the DNA-binding affinity was found to be up to 4.5 fold higher under these conditions (Gomelsky & Kaplan, 1995b; Ponnampalam *et al.,* 1995; Ponnampalam & Bauer, 1997). Today it is known that the formation of intramolecular disulfide bonds between conserved cysteine residues stimulate DNA-binding and thus, the repression of photosynthesis genes by a PpsR tetramer (Masuda *et al.,* 2002; Cheng *et al.,* 2012). PpsR binds to the target sequence TGT-N_{12}-ACA (where N is any nucleotide), which is located in tandem upstream of *puc* and several *crt* and *bch* operons (Ponnampalam & Bauer, 1997; Gomelsky & Kaplan, 1995b; Gomelsky *et al.,* 2000). This binding motif is also found upstream of many genes that are not involved in photosynthesis, so probably the role of PpsR is broader and not only limited to Bchl biosynthesis regulation (Moskvin *et al.,* 2005). A total of 240 potential PpsR binding sites were identified in the genome of *R. sphaeroides,* but it is not known if all binding sites are actually functional. During transcriptome analysis the *hemE* and *hemC* genes were identified as direct targets of PpsR, revealing that it is also involved during early tetrapyrrole synthesis (Moskvin *et al.,* 2005).

Besides many similarities in the regulation of photosynthesis genes between *R. sphaeroides* and *R. capsulatus*, there are also some fundamental differences. One distinction is for instance the presence of a PpsR anti-repressor in *R. sphaeroides*, called AppA, that is completely missing in *R. capsulatus*. AppA is a monomeric protein and the encoding gene was first identified during a genetic screen for mutants lacking the expression of the *puc* operon (Masuda & Bauer, 2002; Gomelsky & Kaplan, 1995a). The gene locus was therefore termed “activation of photopigment and puc expression A” (*appA*) (Gomelsky & Kaplan, 1995a). An *appA-ppsR* double mutant strain of *R. sphaeroides* showed the same phenotype as the *ppsR* mutant strain and therefore it was considered that AppA is not an actual activator of photosynthesis genes, but rather an anti-repressor of PpsR (Gomelsky & Kaplan, 1997). It was also Gomelsky and Kaplan who showed, that AppA is a flavoprotein that binds a flavin adenine

dinucleotide (FAD) cofactor at its N-terminus (Gomelsky & Kaplan, 1998). Later is was found that this FAD serves as chromophore in a new kind of photoreceptor called "blue-light using FAD" (BLUF) (Masuda & Bauer, 2002). Upon blue light illumination the FAD gets excited, which causes an immediate conformational change of the AppA protein (Gauden *et al.,* 2005; Masuda & Bauer, 2002). This finding provided evidence of blue light-dependent control of photosynthesis genes in photosynthetic purple bacteria for the first time. The C-terminus of AppA harbors a "sensor containing heme instead of cobalamin" (SCHIC) domain, binding a heme cofactor (Han *et al.,* 2007). Therefore, AppA is a light and oxygen sensitive anti-repressor that integrates both signals in its regulatory system. Even long before regulators of photosynthesis genes where known it was described, that light and oxygen had the most influence on photopigment biosynthesis in purple bacteria (Cohen-Bazire *et al.,* 1957). Experiments with purified PpsR and AppA proteins showed that both proteins build a stable non covalent AppA-$PpsR_2$ complex under (semi) anaerobic conditions, that is not affected by blue light (Masuda & Bauer, 2002; Winkler *et al.,* 2013). Under anaerobic conditions this protein complex is able to bind to the PpsR DNA-binding sites, preventing a repression of genes by PpsR. Additionally, it is assumed that reduced AppA reduces the disulfide bonds in PpsR that are needed for DNA-binding of the repressor. The blue light induced conformational change of AppA is proposed to weaken the DNA affinity of the AppA-$PpsR_2$ complex. In an aerobic environment AppA is present in its oxidized form and therefore not able to interact with PpsR, which consequently represses transcription of its target genes (Masuda & Bauer, 2002; Masuda & Bauer, 2005; Winkler *et al.,* 2013).

A regulator protein that was found to have an influence on the PpsR activity in *R. capsulatus* is AerR. AerR stands for "aerobic repressor", as it was initially suggested to be involved in the aerobic repression of photosynthesis genes (Dong *et al.,* 2002). A homologue that is involved in photosystem formation was also identified in *R. sphaeroides* and termed PpaA (photopigment and *puc* activator protein) (Gomelsky *et al.,* 2003). Both protein encoding genes were found immediately upstream of *ppsR* within the PGC. Also in other sequenced purple bacteria that contain PpsR, the *aerR*/*ppaA* genes were always found upstream of the *ppsR* gene (Dong *et al.,* 2002; Cheng *et al.,* 2014) (Figure 4).

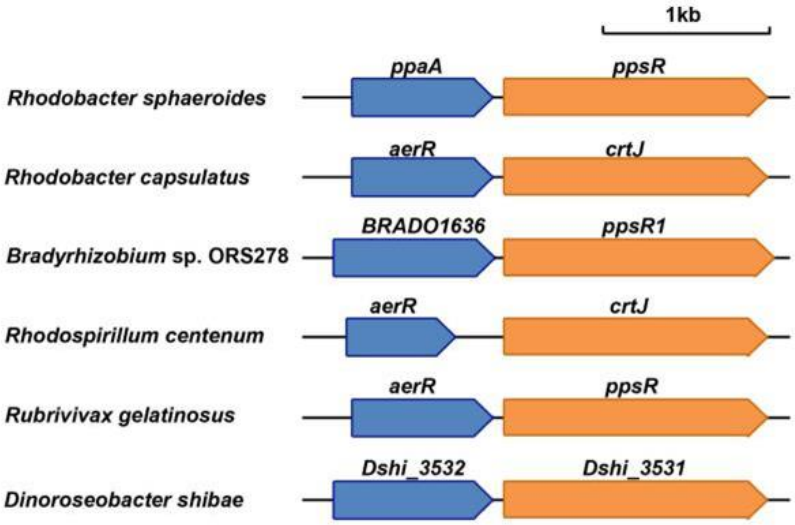

Figure 4: Conserved position of *aerR* and *ppaA* homologues in different bacterial species
The *aerR*/*ppaA* homologues are indicated by blue arrows, *ppsR* homologues by orange arrows. (Cheng *et al.,* 2014, modified)

Surprisingly, the chromosomal deletion of *ppaA* in *R. sphaeroides* led to a completely different phenotype than deletion of *aerR* in *R. capsulatus*. The *R. sphaeroides* Δ*ppaA* strain showed only minor changes in pigmentation compared to the wild type strain (Vermeulen & Bauer, 2015). In contrast, in the Δ*aerR* mutant strain of *R. capsulatus* a strong reduction of pigmentation was observed (Cheng *et al.,* 2014). This implicates, that PpaA in *R. sphaeroides* only plays a minor role in regulation of photosynthesis genes and that probably AppA, which is missing in *R. capsulatus*, is the major anti-repressor of PpsR. Interestingly, overexpression of PpaA in the *R. sphaeroides* Δ*appA* mutant background can restore the Bchl *a* biosynthesis and thus, photosynthetic growth. So it seems that in the presence of AppA, PpaA is not active but if AppA is somehow missing or inactive, PpaA can take over the anti-repressor role (Vermeulen & Bauer, 2015). All PpaA/AerR family members characterized so far, exhibit a SCHIC domain sequence at the N-terminus (Vermeulen & Bauer, 2015). However, their specificity to heme or cobalamin was a matter of dispute. It was postulated that *R. sphaeroides* PpaA binds heme (Moskvin *et al.,* 2010), whereas *R. capsulatus* AerR showed cobalamin binding (Cheng *et al.,* 2014). Vermeulen and Bauer reinvestigated the PpaA tetrapyrrole binding affinity and could clearly demonstrate that the proteins bind cobalamin instead of heme (Vermeulen & Bauer, 2015). Furthermore, they could reveal an interaction between PpaA and PpsR. Also for AerR and PpsR an interaction was experimentally proven and it was found that both proteins form a AerR-$PpsR_2$ complex (Fang & Bauer, 2017). Nevertheless, the mechanism how PpaA and AerR can regulate the PpsR activity

remains largely unclear. The AerR-$PpsR_2$ complex can interact with promoters of photosynthesis genes in a redox-dependent manner and thereby control PpsR repression (Fang & Bauer, 2017). Recently it was found that AerR is translated in two isoform that differ by 41 amino acids at the N-terminus. The ratio of both forms is influenced by light and the cell growth phase. During photosynthetic and exponential growth, the longer AerR variant is dominating and activating photosynthesis genes. The shorter variant is more present under dark conditions and/or during the stationary phase and is involved in repression of photosynthesis genes (Yamamoto *et al.,* 2018). A novel class of photoreceptors was recently described, which use cobalamin as blue light detecting chromophore (Yamamoto *et al.,* 2018). This suggests that PpaA/AerR could be defined as such a photoreceptor.

1.4.2 Photosynthesis in *D. shibae*

D. shibae is able to perform aerobic anoxygenic photosynthesis. First indications were found by Biebl *et al.* (2005), when they described the presence of Bchl *a* and spheroidenone as light absorbing pigments. Furthermore, *in vivo* absorbance spectra implied the presence of the light harvesting complex II and thus, a functional photosynthetic apparatus was predicted (Biebl *et al.,* 2005). In the genome of *D. shibae* all necessary components for aerobic anoxygenic photosynthesis are encoded in the PGC (Wagner-Döbler *et al.,* 2010; Tomasch *et al.,* 2011). The PGC spans the gene loci from Dshi_3501 to Dshi_3547 (Figure 5a), the *puc* operon is located elsewhere in the genome and ranges from Dshi_2897 to Dshi_2900. Within the PGC of *D. shibae* gene copies encoding the transcription factors PpsR (Dshi_3531) and PpaA (Dshi_3532) are located (Tomasch *et al.,* 2011). Similar to *R. capsulatus*, no AppA homologue is present. During long-term cultivation experiments it was found, that a 12 h dark followed by a 12 h light cycle provides the best growth conditions for *D. shibae.* In response to light, O_2 consumption, CO_2 production and Bchl *a* concentration is decreased, whereas the biomass increased. In this situation the respiration of carbon sources is reduced and photophosphorylation is the preferred mechanism for energy generation (Tomasch *et al.,* 2011). Light exposure of *D. shibae* cells can lead to a reduction of the respiration rate of up to 75 %. Additionally, the assimilation rate of carbon sources under light conditions is two times faster than in the dark (Piwosz *et al.,* 2018). The opposite behavior was observed in the dark: a decrease in biomass and O_2 concentration and an increased CO_2 and Bchl *a* level. Here, no cyclic electron transfer is

possible to gain energy and thus, stored carbon is consumed as electron donor for the respiratory chain (Tomasch *et al.,* 2011). Especially under starvation conditions, which are predominant in most oceanic regions, the switch between phototrophic and heterotrophic metabolism is a great survival strategy of *D. shibae*. Under constant dark conditions, where only heterotrophic growth can occur, cell numbers are decreased by a factor of ten (Soora & Cypionka, 2013).

Transcriptome analyses showed a light-dependent expression of most of the PGC genes (Figure 5b) (Tomasch *et al.,* 2011). After exposure of dark cultivated *D. shibae* cells to light, expression of genes involved in Bchl *a* biosynthesis and photosynthesis was immediately shut down. The same genes remained repressed in the first four hours after the cultures were returned to dark conditions and were then upregulated again. Expression of the *ppsR* gene is not influenced by light (Tomasch *et al.,* 2011). The PGC of *D. shibae* contains several PpsR binding sites. Also, outside of the PGC, for instance in the promoter region of the *hemE* (Dshi_2705)/*hemC* (Dshi_2704) operon, PpsR binding sites were identified. This indicates the important role of PpsR as a master regulator of photosynthesis genes in *D. shibae* and the close link to tetrapyrrole biosynthesis (Tomasch *et al.,* 2011).

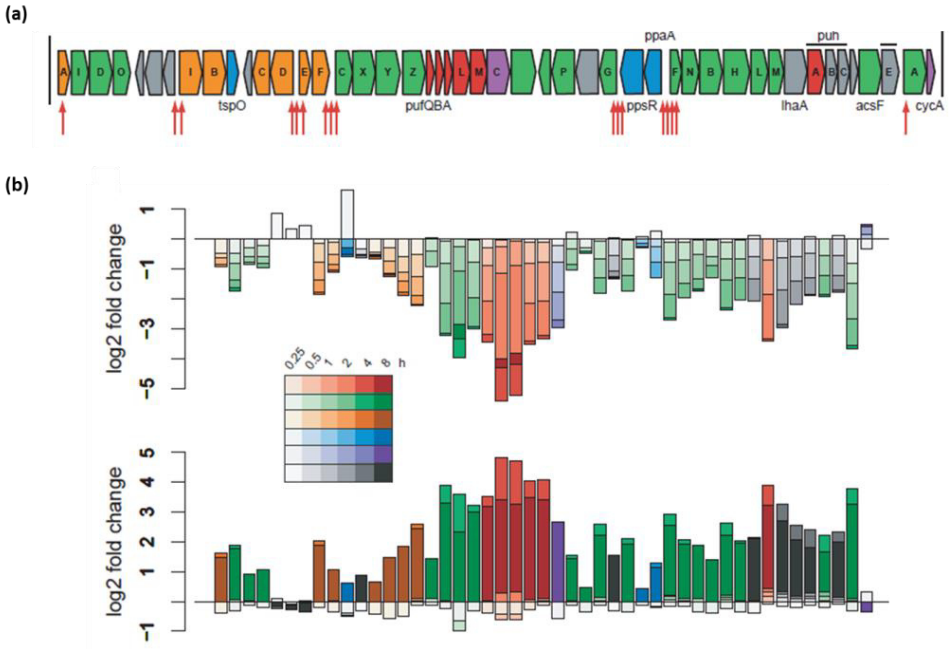

Figure 5: The photosynthetic gene cluster of *D. shibae* and its expression in response to light
(a) Photosynthetic gene cluster of *D. shibae* ranging from Dshi_3501 to Dshi_3547. Related genes are illustrated in the same colors. Green: Bchl *a* biosynthesis, orange: carotenoid biosynthesis, red: structural components of the photosystem, blue: regulatory proteins, velvet: cytochromes, grey: assembly proteins or no function assigned. The red arrows indicate potential PpsR binding sites.
(b) Transcription profile of PGC genes in log2 fold-changes under light conditions (upper row), compared to the dark control (lower row). Order of genes and colors correspond to the PGC described in (a). (Tomasch *et al.,* 2011, modified)

1.4.2.1 High-throughput Screening for Identification of Potential Regulators of Photosynthesis Genes in *D. shibae*

Regulation, especially light-dependent regulation, of photosynthesis and Bchl *a* biosynthesis in *D. shibae* is poorly understood. Therefore, it was aimed in a previous doctoral thesis to identify and characterize new potential regulator proteins involved in this process. The approach was to establish a reliable high-throughput screening of the *D. shibae* transposon mutant library, which comprises almost 10.000 different clones with 3000 different gene loci, to identify mutants with a defect in Bchl *a* biosynthesis (Ebert *et al.,* 2013). These defects might be due to the lack of an important previously unknown regulator, making the coding protein an interesting new candidate for further studies.

The established high-throughput screening enabled the fast identification of *D. shibae* transposon mutant strains with deficiencies in Bchl *a* biosynthesis (Heyber, 2021). A total of 9975 *D. shibae* transposon mutants were analysed regarding their pigmentation phenotype, Bchl *a* absorption spectrum and MPE accumulation. In the screening the

D. shibae wild type strain DFL12^T served as a negative control. As positive control, the *ascF*::Tn mutant strain was chosen, which is missing the oxygen-dependent cyclase AcsF and fails to convert MPE into PChlide *a* (see chapter 1.4). The accumulated MPE shows an autofluorescence under blue light illumination (415 nm) and an altered Bchl *a* absorbance spectrum compared to the wild type, which makes it a suitable marker. In the screening 93 transposon mutants with an altered pigmentation phenotype, 145 transposon mutants with an altered Bchl *a* absorbance spectrum and 34 MPE-accumulating transposon mutants were identified. Of the genes hit by the transposon, 15 were directly related to Bchl *a* biosynthesis and photosynthesis. For instance, the genes encoding the photoreaction center subunits PufL and PufC, the oxygen-independent cyclase BchE, the Mg-chelatase subunits BchI and BchH, the COR subunit BchZ and the PpsR repressor were found. Particularly striking was the bright green pigmentation of the *ppsR*::Tn transposon mutant strain, which is assumed to be due to accumulation of the Bchl *a* biosynthesis intermediate PChlide (Heyber, 2021). However, also mutants were found whose gene products are not directly involved in Bchl *a* biosynthesis, like the *clpX*::Tn and Dshi_1135::Tn mutant strains. Both strains show a faintly beige pigmentation phenotype and therefore a severe deficiency in Bchl *a* and spheroidenone biosynthesis.

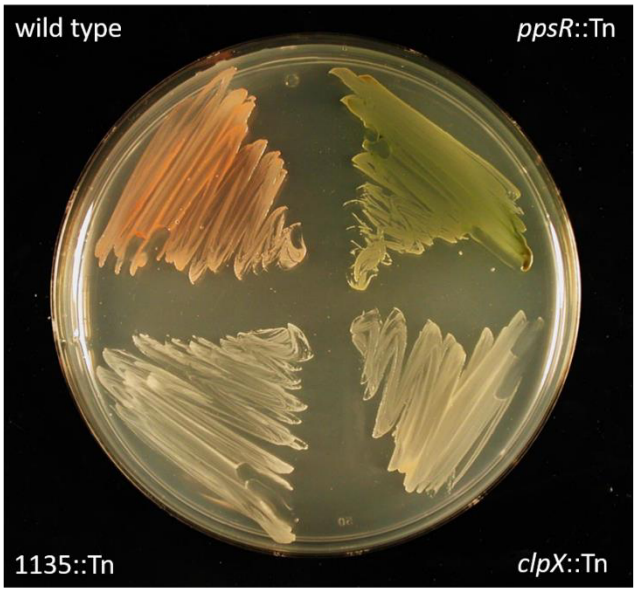

Figure 6: *D. shibae* transposon mutant strains with deficiency in pigment biosynthesis compared to the wild type strain
Top left: *D. shibae* DFL12^T wild type strain with typical pink pigmentation. Top right: *D. shibae ppsR*::Tn transposon mutant strain with deficiency in Bchl *a* biosynthesis, accumulating an unknown pigment. Bottom left: *D. shibae* Dshi_1135::Tn transposon mutant strain showing a complete loss of Bchl *a* biosynthesis. Bottom right: *D. shibae clpX*::Tn showing a complete loss of Bchl *a* biosynthesis.

As described earlier (see chapter 1.4.1.2), PpsR is the master repressor of photosynthesis genes, therefore it is not surprising that the respective mutant strain shows severe deficiencies. The *clpX* gene encodes the ClpX subunit of the ClpXP protease system. Substrate degradation is processive, with cycles of ATP hydrolysis driving unfolding and translocation of the target proteins through ClpX to the ClpP peptidase subunit (Baker & Sauer, 2012). The role of ClpX and the ClpXP protease, respectively, in Bchl *a* biosynthesis is not understood. One hypothesis is that the protease is able to indirectly derepress photosynthesis genes by degrading a repressor protein. Defects in the ClpXP protease system would lead in consequence to a constant repression of Bchl *a* biosynthesis. The gene locus Dshi_1135 codes for a 338 amino acid protein annotated as a Per-Arnt-Sim (PAS) domain-containing protein (NCBI reference: WP_012177807.1), possessing a N-terminal putative PAS photoreceptor domain and a C-terminal histidine kinase (HK) domain. A well-known subset of PAS domains are Light-Oxygen-Voltage (LOV) domains, which belong to the photoreceptor family. They are able to specifically sense blue light, which leads to the activation of a fused effector domain that in turn is often involved in gene regulation. Since a light-dependent regulation of photosynthesis genes was observed in related Rhodobacter species (Shimada, 1992; Braatsch *et al.,* 2004), it was estimated that Dshi_1135 might be a part of a light-dependent regulatory machinery in *D. shibae*. Initial transcriptome analyses of the *D. shibae* wild type and the Dshi_1135::Tn mutant strain under different light conditions revealed that blue light has a positive effect on the expression of photosynthesis genes in the wild type. Furthermore, it seems that this expression is dependent on Dshi_1135. No transcription of the PGC was observed in the Dshi_1135::Tn mutant strain, independent on the light quality (Heyber, 2021). Therefore, the Dshi_1135 gene product might play a role in light-dependent gene regulation of the PGC in *D. shibae*.

1.5 Signal Perception and Photoreceptors in Prokaryotes

All organisms are constantly exposed to everchanging environmental conditions and the resulting various stimuli. Accordingly, many systems and mechanisms have evolved throughout different species to adequately sense, discriminate and respond to these signals and to quickly adapt to altered conditions. As mentioned above one important environmental signal is light. The effect of light on organisms, especially of blue light

on plants, has been known for more than 150 years, but the molecular basis for it has long been unknown. In the mid 1990's the first blue light sensing proteins, called photoreceptors, were identified in *Arabidopsis thaliana* (Ahmad & Cashmore, 1993; Huala *et al.,* 1997). Surprisingly, shortly after such photoreceptors were also found in non-photosynthetic bacteria (Davis *et al.,* 1999; Losi *et al.,* 2002; Losi & Gärtner, 2017). For a long time, it was assumed that light sensing and the ability to respond to the stimulus was exclusive to phototrophs and that other species are insensitive to it. This discovery revealed an unknown role of light in regulating bacterial physiology (Purcell & Crosson, 2008; Gomelsky & Hoff, 2011). With increasing high-throughput sequencing of bacterial genomes, also the number of potential photoreceptors raised and they were identified across a broad range of different taxa (Purcell & Crosson, 2008; Losi & Gärtner, 2008). This has created a kind of gold-rush atmosphere among scientists to study photoreceptors and their role in light-dependent regulation of physiological processes in bacteria.

Photoreceptors are protein domains that bind specific cofactors or chromophores that facilitate the absorption of light in or near the visible spectrum and thus mediate the light sensitivity of the protein (Purcell & Crosson, 2008). Bacterial photoreceptor domains are often part of regulatory systems and are either covalently or non-covalently connected to diverse output domains. One of the most common output domains are HKs (Gomelsky & Hoff, 2011). In bacteria HKs are often part of two-component systems with their cognate response regulator (RR) and catalyze a three-step reaction. First, upon stimulation, ATP gets hydrolyzed to ADP and a conserved histidine residue within the kinase domain gets autophosphorylated, followed by the phosphoryl group transfer to a conserved aspartate residue of the RRs receiver domain. This phosphor-transfer reaction leads to the activation of the RR effector domain, which then undergoes a structural change and is thus able to perform various functions (Jacob-Dubuisson *et al.,* 2018). About 70 % of all RRs are classified as DNA-binding transcriptional regulators. The rest is defined as RNA-or protein binding or enzymatically active RRs (Zschiedrich *et al.,* 2016).

To date, six photoreceptor families are known that exhibit high diversity in terms of spectral, structural, and biophysical properties: rhodopsins using a retinal chromophore, (bacterio)phytochromes using a tetrapyrrole chromophore, photoactive yellow protein (PYP) using *p*-coumaric acid as chromophore, light-oxygen-voltage (LOV) proteins

using a flavin mononucleotide (FMN) chromophore, BLUF proteins using a FAD chromophore and cryptochromes also using a FAD chromophore (Gomelsky & Hoff, 2011; Kottke *et al.,* 2018). The function(s) of most identified bacterial photoreceptors are unclear. One explanation that is discussed is that light provides crucial information about the environmental position of the bacterium and therefore promotes lifestyle decisions, like the switch between single cell or multicellular state, attachment and deattachment to surfaces or the switch between an environmental and pathogenic lifestyle (Gomelsky & Hoff, 2011; Kraiselburd *et al.,* 2017). YtvA of the soil bacterium *Bacillus subtilis* was the first discovered blue light-dependent LOV domain protein in bacteria and is to date one of the most extensively studied photoreceptors (Losi *et al.,* 2002). It is part of the *B. subtilis* stressosome, a kind of signal collection point that converts extracellular stimuli into an intracellular response and is therefore an important key player in stress response (Marles-Wright & Lewis, 2008; Jurk *et al.,* 2013). Stress control in *B. subtilis* is mediated by the alternative sigma factor σ^B, which on the other hand is regulated in a blue light-dependent manner by YtvA (Hecker & Völker, 2001; Gaidenko *et al.,* 2006). Blue light is known for its ability to cause ROS generation in bacterial cells, resulting potentially in severe cell damage. Activation of the σ^B-regulon by YtvA upon blue light illumination results in the expression of gene products that confer resistance towards oxidative damage of cell components. Consequently, the link between light detection and stress response in *B. subtilis* plays an important role in survival in a soil environment (Gaidenko *et al.,* 2006).

Numerous other bacterial photoreceptors with diverse physiological functions were studied in the last decade. Especially photoreceptors sensitive to the blue region of the visible light spectrum gained interest, as they show most diversity (Kraiselburd *et al.,* 2017; Losi & Gärtner, 2012).

1.5.1 Light-Oxygen-Voltage Domains

The in the high-throughput screening identified gene locus Dshi_1135 possesses a potential N-terminal LOV domain and is assumed to be involved in the light-dependent regulation of photosynthesis genes in *D. shibae*. The first LOV domain was identified in *A. thaliana* as part of the blue light receptor phototropin 1 (Phot1), showing a crucial role in phototropism (Christie *et al.,* 1998; Christie *et al.,* 1999). After this breakthrough discovery in environmental photobiology, many other LOV domain containing proteins were found in all three domains of life, but only a small fraction has been investigated

regarding functionality. Especially *in vivo* studies are missing (Losi & Gärtner, 2008; Losi *et al.,* 2014). Evolution of bacterial LOV domains is suggested to be quite complex. An event of multiple HGT events across distant phyla or co-evolution of plants and bacteria is hypothesized. Moreover, it is unclear whether there is a general concept in the mode of action of LOV domains or photoreceptors in general, or whether it is specific to each organism (Losi, 2004; Losi *et al.,* 2015).

LOV proteins share a common domain organization, comparable to other signaling proteins and are highly modular. They consist of an N-terminal sensor domain (LOV domain) fused to a diverse set of C-terminal effector domains, including HKs, second messenger regulators, phosphatases or DNA-binding motifs. LOV HKs are the most common combination (~50 %) found in bacteria and are often involved in blue light-activated gene regulation in combination with their cognate RR (Losi & Gärtner, 2008). For example, the LOV HK LovK of the freshwater bacterium *Caulobacter cresentus* with its cognate RR LovR is part of a two-component system. Blue light activates the LOV domain of LovK, causing autophosphorylation of the effector HK and subsequent activation of LovR by phosphotransfer. The blue light-activated LovK/LovR system was found to enhance the cell-cell and cell-surface attachment of the bacterium (Purcell *et al.,* 2007). *C. cresentus* is capable of living in various depth of the water column and most likely, the cells use light as an environmental signal for the determination of its position in the water. Of all the regions of the visible light spectrum, blue light penetrates water the deepest. Surface waters are often nutrient-poor, whereas the deeper benthic sediments are nutrient-rich. It is therefore assumed, that a blue light signal "guides" *C. cresentus* to a better nutrient supply and provides a growth advantage over other species (Purcell *et al.,* 2007).

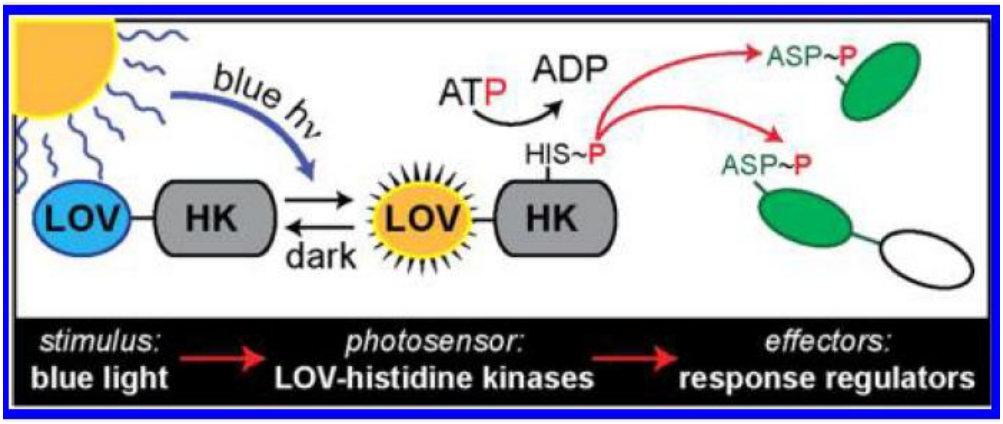

Figure 7: Overview of a blue light activated two-component system
In this two-component pathway the N-terminal LOV domain senses the blue light stimulus, thereupon the C-terminal HK domain gets activated and binds ATP within the catalytic and ATPase domain. Here ATP is hydrolyzed to ADP and the resulting phosphoryl moiety autophosphorylates a conserved histidine residue in the dimerization/ histidine phosphotransfer like domain. The phosphoryl group is then transferred to a conserved aspartate residue in the receiver domain of the cognate RR, which triggers diverse downstream responses (Correa *et al.,* 2013).

Recently also standalone LOV domains without a C-terminal effector domain have been identified in bacterial genomes and where termed short-LOV/ sLOV proteins (Losi & Gärtner, 2008; Krauss *et al.,* 2009; Fraikin *et al.,* 2013; Losi & Gärtner, 2017; Losi, 2013). Although, many LOV protein variants have been identified in 10-12 % of sequenced bacterial genomes since their discovery, little is known about their exact function (Losi & Gärtner, 2012).

Structurally the LOV core domain shows a typical α/β PAS domain fold that consists of about 100 amino acids arranged in five chains of antiparallel β-sheets and four α-helical elements (Crosson & Moffat, 2001; Crosson & Moffat, 2002; Möglich *et al.,* 2009). Embedded within the PAS fold is a single FMN molecule, that is either covalently or non-covalently bound to the protein core, depending on the state of illumination (Sean Crosson, 2005). The FMN molecule serves as a chromophore and facilitates the blue light sensitivity of the protein. Flavins are able of undergoing oxidation-reduction reactions and can easily switch between oxidation states, thus promoting high reactivity to the LOV domain/ protein. In the ground state, also called dark state, the fully oxidized FMN molecule is bound non-covalently to the LOV domain and is held in place by polar interactions and hydrogen bonds (Sean Crosson, 2005). Upon blue light irradiation a covalent bond is formed between a conserved cysteine residue in the LOV domain and the C4a atom within the FMN isoalloxazine ring. At the same time the FMN N5 atom gets protonated. Both events lead to the conversion from the ground state into the signaling state (Crosson & Moffat, 2002; Conrad *et al.,* 2014). The cysteine

residue is located on one of the α-helices in the central core and is part of a highly conserved motif of the LOV domain family (Christie *et al.,* 1999; Herrou & Crosson, 2011). Mutational studies showed that it is not essential for FMN binding, but for a reversible photochemical reaction (Salomon *et al.,* 2000). The conversion of the LOV domain from the ground state to the signaling state is not a one-way reaction, but occurs as a blue light driven photocycle. During the photocycle reaction a series of transient intermediates are formed that return back into the ground state in the dark (Figure 8) (Swartz & Bogomolni, 2005).

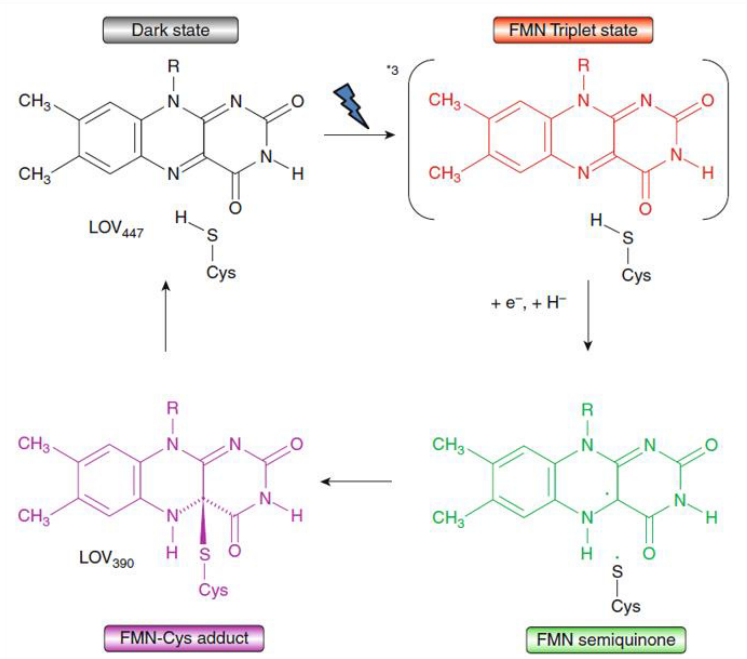

Figure 8: Photocycle reaction of LOV domains
Blue light illumination of the dark state FMN LOV_{447} (gray) leads to FMN triplet state (red) formation. *Via* the fast decay of the FMN triple state and a $FMNH^{\bullet}$-$H_2CS^{\bullet}$ radical pair (green) a covalent bond between the FMN C4a atom and the thiol group of a conserved cysteine residue of the LOV domain is formed, resulting in der LOV_{390} intermediate (purple). Simultaneously, the FMN N5 atom gets protonated. On a second to hour timescale LOV_{390} decays back into the dark state (Losi, 2013).

Blue light excitation of the LOV domain drastically changes the redox potential of FMN, making it a much stronger oxidant compared to unexcited FMN and converts it into the FMN triplet state (Losi, 2007). This intermediate absorbs maximally at 660 nm (LOV_{660}) and decays back within µs into a second metastable LOV_{390} intermediate, called photo-adduct (Swartz *et al.,* 2001). Most likely this reaction is preceded by the formation of transient and thus hard to detect formation of a $FMNH^{\bullet}$-$H_2CS^{\bullet}$ radical pair (Bauer *et al.,* 2011; Kutta *et al.,* 2015; Losi & Gärtner, 2017). It is assumed that the

radical recombination is coupled to the earlier mentioned protonation of the FMN N5 atom and that during this step the covalent bond between FMN chromophore and LOV domain is formed (Losi & Gärtner, 2017). The protonation of the FMN N5 is possibly involved in signal propagation in the LOV domain, as this step might trigger the flipping/ rotation of a glutamine side chain. This event causes a series of structural changes within the LOV domain, finally resulting in the activation of the C-terminal effector domain. In many cases the activated effector domains tend to form dimeric structures, which implies that the dimeric form is the functional one (Losi & Gärtner, 2017).

It is controversially discussed whether covalent bond formation between the LOV domain and the FMN chromophore is the key step for output domain activation, or if the rearrangement of the FMN hydrogen bond network as a result of the glutamine side chain rotation is the cause (Kottke *et al.,* 2018). Studies using a fungal mutant strain, lacking the conserved cysteine residue for photo adduct formation, showed that light induced protonation of the FMN N5 and the resulting hydrogen bond formation with the glutamine side chain is sufficient to induce downstream signaling (Yee *et al.,* 2015). Consequently, proton and electron transfer, changes in hydrogen bond formation and rotation of the glutamine side chain are essential for signal propagation in LOV domains.

The photocycle is completed when the LOV_{390} intermediate decays back into the ground state with breakage of the covalent bond and the FMN N5 deprotonation (Conrad *et al.,* 2014). Depending on the LOV domain protein the duration of the last step is quite variable, ranging from seconds to hours or even days. In rare cases it was observed that activation of the LOV domain can be irreversible (Swartz *et al.,* 2001; Swartz & Bogomolni, 2005; Herrou & Crosson, 2011).

Even though extensive research has been performed on photophysics and photochemistry of LOV domain proteins, the exact mechanism of activation and signal transduction to the downstream effector domain remains poorly understood and elusive. In particular the experimental set-up is limiting and hard to realize due to the light sensitivity and partially ultra-fast kinetics and dynamics of the proteins. Additionally, it cannot be ruled out that there is no general activation mechanism of LOV domain proteins. Despite these challenges, LOV domains are increasingly coming into focus, as they can be used as photoswitches in a broad field of applications like optogenetics,

fluorescence microscopy or regulation of cellular events (Losi & Gärtner, 2017).

In the annotated *D. shibae* DFL12^T genome the three putative LOV photoreceptor encoding genes Dshi_2006, Dshi_1135 and Dshi_1893, were identified by sequence similarity analyses. The respective amino acid sequences showed the necessary features for FMN binding and photocycling in all three proteins (Endres *et al.,* 2015).

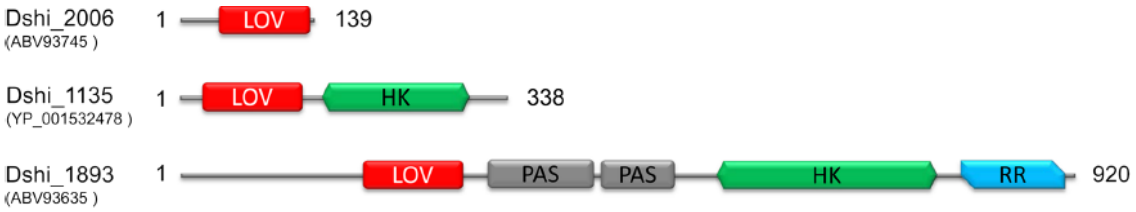

Figure 9: Domain structure of the three potential LOV proteins of *D. shibae*
Three putative LOV proteins were identified by sequence similarity analyses of the annotated *D. shibae* DFL12^T genome. The respective amino acid sequence of Dshi_2006 shows a single LOV domain without a fused effector domain. The amino acid sequence of Dshi_1135 shows an N-terminal LOV domain fused to a C-terminal HK domain. The predicted domain structure of Dshi_1893 consists of an N-terminal LOV domain, followed by two PAS domains, a HK effector domain directly fused to a RR. (Endres *et al.,* 2015)

Dshi_2006 was already investigated regarding its function and structure and was termed DsLOV (Endres *et al.,* 2015). It is a LOV protein with one of the fastest known recovery rates to date at 9.6 seconds. Mutation of the *dslov* gene resulted in a complete loss of pigmentation. Growth experiments of the *D. shibae* DFL12^T and the Δ*dslov* strain under different light conditions revealed a unique role of DsLOV in controlling the biosynthesis of photopigments in *D. shibae* in the absence of blue light. Therefore, DsLOV most likely presents the first LOV photoreceptor that is promoting gene activation in the dark and not in the presence of blue light (Endres *et al.,* 2015). However, the respective Dshi_2006::Tn transposon mutant strain did not appear in the high-throughput screening for identification of potential regulators involved in Bchl *a* biosynthesis. Also, the Dshi_1893::Tn transposon mutant strain was not found in the screening and therefore and it is not clear which role it plays in gene regulation in *D. shibae*. The function of Dshi_1135 is also unclear so far. However, the LOV HK domain structure and the lack of pigmentation of the respective transposon mutant strain suggests a function in the blue light-dependent regulation of the photosynthesis genes in *D. shibae*.

2 Aim of this Study

The marine bacterium *D. shibae* is capable to perform aerobic anoxygenic photosynthesis. Almost all genes for the required components of the photosynthetic apparatus are encoded in the PGC. Under dark conditions expression of the cluster is induced, whereas it is repressed in the presence of light. To date, only little is known about the involved regulators and mechanisms of light-dependent regulation. A previous high-throughput screening of a *D. shibae* transposon mutant library identified the PAS photoreceptor domain containing protein Dshi_1135 as a potential regulator of photosynthesis genes.

Thus, the first objective of this work was the biochemical characterization of the Dshi_1135 protein. For this purpose, a suitable protocol for the heterologous production and purification of the protein had to be established. UV/Vis spectroscopic characterization of purified protein should be used to determine whether Dshi_1135 binds an FMN cofactor typical of LOV domain proteins and is able to perform a blue light-activated photocycle. Amino acid residues necessary for photocycling should be defined by bioinformatic analyses. Their function should be investigated by site-directed mutagenesis of the corresponding Dshi_1135 gene and biochemical characterization of the recombinant mutant proteins. A potential blue light-induced kinase activity of Dshi_1135 was aimed to be proven by autophosphorylation experiments. Furthermore, strategies for the identification of potential response regulators of Dshi_1135 should be tested.

The second objective of this work was the definition of the roles of the regulators Dshi_1135, PpsR and PpaA in light-dependent regulation of photosynthesis genes. For this purpose, a *bchF-lacZ* reporter gene fusion should be generated and promoter activity analysed *via* β-galactosidase activity assays in the *D. shibae* DFL12^T wild type strain and the Dshi_1135::Tn, *ppsR*::Tn and *ppaA*::Tn mutant strains under different light conditions. Furthermore, it was intended to identify and functionally verify potential PpsR binding sites within the *bchF* promoter sequence, by performing β-galactosidase activity assays with mutated *bchF-lacZ* reporter gene fusions.

Overall, this work should contribute to the understanding of the gene regulatory networks in a marine model bacterium.

3 Materials and Methods

3.1 Instruments, Materials and Chemicals

3.1.1 Instruments

Instruments that were used in this study are listed in Table 1.

Table 1: Instruments

Instruments	Model	Manufacturer
Agarose gel documentation	DeVision G system	Science Tec
Agarose gel electrophoresis	Agagel mini	Biometra
	EnduroTM 7.10 Horizontal Gel Box	Labnet International Inc.
Autoclave	LVSA 50/70	Zirbus
	FVA/A1	Fedegari AG
Blotting equipment	Trans-Blot® SD	Bio-Rad
	Trans-Blot® Turbo™	
Blue light transilluminator	Flu-O-Blu	Biozym Scientific
Centrifuges	5424R	Eppendorf
	Avanti® J-26XP	Beckman Coulter
	Avanti® J-E	
	Heraeus Megafuge 8R	Thermo Fisher Scientific
	Megafuge 1.0R	Heraeus
	MiniSpin® plus	Eppendorf
	Optima® L-90K Ultracentrifuge	Beckman Coulter
FPLC	Äkta™ Purifier	GE Healthcare
French Press®	French® Pressure Cell Press	Polytec
French Press® cell	French® Pressure Cell	Thermo Electron Corporation
Gel scanner	BIO-5000 Plus VIS gel scanner	Serva
Incubator	Multitron	Infors HT
LED	IP65 50924914	Barthelme
	IP65 50924915	
	LED growth light, LL-GL001 (blue)	Albrillo
	DF-7012-12 (red)	Conrad

Instruments	Model	Manufacturer
pH determination	GC 842	Schott
Photometer	Ultrospec 2000	Amersham Pharmacia
Power supplies	ENDURO™ Power Supplies 250V	Labnet International Inc.
	Consort EV243	Thermo Fisher Scientific
Real-time PCR	C1000™ Thermal Cycler with	Bio-Rad
	CFX96™ real-time system	
Roller mixer	RM5	Ingenieurbüro CAT, M. Zipperer GmbH
Scales	BP 61S	Sartorius
	Entris 2241-1S	
	Entris 3202I-1S	
SDS-PAGE system	Mini Protean III	Bio-Rad
Shaker	Orbitron	Infors HT
	Multitron	
	TR-150	
Spectralphotometer	NanoDrop™ ND 1000	PEQLAB
Thermocycler	T3 Thermocycler	Biometra
Thermomixer	ThermoMixer C	Eppendorf
UV/Vis spectrophotometer	V-650	Jasco
Vortex	Vortex-Genie 2	Scientific Industries Inc.
Water purification system	Milli-Q® IQ 7000	Merck
	Milli-Q® Synthesis A10	Millipore

3.1.2 Chemicals, Enzymes and Materials

If not indicated otherwise, all chemicals were purchased from the following manufacturers: Merck (Darmstadt, Germany), Sigma-Aldrich (Steinheim, Germany) or Carl Roth (Karlsruhe, Germany).

Table 2: Chemicals, enzymes and materials

Material	Product	Source
Antibodies	Anti-GST-Alkaline Phosphatase Conjugate antibody	Sigma-Aldrich
	Strep-tag® II specific monoclonal antibody (StrepMAB-Classic)	iba
Blotting	transfer membrane ROTI®PVDF 0.45	Carl Roth
	blotting papers ROTILABO® thickness 0,35 mm	Carl-Roth
Chemicals	[γ-^{32}P] ATP	Hartmann Analytic

Material	Product	Source
	5-aminolevulinic acid	Carl Roth
	Albumin Fraction V (BSA)	Carl Roth
	Ampicillin	Carl Roth
	ATP	Sigma-Aldrich
	avidin	Merck, iba
	Bradford reagent	Sigma-Aldrich
	Chloramphenicol	Carl Roth
	dATP's	New England Biolabs
	D-desthiobiotin	Sigma-Aldrich
	dithiothreitol (DTT)	GERBU Biotechnik
	DMSO	Carl Roth
	dNTP's	New England Biolabs
	dTTP's	New England Biolabs
	FMN	Sigma-Aldrich
	Gentamicin	Carl Roth
	Instant Blue	Expedeon
	Isopropyl-β-D-galactopyranoside (IPTG)	GERBU Biotechnik
	Kanamycin	Carl Roth
	L-glutathione (reduced)	Carl Roth
	L-rhamnose	Carl Roth
	2-nitrophenyl-β-D-galactopyranosid (ONPG)	AppliChem, Carl Roth
	Phos-tag™ Acrylamide	FUJIFILM Wako Chemicals Europe
	Sypro®Orange	Life Technologies
	5-brom-4-chlor-3-indoxyl-β-D-galactosid (X-Gal)	Carl Roth
Enzymes	Benzonase®	Merck
	Dnase I	AppliChem
	lysozyme	Fluka
	Phusion High-Fidelity DNA Polymerase	New England Biolabs
	PreScission™ Protease	GE Healthcare
	Q5® High-Fidelity DNA Polymerase	New England Biolabs
	rAPid alkaline phosphatase	Roche
	restriction endonucleases	New England Biolabs
	Rnase I	AppliChem
	T4 DNA Ligase	New England Biolabs

Material	Product	Source
	T4 DNA Polymerase	New England Biolabs
Kits	Gel Filtration Markers Kit for Protein Molecular Weights 12'000-200'000 Da	Sigma-Aldrich
	QIAprep Spin Miniprep Kit	QIAGEN
	QIAquick Gel Extraction Kit	
	QIAquick PCR Purification Kit	
	Q5 Site-Directed Mutagenesis Kit	New England Biolabs
Markers	PageRuler™ Plus Prestained Protein Ladder	Thermo Fisher Scientific
	Quick-Load® Purple 1 kb DNA Ladder	New England Biolabs
	Precision Plus Protein™ Dual Color Standards	Bio-Rad
Protein purification, concentration and reconstitution	Amicon® Ultra 0.5 ml, MWCO: 30 kDa	Merck
	NAP™-25	GE Healthcare
	Poly-Prep® Chromatography Column (0.8 x 4 cm)	Bio-Rad
	Protino™ Glutathion-Agarose 4B	Macherey-Nagel
	Strep-Tactin® Superflow® high capacity	iba
	Superdex™ 200 Increase 5/150 GL	GE Healthcare

3.2 Bacterial Strains, Plasmids and Oligonucleotides

3.2.1 Bacterial Strains

Bacterial strains that were used in this work are listed in Table 3.

Table 3: Bacterial strains

Strain	Genotype	Reference
Escherichia coli		
DH10B	F⁻ *mcrA* Δ(*mrr-hsd*RMS-*mcr*BC) Φ80*lac*ZΔM15 Δ*lac*X74 *rec*A1 *end*A1 *ara*D139 Δ(*ara leu*) 7697 *gal*U *gal*K *rps*L *nup*G λ⁻	Invitrogen, (Carlsbad, CA, USA)
BL21(DE3)	*fhuA2 [lon] ompT gal (λ DE3) [dcm] Δhsds* *λ DE3 = λ sBamHIo ΔEcoRI-B int::(lacI::PlacUV5::T7 gene1) i21 Δnin5*	New England Biolabs (Ipswich, MA, USA)
BL21-CodonPlus(DE3)-RIL	*E. coli B F⁻ ompT hsdS(r_B^- m_B^-) dcm⁺ Tet^r gal λ(DE3) endA Hte [argU ileY leuW Cam^r]*	Stratagene, Santa Clara, CA (USA)

Strain	Genotype	Reference
Lemo21(DE3)	*fhuA2 [lon] ompT gal (λ DE3) [dcm] ΔhsdS/ pLemo*(Cam^R) *λ DE3 = λ sBamHIo ΔEcoRI-B int::(lacI::PlacUV5::T7 gene1) i21 Δnin5* pLemo = pACYC184-*PrhaBAD-lysY*	New England Biolabs (Ipswich, MA, USA)
Tuner™(DE3)	F^- *ompT hsdS*$_B$ (r_B^- m_B^-) *gal dcm lacY1*(DE3)	Novagen, Darmstadt (Germany)
ST18	*E. coli* S17-1*ΔhemA thi pro hsdR*-M-chromosomal integrated [*RP4-2 Tc::Mu:Kmr::Tn7, Tra+ Trir Strr*]	(Thoma & Schobert, 2009)
Vibrio natriegens		
Vmax™ Express	Δ*dns*, IPTG-inducible T7 RNAP, Kan^R (Cat.No. CL1200)	BioCat (Heidelberg, Germany)
Dinoroseobacter shibae		
$DFL12^T$	wild type, isolated from the dinoflagellate *Prorocentrum lima*, type strain, $DSM16493^T$	(Biebl *et al.,* 2005)
DSTn12510	Dshi_1135::Tn, Gm^r	(Ebert *et al.,* 2013)
DSTn3068	Dshi_1011::Tn (*irr*), Gm^r	(Ebert *et al.,* 2013)
DSTn4031	Dshi_3532::Tn, (*ppaA*), Gm^r	(Ebert *et al.,* 2013)
DSTn4634	Dshi_3531::Tn, (*ppsR*), Gm^r	(Ebert *et al.,* 2013)
DS180	$DFL12^T$; pBBR1LIC_*ppaA-lacZ*, Cml^r	This work
DS181	$DFL12^T$; pBBR1LIC_*bchF-lacZ*, Cml^r	This work
DS182	$DFL12^T$; pBBR1LIC_*hemE-lacZ*, Cml^r	This work
DS183	Dshi_1011::Tn (*irr*), Gm^r; pBBR1LIC_*hemE-lacZ*, Cml^r	This work
DS184	Dshi_3531::Tn, (*ppsR*), Gm^r; pBBR1LIC_*hemE-lacZ*, Cml^r	This work
DS185	Dshi_3532::Tn, (*ppaA*), Gm^r; pBBR1LIC_*hemE-lacZ*, Cml^r	This work
DS186	Dshi_1135::Tn, Gm^r; pBBR1LIC_*hemE-lacZ*, Cml^r	This work
DS187	Dshi_3532::Tn, (*ppaA*), Gm^r; pBBR1LIC_*bchF-lacZ*, Cml^r	This work
DS188	Dshi_1135::Tn, Gm^r; pBBR1LIC_*bchF-lacZ*, Cml^r	This work
DS189	Dshi_3531::Tn, (*ppsR*), Gm^r; pBBR1LIC_*bchF-lacZ*, Cml^r	This work
DS190	$DFL12^T$; pBBR1LIC_*bchF*mut1-*lacZ*, mutations in potential PpsR binding sites at positions -79/-77 from TGT to CCA and -30/-28 from ACA to TGG, Cml^r	Bachelor thesis Saskia Pucelik
DS191	$DFL12^T$; pBBR1LIC_*bchF*100bpwt-*lacZ*, Cml^r	Bachelor thesis Saskia Pucelik

Strain	Genotype	Reference
DS192	DFL12^T; pBBR1LIC_*bchF*100bpmut1-*lacZ*, mutations in potential PpsR binding sites at positions -79/-77 from TGT to CCA and -30/-28 from ACA to TGG, Cm^r	Bachelor thesis Saskia Pucelik
DS193	Dshi_1135::Tn, Gm^r; pBBR1LIC_*bchF*mut1-*lacZ*, mutations in potential PpsR binding sites at positions -79/-77 from TGT to CCA and -30/-28 from ACA to TGG, Cm^r	Bachelor thesis Saskia Pucelik
DS194	Dshi_1135::Tn, Gm^r; pBBR1LIC_*bchF*100bpwt-*lacZ*, Cm^r	Bachelor thesis Saskia Pucelik
DS195	Dshi_1135::Tn, Gm^r; pBBR1LIC_bchF100bpmut1-*lacZ*, mutations in potential PpsR binding sites at positions -79/-77 from TGT to CCA and -30/-28 from ACA to TGG, Cm^r	Bachelor thesis Saskia Pucelik
DS204	Dshi_1135::Tn, Gm^r; pBBR1LIC_*ppaA-lacZ*, Cm^r	This work
DS205	Dshi_3531::Tn, (*ppsR*), Gm^r; pBBR1LIC_*ppaA-lacZ*, Cm^r	This work

3.2.2 Plasmids

All plasmids used in this work are listed in Table 4.

Table 4: Plasmids

Plasmid	Description	Reference
pACYCLIC-*lacZ*	vector for LIC, *lacZ* gene, *ori*$_{p15A}$, Cm^r	Anja Hartmann, AG Härtig, TU Braunschweig
pACYCLIC_*bchF-lacZ*	pACYLIC-*lacZ* vector encoding the *bchF* promoter sequence from *D. shibae* fused to a C-terminal *lacZ* reporter gene, inserted *via* LIC, Cm^r	Bachelor thesis Miriam Niewöhner
pBBR1MCSLIC-*lacZ*	vector for diparental mating of *E. coli* and *D. shibae*, LIC site, *lacZ* gene downstream of LIC site, Cm^r	(Kovach *et al.,* 1995)
pBBR1LIC_*bchF-lacZ*	pBBR1MCSLIC-*lacZ* vector encoding sequences from -289 to +41 with respect to the translational start of *bchF* fused to *lacZ*, Cm^r	This work

Plasmid	Description	Reference
pBBR1LIC_*bchF*mut1-*lacZ*	pBBR1MCSLIC-*lacZ* vector encoding sequences from -289 to +41 with respect to the translational start of *bchF* fused to *lacZ*, mutations in potential PpsR binding sites at positions -79/-77 from TGT to CCA and -30/-28 from ACA to TGG, Cml^r	Bachelor thesis Saskia Pucelik
pBBR1LIC_*bchF*100bpwt-*lacZ*	pBBR1MCSLIC-*lacZ* vector encoding sequences from -100 to +41 with respect to the translational start of *bchF* fused to *lacZ*, Cml^r	Bachelor thesis Saskia Pucelik
pBBR1LIC_*bchF*100bpmut1-*lacZ*	pBBR1MCSLIC-*lacZ* vector encoding sequences from -100 to +41 with respect to the translational start of *bchF* fused to *lacZ*, mutations in potential PpsR binding sites at positions -79/-77 from TGT to CCA and -30/-28 from ACA to TGG, Cml^r	Bachelor thesis Saskia Pucelik
pBBR1LIC_*hemE-lacZ*	pBBR1MCSLIC-*lacZ* vector encoding sequences from -144 to +25 with respect to the translational start of *hemE* fused to *lacZ*, Cml^r	This work
pBBR1LIC_*ppaA-lacZ*	pBBR1MCSLIC-*lacZ* vector encoding sequences from -298 to +32 with respect to the translational start of *ppaA* fused to *lacZ*, Cml^r	This work
pET22b(+)Strep	vector for recombinant protein production in *E. coli*, pET22b(+) derivative providing a T7-promoter, an N-terminal *pelB* secretion signal sequence and a C-terminal Strep-tag II cloned into *Hind*III/*Xho*I sites, Amp^r	(Arendt *et al.,* 2013)
pET22b(+)Strep_Dshi1135	pET22b(+)Strep vector carrying the native Dshi_1135 sequence from *D. shibae* fused to a C-terminal Strep-tag II, cloned into in *Nde*I and *Hind*III restriction sites, Amp^r	This work

Plasmid	Description	Reference
pET52b(+)	vector for cloning and recombinant protein production in *E. coli*, provides a T7-promoter and a N-terminal Strep-tag II followed by the sequence or the PreScission™ Protease cleavage site, ori_{pBR322}, *lacI*, Amp^r	Novagen, Darmstadt (Germany)
pET52b(+)_Dshi1135Full	pET52b(+) derivative carrying the native sequence of *D. shibae* Dshi_1135 fused to an N-terminal Strep-tag II, cloned into *Sma*I and *Sac*I restriction sites, specific PreScission™ Protease cleavage site, Amp^r	AG Härtig, unpublished
pET52b(+)_Dshi1135LOV	pET52b(+) derivative carrying the amino acids 1-149 of *D. shibae* Dshi_1135 fused to an N-terminal Strep-tag II, cloned into *Sma*I and *Sac*I restriction sites, specific PreScission™ Protease cleavage site, Amp^r	AG Härtig, unpublished
pET52b(+)_Dshi1406	pET52b(+) derivative carrying the native sequence of *D. shibae* Dshi_1406 fused to an N-terminal Strep-tag II, cloned into *Xma*I and *Sac*I restriction sites, specific PreScission™ Protease cleavage site, Amp^r	This work
pET52b(+)_Dshi1538	pET52b(+) derivative carrying the native sequence of *D. shibae* Dshi_1538 fused to an N-terminal Strep-tag II, cloned into *Bam*HI and *Sac*I restriction sites, specific PreScission™ Protease cleavage site, Amp^r	This work
pET52b(+)_Dshi3837	pET52b(+) derivative carrying the native sequence of *D. shibae* Dshi_3837 fused to an N-terminal Strep-tag II, cloned into *Xma*I and *Not*I restriction sites, specific PreScission™ Protease cleavage site, Amp^r	This work
pET52bTrx	derivative of pET52b(+) carrying the sequence of a TRX-tag upstream of the Strep-tag II, ori_{pBR322}, *lacI*, Amp^r	(Frädrich *et al.,* 2012)

Plasmid	Description	Reference
pET52b(+)Trx_Dshi1135Full	pET52bTrx vector carrying the native *D. shibae* Dshi_1135 gene sequence fused to an N-terminal TRX-tag and Strep-tag II, cloned into *SmaI* and *SacI* restriction sites, specific PreScission™ Protease cleavage site, Amp^r	This work
pET52b(+)Trx_Dshi1135LOV	pET52(+)Trx vector carrying the amino acids 1-149 of *D. shibae* Dshi_1135 fused to an N-terminal TRX-tag and Strep-tag II, cloned into *SmaI* and *SacI* restriction sites, specific PreScission™ Protease cleavage site, Amp^r	This work
pET52b(+)Trx_Dshi1135C61A	derivative of pET52b(+)Trx_Dshi1135Full, amino acid cysteine 61 of Dshi_1135 was changed to alanine, Amp^r	This work
pET52b(+)Trx_Dshi1135C61S	derivative of pET52b(+)Trx_Dshi1135Full, amino acid cysteine 61 of Dshi_1135 was changed to serine, Amp^r	This work
pET52b(+)Trx_Dshi1135H258A	derivative of pET52b(+)Trx_Dshi1135Full, amino acid histidine 258 of Dshi_1135 was changed to alanine, Amp^r	This work
pET52b(+)Trx_Dshi1135H258N	derivative of pET52b(+)Trx_Dshi1135Full, amino acid histidine 258 of Dshi_1135 was changed to asparagine, Amp^r	This work
pET52b(+)Trx_Dshi1135I121A	derivative of pET52b(+)Trx_Dshi1135Full, amino acid isoleucine 121 of Dshi_1135 was changed to alanine, Amp^r	This work
pETDuet1	vector for cloning and coexpression of multiple proteins in *E. coli*, provides two MCS each of which is preceded by a T7 promoter, ori_{pBR322}, *lacI*, Amp^r	Novagen, Darmstadt (Germany)
pETDuet1_Dshi1135	pETDuet1 vector carrying the native *D. shibae* Dshi_1135 sequence in *Xba*I and *Sac*I restriction sites of MCS-1, Amp^r	Bachelor thesis Miriam Niewöhner

Plasmid	Description	Reference
pETDuet1_Dshi1135-Dshi_1406	pETDuet1 vector carrying the native *D. shibae* Dshi_1135 sequence in *Xba*I and *Sac*I restriction sites of MCS-1 and the native sequence of *D. shibae* Dshi_1406 in *Nde*I and *Bgl*II restriction sites of MCS-2, Amp^r	Bachelor thesis Miriam Niewöhner
pETDuet1_Dshi1135-Dshi_1538	pETDuet1 vector carrying the native *D. shibae* Dshi_1135 sequence in *Xba*I and *Sac*I restriction sites of MCS-1 and the native sequence of *D. shibae* Dshi_1538 in *Nde*I and *Bgl*II restriction sites of MCS-2, Amp^r	Bachelor thesis Miriam Niewöhner
pETDuet1_Dshi1135-Dshi_3837	pETDuet1 vector carrying the native *D. shibae* Dshi_1135 sequence in *Xba*I and *Sac*I restriction sites of MCS-1 and the native sequence of *D. shibae* Dshi_3837 in *Nde*I and *Bgl*II restriction sites of MCS-2, Amp^r	Bachelor thesis Miriam Niewöhner
pETDuet1_Dshi_1406	pETDuet1 vector carrying the native *D. shibae* Dshi_1406 sequence in *Nde*I and *Bgl*II restriction sites of MCS-2, Amp^r	Bachelor thesis Miriam Niewöhner
pETDuet1_Dshi_1538	pETDuet1 vector carrying the native *D. shibae* Dshi_1538 sequence in *Nde*I and *Bgl*II restriction sites of MCS-2, Amp^r	Bachelor thesis Miriam Niewöhner
pETDuet1_Dshi_3837	pETDuet1 vector carrying the native *D. shibae* Dshi_3837 sequence in *Nde*I and *Bgl*II restriction sites of MCS-2, Amp^r	Bachelor thesis Miriam Niewöhner
pGEX-6P-1	vector for cloning and recombinant protein production, P_{tac}, ori_{pBR322}, N-terminal glutathione S-transferase (GST)-tag, PreScission™ Protease specific cleavage site, Amp^r	GE Healthcare, Chalfont St Giles (UK)
pGEX-6P-1_Dshi1135Full	pGEX-6P-1 vector containing the native *D. shibae* Dshi_1135 gene fused to the sequence for N-terminal GST-tag, cloned into *Eco*RI and *Bam*HI sites, specific PreScission™ Protease cleavage site, Amp^r	This work

Plasmid	Description	Reference
pGEX-6P-1_Dshi1135LOV	pGEX-6P-1 vector containing amino acids 1-149 of native *D. shibae* Dshi_1135 fused to the sequence for N-terminal GST-tag, cloned into *Eco*RI and *Bam*HI sites, specific PreScission™ Protease cleavage site, Amp^r	This work
pMK-RQ*bchF*mut1	Derivative of pMX cloning vector based on pUC vector series, encodes synthetic *D. shibae bchF* promoter gene sequence with mutations in potential PpsR binding sites, ori_{ColE1}, Kan^r	Thermo Fisher Scientific, Waltham, MA (USA)
pRhokS-2	vector for diparental mating of *E. coli* and *D. shibae*, provides a C-terminal Strep-tag II, P_{aphII}, Cml^r	(Katzke *et al.,* 2010)
pRhokS_Dshi1135	pRhokS vector encoding the native sequence of *D. shibae* Dshi_1135, inserted into *Sac*I and *Nde*I sites, complementation of *D. shibae* Dshi_1135::Tn mutant strain, Cml^r	This work
pRhokS_Dshi1135Strep	pRhokS vector encoding the native sequence of *D. shibae* Dshi_1135, inserted into *Sac*I and *Nde*I sites, C-terminal Strep-tag II, homologous production of Dshi_1135 protein, Cml^r	This work

3.2.3 Oligonucleotides

DNA oligonucleotides used for cloning and sequencing purposes in this study are listed in Table 5. Oligonucleotides for cloning were purchased from Invitrogen (Carlsbad, CA, USA). For DNA sequencing, standard primers provided by Eurofins Genomics (Ebersberg, Germany), were used.

Table 5: Oligonucleotides used for cloning and sequencing

Primer	Sequence (5'-3')
EH636	CCGCTCGAGTTTCCTTACGCGAAATACG
EH649	GGGATGAAGCCACGCACGCTAGGA
EH650	GCGAGCTCAGCCATCTGATTGCGGTC
EH651	GCGAGCTCTCACTGGATGCCGATGAAATA
EH677	CCGCGGGCTTTCCCAGCATGGGATCTTGCAGGTT
EH678	GTTCCTCCTTCCCACCAGTCCGACCCTGTTTTCT
EH679	GTTCCTCCTTCCCACCATGGGATCTTGCAGGTT
EH680	CCGCGGGCTTTCCCAGCAGTCCGACCCTGTTTTCT

Primer	Sequence (5'-3')
EH681	CCGCGGGCTTTCCCAGCTTTTCAAGGGTGAATCGG
EH682	GTTCCTCCTTCCCACCGGAGGAGTTTTTTTCTGTC
EH725	GGAAATTCCATATGAAGCCACGCACGCTAGGA
MIB1	GGGGGATCCATGAAGCCACGCACGCTAGGA
MIB2	GCGAATTCAGCCATCTGATTGCGGTC
MIB3	GCGAATTCTCACTGGATGCCGATG
MIB4	GCCCCGGGATGTCCCAGGTGACTGATACATCG
MIB5	GCGCGGCCGCTTACGCCTTCAACGTCTCGGTCGA
MIB6	GCGGATCCTGTGTCCGACCAACCCACC
MIB7	GCGAGCTCTCAGCCGAGCGCGTAGCC
MIB8	GCCCCGGGATGGCGAAAACCGTTCTG
MIB9	GCGAGCTCTCAGCCTCCCAGCTCCCG
MIB14	CGGCCGGAACGCGCGGTTCCTGCAAGGCAGC
MIB15	ATCGCCGCGGTGCGCGAA
MIB16	CGGCCGGAACAGCCGGTTCCTGC
MIB17	ATCGCCGCGGTGCGCGAA
MIB18	CGCATTCCAGGCGGCCTTTGTCGGG
MIB19	TTGGTAAGCACTTCCGAC
MIB20	CGCATTCCAGAACGCCTTTGTCG
MIB21	TTGGTAAGCACTTCCGAC
MIB22	TCACTATTTCGCGGGCATCCAGAAGGC
MIB23	CATTTGCCGTCGTCTGAT
MIB27	GGAATTCCATATGGCAAGCTGGAGCCACCCGC
MIB28	GGAAGATCTAGCGGAACTACCGCGTGGCAC
MIB29	CCGCTCGAGATTGCCCGCGGGCAC
MIB30	CCCAAGCTTATTGCCCGCGGGCACGTC
Duet Upstream	GATGCGTCCGGCGTAGAGG
M13-RP	CAGGAAACAGCTATGACC
pACYCDuetDown1	GATTATGCGGCCGTGTACAA
pACYCDuetUP2	TTGTACACGGCCGCATAATC
pET-RP	CTAGTTATTGCTCAGCGG
pGEX3	GGAGCTGCATGTGTCAGAG
pGEX5	CTGGCAAGCCACGTTTGG
T7	TAATACGACTCACTATAGGG

3.2.4 Synthetic Genes

Synthetic genes in this study were purchased as GeneArt® Strings™ DNA fragments or as cloned genes in pMK cloning vectors (Thermo Fisher Scientific, Waltham, MA, USA) and are listed in Table 6.

Table 6: Synthetic gene sequences

Name	Sequence (5'-3')
*bchF*mut1	CCGCGGGCTTTCCCAGCATGGGATCTTGCAGGTTGTC CGGGGTGGACATTTTTCCTGTGTCAGTATCGCGCACC GGACCACTATTGTCAAAGTTATTGGACACCAGCGCCC GGAAGGCGGCCACCTCGGCGTCCGGCGAGGATTCGG CGCGCATATTCTCTTTGTTTATTAGGTCTTTCATGGCC GAATCACCCGTGCTGTCTCTTCTCCAGTATTCCCCAGC ATTG**CCA**AAGTTTTAGTTGACACTTTCAACTGCTCATAT GTAAATTCGACAAA**TGG**GTCATTTACCGGAGGGGGAG TCGCCGGATGTCAACCGGTCTGAACACCCAAGAAAAC AGGGTCGGACTGGTGGGAAGGAGGAAC
*bchF*100bpwt	CCGCGGGCTTTCCCAGCCTCCAGTATTCCCCAGCATT GTGTAAGTTTTAGTTGACACTTTCAACTGCTCATATGTA AATTCGACAAAACAGTCATTTACCGGAGGGGGAGTCG CCGGATGTCAACCGGTCTGAACACCCAAGAAAACAGG GTCGGACTGGTGGGAAGGAGGAAC
*bchF*100bpmut1	CCGCGGGCTTTCCCAGCCTCCAGTATTCCCCAGCATT G**CCA**AAGTTTTAGTTGACACTTTCAACTGCTCATATGT AAATTCGACAAA**TGG**GTCATTTACCGGAGGGGGAGTC GCCGGATGTCAACCGGTCTGAACACCCAAGAAAACAG GGTCGGACTGGTGGGAAGGAGGAAC

LIC sequences are underlined and mutated areas are highlighted in bold font.

3.3 Sterilization, Growth Media and Media Additives

3.3.1 Sterilization

Media, solutions and items used in this study were vapor sterilized at 121 °C and 1 bar overpressure for 20 min. Temperature sensitive materials were sterilized by filtration (pore size 0.2 µm).

3.3.2 Growth Media

3.3.2.1 Lysogeny Broth

If not indicated otherwise, Lysogeny Broth (LB) (Sambrook & Russell, 2001) was used as standard medium for the cultivation of *E. coli* cells. For solid medium, 1.5 % (w/v) agar-agar were added prior to sterilization.

LB medium	10 g/l	tryptone
	5 g/l	yeast extract
	5 g/l	NaCl

For the recombinant protein production of Dshi_1135 *via* auto-induction in *E. coli*, LB medium was supplemented with self-inducing reagents for the T7 promoter according to Studier (Studier, 2005). 50 x 5052 was sterilized by filtration (pore size 0.2 µm), whereas the 20 x NPS buffer was autoclaved.

Auto-induction medium	930 ml	LB medium
	1 ml	1 M $MgCl_2$
	20 ml	50 x 5052
	50 ml	20 x NPS
50 x 5052	250 g/l	glycerol
	25 g/l	glucose
	100 g/l	α-lactose
20 x NPS	500 mM	$(NH_4)_2SO_4$
	1 M	$Na_2HPO_4 \cdot 7\ H_2O$
	1 M	KH_2PO_4

3.3.2.2 Terrific Broth

Terrific broth (TB) is a nutrient rich medium that was designed for high cell density cultivation of *E. coli* (Tartoff & Hobbs, 1987). In this study TB was used for overexpression of recombinant proteins in *E. coli*. TB basic and TB-salts were autoclaved separately.

TB	900 ml	TB basic
	100 ml	10 x TB-salts

TB basic	12 g/l	tryptone
	24 g/l	yeast extract
	5 g/l	glycerol
10 x TB-salts	0.17 M	KH_2PO_4
	0.72 M	K_2HPO_4

3.3.2.3 LB Miller Agar

LB Miller agar was used for *Vibrio natriegens* cultivation on solid medium. The medium was sterilized by autoclaving.

LB Miller agar	10 g/l	tryptone
	5 g/l	yeast extract
	10 g/l	NaCl
	15 g/l	agar-agar

3.3.2.4 LB3 Medium

For cultivation of *V. natriegens* in liquid cultures, LB3 medium according to Lee and colleagues was used (Lee *et al.,* 2019). Before use, the medium was vapor sterilized.

LB3 medium	10 g/l	tryptone
	5 g/l	yeast extract
	30 g/l	NaCl

3.3.2.5 Marine Broth

For cultivation of *D. shibae* strains in a full medium Marine Broth (MB) was used. If selective antibiotics were needed, half-concentrated MB (hMB) medium was used. For solid medium, 1.5 % (w/v) agar-agar were added prior to sterilization.

MB medium	40.1 g/l	Marine-Bouillon
hMB medium	20.05 g/l	Marine-Bouillon

3.3.2.6 Artificial Saltwater Medium

Artificial saltwater medium (SWM) was used as a minimal medium for the cultivation of *D. shibae* under defined growth conditions. Therefore, SWM Basic and the 10x $NaHCO_3$ solution were prepared in Milli Q H_2O and sterilized by autoclaving. All other components were prepared as stock solutions in Milli Q H_2O and sterile-filtered (pore size 0.2 µm) and added to the sterile SWM Basic to obtain SWM.

SWM	800 ml/l	SWM Basic
	100 ml/l	10 x $NaHCO_3$
	10 ml/l	100 x vitamin solution
	2 ml/l	500 x trace elements
	1 ml/l	1000 x Fe-solution
	87 ml/l	Milli Q H_2O
SWM Basic	4 g/l	Na_2SO_4
	0.25 g/l	NH_4Cl
	20 g/l	NaCl
	3 g/l	$MgCl_2 \cdot 6\ H_2O$
	0.5 g	KCl
	0.15 g/l	$CaCl_2 \cdot 2\ H_2O$
	0.2 g/l	KH_2PO_4
	2 g/l	succinate
	1.2 g	NaOH

All components were dissolved in 800 ml Milli Q H_2O and the pH was adjusted to 7.0 by NaOH.

10 x $NaHCO_3$solution	1.9 g/l	$NaHCO_3$
100 x vitamin solution	200 mg/l	biotin
	2 g/l	nicotinic acid
	800 mg/l	4-aminobenzoic acid

500 x trace elements	5.2 g	TitriplexIII (Na_2EDTA)
	6.5 ml	HCl (25 % (v/v))
	→ adjust pH to 6.0-6.5 with NaOH, add the following components afterwards:	
	30 mg/l	H_3BO_3
	100 mg/l	$MnCl_2 \cdot 4\ H_2O$
	190 mg/l	$CoCl_2 \cdot 6\ H_2O$
	24 mg/l	$NiCl_2 \cdot 6\ H_2O$
	2 mg/l	$CuCl_2 \cdot 2\ H_2O$
	144 mg/l	$ZnSO_4 \cdot 7\ H_2O$
	38 mg/l	Na_2MoO_4
1000 x Fe-solution	4.17 g/l	$FeSO_4 \cdot 7\ H_2O$
	25 ml/l	0.1 M HCl

3.3.3 Media Additives

All used media additives were prepared as concentrated stock solutions, sterile-filtered (pore size 0.2 µm) and stored at -20 °C. Addition of the additives occurred under sterile conditions to lukewarm media. ALA stock solutions were covered in aluminum foil, due to its light sensitivity. The used final concentrations of the respective additives are listed in Table 7.

Table 7: Media additives

Substance	Stock solution	Final concentration	Organism
5-aminolevulinic acid (ALA)	50 mg/ml in dH_2O	50 µg/ml	*E. coli*
Ampicillin (Amp)	100 mg/ml in dH_2O	70-100 µg/ml 25-75 µg/ml	*E. coli* *V. natriegens*
Chloramphenicol (Cml)	34 mg/ml in 70 % (v/v) ethanol	25-34 µg/ml 10-20 µg/ml 10 µg/ml	*E. coli* *D. shibae* *V. natriegens*
Gentamicin (Gm)	10 mg/ml in dH_2O	80 µg/ml	*D. shibae*
isopropyl-β-D-galacto-pyranoside (IPTG)	1 M in dH_2O	50-500 µM 400 µM	*E. coli* *V. natriegens*
Kanamycin (Kan)	50 mg/ml in dH_2O	50 µg/ml 12.5 µg/ml	*E. coli* *V. natriegens*

Substance	Stock solution	Final concentration	Organism
L-rhamnose	1 M in dH_2O	0-2000 µM	*E. coli*

3.4 Microbiological Techniques

3.4.1 Cultivation of *E. coli*

For the cultivation of *E. coli* cells on solid media 5-250 µl of a respective bacterial suspension were plated onto LB agar plates with a drigalski spatula. Alternatively, cell material from a glycerol stock was streaked out with an inoculation loop. If necessary, corresponding antibiotics or other additives were added to the LB agar medium before use. Plates were incubated overnight at 37 °C.

Liquid pre-cultures were prepared in 10-50 ml LB medium, supplemented with the respective antibiotics, in either baffled flasks or test tubes. The medium was inoculated with a single colony from a plate culture or directly from a glycerol stock. Cultures were incubated overnight at 37 °C under vigorous shaking (200 rpm).

3.4.2 Cultivation of *V. natriegens*

Plate cultures of *V. natriegens* were obtained by plating of a cell suspension onto LB Miller agar plates, containing the respective antibiotics. Alternatively, cell material from a glycerol stock was streaked with an inoculation loop. Cultivation occurred over night at 37 °C, if kanamycin was used for selection incubation was performed at 30 °C.

Liquid *V. natriegens* cultures were grown in LB3 medium supplemented with the respective antibiotics. For pre-cultures 100 ml LB3 medium in a 300 ml baffled flask were inoculated with cell material from a plate culture or directly from a glycerol stock. The cells were cultivated overnight at 37 °C (without kanamycin) or 30 °C (with kanamycin), respectively, at 200 rpm.

3.4.3 Cultivation of *D. shibae*

For *D. shibae* plate cultures cell material from a glycerol stock was streaked out with an inoculation loop on MB agar plates. hMB agar plates were used when antibiotics were mandatory for strain cultivation, due to their instability under high salt concentrations. Plates were incubated for 3-5 days at 30 °C.

Liquid pre-cultures of *D. shibae* were inoculated with a single colony from a respective plate culture in 30 ml MB medium in baffled flasks. The cells were grown for three days at 30 °C under continuous shaking (200 rpm).

3.4.4 Determination of Cell Density

To determine the cell density of a bacterial culture the optical density (OD) at a wavelength of 578 nm (OD_{578}) was measured *via* photometry. For cell densities < 0.8, samples were diluted 1:10 in the respective growth medium. An OD_{578}= 1 corresponds to approximately $1 \cdot 10^9$ cells/ml.

3.4.5 Storage of Bacteria

Short term storage of *E. coli* and *D. shibae* occurred on solid media plates for a maximum of four weeks at 4 °C. *V. natriegens* plate cultures were unsuitable for storage at 4 °C and were therefore kept at room temperature for approximately 5-7 days. For long term storage, glycerol stocks of the bacterial strains were prepared. For *E. coli* glycerol stocks 1.2 ml of an overnight culture were mixed with 400 µl of sterile 80 % (v/v) glycerol, to yield a final concentration of 20 % (v/v) glycerol. For the generation of *D. shibae* glycerol stocks, 1 ml of a well grown culture was sedimented (1 min, 11'337 x g) and resuspended in another 1 ml of cell culture. Afterwards, 600 µl of sterile 80 % (v/v) were added and the suspension was well mixed to obtain a final glycerol concentration of 30 % (v/v). *V. natriegens* glycerol stocks were prepared by mixing 1.1 ml of a well grown over night culture with 0.5 ml sterile 80 % (v/v) glycerol (final glycerol concentration 25 % (v/v). All glycerol stocks were stored at -80 °C.

3.5 Molecular Biological Techniques

3.5.1 Preparation of Plasmid DNA (Miniprep)

High quality plasmid DNA was isolated out of *E. coli* cells using the QIAprep Spin Miniprep Kit according to manufacturer's instructions (QIAGEN, Hilden, Germany). For DNA elution from the column, heated dH_2O at 65 °C was used instead of the provided elution buffer. The obtained plasmid DNA was used for cloning and sequencing purposes.

3.5.2 Preparation of Genomic DNA of *D. shibae*

For the isolation of genomic *D. shibae* $DLF12^T$ DNA, 40 ml MB medium in a baffled flask were inoculated with a single colony from a respective plate culture and incubated for 2-3 days at 30 °C and continuous shaking (200 rpm). After reaching the stationary phase the cell culture was transferred into a 50 ml screw cap tube, harvested by centrifugation (15 min, 2500 x g) and the resulting cell pellet was resuspended in 564 µl TE-buffer. This cell suspension was divided into two 2 ml reaction tubes and for the

removal of RNA and proteins, 6 µl RNase (10 mg/ml) and 10 µl lysozyme-solution (10 mg/ml) were carefully added and the cells were incubated at 37 °C for 20 min. In the next step, 6 µl Proteinase K (20 mg/ml) and 30 µl SDS-solution (20 % (w/v)) were added and the cell suspension was incubated at 37 °C until it became clear. Then, 100 µl 5 M NaCl-solution were pipetted to the mixture and an additional incubation step at 37 °C for 2 min followed. For purification of the genomic DNA, a phenol/chloroform extraction was performed, followed by subsequent precipitation and washing with 100 % (v/v) isopropanol and 70 % (v/v) ethanol, respectively. The resulting pellet was dried and then dissolved in 200 µl TE-buffer and the DNA concentration was determined, using a Nano Drop. Storage of the genomic *D. shibae* DNA occurred at 4 °C.

TE-buffer	10 mM	Tris-HCl, pH 8.0
	1 mM	EDTA, pH 8.0
Lysozyme-solution	10 mg/ml	lyzozyme
Proteinase K	20 mg/ml	Proteinase K
RNase (DNase free)	10 mg/ml	RNase A
	10 mM	sodium acetate, pH 5.2
	1 M	Tris-HCl, pH 8.0

3.5.3 Preparation of Chemically Competent *E. coli* Cells

3.5.3.1 $CaCl_2$ Method

For the preparation of $CaCl_2$ competent *E. coli* cells, 100 ml LB medium in a 500 ml baffled flask were inoculated with a respective pre-culture in a ratio of 1:100 and subsequently incubated at 37 °C and 200 rpm. After reaching an OD_{578}= 0.6-0.8 the cells were transferred into two 50 ml screw cap tubes and harvested by centrifugation (10 min, 3000 x g, 4 °C). The supernatant was discarded, the resulting cell pellet was gently resuspended in 10 ml ice-cold $CaCl_2$-solution and the cells were incubated for 15 min on ice. In a second centrifugation step, the cells were sedimented again (10 min,

3000 x g, 4 °C) and subsequently dissolved in 1 ml ice-cold $CaCl_2$-solution on ice. Aliquots of the $CaCl_2$ competent cells were stored at -80 °C.

$CaCl_2$-solution	100 mM	$CaCl_2$
	10 % (v/v)	glycerol

3.5.3.2 RbCl Method

A pre-culture of the desired *E. coli* strain was prepared and used for the inoculation of 250 LB medium, supplemented with 20 mM $MgSO_4$, in a 500 ml baffled flask in a ratio of 1:100. The cells were grown at 37 °C and 200 rpm until an OD_{578}= 0.6-0.8 was reached. Subsequently the cells were transferred into 50 ml screw cap tubes and sedimented by centrifugation (10 min, 3000 x g, 4 °C). The resulting cell pellets were each dissolved in 100 ml ice-cold TFB-I buffer and incubated on ice for 5 min. Afterwards, cells were centrifuged (10 min, 3000 x g, 4 °C) and resuspended in 2 volumes of buffer TFB-II, referring to volume of the cell pellet. After incubation on ice for 1 h, cells were divided into aliquots and stored at -80 °C.

TFB-II	30 mM	potassium acetate
	10 mM	$CaCl_2$
	50 mM	$MnCl_2$
	100 mM	RbCl
	15 % (v/v)	glycerol
	⟶ pH 5.8 (adjusted with acidic acid)	
	⟶ sterile filtered (pore size 0.2 µm)	

TFB-II	10 mM	MOPS-KOH (pH 6.5)
	75 mM	$CaCl_2$
	10 mM	RbCl
	15 % (v/v)	glycerol
	⟶ pH 6.5 (adjusted with KOH)	
	⟶ sterile filtered (pore size 0.2 µM)	

3.5.4 Transformation of Plasmid DNA into Competent *E. coli* Cells

The transformation of $CaCl_2$ or RbCl competent *E. coli* cells was performed according to the heat shock protocol. Therefore, 1 µl plasmid DNA was mixed with 49 µl competent *E. coli* cells and incubated on ice for 20 min. Afterwards, the heat shock was performed at 42 °C for exactly 45 sec and then the cells were stored on ice again for 2 min immediately. For recovery of the cells, 250 µl LB medium were added to the transformation mix, followed by an incubation step for 1 h at 37 °C and 300 rpm. To obtain single colonies of transformed cells, 20-200 µl of the transformation mix were plated onto LB agar plates, containing the respective antibiotic(s). The plates were incubated overnight at 37 °C.

3.5.5 Transformation of Plasmid DNA into Competent *V. natriegens* Cells

50 µl of commercially purchased competent *V. natriegens* Vmax™ Express (BioCat, Heidelberg, Germany) were thawed on ice for 10 min, then mixed carefully with 1 µl of plasmid DNA in a 1.5 ml reaction tube and incubated for 1 h on ice. Afterwards the cells heat shocked at 42 °C for 30 sec and then immediately stored on ice for 2 min. Carefully, 1 ml of SOC3 medium (Lee *et al.,* 2019), preheated to 37 °C, was added and the cell suspension was incubated for 2 h at 37 °C and 600 rpm. After expiry of the time 200 µl of the transformed *V. natriegens* cells were plated onto LB Miller agar, containing the respective antibiotics. The residual cells were sedimented (2 min, 2415 x g), resuspended in the reflux after the supernatant was discarded and then also plated onto LB Miller agar plates with the respective antibiotics. If the medium contained kanamycin incubation occurred at 30 °C, otherwise at 37 °C overnight.

SOC3 medium	20 g/l	tryptone
	5 g/l	yeast extract
	30 g/l	NaCl
	2.5 mM	KCl
	10 mM	$MgCl_2$
	10 mM	$MgSO_4$
	20 mM	glucose

3.5.6 Diparental Mating with *D. shibae*

Diparental mating is a method, where plasmid DNA is transferred directly from a donor strain to a recipient strain *via* cell-to-cell contact. Therefore, the donor strain produces a pilus, which can connect both the donor and recipient strain and enables the exchange of genetic material.

Here, the 5-aminolevulinic acid (ALA) auxotrophic strain *E. coli* ST18 (Thoma & Schobert, 2009) was used as donor strain for the transfer on plasmid DNA into different *D. shibae* (recipient) strains. Therefore, RbCl competent *E. coli* ST18 cells were transformed with the desired plasmid. For the generation of *D. shibae* main cultures, 30 ml hMB medium were inoculated with a respective pre-culture in a baffled flask with an OD_{578}= 0.05 and incubated at 30 °C and 200 rpm to a final OD_{578}= 0.5-0.8. *E. coli* ST18 main cultures were obtained by inoculating 50 ml LB medium containing 50 µg/ml ALA in a baffled flask, with a pre-culture carrying the desired plasmid, with an OD_{578}= 0.1. Incubation occurred overnight at 37 °C and 200 rpm, until an OD_{578}= 0.5-0.6 was reached. After both strains grew to the desired OD_{578}, 1 ml of the *D. shibae* recipient strain was transferred into a 15 ml screw cap tube and sedimented by centrifugation (5 min, 2500 x g). The resulting cell pellet was resuspended and mixed with five volumes of the *E. coli* ST18 donor strain, referring to the OD_{578} of the *D. shibae* recipient strain. The cell suspension was centrifuged (5 min, 2500 x g), the supernatant was discarded and the pellet was gently dissolved in the remaining medium. This mixture of donor and recipient strain was carefully applied onto a sterile membrane filter (GVS North America, Ø 25 mm, pore size 0.2 µm) on a LB agar plate, containing 50 µg/ml ALA. After incubation at 30 °C for 3 days, the membrane filter was transferred into a 2 ml reaction tube and the cells were washed off with 1 ml MB medium. By vortexing the conjugation process was stopped and the cells were harvested by centrifugation (5 min, 2415 x g). The obtained cell pellet was resuspended in 500 µl MB medium and subsequently serial dilutions from 10^{-1} to 10^{-3} were prepared. Of each dilution 100 µl were plated onto hMB agar plates supplemented with 10-20 µg/ml Cml. Plates were cultivated for 3-10 days at 30 °C to obtain the desired *D. shibae* transformants.

3.5.7 Determination of DNA Concentration

Spectral photometric analysis was employed for the determination of DNA concentrations. Therefore, 1 µl of the DNA sample was applied to the sensor of the

NanoDrop™ ND-1000 (PEQLAB Biotechnology GmbH, Erlangen, Germany) and the absorbance at 260 nm and 280 nm were measured. An $A_{260\ nm}$=1 of a pure DNA solution corresponds to a concentration of 50 µg/ml double-stranded DNA. Potential impurities of the DNA solution with proteins were determined by calculating the ratio of $A_{260\ nm}$ to $A_{280\ nm}$. Here, a value of 1.8-2 accounts for pure DNA.

3.5.8 Agarose Gel Electrophoresis

Agarose gel electrophoresis was used for analytical separation of DNA fragments. Therefore, depending on the size of the DNA fragment, agarose gels with 1 % (w/v) or 2 % (v/v) agarose in 1x TAE buffer were prepared and placed into an appropriate electrophoresis chamber, filled with 1x TAE buffer. The DNA samples were mixed with 6x DNA loading dye and loaded subsequently on the gel. Additionally, the size marker Quick-Load® 2-Log DNA Ladder (New England Biolabs, Ipswich, MA, USA) was applied according to the manufacturer's instructions, to allow DNA fragment size determination of the sample. Depending on the size of the gel, an electric field with a voltage of 100-120 V was applied. Due to the negatively charged phosphate groups of the DNA, fragments migrate towards the anode with proportional velocity to the negative logarithm of their size. After the run, the gel was stained in a 0.1 % (v/v) ethidium bromide solution for 15 min and then adequately rinsed with dH_2O. Visualization and documentation of DNA was enabled by its fluorescence under UV light (λ=312 nm), using the GelDoc (Wealtec Europe, Cambridge, UK).

TAE buffer	40 mM	Tris-acetate
	1 mM	EDTA
6x DNA loading dye	350 µM	bromophenol blue
	450 µM	xylene cyanol FF
	0.25 % (w/v)	orange G
	50 % (v/v)	glycerol

3.5.9 Cloning of DNA

3.5.9.1 DNA Amplification by Polymerase Chain Reaction

With the method of polymerase chain reaction (PCR) it is possible to amplify a specific DNA region of interest. Therefore, appropriate oligonucleotide primers with the desired recognition sequences for restriction endonucleases were designed to bind to the start and to the end of the DNA target (Table 5). As DNA template either plasmid DNA, genomic DNA or a single bacterial colony was used, respectively. If a single colony was employed as template, it was dissolved in 50 µl dH_2O immediately before use. Additionally, the PCR reaction mix contained a deoxynucleotide triphosphate (dNTP) mix, the Phusion® High-Fidelity DNA Polymerase and its corresponding 5x Phusion® HF Buffer (all New England Biolabs, Ipswich, MA, USA). For the amplification of GC rich DNA regions, the Q5® High-Fidelity DNA Polymerase together with its corresponding buffer and 1.5 % (v/v) DMSO was used. All PCR reactions were either performed in a total volume of 20 µl or 50 µl.

Standard PCR reaction:

DNA template	5-100 ng
forward primer (100 pmol/µl)	1 µl
reverse primer (100 pmol/µl)	1 µl
dNTP mix (2.5 mM)	5 µl
Phusion® HF Buffer (5x)	10 µl
Phusion® High-Fidelity DNA Polymerase (5 U/µl)	0.5 µl
dH_2O	adjust to 20-50 µl

Standard colony PCR reaction:

DNA template	5 µl
forward primer (100 pmol/µl)	1 µl
reverse primer (100 pmol/µl)	1 µl
dNTP mix (2.5 mM)	5 µl
Phusion® HF Buffer (5 x)	10 µl
Phusion® High-Fidelity DNA Polymerase (5 U/µl)	0.5 µl
dH_2O	adjust to 50 µl

In an initial denaturation step at 98 °C, the DNA template is separated into single strands. PCR then continues with a repeat cycle (25 x) of denaturation (98 °C), primer annealing (55-72 °C) to allow binding of the primers to the single stranded DNA and primer elongation (72 °C) for generation of a new complementary DNA strand. In the end a final elongation step (72 °C) occurs to terminate the PCR reaction.
The annealing temperature was adjusted according to the calculated primer melting temperature to ensure specific primer-DNA hybridization. Dependent on the length of the desired DNA fragment and employed DNA polymerase, the elongation time was set.

Standard thermocycler program:

Initial denaturation	1 min	98 °C	
Denaturation	30 sec	98 °C	25 x
Annealing	30 sec	55-72 °C	
Elongation	30 sec/kb	72 °C	
Final elongation	5 min	72 °C	

Standard thermocycler program for colony PCR:

Initial denaturation	5 min	98 °C	
Denaturation	30 sec	98 °C	25 x
Annealing	30 sec	55-72 °C	
Elongation	30 sec/kb	72 °C	
Final elongation	5 min	72 °C	

3.5.9.2 Restriction of DNA

Plasmid DNA (vectors) and PCR products (inserts) were digested by restriction endonucleases purchased from New England BioLabs (Ipswich, MA, USA). Concentrations of DNA, enzymes and reaction buffers, as well as incubation temperature and time were chosen according to manufacturer's instructions.

3.5.9.3 Phenol/Chloroform/Isoamyl Alcohol Extraction of DNA

If necessary, DNA was extracted and purified *via* phenol/chloroform/isoamyl alcohol

treatment. Therefore, the samples, containing the desired DNA, were filled up to a minimal volume of 150 µl with dH_2O and mixed thoroughly with an equal volume of phenol and afterwards with one volume of chloroform/isoamyl alcohol (24:1). After centrifugation for 2 min at 11'337 x g the aqueous phase was carefully transferred into a fresh 1.5 ml reaction tube and subsequently, two volumes of chloroform/isoamyl alcohol (24:1) were added and the approach was adequately mixed by vortexing. The resulting mixture was then centrifuged again (2 min, 11'337 x g) and the resulting upper aqueous phase, containing the DNA, was carefully removed and transferred into another fresh 1.5 ml reaction tube. Precipitation of the extracted DNA occurred by addition of 1 ml ice-cold 100 % (v/v) ethanol and incubation at -20 °C for 30 min. Afterwards the DNA was sedimented (10 min, 11'337 x g), the supernatant was discarded and to yield pure DNA, the pellet was washed twice with 500 µl of 70 % (v/v) ethanol for 30 min at 50 °C. After each washing step the sample was centrifuged for 10 min at 11'337 x g and finally the resulting pellet was incubated at 50 °C to complete dryness. The DNA pellet was dissolved in 20-40 µl sterile dH_2O and stored appropriately.

3.5.9.4 Purification of PCR Products and Vectors

PCR products were purified using the QIAquick PCR Purification Kit (QIAGEN, Hilden, Germany) according to the manufacturer's instructions. For DNA elution from the column, heated dH_2O at 65 °C was used instead of the provided elution buffer.

For the removal of restriction endonucleases after digest of vector DNA agarose gel electrophoresis was performed. After the run the gel was stained with 0.1 % (v/v) ethidium bromide solution for 15 min and rinsed with dH_2O adequately. The DNA was visualized *via* its fluorescence under UV light (λ=312 nm) and the corresponding band was excised from the gel. For purification of the vector DNA the QIAquick Gel Extraction Kit (QIAGEN, Hilden, Germany) was used according to the manufacturer's instructions. Again, heated dH_2O at 65 °C was used for DNA elution from the column instead of the provided elution buffer.

3.5.9.5 Dephosphorylation of Vector DNA

In order to prevent self-ligation of free 5'ends of the linearized vector DNA, it was dephosphorylated, using rAPid Alkaline Phosphatase according to manufacturer's instructions (Roche, Basel, Schweiz).

3.5.9.6 Ligation of DNA

For ligation of DNA fragments the T4 DNA Ligase (New England BioLabs, Ipswich, MA, USA) was used according to manufacturer's instructions.

In general, vector DNA and insert DNA were mixed in a molar ratio of 1:5 and incubation occurred overnight at 17 °C or for 2 h at 25 °C, respectively. Afterwards 5 µl of the reaction mixture were transformed into 45 µl of chemically competent *E. coli* DH10B cells. Successful cloning was checked by colony PCR and verified by DNA sequencing.

3.5.9.7 Ligation Independent Cloning

The method of ligation independent cloning (LIC) was developed as an alternative cloning strategy to restriction endonuclease/ ligase cloning. Here, the 3'⟶5' exonuclease activity of the T4 DNA polymerase is used to create specific DNA overhangs, that are complementary between vector and insert. For the generation of these overhangs in the vector a special LIC-site is contained that possesses a restriction site for blunt end digestion. After linearization, the vector is treated with the T4 DNA polymerase in the presence of dATP's. This leads to a removal of bases in 3'⟶5' direction until the first thymidine residue of the complementary strand is reached and an adenosine is incorporated, resulting in two specific overhangs. For the creation of inserts with compatible overhangs, special primers with LIC tails are needed. Both, forward and reverse primer must contain the sequence of the complementary overhangs and a long enough overlap with of the gene of interest. After amplification of the desired gene region by PCR, the PCR product is also treated with the T4 DNA polymerase together with dTTP's. Here again the bases are removed in 3'⟶5'direction until the first adenosine of the complementary strand is reached and a thymidine can be incorporated. Also, here an overhang is created that now perfectly matches with the vector overhangs. In a last and enzyme free annealing step, vector and insert can be ligated.

In this study, LIC was used for the generation promoter-reporter gene fusions, to analyse the activity of promoters of interest in different *D. shibae* strains under different light conditions. As vector pBBR1MCS LIC-*lacZ* was used, that contains a *Sma*I restriction site for linearization. After linearization the vector was purified *via* phenol/chloroform/isoamyl alcohol extraction. The promoters of interest were PCR amplified from genomic *D. shibae* DNA and then purified, using the QIAquick PCR

Purification Kit. Vector and insert were treated with the T4 DNA polymerase (New England BioLabs, Ipswich, MA, USA) and the respective deoxynucleotide for 20 min at 22 °C. Subsequently, the reaction mixture was heated up to 75 °C for 30 min. The exact pipetting scheme is shown in Table 8.

Table 8: Pipetting scheme for T4 DNA polymerase treatment of vector and insert DNA

	Vector	Insert
pBBR1MCS LIC-*lacZ* (linearized and purified)	~ 100 ng	
Insert (PCR purified)		~ 300 ng
NEB Buffer 2 (10 x)	4 µl	4 µl
BSA (10 mg/ml)	0.4 µl	0.4 µl
dATP's (2.5 mM)	1 µl	
dTTP's (2.5 mM)		1 µl
T4 DNA polymerase (3 U/µl)	2 µl	2 µl
dH_2O	adjust to 40 µl	adjust to 40 µl

After the T4 DNA polymerase treatment 2 µl of each, vector DNA and insert DNA were mixed in a PCR reaction tube and incubated for 10 min at room temperature for the annealing reaction. Finally, 4 µl of this reaction mix were transformed into chemically competent *E. coli* DH10B cells and plated onto LB agar plates supplemented with 34 µg/ml Cml. Potentially positive clones were identified *via* colony PCR and verified by DNA sequencing.

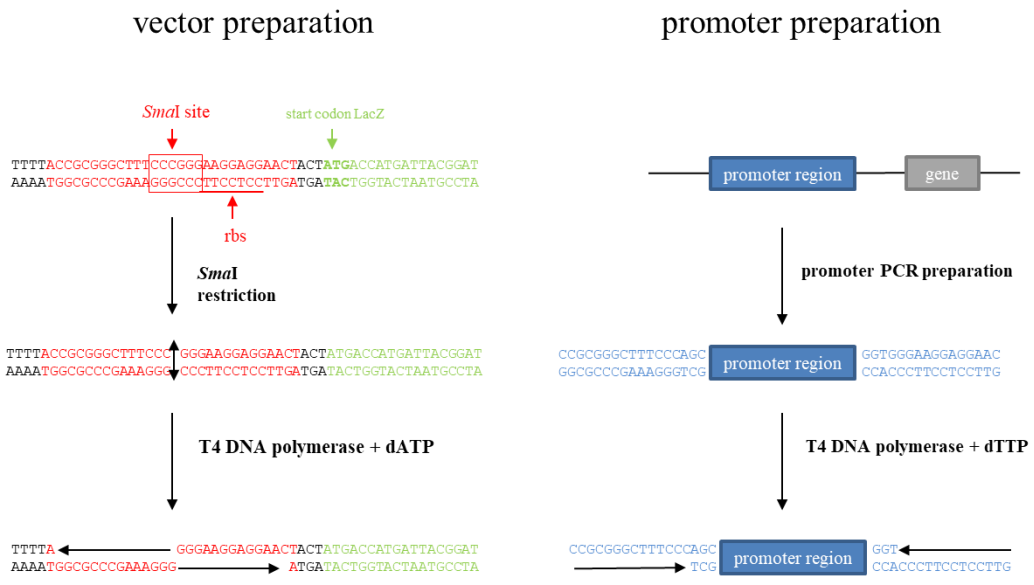

Figure 10: Scheme of ligation independent cloning
Overview of the ligation independent cloning (LIC) method. Vector preparation is shown in red, insert (promoter) preparation in blue (Botella *et al.*, 2010).

3.5.9.8 Site-directed Mutagenesis

Single amino acids in a protein of interest can be exchanged by the insertion of a specific mutation into the DNA sequence of the corresponding gene.

In this study, the Q5® Site-Directed Mutagenesis Kit (New England BioLabs, Ipswich, MA, USA) was used for this purpose according to manufacturer's instructions. Beforehand, specific primers that are complementary to the opposite strands of the plasmid DNA and carry the desired mutation were designed, using the NEBase Changer Tool (New England BioLabs, Ipswich, MA, USA). As template a dsDNA plasmid, carrying the gene of interest, was used. In a PCR reaction the primers can anneal to the complementary DNA strands and synthesize the new mutated plasmid. Afterwards, the PCR product is treated with the endonuclease *Dpn*I, which specifically cleaves methylated DNA. Thereby, only parental plasmid DNA gets digested and the newly *in vitro* synthesized mutated unmethylated plasmid DNA remains. The modified plasmid was transformed into chemically competent *E. coli* DH10B cells and potentially positive colonies were selected on LB agar plates with the respective antibiotic. Successful amino acid exchange was checked *via* DNA sequencing.

3.5.10 Construction of Vectors

3.5.10.1 Plasmids for Heterologous Production of Dshi_1135

Three different expression vectors were designed and tested for the heterologous production of the *D. shibae* Dshi_1135 protein.

First, the Dshi_1135 gene was cloned into the pET52bTrx vector, which carries the sequence for an N-terminal thioredoxin tag to increase protein solubility, followed by a Strep-tag II for affinity chromatography. Therefore, the Dshi_1135 gene was PCR amplified from genomic *D. shibae* DNA, using the primer pair EH649/ EH650. The resulting PCR product was digested with *Sac*I-HF (New England BioLabs, Ipswich, MA, USA) and ligated into the *Sma*I/ *Sac*I site of pET52bTrx, resulting in the plasmid pET52b(+)Trx_Dshi1135Full. Positive clones were identified by DNA sequencing with the standard sequencing primers T7 and pET-RP by Eurofins Genomics (Ebersberg, Germany). Protein production occurred in *E. coli* BL21-CodonPlus(DE3)-RIL and *E. coli* Lemo21(DE3) cells, respectively and resulted in a TRX-Strep-tag II-Dshi_1135 fusion protein containing a HRV-3C protease/ PreScission™ Protease cleavage site to remove the N-terminal TRX-Strep-tag II.

Second, the plasmid pGEX-6P-1_Dshi1135Full was generated. This expression vector contains the sequence for an N-terminal GST-tag and therefore enables affinity chromatographic purification of target proteins *via* a glutathione sepharose resin. Here, the Dshi_1135 gene was amplified by PCR with primers MIB1 and MIB2 that contained the restriction sites for *Eco*RI and *Bam*HI, respectively. Both, vector and insert were initially digested with *Eco*RI-HF and *Bam*HI-HF and then ligated, yielding the plasmid pGEX-6P-1_Dshi1135Full. DNA sequencing with the Eurofins Genomics (Ebersberg, Germany) standard sequencing primers pGEX5 and pGEX3 confirmed the correct integration of the Dshi_1135 gene into the vector. The plasmid was used for recombinant production of a GST-tag Dshi_1135 fusion protein in *E. coli* BL21-CodonPlus(DE3)-RIL or *V. natriegens* Vmax™ Express cells.

Third, the Dshi_1135 gene was cloned into the pET22b(+)Strep vector, which carries the sequence for a C-terminal Strep-tag II for affinity chromatography *via* the Strep-tag® system. To yield pET22b(+)Strep_Dshi1135, the DNA sequence of the corresponding gene was amplified with the primers EH725 and MIB30 *via* PCR from genomic *D. shibae* DNA. The resulting DNA fragment was digested with *Nde*I and *Hind*III (New England BioLabs, Ipswich, MA, USA) and inserted into the identically cleaved vector. The DNA sequence of the integrated fragment into the vector was obtained by DNA sequencing by Eurofins Genomics (Ebersberg, Germany) with the standard sequencing primers T7 and pET-RP. Expression of the cloned DNA fragment in *E. coli* BL21(DE3) cells resulted in a Dshi_1135-Strep-tag II fusion protein, without the N-terminal *E. coli pelB* signal sequence for periplasmic export.

3.5.10.2 Plasmids for Heterologous Production of Dshi_1135$_{LOV}$

For recombinant production of the Dshi_1135 LOV domain (amino acids 1-149) in *E. coli* BL21-CodonPlus(DE3)-RIL cells, the gene sequence encoding the corresponding amino acids was introduced into the pET52bTrx and pGEX-6P-1 vector, respectively.

To yield the plasmid pET52b(+)Trx_Dshi1135LOV, the desired Dshi_1135 gene sequence was PCR amplified from genomic *D. shibae* DNA with the primer pair EH649/ EH651, the resulting DNA fragment was digested with *Sac*I-HF (New England BioLabs, Ipswich, MA, USA) and subsequently ligated into the *Sma*I/ *Sac*I site of pET52bTrx.

By using primers MIB1 and MIB3 the Dshi_1135 LOV domain DNA sequence was

amplified from genomic *D. shibae* DNA. The PCR product was treated with *Eco*RI-HF and *Bam*HI-HF (New England BioLabs, Ipswich, MA, USA) and ligated into pGEX-6P-1, resulting plasmid pGEX-6P-1_Dshi1135LOV.

For both plasmids successful cloning was verified *via* DNA sequencing. Standard Eurofins Genomics (Ebersberg, Germany) primers T7 and pET-RP were used for pET52b(+)Trx_Dshi1135LOV sequence determination. For sequencing of pGEX-6P-1_Dshi1135LOV, primers pGEX5 and pGEX3 (Eurofins Genomics, Ebersberg, Germany) were used.

3.5.10.3 Plasmids for Homologous Production of Dshi_1135

To enable homologous production of the Dshi_1135 protein in *D. shibae* cells, the pRhokS vector system was used. This vector possesses an *aphII* promoter for constitutive gene expression and a sequence for a C-terminal Strep-tag II for affinity purification. The Dshi_1135 gene sequence was amplified using the pET52b(+)_Dshi1135Full plasmid as template and primers EH725 and MIB29 in a PCR reaction. The resulting DNA fragment and the pRhokS vector were initially digested with *Nde*I and *Xho*I (New England BioLabs, Ipswich, MA, USA) and then ligated, yielding the plasmid pRhokS_Dshi1135Strep. After DNA sequence determination of the integrated Dshi_1135 gene by Eurofins Genomics (Ebersberg, Germany) with the standard sequencing primers T7 and pET-RP, the plasmid was transformed into *E. coli* ST18 cells for diparental mating into the *D. shibae* wild type and Dshi_1135::Tn mutant strain, respectively.

3.5.10.4 Plasmids for Heterologous Production of Dshi_1135 Mutant Proteins

For the investigation of the role of specific amino acid residues in photo adduct formation and histidine kinase activity of the Dshi_1135 protein, different mutant proteins were generated *via* site-directed mutagenesis (see chapter 3.5.9.8).

Here, the pET52b(+)Trx_Dshi1135Full plasmid was used as matrix. All utilized primers and generated plasmids are listed in Table 9.

Table 9: Generated Dshi_1135 mutant proteins and used primers for site directed mutagenesis

Mutation	Primer pair	Resulting plasmid
C61A	MIB14, MIB15	pET52b(+)Trx_Dshi1135C61A
C61S	MIB16, MIB17	pET52b(+)Trx_Dshi1135C61S
H258A	MIB18, MIB19	pET52b(+)Trx_Dshi1135H258A
H258N	MIB20, MIB21	pET52b(+)Trx_Dshi1135H258N
I121A	MIB22, MIB23	pET52b(+)Trx_Dshi1135I121A

Successful mutagenesis was checked by DNA sequencing with the standard sequencing primers T7 and pET-RP (Eurofins Genomics, Ebersberg, Germany).

3.5.10.5 Plasmids for Heterologous Production of Potential Response Regulators of Dshi_1135

The gene loci Dshi_3837, Dshi_1538 and Dshi_1406 were identified in an initial bioinformatic search to be potential response regulators of the LOV histidine kinase Dshi_1135. For further investigations they were cloned into the pET52b(+) expression vector system and produced in *E. coli* BL21-CodonPlus(DE3)-RIL cells.

All used primers for gene amplification, restriction sites and resulting plasmids are listed in Table 10.

Table 10: Used primers and restriction sites for cloning of potential response regulators of Dshi_1135

Gene locus	Primer pair	Restriction sites	Resulting plasmid
Dshi_3837	MIB4, MIB5	*Xma*I, *Not*I	pET52b(+)_Dshi3837
Dshi_1538	MIB6, MIB7	*Bam*HI, *Sac*I	pET52b(+)_Dshi1538
Dshi_1406	MIB8, MIB9	*Xma*I, *Sac*I	pET52b(+)_Dshi1406

All newly generated plasmids were examined for correct insert integration *via* DNA sequencing, with standard sequencing primers T7 and pET-RP (Eurofins Genomics, Ebersberg, Germany).

3.5.10.6 Plasmids for Coexpression of Dshi_1135 and Potential Response Regulators

For a heterologous test system for response regulator identification of Dshi_1135 in *E. coli*, several plasmids were generated.

The vector pETDuet1, which encodes two multiple cloning sites (MCS) with each a T7 promoter, *lac* operator and ribosome binding sites, was used for coexpression of Dshi_1135 and one of the potential response regulators Dshi_3837, Dshi_1538 and Dshi_1406, respectively.

The Dshi_1135 gene sequence was subcloned from pET52b(+)_Dshi1135Full into the *Xba*I and *Sac*I restriction sites of pETDuet1 MCS-1, resulting in the plasmid pETDuet1_Dshi1135. With the primer pair MIB27/ MIB28 all three potential response regulators were PCR amplified, using the plasmids pET52b(+)_Dshi3837, pET52b(+)_Dshi1538 and pET52b(+)_Dshi1406 as templates, respectively. The resulting PCR products were digested with *Nde*I and *Bgl*II (New England BioLabs,

Ipswich, MA, USA) and ligated into the MCS-2 of the linearized pETDuet1 vector to yield the plasmids pETDuet1_Dshi3837, pETDuet1_Dshi1538 and pETDuet1_Dshi1406. Additionally, the genes Dshi_3837, Dshi_1538 and Dshi_1406 were cloned into the MCS-2 of pETDuet1_Dshi1135 as described above, to obtain plasmids pETDuet1_Dshi1135-Dshi3837, pETDuet1_Dshi1135-Dshi1538 and pETDuet1_Dshi1135-Dshi1406. All newly generated plasmids were checked for correct insert integration by DNA sequencing (Eurofins Genomics, Ebersberg, Germany), using sequencing primers Duet Upstream and pACYCDuetDown1 for MCS-1 and primer pACYCDuetUP2 for MCS-2.

All plasmid variants were separately transformed into *E. coli* BL21(DE3) or *E. coli* NovaBlue(DE3) cells, respectively, for expression analyses of the respective protein(s).

3.5.10.7 Plasmids for Reporter Gene Fusions

Reporter gene fusions were generated with the pBBR1MCSLIC-*lacZ* vector that allows integration of a promoter sequence of interest *via* LIC.

The promoter regions of the *bchF*, *ppaA* and *hemE* genes were amplified from genomic *D. shibae* DNA, using the primer pairs EH677/ EH678, EH679/ EH680 and EH681/ EH682, respectively and subsequently integrated into the pBBR1MCSLIC-*lacZ* vector by LIC as described in chapter 3.5.9.7. This resulted in the plasmids pBBR1LIC_*bchF*-*lacZ*, pBBR1LIC_*ppaA*-*lacZ* and pBBR1LIC_*hemE*-*lacZ*, which were verified by DNA sequencing with standard sequencing primers T7 and M13-RP (Eurofins Genomics, Ebersberg, Germany). Positive plasmids were transformed into *E. coli* ST18 cells for diparental mating into different *D. shibae* strains. Resulting *D. shibae* colonies were checked for successful gene transfer *via* colony PCR with the T7 and EH636 primers.

Mutated *bchF* promoter fragments were commercially obtained as GeneArt® Strings™ DNA fragments (*bchF*100bpwt and *bchF*100bpmut1), or as synthetic gene cloned into the pMK-RQ vector (*bchF*mut1) (Thermo Fisher Scientific, Waltham, MA, USA). The *bchF*mut1 fragment was initially resected from pMK-RQ*bchF*mut1 with *Sma*I (New England BioLabs, Ipswich, MA, USA) and then inserted into pBBR1LIC-*lacZ*. The *bchF*100bpwt and *bchF*100bpmut1 fragments could be used directly for LIC into pBBR1MCSLIC-*lacZ*. Here, the plasmids pBBR1LIC_*bchF*mut1, pBBR1LIC_*bchF*100bpwt and pBBR1LIC_*bchF*100bpmut1 were obtained, checked by DNA sequencing (T7 primer, Eurofins Genomics, Ebersberg, Germany) and employed for diparental mating *via E. coli* ST18 into different *D. shibae* strains.

For construction of pACYCLIC-*bchF-lacZ*, the *bchF* promoter region was amplified with primers EH677 and EH678 of the template pBBR1LIC_*bchF-lacZ* and inserted *via* LIC into pACYCLIC-*lacZ*. Correct integration of the promoter fragment was verified by DNA sequencing, using the T7 primer (Eurofins Genomics, Ebersberg, Germany). The final plasmid was part of the heterologous *in vivo* test system for response regulator identification of Dshi_1135.

3.5.10.8 Plasmid for Complementation of *D. shibae* Dshi_1135::Tn

For complementation of the transposon mutant strain *D. shibae* Dshi_1135::Tn the vector pRhokS was used, which allows integration of a DNA sequence downstream of the constitutive *aphII* promoter.

The Dshi_1135 gene was PCR amplified from genomic *D. shibae* DNA with the primer pair EH725/ EH650 with its native stop codon and the resulting product was cloned into the *Sac*I and *Nde*I sites of pRhokS, yielding the plasmid pRhokS_Dshi1135. DNA sequencing with standard primer T7 (Eurofins Genomics, Ebersberg, Germany) was performed to confirm successful cloning. For diparental mating into *D. shibae* Dshi_1135::Tn, the plasmid was transformed into *E. coli* ST18 cells.

3.5.11 DNA Sequencing

For the conformation of successful DNA modification (cloning and site directed mutagenesis), the sequence of the respective DNA region was determined by the company Eurofins Genomics (Ebersberg, Germany) according to the sanger method (Sanger *et al.,* 1977). Resulting sequence files were analysed with the Lasergene® software package (DNASTAR, Madison, WI, USA) or the multiple sequence alignment program Clustal Omega.

3.6 Protein Biochemical Methods

3.6.1 Recombinant Protein Production

3.6.1.1 Expression Analysis of Recombinant Protein Production

Expression analyses were performed to determine optimal time and temperature and additive and IPTG concentrations for the recombinant production of different proteins used in this study, using different expression strains and plasmid combinations.

For this purpose, 30 ml LB medium were supplemented with the respective antibiotics

and additives and then inoculated with a pre-culture, carrying the desired expression plasmid (start OD_{578}= 0.05). Cells were grown at 37 °C and 200 rpm to an OD_{578}= 0.5-0.6. IPTG was used at concentrations between 50 µM and 1 mM to induce protein expression and further cultivation was carried out at 17 °C, 25 °C, 30 °C and 37 °C, respectively, and shaking at 180 rpm overnight. Samples for optical cell density measurements of the cultures were taken after 0 h (before induction), 1 h, 2 h, 3 h, 4 h and 18 h after induction. In parallel, samples corresponding to an OD_{578}= 2 were additionally taken at the indicated time points for expression analyses and transferred into 1.5 ml reaction tubes. Cells were sedimented (1 min, 11'337 x g) and the liquid medium was decanted. The obtained cell pellets were solubilized in 40 µl of lysis buffer and incubated for 1 h at 25 °C for cell lysis. To obtain the soluble and insoluble protein fractions, the lysed cells were centrifuged for 1 h at 9'391 x g and 4 °C. The supernatants, containing the soluble protein fraction, were transferred into fresh 1.5 ml reaction tubes, the sediments, containing the insoluble protein fraction, were dissolved in 20 µl dH_2O. All samples were mixed with 2x SDS loading dye, denatured for 10 min at 95 °C and analysed by SDS-PAGE.

Lysis buffer	0.5 mg/ml	lysozyme in Z-buffer
Z-buffer	60 mM	Na_2HPO_4
	40 mM	NaH_2PO_4
	10 mM	KCl
	1 mM	$MgSO_4$
2x SDS loading dye	50 mM	Tris-HCl (pH 6.8)
	10 % (v/v)	glycerol
	2 mM	β-mercaptoethanol
	2 % (w/v)	SDS
	0.1 % (w/v)	bromophenol blue

3.6.1.2 Production of Dshi_1135 Protein Variants from *D. shibae* in *E. coli* BL21-CodonPlus(DE3)-RIL

For recombinant production of the Dshi_1135 protein from *D. shibae* and the corresponding mutant proteins, 500 ml LB medium in a baffled flask supplemented with 100 µg/ml Amp were inoculated with an *E. coli* BL21-CodonPlus(DE3)-RIL pre-culture, carrying the desired plasmid, with an OD_{578}= 0.05. Cultures were incubated at 37 °C and 200 rpm to an OD_{578}= 0.5-0.6. Recombinant protein production was then induced by the addition of 50 µM IPTG to the culture. From that time point, cultures were kept in the dark by using special flask covers (aquila biolabs, Baesweiler, Germany), due to the light sensitivity of the Dshi_1135 protein. Cultivation was continued at 17 °C and 180 rpm overnight. Cells were transferred into 1 L centrifugation bottles and harvested by centrifugation (20 min, 3000 x g, 4 °C). The supernatant was discarded and the remaining cell pellet was resuspended in 15 ml of cold disruption buffer A und subsequently employed for protein purification. All steps after the cultivation of cells were performed under dim red light, using a red light LED (DF-7012-12, Conrad, Hirschau, Germany).

Disruption buffer A	50 mM	Tris-HCl (pH 8.2)
	500 mM	NaCl

3.6.1.3 Production of Dshi_1135 from *D. shibae* in *E. coli* Lemo21(DE3)

Alternatively to the *E. coli* BL21-CodonPlus(DE3)-RIL expression strain, *E. coli* Lemo21 (DE3) was used for the recombinant production of Dshi_1135 protein. This strain is an *E. coli* BL21 (DE3) derivative and contains an additional plasmid called pLemo that carries the *lysY* gene under control of the *rha*BAD promoter. The *lysY* gene codes for T7 lysozyme, a natural inhibitor of the T7 RNA polymerase. Expression of the *lysY* gene can be modulated by the addition of L-rhamnose and thus, the concentration of L-rhamnose also tunes the T7 RNA polymerase activity and expression of the target protein. Therefore, this tunable T7 expression system that is provided by *E. coli* Lemo21 (DE3) can alleviate inclusion body formation of challenging proteins and results in higher amounts of soluble protein.

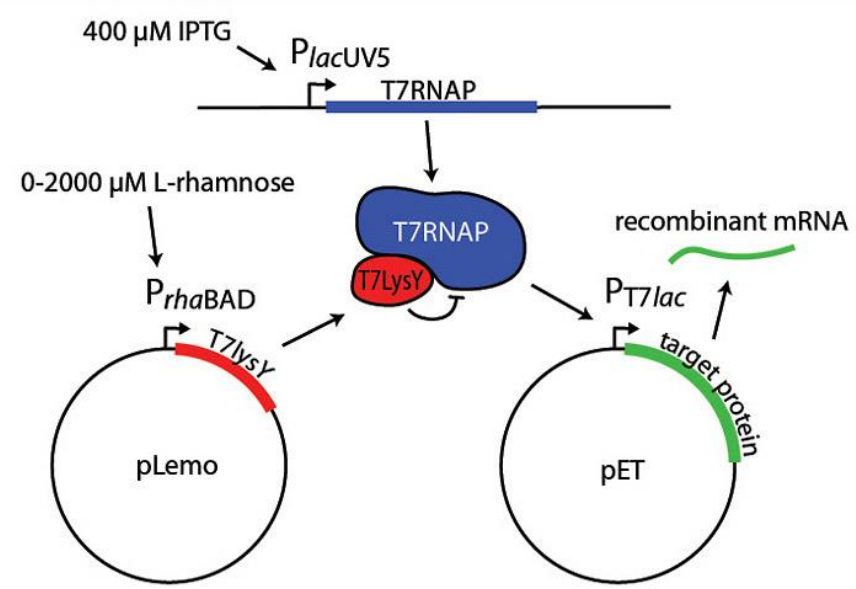

Figure 11: Tunable T7 expression strain *E. coli* Lemo21 (DE3)
Overview of the *E. coli* Lemo21 (DE3) expression system (NEB application note). The *E. coli* Lemo21 (DE3) host strain harbors the typical features for a T7 RNA polymerase dependent expression of target proteins. Additionally, the strain contains the pLemo plasmid that carries a T7 *lysY* gene copy encoding for T7 lysozyme, a natural inhibitor of T7 RNA polymerase. T7 lysozyme is expressed from a well L-rhamnose titratable *rha*BAD promoter. T7 RNA polymerase activity can be modulated by varying levels of L-rhamnose, which results in different levels of protein expression.
Overview from NEB application note for *E. coli* Lemo21(DE3) competent cells (New England BioLabs, Ipswich, MA, USA).

In this study *E. coli* Lemo21 (DE3) cells were used for the recombinant production of StrepII-tagged Dshi_1135 protein. Pre-cultures of with the respective expression plasmid were prepared in LB medium supplemented with 100 µg/ml Amp and 34 µg/ml Cml, to maintain the expression plasmid and pLemo. For protein production in baffled flasks, 500 ml LB medium containing 100 µg/ml Amp, 34 µg/ml Cml and 750 µM L rhamnose were inoculated with an OD_{578}= 0.05, using the prepared pre-culture. Cultures were grown at 37 °C and 200 rpm until an OD_{578}= 0.5-0.6 was reached and expression of Dshi_1135 was induced by addition of 400 µM IPTG to the medium. Further incubation was performed at 25 °C and 180 rpm overnight. Because of the light sensitivity of Dshi_1135, special black flask covers (aquila biolabs, Baesweiler, Germany) were used during cultivation to prevent light exposure. The cell culture was transferred into centrifugation bottles and cells were harvested for 20 min at 3000 x g and 4 °C. The resulting supernatant was discarded and the cell sediment was dissolved in 15 ml of cold disruption buffer A and directly used for protein purification. All steps after cell harvesting were performed under dim red light (DF-7012-12 (red), Conrad, Hirschau, Germany).

3.6.1.4 Production of Dshi_1135 from *D. shibae* Using Self-Inducing Reagents

Self-inducing reagents (Studier, 2005) can be applied for protein production in T7-regulated bacterial expression systems. Here, no monitoring of cell optical density and IPTG induction are necessary.

For overproduction of StrepII-tagged Dshi_1135 protein 930 ml LB medium were supplemented with 100 µg/ml Amp and self-inducing reagents (see chapter 3.3.2.1) in a 2 L Erlenmeyer flask. The medium was inoculated with an *E. coli* BL21-CodonPlus(DE3)-RIL pre-culture carrying the pET52b(+)Dshi1135Full plasmid in a ratio of 1:100 and cells were grown overnight at 17 °C and 180 rpm. The next day the obtained culture was transferred into a 1 L centrifuge bottle and cells were harvested by centrifugation (20 min, 3000 x g, 4 °C). Cell sediment was dissolved in 15 ml of cold disruption buffer A and used for protein purification.

3.6.1.5 Production of Dshi_1135 from *D. shibae* in *V. natriegens* Vmax™ Express Cells

The Vmax™ Express system is a novel bacterial strain that was designed for fast and high yield protein expression. Vmax™ Express cells are derived from the marine bacterium *V. natriegens*. With a doubling time of less than 15 min *V. natriegens* is almost twice as fast as *E. coli* and therefore is the microorganism with the fastest known growth rate.

In this study, Vmax™ Express cells were used for the overproduction of GST-tagged Dshi_1135 protein. For this purpose, 500 LB3 medium in a baffled flask, containing 75 µg/ml Amp, were inoculated with a respective pre-culture in a ratio of 1:100. Afterwards cells were aerobically cultivated at 30 °C and 200 rpm to an OD_{578}= 0.5-1. Protein production was induced by adding 1 mM of IPTG and cultures were immediately covered with special flask covers (aquila biolabs, Baesweiler, Germany) to prevent illumination of the cells. Further growth occurred for 4 h or overnight at 30 °C and 200 rpm, respectively. For cells harvesting cultures were transferred into 1 L centrifuge bottles and centrifuged for 20 min at 3000 x g and 4 °C. The obtained cell pellet was resuspended in 15 ml of cold disruption buffer and the suspension was directly employed for protein purification.

3.6.1.6 Heterologous Production of Dshi_3837, Dshi_1538 and Dshi_1406 from *D. shibae* in *E. coli* BL21-CodonPlus(DE3)-RIL

The three potential response regulators Dshi_3837, Dshi_1538 and Dshi_1406 were produced in *E. coli* BL21-CodonPlus(DE3)-RIL containing the respective expression plasmid.

For each protein 500 ml LB medium and 100 µg/ml Amp in a baffled flask were inoculated with a pre-culture (OD_{578}= 0.05) and grown at 37 °C and 200 rpm to an OD_{578}= 0.5-0.6. Expression was induced by addition of IPTG to a final concentration of 50 µM and incubation was continued overnight at 17 °C and 180 rpm. For cell harvesting the cultures were transferred into 1 L centrifuge bottles and spun down for 20 min at 3000 x g and 4 °C. The supernatant was decanted and the resulting cell pellet was solubilized in 15 ml of cold disruption buffer B. Cell suspensions were either stored at -20 °C or directly used for protein purification.

Disruption buffer B	50 mM	Tris-HCl (pH 7.5)
	500 mM	NaCl

3.6.2 Cell Disruption and Ultracentrifugation

For purification of heterologously produced proteins used in this study the corresponding cell suspensions were supplemented with 1 µl Benzonase® Nuclease (Merck, Darmstadt, Germany) and subsequently disrupted by a single or double passage through a hydraulic French® Press at 19'200 p.s.i. To pellet the insoluble cell components after cell lysis, the obtained extracts were centrifuged for 1:05 h at 110'000 x g and 4 °C. The resulting supernatant, containing the soluble protein fraction, was directly used for protein purification *via* affinity chromatography.

Due to the light sensitivity of the Dshi_1135 protein, all steps were performed under dark or red light conditions, respectively.

3.6.3 Protein Purification by Affinity Chromatography

3.6.3.1 Affinity Chromatography of StrepII-Tagged Proteins

Purification of StrepII-tagged Dshi_1135 was performed at 4 °C and under dark or dim red light conditions, respectively. For purification of StrepII-tagged proteins Poly-Prep® Chromatography columns (Bio-Rad, Hercules, CA, USA) were packed with 1 ml Strep-

Tactin® Superflow® high-capacity resin (iba, Göttingen, Germany) and equilibrated with 10 column volumes (CV) washing buffer. Washing buffer A1 was used as standard washing buffer, washing buffer A2 und A3 were modified washing buffers to enhance protein solubility. To mask biotinylated proteins, the soluble protein fraction after ultracentrifugation was supplemented with avidin (150 µl per 1 L cell culture; stock: 2 mg/ml) and incubated for 15 min at 4 °C on a roller mixer. Afterwards, the cell free extract was loaded onto the prepared column to allow binding of StrepII-tagged proteins by gravity flow. Extensive washing with 2x 10 CV of washing buffer was performed to remove non-specifically bound proteins from the resin. For elution of the protein of interest, the column was sealed at the bottom and 1 CV of elution buffer A was added. The column was incubated for 5 min and then opened for elution of the protein fraction. This step was repeated 6 times. The obtained protein fractions were stored constantly in the dark at 4 °C until further use.

Buffers for purification of Dshi_1135 from *D. shibae*:

Washing buffer A1	50 mM	Tris-HCl (pH 8.2)
	150 mM	NaCl
	5 mM	$MgCl_2$
	10 % (v/v)	glycerol
Washing buffer A2	50 mM	Tris-HCl (pH 8.2)
	150 mM	NaCl
	5 mM	$MgCl_2$
	10 % (v/v)	glycerol
	0.1 % (w/v)	Triton X-100
Washing buffer A3	50 mM	Tris-HCl (pH 8.2)
	500 mM	NaCl
	5 mM	$MgCl_2$
	10 % (v/v)	glycerol
	0.1 % (w/v)	Triton X-100

Elution buffer A	2.5 mM	D-desthiobiotin
	in washing buffer A1, A2 or A3, respectively	

Buffers for purification of Dshi_3837, Dshi_1538 and Dshi_1406 from *D. shibae*:

Washing buffer B	50 mM	Tris-HCl (pH 7.5)
	150 mM	NaCl
Elution buffer B	2.5 mM	D-desthiobiotin
	in washing buffer B	

3.6.3.2 Affinity Chromatography of GST-tagged Proteins

All purification steps of GST-tagged Dshi_1135 were performed at 4 °C and dark and dim red light conditions, respectively. GST-tagged proteins were purified using a Poly-Prep® Chromatography column (Bio-Rad, Hercules, CA, USA) packed with 1 ml Protino® Glutathione Agarose 4 B resin (Macherey-Nagel, Düren, Germany) that was equilibrated with 10 CV washing buffer B. The cell free extract after ultracentrifugation, containing the protein of interest, was loaded onto the prepared column and protein binding to the resin was allowed by gravity flow. After complete flow through, the resin was washed twice using 10 CV washing buffer B and then proteins were eluted with 6x 1 CV elution buffer C and constantly stored in the dark at 4 °C.

Elution buffer C	20 mM	glutathione
	in washing buffer B	

3.6.4 Protease Digestion for Removal of Affinity Tags

For on-column cleavage of affinity tags during protein purification, proteins bound to the resin were incubated overnight with PreScission™ Protease (GE Healthcare, Chalfont St Giles, UK).

Therefore, 1.2 CV of the respective washing buffer were loaded onto the sealed column after the washing steps occurred and 200 U PreScission™ Protease were added. Incubation occurred overnight at 4 °C under constant rolling. Proteins were eluted with

6x 1 CV of the desired washing buffer. If necessary, the GST-tagged PreScission™ Protease was removed from the elution fractions, using a second Poly-Prep® Chromatography column with Protino® Glutathione Agarose 4 B resin. Storage of purified proteins occurred in the dark at 4 °C.

3.6.5 Protein Concentration

Purified Dshi_1135 protein was concentrated up to a desired concentration using a centrifugal filter device with a molecular weight cut off (MWCO) of 30 kDa (Amicon® Ultra 0.5, Merck, Darmstadt, Germany) according to manufacturer's instructions.

3.6.6 Determination of Protein Concentration

Protein concentrations were determined photometrically, using the Bradford method (Bradford, 1976) that is based on an absorbance shift of the dye Coomassie Brilliant Blue G-250 from 465 nm to 595 nm when complexed with proteins.

1 ml Bradford reagent (Sigma-Aldrich, St. Louis, MO, USA) was mixed with 30 µl of a purified protein sample and incubated at room temperature for 15 min in the dark. Afterwards the absorbance was measured at 595 nm and protein concentration was calculated using an appropriate Bovine Serum Albumin (BSA) calibration curve.

3.6.7 Determination of FMN Content

The FMN content of purified Dshi_1135 protein was quantified by UV/Vis spectroscopy using an extinction coefficient of ε_{280}= 30'535 $M^{-1} \cdot cm^{-1}$ for Dshi_1135 and ε_{450}= 12'200 $M^{-1} \cdot cm^{-1}$ for FMN.

3.6.8 Reconstitution of Dshi_1135 Protein with FMN

For reconstitution of purified Dshi_1135 protein with FMN the elution fractions E1 and E2 were pooled in a 1.5 ml reaction tube and 100 µM FMN solution (stock: 10 mg/ml in dH_2O) were added and the components were well mixed. The solution was incubated for 30 min at 4 °C under constant rolling. To remove unbound FMN from the protein, the protein-FMN mixture was loaded onto a NAP-25 Column (GE Healthcare, Munich, Germany) that was prepared according to manufacturer's instructions. The protein was eluted in the desired washing buffer and stored at 4 °C under dark conditions. All steps were performed at 4 °C under dim red light.

3.6.9 UV/Visible Light Absorption Spectroscopy

UV/Vis spectroscopy was used for cofactor determination and photocycle experiments of the Dshi_1135 protein. Spectra were recorded at room temperature from 200-700 nm on a V-650 spectrophotometer (Jasco, Groß Umstadt, Germany), using a quartz cuvette with 10 mm path length.

For cofactor determination and analyses of the ground state of Dshi_1135, the protein was kept in the dark and only handled under dim red light conditions before spectra recording. For signaling state experiments the protein was illuminated with blue light (LED growth light, LL-GL001, Albrillo) for 5 min before immediate data collection.

Additionally, UV/Vis spectroscopy was used for analyses of extracted bacteriochlorophyll *a* and carotenoid compounds of different *D. shibae* strains. The absorbance was measured using a V-650 spectrophotometer (Jasco, Groß Umstadt, Germany) in quartz cuvettes (path length 10 mm) from 200-900 nm.

All spectra were analysed using the JASCO software Spectra Manager™.

3.6.10 Discontinuous SDS Polyacrylamide Gel Electrophoresis (SDS-PAGE)

Discontinuous sodium dodecyl sulfate polyacrylamide gel electrophoresis (SDS-PAGE) is a method where proteins are electrophoretically separated according to their molecular masses (M_r). In this study SDS-PAGE was performed according to Laemmli (Laemmli, 1970) with modifications by Righetti (Righetti, 1990) for discontinuous SDS-PAGE.

For SDS-PAGE analysis, proteins were mixed with 2x SDS loading dye and denatured for 10 min at 95 °C. Afterwards, samples were loaded onto 12 % (w/v) or 15 % (w/v) SDS gels, respectively, depending on the M_r of the protein. The gels were run in electrophoresis buffer at a current intensity of 45 mA until the bromophenol blue dye band reached the lower end of the gel. During electrophoresis proteins are focused first in the stacking gel and subsequently separated according to their M_r in the running gel. As protein size standard the PageRuler™ Prestained Protein Ladder, 10 to 180 kDa (Thermo Fisher Scientific, Waltham, MA, USA) was used. After the run, gels were stained in Coomassie Brilliant Blue G-250 solution for 2 h or overnight and subsequently destained until distinct protein bands became visible. Alternatively, InstantBlue™ (Expedeon Inc., San Diego, CA, USA) was used for gel staining according to manufacturer's instructions. Gels were documented on a BIO-5000 Plus VIS gel scanner (Serva, Heidelberg, Germany).

Running gel, 12 % (w/v)	2 ml	Rotiphorese® Gel 30 (37.5:1)
	1.25 ml	1.5 M Tris-HCl, pH 8.8 with 0.4 % (w/v) SDS
	1.75 ml	dH_2O
	50 µl	10 % (w/v) ammonium peroxodisulphate (APS)
	5 µl	N,N,N',N',-tetramethyl ethylene diamine (TEMED)
Running gel, 15 % (w/v)	2.5 ml	Rotiphorese® Gel 30 (37.5:1)
	1.25 ml	1.5 M Tris-HCl, pH 8.8 with 0.4 % (w/v) SDS
	1.25 ml	dH_2O
	50 µl	10 % (w/v) APS
	5 µl	TEMED
Stacking gel, 6 % (w/v)	0.5 ml	Rotiphorese® Gel 30 (37.5:1)
	625 µl	0.5 M Tris-HCl, pH 6.8 with 0.4 % (w/v) SDS
	1.375 ml	dH_2O
	25 µl	10 % (w/v) APS
	2.5 µl	TEMED
Electrophoresis buffer	50 mM	Tris-HCl (pH 8.4)
	380 mM	glycine
	0.1 % (w/v)	SDS
Staining solution	10 % (v/v)	acidic acid
	30 % (v/v)	ethanol
	0.25 % (w/v)	Coomassie Brilliant Blue
Destaining solution	10 % (v/v)	acidic acid
	30 % (v/v)	ethanol

3.6.11 Immunochemical Detection of Proteins by Western Blot

3.6.11.1 Detection of GST-tagged Proteins

For immunochemical detection the GST-tagged proteins were first separated by SDS-PAGE and then transferred onto a polyvenylidene difluoride (PVDF) membrane (Immobilon-P Transfer Membrane with a pore size of 0.45 µm, Merck, Darmstadt, Germany) using the semi-dry Trans-Blot® Turbo™ system (Bio-Rad, Hercules, CA, USA).

First, the PVDF membrane was activated for 15 min in methanol and then subsequently equilibrated in Towbin buffer. After SDS-PAGE the unstained gel, together with two pieces of Whatman paper, was equilibrated in Towbin buffer as well for 15 min. For the semi-dry blotting apparatus all components were assembled in the following order: anode, blotting paper, membrane, SDS gel, blotting paper, cathode. Blotting of the proteins onto the membrane occurred at 25 V for 16 min. Next, the membrane was blocked overnight at 4 °C in blocking solution and washed afterwards three times in washing buffer C for 5 min. For detection of GST-tagged proteins the membrane was incubated in washing buffer C, containing 1:20'000 diluted Anti-GST-Alkaline Phosphatase Conjugate antibody (Sigma-Aldrich, Steinheim, Germany) for 2 h. Afterwards the membrane was washed three times with washing buffer C for 5 min and subsequently proteins were visualized by incubation of the membrane in reaction buffer. The reaction was stopped by several washing steps with dH_2O after the desired protein band intensity was reached.

Towbin buffer	25 mM	Tris-HCl (pH 9.5)
	192 mM	glycine
10 x PBS	1.37 M	NaCl
	27 mM	KCl
	100 mM	Na_2HPO_4
	20 mM	KH_2PO_4
Blocking solution	5 % (w/v)	BSA
	10 % (v/v)	10 x PBS
	0.5 % (v/v)	Tween 20

Washing buffer C	1 % (v/v)	BSA
	10 % (v/v)	10 x PBS
	0.5 % (v/v)	Tween 20
AP buffer	100 mM	Tris-HCl (pH 9.5)
	100 mM	NaCl
	5 mM	$MgCl_2$
NBT solution	100 mg/ml	NBT in 70 % (v/v) DMF
BCIP solution	50 mg/ml	BCIP in 100 % (v/v) DMF
Reaction buffer	50 ml	AP buffer
	165 µl	NBT solution
	165 µl	BCIP solution

3.6.11.2 Detection of Strep-Tagged Proteins

For immunochemical detection of Strep-tagged proteins, proteins of interest were electrophoretically separated by SDS-PAGE and the resulting unstained gel was blotted onto a PVDF membrane (Immobilon-P Transfer Membrane with a pore size of 0.45 µm, Merck, Darmstadt, Germany), using a Trans-Blot® SD Semi-Dry Transfer Cell (Bio-Rad, Hercules, CA, USA).

Initially, the membrane was activated in methanol for 15 min and subsequently equilibrated in Towbin buffer. The unstained SDS gel was also equilibrated in Towbin buffer for 15 min, together with ten pieces of Whatman paper. For the semi-dry blotting apparatus all components were assembled in the following order: anode, blotting paper, membrane, SDS gel, blotting paper, cathode. Proteins were transferred onto the prepared PVDF membrane at 10 V for 30 min according to the semi dry method. Afterwards the membrane was blocked at room temperature for 1 h or alternatively at 4 °C overnight in blocking solution und subsequently washed three times in PBST for 10 min. To avoid unspecific binding of the used Strep-tag® II specific monoclonal antibody (StrepMAB-Classic, iba, Göttingen, Germany) to biotinylated molecules, the membrane was incubated in PBST, containing 10 µl avidin solution (stock: 2 mg/ml)

for 10 min. Then, 2.5 µl of the antibody were added to the buffer and the membrane was incubated for 1 h at room temperature. After incubation the membrane was washed twice in PBST for 2 min, followed by two washing steps with PBS for 2 min. Visualization of protein bands occurred in reaction buffer as described for GST-tagged proteins (see chapter 3.6.11.1).

PBST	10 % (v/v)	10 x PBS
	0.1 % (v/v)	Tween 20

3.6.12 Determination of Native Molecular Mass

To determine the native molecular mass and the oligomeric state of the Dshi_1135 protein, analytical gel permeation chromatography (GPC) was performed, using the Superdex™ 200 Increase 5/150 GL column (GE Healthcare, Chalfont St Giles, UK), equilibrated with GPC buffer A, B or C, respectively. GPC buffer A was used as standard buffer, GPC buffers B and C were used to enhance protein stability. For column calibration and generation of a calibration curve, several protein standards from the Gel Filtration Markers Kit for Protein Molecular Weights 12'000-200'000 Da (Sigma-Aldrich®, St. Louis, MO, USA) were used.

Sample volumes of 5-150 µl were loaded onto the column and eluted at a constant flow rate of 0.45 ml/min over a period of 1.5 CV. Absorbance at 260 nm and 280 nm was recorded to monitor DNA and protein elution, respectively. Native molecular masses were calculated with the generated calibration curve and detected elution volumes of injected protein samples and protein standards.

GPC buffer A	50 mM	Tris-HCl (pH 8.2)
	150 mM	NaCl
	5 mM	$MgCl_2$
	10 % (v/v)	glycerol

GPC buffer B	50 mM	Tris-HCl (pH 8.2)
	150 mM	NaCl
	5 mM	$MgCl_2$
	10 % (v/v)	glycerol
	0.1 % (w/v)	Triton X-100
GPC buffer C	50 mM	Tris-HCl (pH 8.2)
	500 mM	NaCl
	5 mM	$MgCl_2$
	10 % (v/v)	glycerol
	0.1 % (w/v)	Triton X-100

3.6.13 Thermal Shift Assay

Thermal shift assays can be used to determine the stability and the specific melting temperature of a protein of interest. During the assay, the protein sample is mixed with the fluorescence dye SYPRO® Orange and exposed to increasing temperatures. When the protein starts to denature it loses its tertiary structure and hydrophobic amino acid residues are exposed to the surface. At this time point, SYPRO® Orange binds to these hydrophobic areas, which leads to an increase in fluorescence. A melting curve is recorded, using the detected intensities and the maximum of the first derivative of this curve corresponds to the specific melting temperature of the protein (Niesen *et al.,* 2007).

For the thermal shift assay 40 µl protein buffer, 5 µl protein sample (0.5, 1 and 2 mg/ml) and 5 µl SYPRO® Orange Protein Gel Stain (Thermo Fisher Scientific, Waltham, MA, USA) solution (10 x, 50 x or 100 x) were mixed in a 96 well micro titer plate (Bio-Rad, Hercules, CA, USA) and sealed air tight. The melting curve was recorded in a real-time PCR machine (C1000™ Thermal Cycler with CFX96™ real-time system, Bio-Rad, Hercules, CA, USA) and the samples were heated from 10 °C to 90 °C in 0.5 °C steps. In parallel, the fluorescence was recorded at 570 nm in 15 sec intervals. Melting points were calculated with the CFX Manager software (Bio-Rad, Hercules, CA, USA).

3.6.14 Autophosphorylation Assay

For autophosphorylation assays 10 µM of purified Dshi_1135 protein were mixed with 5 µCi [γ-^{32}P] ATP (Hartmann Analytic, Braunschweig, Germany) and 100 µM ATP solution at room temperature under dim red light conditions. Afterwards, samples were either further incubated in the dark or immediately illuminated with a camera flash (Nikon D3300), followed by exposure to blue light (LED growth light, LL-GL001, Albrillo). At desired time points samples were quenched by adding 2x SDS loading dye and subsequent flash freezing in liquid nitrogen. Samples were denatured for 10 min at 95 °C and employed for SDS-PAGE on a 12 % (w/v) SDS gel. After the run the resulting gel was transferred onto a piece of Whatman paper and wrapped in cling film. In the darkroom under red light conditions an X-ray film (Fuji Medical X-Ray Film Super RX-N, Fujifilm, Minato, Tokyo, Japan) was applied on the gel and exposure occurred overnight at room temperature. Visualization of ^{32}P incorporation was enabled *via* autoradiography.

3.6.15 Autoradiography

This technique was used to visualize the incorporation of the isotope ^{32}P into the Dshi_1135 protein after autophosphorylation experiments. The exposed X-ray film was processed in the darkroom, using Adelfo Citroline 2000 and Adefofix Fixer (Adefo Chemie, Neu-Isenburg, Germany) according to manufacturer's instructions.

3.6.16 Phos-tag™ SDS-PAGE

Phos-tag™ was developed by Kinoshita *et al*. at the Department of Functional Molecular Science at Hiroshima University (Japan) and is a functional molecule that was designed from the catalytic domain of an alkaline phosphatase and is capable to specifically capture phosphorylated amino acid residues, such as serine, aspartate or histidine.

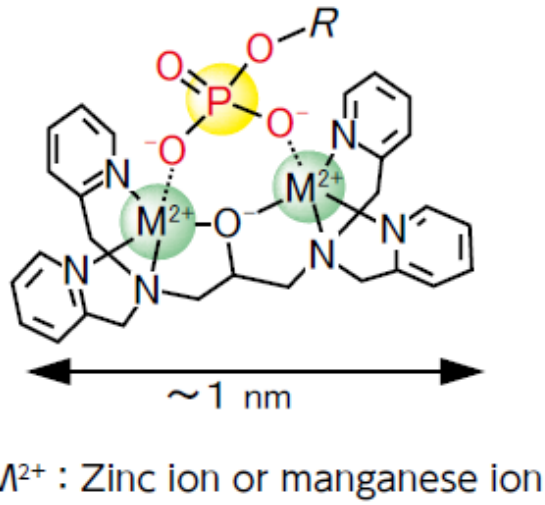

Figure 12: Phos-tag™ structure
Phos-tag™ is a functional molecule that is able to trap phosphorylated proteins with divalent metal ions like zinc or manganese during migration in an SDS gel and forms a stable complex under physiological conditions. It is derived from a catalytic domain of an alkaline phosphatase.
Overview from the Phos-tag™ SDS-PAGE guidebook (FUJIFILM Wako Chemicals Europe, Neuss, Germany).

Divalent metal ions like zinc or manganese are incorporated in the Phos-tag™ molecule and are able to trap phosphorylated proteins by building a non-covalent complex. Multiple applications for the Phos-tag™ are available; one is the Phos-tag™ SDS-PAGE. Using this method, it is possible to separate phosphorylated and non-phosphorylated proteins during electrophoresis by adding either $ZnCl_2$ or $MnCl_2$, respectively, as metal ions and the Phos-tag™ to the SDS running gel. During electrophoresis, phosphorylated proteins are trapped earlier in the gel than non-phosphorylated proteins and therefore separation is dependent on the phosphorylation level and not on the relative molecular mass. In general, the migration velocity of proteins gets slower, the higher the level of phosphorylation is.

In this study Phos-tag™ SDS-PAGE was performed to show the blue light induced autophosphorylation of the Dshi_1135 protein. For this purpose, 4-15 µM of the purified protein were mixed with ATP (1 µM-40 mM) under red light conditions at room temperature and then either incubated in the dark for 2 to 24 hours or immediately exposed with a camera flash and then also incubated for 2 to 24 hours under blue light (LED growth light, LL-GL001, Albrillo) irradiation. After incubation of the samples the reaction was stopped by the addition of 2x SDS loading dye, but the samples were not denatured to prevent possible heat sensitive phosphorylation from being destroyed. Subsequently, 10 % SDS gels supplemented with 20-100 µM Phos-tag™ and 40-

200 µM $MnCl_2$ were prepared according to manufacturer's instructions (FUJIFILM Wako Chemicals Europe, Neuss, Germany). Samples were loaded onto the gel and electrophoretic separation occurred at 30-60 mA in electrophoresis buffer until the bromophenol blue dye front reached the lower end of the gel. As positive control, an α-casein solution (FUJIFILM Wako Chemicals Europe, Neuss, Germany), composed of phosphorylated and non-phosphorylated molecules, was used. After the run the proteins in the gel were fixed according to manufacturer's instructions and then visualized either by Coomassie Brilliant Blue staining or InstantBlue™ (Expedeon Inc., San Diego, CA, USA), respectively.

3.6.17 Acetone/Methanol Extraction of Pigments

For pigment extraction cells corresponding to an OD_{578}= 2.5 of the desired *D. shibae* strain were transferred into a 15 ml screw cap tube and sedimented by centrifugation (10 min, 2500 x g, 4 °C). The supernatant was discarded and the pellet was dissolved in 1 ml acetone/methanol (7:2) solution. Afterwards, incubation of the cell solution occurred on a tumbler mixer at room temperature for 1 h in the dark. Subsequently cell debris was removed by centrifugation for 5 min at 2500 x g and the resulting supernatant was transferred into a quartz cuvette for UV/Vis spectroscopy. The aceton/methanol (7:2) solution served as blank.

3.6.18 β-Galactosidase Activity Assay

To test the activity of different promoter-*lacZ* reporter gene fusions, β-galactosidase activity assays were performed. *D. shibae* strains carrying the desired plasmid were grown in SWM medium at 25 °C and 180 rpm under different light conditions (dark, blue light or white light, respectively) to an OD_{578}= 0.5 to 0.8. Then, 250 µl, 500 µl and 1 ml samples of the cultures were taken and transferred into fresh 2 ml reaction tubes and the cells were pelleted by centrifugation (5 min, 11'337 x g). Supernatants were discarded and the resulting pellets were dissolved in 800 µl Z-buffer supplemented with 50 mM β- mercaptoethanol and 5 µl lysozyme-DNase solution and then incubated for 30 min at 37 °C for cell lysis. Afterwards, the β-galactosidase activity assay was started by adding 200 µl *ortho*-nitrophenyl-β-galactoside (ONPG) solution and thorough mixing of the samples. Immediately when a color change from colorless to yellow was observed, the reaction was stopped by adding 500 µl of 1 M Na_2CO_3 and the time required between start and stop was noted. At the end all samples were centrifuged (5

min, 11'337 x g) and the OD_{420} and OD_{550} of the supernatants were determined. All β-galactosidase activity assays were performed in biological and technical triplicates. β-galactosidase activity was expressed in Miller Units (MU) (Miller, 1992) and calculated using the following equation:

$$\text{Miller Units} = \frac{A_{420} - (1.75 \cdot A_{550})}{V \cdot t \cdot OD_{578}} * 1000$$

A_{420}:	absorbance at a wavelength of 420 nm
A_{550}:	absorbance at a wavelength of 550 nm
OD_{578}:	optical density of the employed cell culture
V [ml]:	volume of the employed cell culture
t [min]:	time of enzymatic reaction

DNase solution	10 µl/ml	sodium acetate (3 M)
	25 mg/ml	DNase/ bovine pancreas grade II
Lysozyme-DNase solution	7 mg/ml	lysozyme
	50 µg/ml	DNase solution
ONPG solution	4 mg/ml	*ortho*-nitrophenyl-β-galactopyranoside

4 Results and Discussion

The *D. shibae* transposon mutant library was screened for the identification of new potential regulators involved in the regulation of Bchl *a* biosynthesis (Heyber, 2021). Among others, the Dshi_1135::Tn mutant strain, which completely lacks pigmentation and Bchl *a* absorption, was identified. According to the *D. shibae* genome annotation, the Dshi_1135 gene locus encodes a PAS domain-containing protein. LOV photoreceptors are often defined as PAS domain-containing proteins, indicating a role of Dshi_1135 in the regulation of photosynthesis genes. The light-dependent regulation of the PGC has been shown by transcriptome analyses in the group of Irene Wagner-Döbler (Tomasch *et al.,* 2011). However, the exact regulatory mechanism was not elucidated until today. To investigate the role of the newly identified potential regulator Dshi_1135 in more detail, gene expression analyses were performed under different light conditions in the *D. shibae* wild type and Dshi_1135::Tn mutant strain. Here, it was evident that genes of the PGC were no longer activated in the Dshi_1135::Tn transposon mutant strain, independent of the light quality (Heyber, 2021). The Dshi_1135 protein has not yet been studied in detail. Therefore, a first aim of the present work was to characterize Dshi_1135 biochemically and to address the question, if the protein is actually a blue light-dependent LOV protein.

4.1 Biochemical Characterization of *D. shibae* Dshi_1135

4.1.1 Bioinformatic Analysis of Dshi_1135

The basic local alignment search tool (BLAST) is a bioinformatic program, to find regions of local similarity between sequences. It is commonly used to compare nucleotide or protein sequences to sequence databases and calculates the statistical significance of matches (Altschul *et al.,* 1990). During a BLAST search, the sequence of interest, called query, is compared with a database of known annotated sequences and genomes, with the objective to identify homologous genes or proteins.

During an initial BLAST analysis, using the Dshi_1135 amino acid sequence as query, the protein EL346 (locus tag ELI_04860) of the related organism *Erythrobacter litoralis HTCC2594* was identified with an identity score of 42 % and therefore considered a homolog. The EL346 protein is a well-studied monomeric LOV HK that consists of a N-terminal LOV domain, a dimerization/histidine phosphotransfer like domain (DHpL)

and a C-terminal catalytic domain (CA). It was shown to possess a FMN cofactor to undergo a photocycle under blue light illumination, which triggers HK activity (Swartz *et al.,* 2007; Rivera-Cancel *et al.,* 2014). The conversion into the active state is initiated by the destabilization of the LOV-DHpL domain interface. This causes the release of the CA domain that in turn is no longer in its inhibited conformation (Dikiy *et al.,* 2019). Phosphotransfer experiments revealed the proteins EL_PhyR and EL_LovR as target RRs of EL346. These proteins are known to participate in general stress response in α-Proteobacteria (Anna Staroń & Thorsten Mascher, 2010; Foreman *et al.,* 2012). Therefore, it is assumed that EL346 is part of a two-component system, involved in stress response in *E. litoralis* (Correa *et al.,* 2013).

The amino acid alignment of Dshi_1135 and EL346 showed some highly conserved regions (Figure 13). The GRNCRFLQ motif was found within the LOV domain of EL346 and Dshi_1135 and contains the essential cysteine residue for photo adduct formation. Between the LOV domain and DHpL domain of EL346 at amino acid position 118 a conserved glutamine residue is located. It is potentially involved in changes of hydrogen bond interactions upon blue light illumination and FMN N5 protonation. It is assumed that these alterations in the hydrogen bonding pattern contribute to the activation of the output domain (Nash *et al.,* 2008; Losi & Gärtner, 2017; Rivera-Cancel *et al.,* 2014). A homologous glutamine residue was found in the amino acid sequence of Dshi_1135 at position 124 and is therefore assumed to be involved in the activation of the output domain. Surprisingly, no homologous histidine residue for autophosphorylation was found in Dshi_1135 compared to the DHpL domain of EL346. In EL346 H142 was experimentally verified as the phosphoacceptor histidine (Rivera-Cancel *et al.,* 2014). At this position Dshi_1135 carries an arginine residue instated. However, two homologous histidine residues to EL346 were identified in the CA domain of Dshi_1135 at positions 218 and 258. This result provided the first indication that Dshi_1135 may be a blue light-activated LOV protein. For hypothesizing the kinase function of Dshi_1135, the results of bioinformatic analysis are not sufficient at this point.

Figure 13: Alignment of amino acid sequences of Dshi_1135 and EL346
The amino acid sequence of Dshi_1135 (*D. shibae*) was aligned against die amino acid sequence of EL346 (*E. litoralis*) and shows 42 % identity. The LOV domain, containing the conserved GRNCRFLQ motif (amino acid position 58-65) and the photoactive cysteine residue at position 61 are marked in blue. A conserved glutamine residue for activation of the output domain is marked in orange. The DHpL domain with the phosphor-accepting histidine 142 of EL346 and the arginine residue 148 of Dshi_1135 are marked in red. The CA domain is marked in green, containing two homologous histidine residues at amino acid positions 218 and 258 in Dshi_1135. Conserved H-, N-, D- and G-boxes are labelled. Asterisks indicate identical amino acids; dots indicate homologous amino acids. The amino acid alignment was generated using the multiple sequence alignment tool Clustal W (Larkin *et al.,* 2007).

To further classify Dshi_1135 as a LOV protein with potential kinase function, the protein sequence was compared to other known LOV HK amino acid sequences. Here, LovhK of *Brucella abortus*, LovK of *E. litoralis* DSM8509 and LovK of *C. cresentus* were chosen. All three proteins were shown to be blue light activated LOV HKs and are involved in general stress response in the respective organism (Kim *et al.,* 2014; Swartz *et al.,* 2007; Fiebig *et al.,* 2019; Foreman *et al.,* 2012). Overall, the proteins did not show sufficient similarity scores to classify them as homologs. However, some highly conserved regions and matching motifs important for LOV and HK domain activity were found in the sequences. In all protein sequences the GRNCRFLQ motif, containing the photoactive cysteine, was found. Furthermore, they shared the glutamine residue, that is most likely involved in activation of the output domain. All HKs share short blocks of conserved sequence motifs, called H-, N-, D-, F-, and G-boxes, resulting from their characteristic amino acid residues (Stock *et al.,* 1988; Stock *et al.,* 1995; Parkinson & Kofoid, 1992). According to the arrangement of these boxes, HKs can be classified into 11 subfamilies (Grebe & Stock, 1999). Based on the found homology boxes in the amino acid sequences, Dshi_1135 and the other HKs can be assigned to the HPK_{11} (histidine protein kinase) type (Figure 13). This classification has also been postulated by Rivera-Cancel *et al*. (2014) for *E. litoralis* EL346. The H-box is the most

variable sequence motif and is located on the N-terminal half of the HK domain and contains the phosphor-accepting histidine residue for autophosphorylation activity (Parkinson & Kofoid, 1992). All analysed protein sequences, besides Dshi_1135, possessed the conserved histidine residue within the H-box. As mentioned before, at this position in Dshi_1135, instead of the histidine, an arginine residue is located. Furthermore, the N, D and G-boxes were found in all protein sequences. The F-box is missing, which is not uncommon in this HPK subfamily (Wolanin *et al.,* 2002).

The high conservation of the GRNCRFLQ motif very clearly indicated that Dshi_1135 is a LOV protein. In contrast, no clear statement could be made about a potential HK activity. The conserved homology boxes suggested that Dshi_1135 is a HK, but the H-box lacks the histidine residue, which is required for autophosphorylation. In some cases, it was reported that HKs of the CheA family are completely missing the H-box and use a histidine residue near the N-terminus for autophosphorylation instead (Parkinson & Kofoid, 1992). It was also observed that in some kinases the conserved H-box histidine was substituted by other amino acids and autophosphorylation could still occur (Grebe & Stock, 1999; Wu *et al.,* 1999). For instance, rare cases of arginine kinases were found in bacteria. For the kinase Ark of *Myxococcus xanthus* it was demonstrated that it catalyzes the phosphorylation of an arginine by using ATP and is involved in fruiting body formation, cell differentiation and stress response (Bragg *et al.,* 2012). It would therefore be interesting to investigate if Dshi_1135 possesses an autophosphorylation activity and if one of the histidine residues or even the arginine residue is involved in autophosphorylation.

4.1.2 Improving the Efficiency of Heterologous Production and Purification of Dshi_1135

For the envisioned biochemical analyses of the Dshi_1135 protein it was necessary to produce and purify it in high yields and purity. For first overexpression experiments an *E. coli* BL21-CodonPlus(DE3)-RIL strain, carrying the pET52b(+)_Dshi1135Full plasmid (AG Härtig, TU Braunschweig, unpublished data) was used. The expression vector backbone carries the sequences for the inducible T7 promoter that enables controlled expression of the protein of interest, an Amp resistance cassette for selection, an N-terminal Strep-tag II for affinity chromatography and a PreScission™ Protease cleavage site for affinity tag removal. *E. coli* BL21-CodonPlus(DE3)-RIL is a commonly used T7 expression host, as it carries the gene sequence of the T7 RNA

polymerase under the control of an IPTG inducible promoter and thus enables the overexpression of the plasmid-encoded protein. In order to determine optimal conditions for the recombinant production of Dshi_1135, expression analyses were performed, using different cultivation temperatures and/ or different concentrations of inducing IPTG. Therefore, 100 ml LB medium were inoculated with an OD_{578}= 0.05 using a respective pre-culture and cells were grown at 37 °C and 200 rpm to an OD_{578}= 0.5-0.6. Subsequently protein expression was induced by adding 50 µM and 300 µM of IPTG, respectively. Cultivation of the cells was performed at 17 °C, 25 °C and 30 °C, respectively, and constant shaking for 18 h. Samples of each culture were taken and cells were disrupted and fractionated into the soluble and insoluble protein fraction by lysozyme treatment and subsequent centrifugation. The resulting protein samples were analysed *via* SDS-PAGE and Coomassie Brilliant Blue staining (Figure 14).

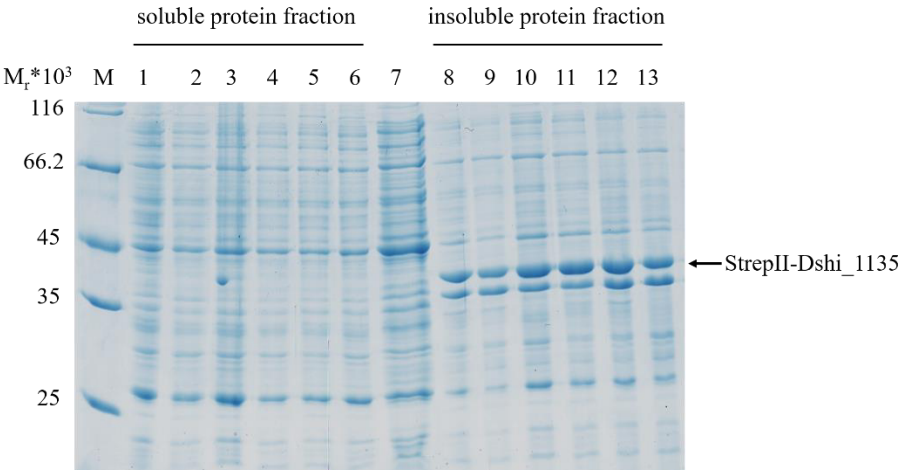

Figure 14: Determination of amount and localization of heterologously produced Strep-Dshi_1135 in *E. coli* BL21-CodonPlus(DE3)-RIL
Initial tests were performed by using 50 µM and 300 µM of IPTG for induction and cultivation at 17 °C, 25 °C and 30 °C, respectively. Samples were taken after 18 h of cultivation, fractionated by lysozyme digestion and subsequent centrifugation. The resulting soluble and insoluble protein fractions were mixed with 2x SDS loading dye and denatured at 95 °C for 10 min. Equal amounts of protein (corresponding to the OD_{578}) were analysed on 12 % SDS gels and visualized *via* Coomassie Brilliant Blue staining.
Lane M: molecular mass marker (relative molecular masses (*1'000) are indicated. Lane 1: 17 °C, 50 µM IPTG, Lane 2: 17 °C, 300 µM IPTG, Lane 3: 25 °C, 50 µM IPTG, Lane 4: 25 °C, 300 µM IPTG, Lane 5: 30 °C, 50 µM IPTG, Lane 6: 30 °C, 300 µM IPTG, Lane 7: before induction t_0, Lane 8: 17 °C, 50 µM IPTG, Lane 9: 17 °C, 300 µM IPTG, Lane 10: 25 °C, 50 µM IPTG, Lane 11: 25 °C, 300 µM IPTG, Lane 12: 30 °C, 50 µM IPTG, Lane 13: 30 °C, 300 µM IPTG.
The arrow highlights the protein band corresponding to StrepII-Dshi_1135 with an approximate relative molecular weight of 40'000.

The calculated molecular mass (M_r) of the StrepII-Dshi_1135 fusion protein is 39'400 Da and accordingly bands with this size were expected after successful production of StrepII-Dshi_1135 protein. However, no distinct bands were found in the

soluble protein fractions independent of growth temperature and IPTG concentration (Figure 14, lanes 1-6). In contrast in the insoluble protein fractions (Figure 14, lanes 8-13), two prominent bands with the relative M_r of 38'000 and 40'000 were detected in all samples with comparable intensity. The band with the relative M_r of 40'000 correlates well with the calculated M_r of StrepII-Dshi_1135. The lower band with a M_r of 38'000 might be attributed to degraded StrepII-Dshi_1135 protein. Both bands were not present in the t_0 sample prior to induction (Figure 14, lane 7), indicating a high repression of the T7 promoter in the absence of IPTG. The obtained results indicate that StrepII-Dshi_1135 was successfully but insolubly produced in *E. coli* BL21-CodonPlus(DE3)-RIL cells. The formation of such protein aggregates is a widespread problem during recombinant protein expression in *E. coli* and causes the formation of inclusion bodies. It is assumed that around 70 % of all recombinant proteins are overexpressed in inclusion bodies, which is the main limiting factor of the *E. coli* expression system (Yang *et al.,* 2011). A reason for aggregation during overexpression can be the fast translation machinery and the application of strong promoters, consequently causing unnaturally high protein concentration in the host cell. Fast overproduction is often accompanied by protein misfolding and thus inclusion body formation. Especially regulator proteins, as Dshi_1135 potentially is one, are prone to form aggregates in heterologous expression systems, because under physiological conditions they are only present in minor amounts.

To overcome the issue of protein aggregation, several approaches are available and described in the literature. One frequently used but often uncertain and inefficient method is refolding of the protein of interest from inclusion bodies, using denaturing and refolding reagents. However, attempts can also be made to prevent the formation of inclusion bodies in the first place and thus increase the amount of soluble protein. For instance, a slower expression can promote the correct protein folding and can be achieved by the employment of weaker promoters, a low copy expression plasmid, reduction of expression temperature or decreased inducer concentrations. In the past also several engineered *E. coli* expression strains were introduced for difficult target proteins. For example strains were modified to co-express specific chaperones that help with correct protein folding, or to encode the natural inhibitor of the T7 RNA polymerase T7 lysozyme and thus, reduce the expression level of the target protein (Samuelson, 2011). Along with *E. coli* also other expression hosts, which confer certain

benefits, can be used for heterologous protein production. Besides strain selection, expression plasmid selection should also be considered, when dealing with insolubly produced proteins. Some expression vectors carry the gene sequences for solubility tags. These fusion partners can greatly improve the chance to obtain good amounts of soluble target proteins. Today a wide set of solubility tags is existing to choose from e.g., the MBP (maltose-binding protein), TRX (thioredoxin), GST (Glutathione-S-transferase) or SUMO (Small ubiquitin modified) tag (Costa *et al.,* 2014).

Although an array of options is available to enhance protein solubility, not every method is suitable for every protein and it is therefore always a try and error experience. As described, the first attempt to produce soluble Dshi_1135 protein, using the *E. coli* BL21-CodonPlus(DE3)-RIL expression host and pET52b(+) expression vector, failed. To address this problem, a number of the suggested approaches above were employed and are described in the following.

4.1.2.1 Test of different Media for soluble Expression of Dshi_1135

In a first optimization approach it was tried to improve Dshi_1135 solubility by using different media for cultivation of the *E. coli* BL21-CodonPlus(DE3)-RIL strain, carrying the pET52b(+)_Dshi1135Full plasmid, since a low growth temperature of 17 °C and IPTG concentration of 50 µM did not yield in the desired result. By default, LB medium was used to grow *E. coli*. However, LB medium only exhibits a limited buffer capacity and is therefore susceptible to pH-fluctuations caused by emerging side products during cultivation. This could cause an unfavorable growth milieu for *E. coli* and might trigger incorrect protein folding. In respect to this issue, Terrific Broth (TB) is superior over LB medium. TB is also a nutrient rich medium, but provides increased concentrations of peptone and yeast extract, additional glycerol as carbon source and phosphate buffer components (Tartoff & Hobbs, 1987; Kram & Finkel, 2015). Due to the higher availability of nutrients, *E. coli* cells can reach higher cell densities and additionally remain in the stationary phase longer, as cell death by toxic side products is prevented by the phosphate buffer system. In the best case, this results in more and properly folded target protein. For expression analysis of Dshi_1135 in TB, 500 ml of the medium were inoculated using a respective pre-culture and cells were grown to an OD_{578} of 0.5 at 37 °C and 200 rpm. Protein expression was induced by addition of 50 µM IPTG and the cultivation was performed at 17 °C and 180 rpm for 18 h. Two different approaches were followed for separation into the soluble and insoluble protein

fractions. One portion of the culture was treated with lysozyme and the other part of the culture was disrupted *via* French Press. Cell debris and insoluble proteins in all samples were removed by centrifugation. All resulting samples were all analysed *via* SDS-PAGE (see appendix Figure 48). Unfortunately, no detectable amounts of soluble StrepII-Dshi_1135 were expressed and Dshi_1135 was still predominately found in inclusion bodies. Therefore, this production strategy was dismissed.

As a second alternative to classic cultivation in LB medium and IPTG-induced protein expression, an autoinduction medium according to Studier was tested (Studier, 2005). Again, an expression analysis was performed initially. Therefore, LB medium was supplemented with self-inducing reagents consisting of glucose, α-lactose and glycerol in an optimal ratio and subsequently inoculated (ratio 1:500) with an *E. coli* BL21 (DE3)+pET52b(+)_Dshi1135Full starter culture. Cultures were grown overnight at 17 °C and as the name of the medium suggest, the addition of an inducer is not necessary to start protein expression. In *E. coli* glucose is the preferred carbon source and is metabolized first accordingly. Once the glucose is depleted in the medium, the cells initiate the uptake of α-lactose. The enzyme β-galactosidase converts the α-lactose into allolactose, which is the natural activator of the *lac*-promoter. This results in the slow expression of the T7 RNA polymerase, followed by subsequent controlled expression of the Dshi_1135 target protein. It was assumed that the slow production of Dshi_1135 would yield in good amounts of soluble protein. After the cells were grown overnight in autoinduction medium, one part of the culture was treated with lysozyme for obtaining the soluble and insoluble protein fraction. The other portion of the cells was disrupted by French Press und subsequently centrifuged to separate soluble and insoluble proteins. All obtained samples were analysed *via* SDS-PAGE and the resulting gels were investigated for desired bands in the soluble fractions (see appendix Figure 48). Again, most of the StrepII-Dshi_1135 protein was found as aggregates in the insoluble pellet fraction. No improvement was achieved by using autoinduction medium for expression of Dshi_1135, compared with conventional expression using IPTG as inducer.

4.1.2.2 Cloning of alternative Expression Vectors for Expression of soluble Dshi_1135 Protein

Alternative media for overproduction of the Dshi_1135 protein, using the pET52b(+)_Dshi1135Full plasmid, did not solve the problem of inclusion body formation. Therefore, it was decided to clone alternative expression vectors for the expression Dshi_1135. As one variant, the Dshi_1135 gene was cloned into the pGEX6P-1 vector, resulting in pGEX6P-1_Dshi1135Full. This expression vector harbors all needed features for T7 expression, an Amp resistance cassette for selection, the gene sequence for an N-terminal GST-tag and a PreScission™ Protease recognition site for tag removal. The GST-tag is well established affinity and solubility tag and is often used for proteins that are difficult to express in soluble form (Smith & Johnson, 1988; Harper & Speicher, 2011). In contrast to other fusion tags, the GST-tag is rather large with 26 kDA. GST itself folds quickly into a stable and highly soluble protein and thus, promotes greater expression and solubility of the fused protein of interest. Additionally, the GST-tag is a two-in-one fusion tag. Besides being a solubility tag it also serves as an affinity tag for protein purification. It tightly binds to its substrate glutathione (GSH), which is used as resin during affinity chromatography.

After successful cloning, the new construct was transformed into *E. coli* BL21-CodonPlus(DE3)-RIL cells and expression analyses were performed. A respective pre-culture was used for the inoculation of 100 ml main cultures in LB medium with a start OD_{578} of 0.05. After growth at 37 °C and 200 rpm and reaching an OD_{578} of 0.5-0.6, protein expression was induced by addition of 50 µM and 300 µM IPTG, respectively. Further cultivation occurred at 17 °C and 30 °C and 180 rpm and samples corresponding to an OD_{578} of 2 for later analysis were taken 1 h, 2 h, 3 h, 4 h and 18 h after induction. All samples were separated into the soluble and insoluble protein fraction and subsequently analysed by SDS-PAGE and Coomassie Brilliant Blue staining (Figure 15).

It was expected that after induction with the progression of time GST-Dshi_1135 is expressed continuously, which would result in increasing protein amounts within the cells. This in turn should be visible in the SDS gels as bands with increasing intensities that correlate to the calculated molecular weight of 63’800 Da of GST-Dshi_1135.

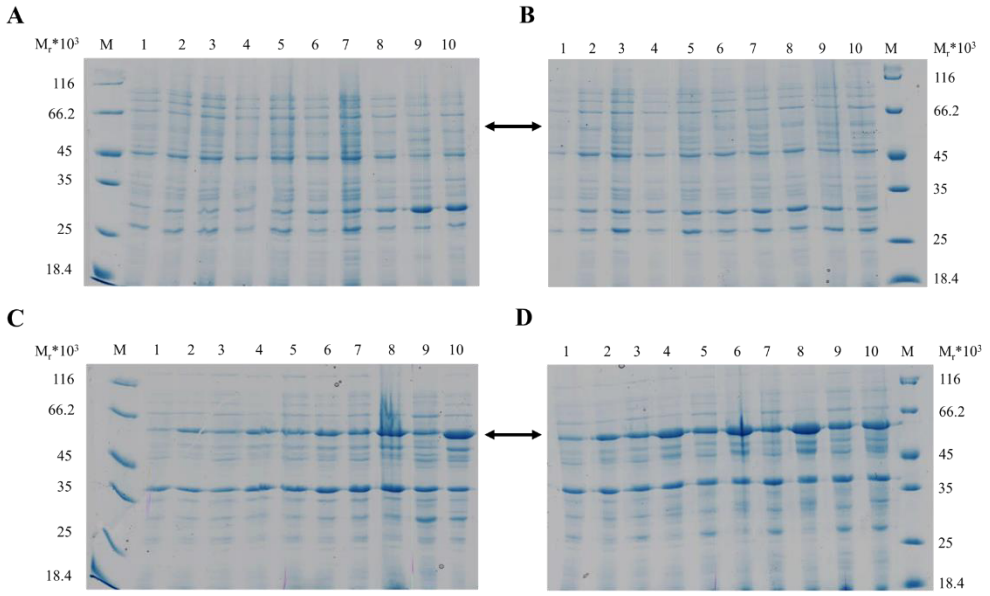

Figure 15: Determination of expression efficiency of GST-Dshi_1135 fusion protein dependent on cultivation temperature and IPTG concentration
Dshi1135 produced as GST-Dshi_1135 from plasmid pGEX6P-1_Dshi1135Full in *E. coli* BL21-CodonPlus(DE) after induction with 50 µM and 300 µM of IPTG and cultivation at 17 °C and 30 °C, respectively. Samples were taken 0 h, 1 h, 2 h, 3 h, 4 h and 18 h after induction and fractionated by lysozyme digestion and subsequent centrifugation. The resulting soluble and insoluble protein fractions were mixed with 2x SDS loading dye and denatured at 95 °C for 10 min. Equal amounts of protein (corresponding to the OD_{578}) were analysed on 12 % SDS gels and visualized *via* Coomassie Brilliant Blue staining.
(A) 17 °C, soluble fraction (B) 30 °C soluble fraction (C) 17 °C, insoluble fraction (D) 30 °C insoluble fraction. Lane M: molecular mass marker (relative molecular masses (*1'000) are indicated. Lane 1: 1 h after induction with 50 µM IPTG. Lane 2: 1 h after induction with 300 µM IPTG. Lane 3: 2 h after induction with 50 µM IPTG. Lane 4: 2 h after induction with 300 µM IPTG. Lane 5: 3 h after induction with 50 µM IPTG. Lane 6: 3 h after induction with 300 µM IPTG. Lane 7: 4 h after induction with 50 µM IPTG. Lane 8: 4 h after induction with 300 µM IPTG. Lane 9: 18 h after induction with 50 µM IPTG. Lane 10: 18 h after induction with 300 µM IPTG.
The double arrow highlights the protein band corresponding to GST-Dshi_1135 with an approximate relative molecular weight of 64'000.

In the soluble protein fractions of the cells that were grown at 17 °C (Figure 15 A) bands with the respective size of GST-Dshi_1135 (indicated by the double arrow) can only hardly be seen. Over the time, the intensity of the bands only increases slightly (Figure 15 A, lanes 1-10), indicating that GST-Dshi_1135 appears to be poorly expressed in soluble form. The same result was observed for the soluble protein fractions that were extracted from cells cultivated at 30 °C (Figure 15 B). Moreover, the concentration of applied IPTG did not seem to influence the amount of soluble GST-Dshi_1135 protein. Analysis of the insoluble protein fractions on SDS gels resulted in a different picture. Here, a dominant band with a M_r of 64'000 was detected in almost all fractions and even stronger in those fractions derived from cells cultivated at 30 °C (Figure 15 C+D). In the cells that were grown at 17 °C, expression was a little

hampered compared to cells that were cultivated at 30 °C (Figure 15 A+B, lanes 1-8). Due to the fact, that the temperature optimum of *E. coli* lies at 37 °C, lower temperatures decelerate cell growth, which is obviously accompanied by lower protein expression. The 17 °C cultured cells grew slower than the cells cultivated at 30 °C, but both approximately reached the same final OD_{578} of 6 after 18 h of cultivation. Almost comparable amounts of GST-Dshi_1135 were produced in cells cultured at 30 °C independent of the IPTG concentration and in cells induced with 300 µM IPTG and grown at 17 °C. A lower IPTG concentration and cultivation at 17 °C obviously reduced expression of GST-Dshi_1135 (Figure 15 C+D, lanes 9-10). In general, larger quantities of GST-Dshi_1135 protein were produced in cells that were induced 300 µM IPTG, compared to cultures induced with 50 µM of IPTG, indicating a stronger activation of the *lac*-promoter and thus also of the T7-promoter (exemplarily see Figure 15 D, lanes 7-8).

In conclusion, the expression of GST-Dshi_1135 works in principle, but resulted mainly in insoluble protein. As mentioned before, it was presumed that a minor part of the GST-Dshi_1135 protein might be present in the soluble cytosolic fraction nonetheless. To check this assumption, 1 L of GST-Dshi_1135 overproducing *E. coli* cells were cultivated for 18 h, disrupted *via* French Press and proteins were separated into the soluble and insoluble fraction by high-speed centrifugation. The whole cell sample after French Press and the cytosolic protein fraction after ultracentrifugation were separated *via* SDS-PAGE and subsequently transferred onto a PVDF membrane by Western Blotting (Figure 16). The employed Anti-GST-Alkaline Phosphatase Conjugate antibody for protein visualization detected a striking band with a M_r of 64'000, corresponding to the GST-Dshi_1135 protein, in the whole cell sample after French Press disruption (Figure 16, lane 1). Only a negligibly small amount of soluble GST-Dshi_1135 was found in the cytosolic fraction, using this method (Figure 16, lane 2).

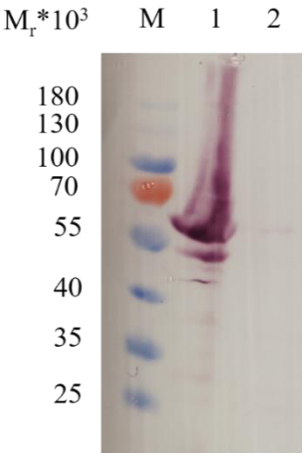

Figure 16: Localization of the GST-Dshi_1135 fusion protein in cell fractions after lysis
GST-Dshi_1135 containing cells were disrupted *via* French Press and a sample was taken for SDS-PAGE. The remaining cells were pelleted by ultracentrifugation and a sample of the resulting cytosolic protein fraction was taken for SDS-PAGE. The proteins in the resulting SDS gel were transferred onto a PVDF membrane by Western Blotting and an Anti-GST- Alkaline Phosphatase Conjugate antibody was employed for detection of GST-Dshi_1135.
Lane M: prestained molecular mass marker (relative molecular masses (*1'000) are indicated. Lane 1: whole cells after French Press, Lane 2: cytosolic protein fraction after ultracentrifugation.

This additional experiment confirmed the result of the expression analysis, that GST-Dshi_1135 is produced but is not present in a soluble form. Consequently, this expression strain was not used for future experiments

The TRX-tag, derived from the *E. coli* thioredoxin gene, is also often used to assist the proper folding of proteins and keep them from precipitation. Therefore, the Dshi_1135 encoding gene sequence was cloned into the pET52bTrx vector (Frädrich *et al.,* 2012), resulting in pET52b(+)Trx_Dshi1135Full. The pET52bTrx vector is a derivative of pET52b(+), carrying the sequence of the TRX-tag upstream of the Strep-tag II, a PreScission™ Protease cleavage site, an Amp resistance cassette and the T7 promoter. Similar to the previously described GST-tag, the TRX-tag is a solubility tag that is commonly used for difficult to express proteins in *E. coli*. Advantages of the TRX-tag are that it is rather small with ca. 12 kDa and that C- and N-termini are accessible on the molecules' surface. Thus, protein fusion partners can easily be attached. Furthermore, the TRX-tag is thermally stable which prevents degradation and it does not aggregate even in very high concentrations and allows time for proper folding of the fusion protein (LaVallie *et al.,* 1993).
The newly cloned pET52b(+)Trx_Dshi1135Full expression plasmid was transformed into *E. coli* BL21-CodonPlus(DE3)-RIL cells and identical to previously described

expression strains, expression analysis was performed to determine optimal conditions for soluble production of Dshi_1135. The resulting SDS gels showed that large portions of the TRX-StrepII-Dshi_1135 protein were expressed in inclusion bodies but however, also a not negligible amount of the protein was detected in the soluble fractions. Best results were obtained when the protein expression was induced with 50 µM of IPTG and cultivation was carried out at 17 °C for 18 h (see appendix Figure 49).

Now it was of interest, whether TRX-StrepII-Dshi_1135 can successfully be expressed in soluble form in larger quantities and purified *via* affinity chromatography. Since a light-sensitivity was postulated for Dshi_1135 as a blue light-sensor, all steps during production and purification were performed under dim red light conditions according to Correa *et al*. (2013) and strictly at 4 °C to prevent stability problems. For production of the TRX-StrepII-Dshi_1135 fusion protein 1 L LB medium was inoculated with an *E. coli* BL21(DE3) starter culture, carrying the pET52b(+)Trx_Dshi1135Full plasmid, and cultivated at 37 °C and 200 rpm to an OD_{578}= 0.5-0.6. Induction of protein expression was initiated by addition of 50 µM IPTG and cells were grown overnight at 17 °C. The cells were harvested and subsequently disrupted by a double French Press passage. Cell debris and insoluble proteins were removed by high-speed centrifugation and the cell free extracts, containing the soluble protein fraction, were used for affinity chromatography *via* a 1 ml Strep Tactin® Superflow matrix gravity flow column. After the sample entered the column bed completely, the column was washed twice to remove potential impurities and afterwards the bound TRX-StrepII-Dshi_1135 protein was eluted using the competitive ligand D-desthiobiotin. Throughout the entire procedure samples were taken and separated *via* SDS-PAGE to trace and analyse all production and purification steps (Figure 17).

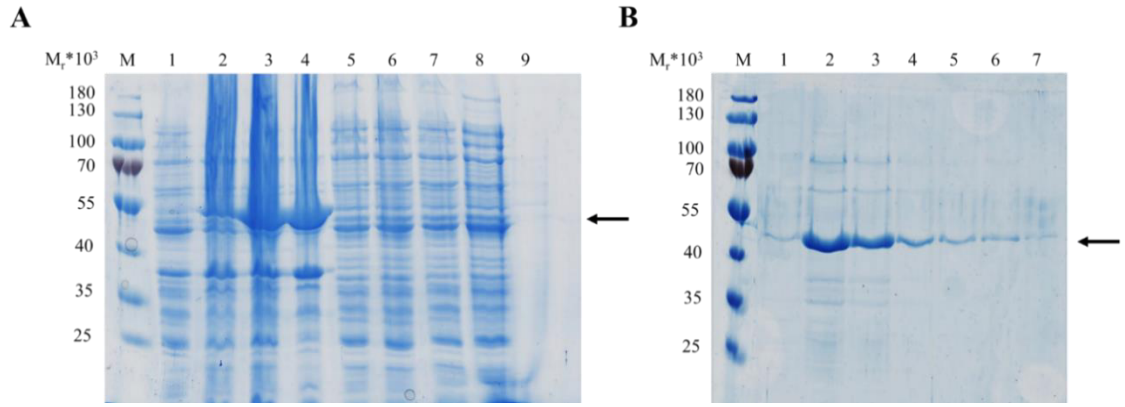

Figure 17: Heterologous production of TRX-StrepII-Dshi_1135 fusion protein in *E. coli* BL21-CodonPlus(DE3)-RIL cells and subsequent purification by affinity chromatography
The TRX-StrepII-Dshi_1135 fusion protein was recombinantly overexpressed in *E. coli* BL21-CodonPlus(DE3)-RIL cells and subsequently purified *via* affinity chromatography using the Strep Tactin® Superflow matrix. All samples were mixed with 2x SDS-loading dye, denatured at 95 °C for 10 min, subsequently analysed on 12 % SDS gels and visualized *via* Coomassie Brilliant Blue staining. Arrows indicate the TRX-StrepII-Dshi_1135 protein.
(A) Samples taken during purification of TRX-StrepII-Dshi_1135 before elution. Lane M: prestained molecular mass marker (relative molecular masses (*1'000) are indicated. Lane 1: before induction. Lane 2: 18 h after induction. Lane 3: disrupted cells. Lane 4: pellet fraction. Lane 5: cell free extracts. Lane 6: flow-through fraction I. Lane 7: flow-through fraction II. Lane 8: washing step I. Lane 9: washing step II.
(B) Elution fractions after affinity chromatography. Lane M: prestained molecular mass marker (relative molecular masses (*1'000) are indicated. Lane 1: pre-elution step. Lane 2: elution fraction I. Lane 3: elution fraction II. Lane 4: elution fraction III. Lane 5: elution fraction IV. Lane 6: elution fraction V. Lane 7: elution fraction VI.

Lanes 1 and 2 show the total protein content of whole *E. coli* BL21-CodonPlus(DE3)-RIL cells, containing the pET52b(+)Trx_Dshi1135Full plasmid, before and after IPTG induction (Figure 17 A). A clearly induced band with a M_r of 52'000 was determined, which corresponds well to the calculated molecular mass of 51'650 Da for TRX-StrepII-Dshi_1135, indicating a successful expression of the protein. After cell disruption (Figure 17 A, lane 3) and high-speed centrifugation a large portion of the TRX-StrepII-Dshi_1135 protein was found in the insoluble pellet fraction (Figure 17 A, lane 4) and only minor amounts are predicted in the soluble cytosolic fraction (Figure 17 A, lane 5). The flow-through contains all unbound proteins (Figure 17 A, lanes 6 and 7). Most of the soluble unbound proteins were removed from the column by two extensive washing steps (Figure 17 A, lanes 8 and 9). In a pre-elution step (Figure 17 B, lane 1) the remaining washing buffer in the column bed was displaced by addition 0.5 CV of elution buffer, to prevent dilution of the first elution fraction. Elution of the specifically bound TRX-StrepII-Dshi_1135 protein was performed in six steps using 1 CV of elution buffer each. Despite the great loss of produced TRX-StrepII-Dshi_1135 in inclusion bodies, elution resulted in protein of apparent homogeneity and a M_r of

approximately 52’000 (Figure 17 B, lanes 2-7). Most of the protein was found the elution fractions 1 and 2. Two prominent contaminating proteins with M_r of 60’000 and 70’000, respectively, were identified in all elution fractions. Since Dshi_1135 seems to have a severe insolubility and stability issues it is most likely, that these bands correspond to the *E. coli* chaperones GroEL and DnaK. For validation of this hypothesis further experiments, like N-terminal sequencing, would have to be considered. Protein concentrations in the elution fractions were calculated using a Bradford calibration curve. The mean yield of TRX-StrepII-Dshi_1135 throughout this study, using this combination of expression strain and plasmid, was 0.52 mg ± 0.1 mg per 1 L of cell culture in final concentrations of approximately 0.5 mg/ml. This was the best result of all methods tested so far for the production and purification of the Dshi_1135 protein. The use of the TRX-tag greatly improved the solubility of Dshi_1135 during heterologous production and enabled successful purification of the protein in small amounts and apparent homogeneity.

4.1.2.3 Alternative Expression Strains for Heterologous Production of Dshi_1135

For certain experiments higher protein concentrations are beneficial. Therefore, it was targeted to further optimize the solubility and yield of the Dshi_1135 protein. Having already found a suitable expression vector, two new expression strains should be tested.

As a first promising candidate the *V. natriegens* strain Vmax™ Express was chosen. *V. natriegens* is a Gram-negative non-pathogenic marine bacterium and was initially described to have a doubling rate of less than 10 minutes (Payne, 1958) and is therefore twice as fast as *E. coli*. This fast growth rate has been taken advantage of and the bacterium was biotechnologically engineered regarding recombinant protein production and is now advertised to express proteins in high yields and solubility (Weinstock *et al.,* 2016). The strain is compatible with diverse commonly used protein expression vectors, like the pET-derived plasmid series that uses the T7 expression system. As mentioned above, *V. natriegens* is a marine bacterium and requires high salinity for optimal growth. Since *D. shibae* is also a marine organism, it was hypothesized that these conditions provided by *V. natriegens* might be more physiological and contribute to the solubility of Dshi_1135.

For the production of Dshi_1135 the expression plasmid pET52b(+)Trx_Dshi1135Full should be transformed into Vmax™ Express cells. However, even after several attempts it was not possible to obtain positive colonies and the approach was rejected.

Alternatively, the pGEX6P-1_Dshi1135Full plasmid was used and was successfully transformed into Vmax™ Express cells. First expression analyses with the constructed strain showed good expression of GST-Dshi_1135 as a soluble protein (see appendix Figure 50). Surprisingly, the subsequent purification approaches did not result in satisfactory yields of protein, as only ~ 0.2 mg per liter of cell culture could be obtained (see appendix Figure 51). This corresponds to only about 38.5 % of the amount of Dshi_1135 protein achieved with the pET52b(+)Trx_Dshi1135Full plasmid in *E. coli* BL21-CodonPlus(DE3)-RIL cells. Thereupon, the use of *V. natriegens* as expression strain was no longer pursued.

As a second alternative expression strain *E. coli* Lemo21(DE3) was employed. This strain is an *E. coli* BL21(DE3) derivative that was designed for the expression of challenging target proteins and was launched in 2010 by NEB (New England BioLabs, Ipswich, MA, USA). In addition to the IPTG inducible T7 system, *E. coli* Lemo21(DE3) harbors the pLemo plasmid, which carries the gene sequence for the natural inhibitor of T7 RNA polymerase, T7 lysozyme. This gene in turn is under the control of the very well titratable *rha*BAD promoter. Thus, the T7 RNA polymerase activity can be precisely controlled by the addition of different L-rhamnose concentrations during protein expression. This offers the advantage that the optimal expression conditions at which the target protein is soluble can be determined using only one strain and testing a small number of cultivation and induction conditions.

For the expression of TRX-StrepII-Dshi_1135, the plasmid pET52b(+)Trx_Dshi1135Full was transformed into *E. coli* Lemo21(DE3) cells and expression analysis was performed. In addition to different growth temperatures and IPTG concentrations, L-rhamnose concentrations between 100-2000 µM were tested to determine optimal conditions for soluble production of TRX-StrepII-Dshi_1135 (see appendix Figure 52). It was found that the use of 400 µM IPTG and 750 µM L-rhamnose in combination with cultivation at 17 °C after induction resulted in the highest yield of soluble protein. Subsequently, TRX-StrepII-Dshi_1135 was produced on a larger scale, using 6 L culture volume, under the conditions described above. After 18 h of expression, the cells were harvested, disrupted by a double French Press passage and all cell debris was removed by high-speed centrifugation. The resulting supernatant, containing the soluble protein fraction, was loaded onto an equilibrated column packed with Strep Tactin® Superflow resin to allow purification of TRX-StrepII-Dshi_1135 by

affinity chromatography. All steps were strictly performed under dim red light conditions and 4 °C. The SDS-PAGE analysis of all production and purification steps is depicted in Figure 18.

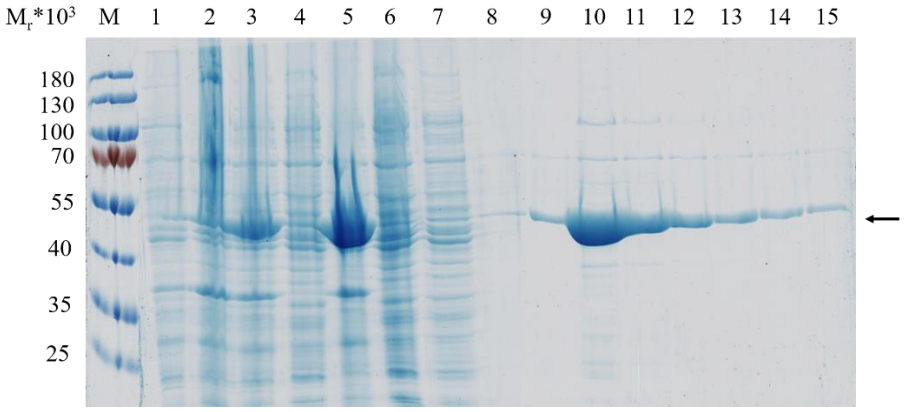

Figure 18: SDS-PAGE analysis of the heterologously produced TRX-StrepII-Dshi_1135 fusion protein in *E. coli* Lemo21(DE3) and subsequent purification by affinity chromatography
The TRX-StrepII-Dshi_1135 fusion protein was recombinantly expressed in *E. coli* Lemo21(DE3) cells after induction with 400 µM IPTG, 750 µM L-rhamnose and cultivation at 17 °C. Produced protein was and subsequently purified *via* affinity chromatography using the Strep Tactin® Superflow matrix. All samples were mixed with 2x SDS-loading dye, denatured at 95 °C for 10 min, subsequently analysed on 12 % SDS gels and visualized *via* Coomassie Brilliant Blue staining. The arrow indicates the TRX-StrepII-Dshi_1135 protein.
Lane M: prestained molecular mass marker (relative molecular masses (*1'000) are indicated. Lane 1: before induction. Lane 2: 18 h after induction. Lane 3: disrupted cells. Lane 4: cell free extracts. Lane 5: pellet fraction. Lane 6: flow-through fraction I. Lane 7: washing step I. Lane 8: washing step II. Lane 9: pre-elution step. Lane 10: elution fraction I. Lane 11: elution fraction II. Lane 12: elution fraction III. Lane 13: elution fraction IV. Lane 14: elution fraction V. Lane 15: elution fraction VI.

Comparing the uninduced sample and the sample after IPTG induction (Figure 18, lanes 1 and 2), the occurrence of an additional protein band with a M_r of 52'000 was determined, indicating the successful expression of TRX-StrepII-Dshi_1135 with a calculated molecular mass of 51'650 Da. Only small amounts of TRX-StrepII-Dshi_1135 were detected in the cell free extract (Figure 18, lane 4), whereas most of the produced TRX-StrepII-Dshi_1135 protein was found in the pellet fraction after high-speed centrifugation (Figure 18, lane 5). This indicated that the majority of produced target protein still appears to be present as insoluble protein in inclusion bodies. After the cell free extracts were loaded onto the column for affinity chromatography (Figure 18, lane 6), two extensive washing steps removed all weakly and non-bound proteins (Figure 18, lanes 7 and 8). In the elution fractions 1-6 successfully purified TRX-StrepII-Dshi_1135 protein in apparent homogeneity was indicated by a clear and prominent band with a M_r of 52'000 (Figure 18, lanes 10-15). An amount of 1.5 mg ±

0.14 mg per L cell culture with concentrations of 1-1.5 mg/ml was yielded throughout this study, when *E. coli* Lemo21(DE3) was used to express TRX-StrepII_Dshi1135. This yield is two to three times higher compared to the until now highest protein yield, when production was performed in the *E. coli* BL21-CodonPlus(DE3)-RIL strain using the same expression plasmid.

In summary, after several optimization steps, it was possible to successfully produce and purify the Dshi_1135 protein in adequate amounts and purity. The use of the TRX solubility tag greatly improved the solubility of the protein. Application of *E. coli* Lemo21(DE3) as expression host was able to further increase the soluble protein yield by threefold. This suggests that in the case of Dshi_1135 the fast expression primarily leads to inclusion body formation. However, throughout all performed production and purification experiments in this study it was observed, that also under optimized conditions, most of the target protein was lost in unavailable inclusion bodies. For certain analyses, like crystallization approaches, much higher protein amounts and concentrations up to 10 mg/ ml or even more will be necessary. Attempts to increase concentration of TRX-StrepII_Dshi1135 by using centrifugal filter devices with a MWCO of 30 kDa failed. Consequently, further optimization of the production and purification protocol for Dshi_1135 might need to be considered.

4.1.3 Purified Dshi_1135 tends to aggregate and precipitate strongly

For all biochemical experiments protein stability is of great importance. To gain clarity according to the thermostability of Dshi_1135, a stability assay at different temperatures was performed. Therefore, TRX-StrepII-Dshi_1135 was produced and subsequently purified *via* a Strep Tactin® Superflow column. The obtained elution fractions were stored in aliquots at room temperature, 4 °C and -20 °C, respectively, for 14 days. Because the stability of proteins in aqueous solutions is known to be enhanced by addition of glycerol (Vagenende *et al.,* 2009), it was tested as cosolvent in different concentrations. After 14 days all samples were analysed by SDS-PAGE (Figure 19).

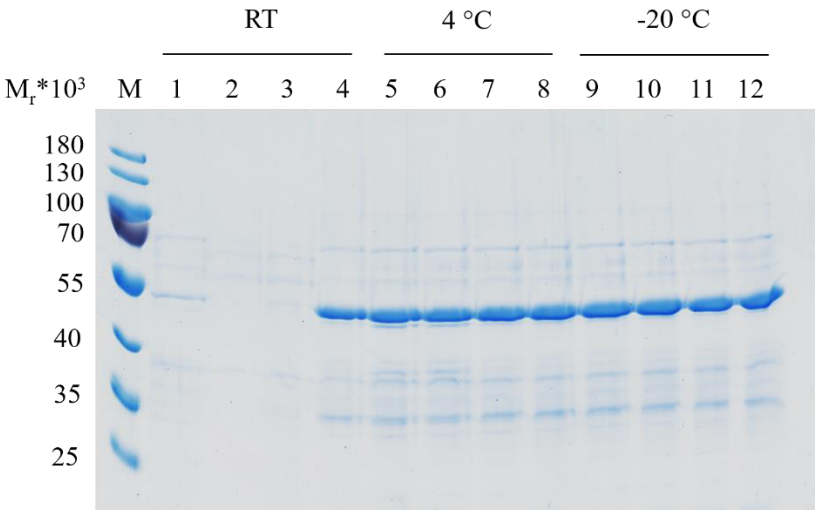

Figure 19: Thermostability test of purified TRX-StrepII-Dshi_1135 protein
Freshly purified TRX-StrepII-Dshi_1135 protein was divided into aliquots for storage over 14 days at room temperature (RT), 4 °C and -20 °C, respectively. The individual samples were either stored in elution buffer or were supplemented with 2 %, 5 % or 10 % (v/v) glycerol, respectively. After 14 days all samples were mixed with 2x SDS loading dye and denatured for 10 min at 95 °C. Proteins were separated on 12 % SDS gels and visualized by Coomassie Brilliant Blue staining.
Lane M: prestained molecular mass marker (relative molecular masses (*1'000) are indicated. Lanes 1,5 and 9=: TRX-StrepII-Dshi_1135 in elution buffer. Lanes 2,6 and 10: TRX-StrepII-Dshi_1135 in elution buffer + 2 % glycerol (v/v). Lanes 3,7 and 11: TRX-StrepII-Dshi_1135 in elution buffer + 5 % glycerol (v/v). Lanes 4,8 and 12: TRX-StrepII-Dshi_1135 in elution buffer + 10 % glycerol (v/v).

Storage of TRX-StrepII-Dshi_1135 at room temperature with glycerol concentrations up to 5 % (v/v) (Figure 19, lanes 1-3) resulted in complete loss of the protein. Concentration of 10 % (v/v) glycerol had a stabilizing effect on TRX-StrepII-Dshi_1135 at room temperature (Figure 19, lane 4). Independent of the glycerol concentration no decrease of TRX-StrepII-Dshi_1135 concentration was observed in samples that were stored at 4 °C or at -20 °C, respectively (Figure 19, lanes 5-12). Based on these results, all buffers used during purification of TRX-StrepII-Dshi_1135 were supplemented with 10 % (v/v) glycerol and the purified protein was stored at 4 °C as standard.

Loss of protein may occur due to proteolysis or aggregation and precipitation of the TRX-StrepII-Dshi_1135 protein. Since all purification steps of the Dshi_1135 protein were performed under red light conditions, it was not possible to examine the elution fractions with respect to turbidity, which would indicate precipitation of the protein. Therefore, this issue was investigated as follows. An aliquot of purified TRX-StrepII-Dshi_1135 was taken and centrifuged for 30 min at 4 °C and at maximum speed in a tabletop centrifuge. This would cause pelleting of potential precipitated protein. After

centrifugation the supernatant was transferred into a fresh reaction tube and the potential protein pellet was resuspended in washing buffer. Both fractions were analysed by SDS-PAGE (Figure 20).

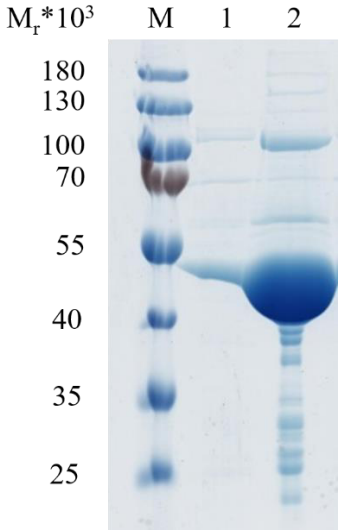

Figure 20: SDS-PAGE analysis regarding precipitation and degradation of the Dshi_1135 protein
Dshi_1135 was purified using a Strep Tactin® Superflow column and subsequently centrifuged for 30 min at 4 °C and maximum speed to separate soluble and potentially precipitated protein. Samples of the supernatant and the dissolved pellet were taken, mixed with 2x SDS loading dye and denatured at 95 °C for 10 min. The proteins were analysed on 12 % SDS gels.
Lane M: prestained molecular mass marker (relative molecular masses (*1'000) are indicated. Lane 1: supernatant (soluble proteins). Lane 2: pellet (precipitated proteins).

A strong band with a M_r of 52'000, that correlates well with the calculated molecular weight of TRX-StrepII-Dshi_1135, in the pellet fraction (Figure 20, lane 2) clearly indicated that about 90-95 % of the protein precipitated right after elution from the column. Only 5-10 % remained as soluble protein (Figure 20, lane 1).

Aggregation of Dshi_1135 was also determined by GPC analyses that were performed to investigate the oligomeric state of TRX-StrepII-Dshi_1135. Many LOV HKs studied to date were found to form dimers in their active state, but interestingly this does not apply to the Dshi_1135 homologue EL346 of *E. litoralis*. Instead, the compact structure of the protein prevents dimerization and it functions as a monomer (Rivera-Cancel *et al.,* 2014). For analytical GPC analyses of TRX-StrepII-Dshi_1135, the protein was heterologously expressed and purified *via* affinity chromatography as described above. The employed Superdex™ 200 Increase 5/150 column for GPC was equilibrated with the respective GPC buffer and subsequently calibrated with reference proteins (carbonic

anhydrase, M_r of 29'000, elution volume 2.21 ml; BSA, M_r of 66'000, elution volume 1.92 ml; β-amylase, M_r of 200'000, elution volume 1.62 ml). Afterwards 100 µl of purified TRX-StrepII-Dshi_1135 protein were injected into the ÄKTA Purifier™ system and separated at a constant flowrate of 0.45 ml/min. For determination of protein elution, absorbance was monitored at 280 nm. Due to the postulated light sensitivity of Dshi_1135, the injection-syringe and the chromatography column were wrapped in aluminum foil, to prevent light exposure. The obtained elution chromatogram is shown in Figure 21.

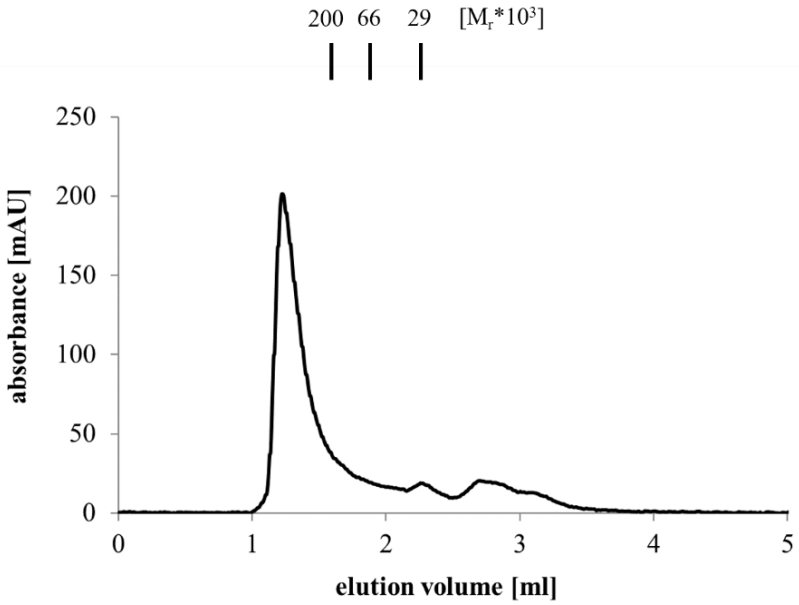

Figure 21: Analytical GPC analysis of Dshi_1135
For analytical GPC 100 µl Dshi_1135 were injected and loaded onto a Superdex™ 200 Increase 5/150 column and subsequently separated at a constant flow rate of 0.45 ml/min. Protein elution was monitored at an absorbance of 280 nm. Employed standard proteins for calibration (relative molecular masses are indicated by black bars): carbonic anhydrase (M_r= 29'000), BSA (M_r= 66'000) and β-amylase (M_r= 200'000).

The elution chromatogram exhibited one major peak at an elution volume of 1.23 ml and two minor peaks at elution volumes of 2.31 and 2.74 ml. Based on the prepared calibration curve, the respective relative molecular masses were calculated. Accordingly, the peak at 1.23 ml corresponds to a M_r of 688'000. This peak runs in the void volume (V_0) of the utilized chromatography column and cannot be attributed to a higher ordered protein complex of TRX-StrepII-Dshi_1135. It is most likely, that this peak was caused by highly aggregated TRX-StrepII-Dshi_1135 protein. Peaks at 2.31 ml and 2.74 ml correspond to relative molecular masses of 20'000 and 4'900, respectively. Since these determined molecular masses did not correspond to the

calculated molecular mass of TRX-StrepII-Dshi_1135 of 51´650 Da, these peaks were presumably caused by impurities or degraded protein. Based on these results it was not possible to make a statement about the oligomeric state of Dshi_1135, but once more it became evident that the protein has severe stability problems and is prone to aggregation. The GPC experiment was repeated several times using the optimizes GPC buffers B (50 mM Tris-HCl pH 8.2, 150 mM NaCl, 5 mM $MgCl_2$, 10 % (w/v) glycerol and 0.1 % (w/v) triton X-100) and C (50 mM Tris-HCl pH 8.2, 500 mM NaCl, 5 mM $MgCl_2$, 10 % (w/v) glycerol and 0.1 % (w/v) triton X-100) to stabilize TRX-StrepII-Dshi_1135, but always resulted in the same unsatisfactory results.

The solubility in aqueous solutions is individual for every protein and is dependent on many parameters. According to thermodynamics, protein solubility is defined as the concentration of a protein in a saturated solution that is in equilibrium with a solid phase under a given set of conditions. These conditions can be for instance pH, ionic strength, temperature or solvent additives (Riès-kautt & Ducruix, 1997). But also, amino acid composition, protein conformation and the content of polar and nonpolar amino acids have a great influence on protein solubility. Proteins with a more negative surface charge tend to aggregate less because they are able to bind water strongly due to their acidic amino acids. (Kramer *et al.,* 2012).

A simple method to rapidly evaluate the influence of different temperatures, buffers, pH values and solvent additives on protein stability is the thermal shift assay, often also referred to as Thermofluor Assay. During the assay the protein of interest is mixed with the fluorescent dye SYPRO® Orange and is then gradually heated from 10 to 90 °C. When the protein starts to denature it unfolds and the hydrophobic amino acid residues are exposed to the surface. SYPRO® Orange specifically binds to these amino acids, causing an increase in the fluorescence signal and thus, the melting point of the protein can be calculated on basis of the signal intensities. Protein aggregation, however, quenches the fluorescence signal towards the end of the assay (Niesen *et al.,* 2007).

In a first test different protein (0.5, 1 or 2 mg/ml) and SYPRO® Orange (10x, 50x or 100 x) concentrations were tested to determine an optimal protein to dye ratio. For this test purified TRX-StrepII-Dshi_1135 protein in buffer A1 (50 mM Tris-HCl, pH 8.2; 150 mM NaCl, 5 mM $MgCl_2$; 10 % (v/v) glycerol) was used. The obtained melting curves are depicted in Figure 22 A, where the derivative of the relative fluorescence is

plotted over the tested temperatures. Under optimal conditions the melting point of the protein can be determined from the distinct minimum of the melting curve. However, no melting curves were obtained for TRX-StrepII-Dshi_1135. To exclude that the experimental performance was cause of the negative outcome, the concentration test of the Thermofluor Assay was repeated with a positive control. As positive control the heterologously produced and purified *D. shibae* IscR protein (buffer: 100 mM Tric-HCl, pH 7.5; 150 mM NaCl, 5 mM DTT) (kindly provided by Lisa Plötzky, TU Braunschweig) was used.

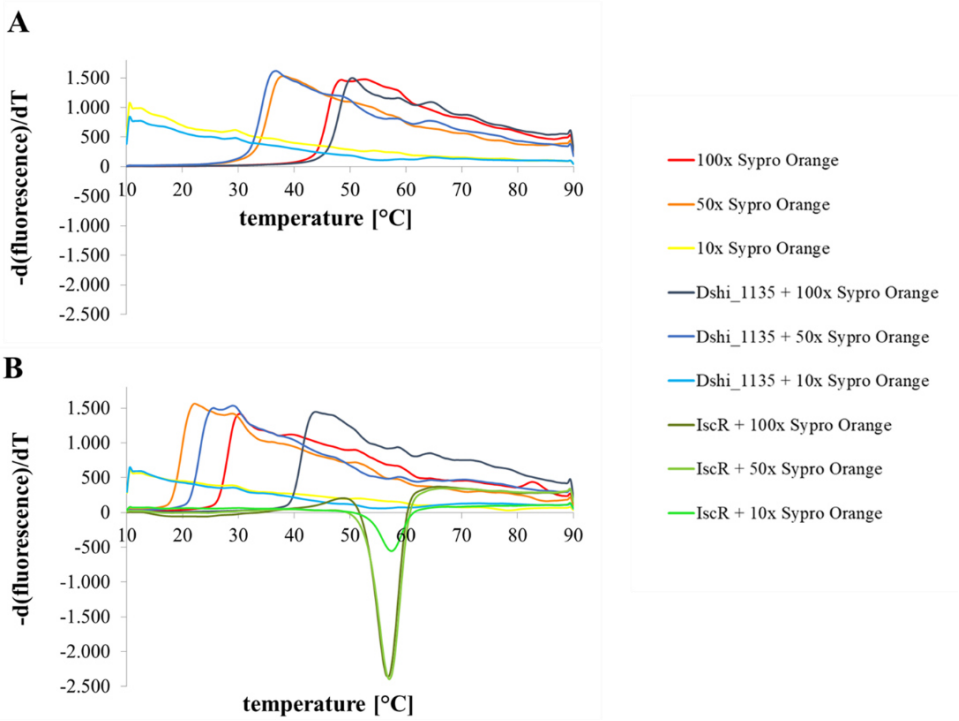

Figure 22: First derivatives of the obtained melting curves of Dshi_1135
Dshi_1135 melting curves were aimed to determine by Thermal Shift Assays. Therefore, different protein concentrations (0.5, 1 or 2 mg/ml) and SYPRO® Orange concentrations (10 x, 50 x or 100 x) were tested. The heating process ranged from 10-90 °C and fluorescence was measured in 0.5 °C steps. Melting points were calculated with the CFX Manager software (Bio-Rad, Hercules, CA, USA).
(A) Melting curves of Dshi_1135 and (B) melting curves of Dshi_1135 and IscR (positive control).

Figure 22 B shows the first derivative of the obtained melting curve. An optimal curve shape with a distinct minimum indicates the melting temperature of IscR at 57 °C. This demonstrates the correct performance of the experimental procedure. For the TRX-StrepII-Dshi_1135 protein however, the same results were obtained again and no melting temperature could be determined. As described earlier, protein aggregation leads to the quenching of the fluorescence signal of SYPRO® Orange. It must therefore be assumed that TRX-StrepII-Dshi_1135 was already present in aggregated form at the

start of the assay. Due to this circumstance, it was not possible to continue the Thermofluor Assay to test different buffer systems and additives to improve protein stability. This result clearly highlights the strong tendency of Dshi_1135 to aggregate and precipitate and supports the previous findings.

The reason for the instability of Dshi1135 could possibly be within the kinase domain. In addition to full length Dshi_1135, the single LOV domain of Dshi_1135 corresponding to amino acids 1-149, was produced and analysed according to stability. The LOV domain of Dhsi_1135 could be produced soluble form in significantly higher yields of ~1.5 mg/ml. In addition, it exhibited higher stability over time compared to full length Dshi_1135 in the thermostability test described above and displayed in Figure 19. Accordingly, one approach to increase the stability of Dshi_1135 could be the investigation and adjustment of the amino acid sequence of the kinase domain by site-directed mutagenesis.

4.1.4 Dshi_1135 binds FMN as Cofactor

Common to all functional LOV proteins is the blue light sensitive flavin chromophore, which in the signaling state is covalently linked to the protein core via an adjacent cysteine residue. Binding sites for the FMN cofactor were identified in *A. thaliana* Phot1, the first discovered LOV protein (Christie *et al.,* 1999). Moreover, EL346 from *E. litoralis* was shown to bind FMN for LOV domain activity (Swartz *et al.,* 2007). Therefore, it was investigated, if Dshi_1135 possesses a FMN cofactor. Due to their peptide bonds and aromatic amino acid side chains, all proteins are able to absorb light in the UV region of the spectrum between 200-280 nm. Proteins with bound cofactors or prosthetic groups are additionally able to absorb light in the visible light region (Holtzhauer, 1996). Flavoproteins are for instance recognizable by their bright yellow color and their ability to fluoresce under UV light. Thus, UV/Vis spectroscopy provides a suitable method to investigate proteins regarding potential cofactors.

A first indication for FMN binding of Dshi_1135 was given by the yellow fluorescence of the purified and reconstituted protein under UV light (Figure 23 A). UV/Vis spectroscopy of the same sample was performed under dark/ dim red light conditions due to the proposed light sensitivity of Dshi_1135. A typical absorption spectrum for FMN-binding LOV proteins in the ground state with maxima at 380 and 450 nm was recorded (Figure 23 B and C).

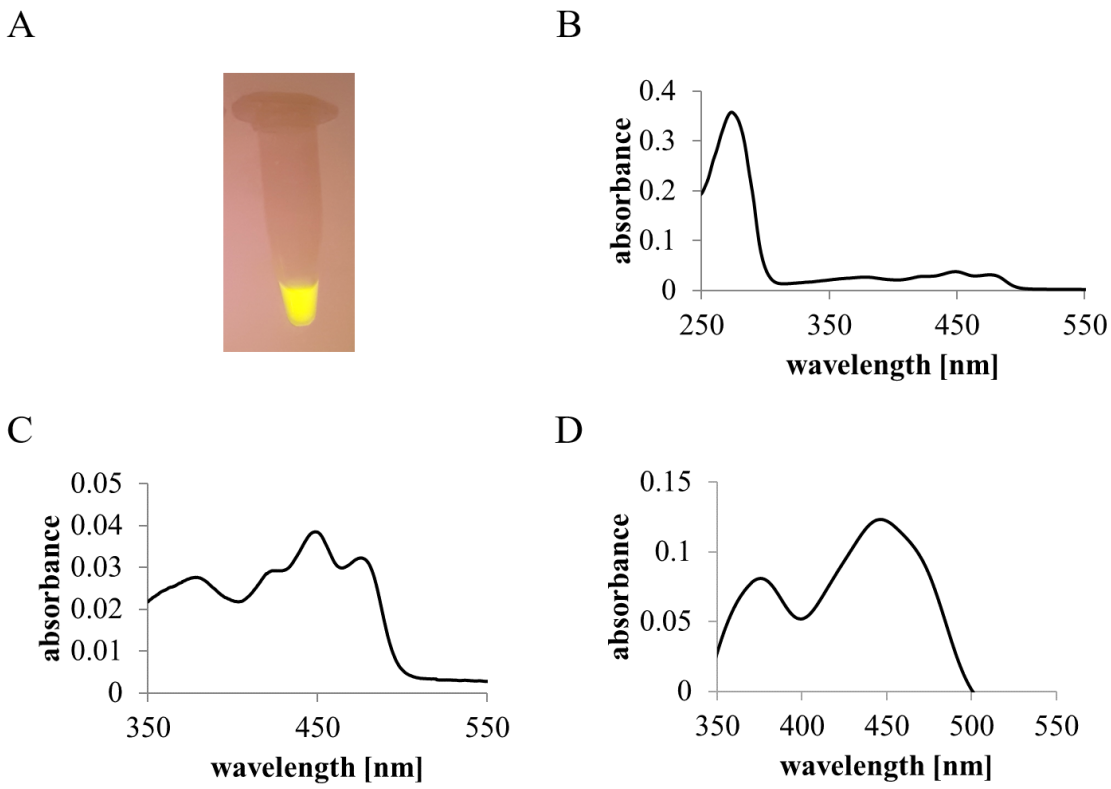

Figure 23: Identification of the FMN cofactor of Dshi_1135
(A) Purified and reconstituted TRX-StrepII-Dshi_1135 protein under UV light shows the typical yellow fluorescence indicative for an FMN cofactor. (B) UV/Vis spectrum of purified and reconstituted TRX-StrepII-Dshi_1135 with a protein peak at 280 nm and peaks indicative for FMN at 380 and 450 nm. (C) Enlarged section of the UV/Vis spectrum of TRX-StrepII-Dshi_1135 with peak maxima at 380 and 450 nm and clear vibronic structure at 425 and 475 nm. (D) UV/Vis spectrum of 20 µM FMN solution in washing buffer A1 with peak maxima at 380 and 450 nm, without vibronic structures.

Additionally, a vibronic structure at 425 and 475 nm was detected (Figure 23 C). This vibronic structure is absent in absorbance pattern of free FMN (Figure 23 D) and indicates the tight binding within the FMN-binding pocket by hydrogen bonding and hydrophobic interactions (Swartz & Bogomolni, 2005). Between 2-30 % FMN occupancy were calculated for purified TRX-StrepII-Dshi_1135 protein, using the respective extinction coefficients. The occupancy was successfully increased up to 60 % by establishing a reconstitution protocol. Recorded spectra of reconstituted Dshi_1135 protein showed the vibronic bands of FMN, indicating that the added cofactor is actually bound to the protein and not just free in solution.

4.1.5 Dshi_1135 undergoes a Blue Light driven Photocycle

Upon blue light illumination LOV proteins typically undergo a photocycle, where a covalent bond is formed between the FMN cofactor and the photoactive cysteine of the LOV domain (see chapter 1.5.1). The covalent bond formation results in a metastable

intermediate that absorbs maximally at 390 nm (LOV_{390}) and is also called the signaling state of the LOV domain. Depending on the LOV domain, the lifetime of the signaling state is quite variable and can reach from seconds to hours or even days. Finally, when the intermediate decays back into the ground state, the photocycle is completed.

To investigate if Dshi_1135 is capable of performing such a photocycle reaction, an absorption spectrum of the purified and reconstituted protein was initially recorded under dim red light conditions. As previously shown, red light has no influence on Dshi_1135 activity and thus simulates a dark environment. After confirming the ground state of Dshi_1135, the same sample was illuminated with blue light (λ=470 nm) for 5 min and then the spectrum was recorded again (Figure 24).

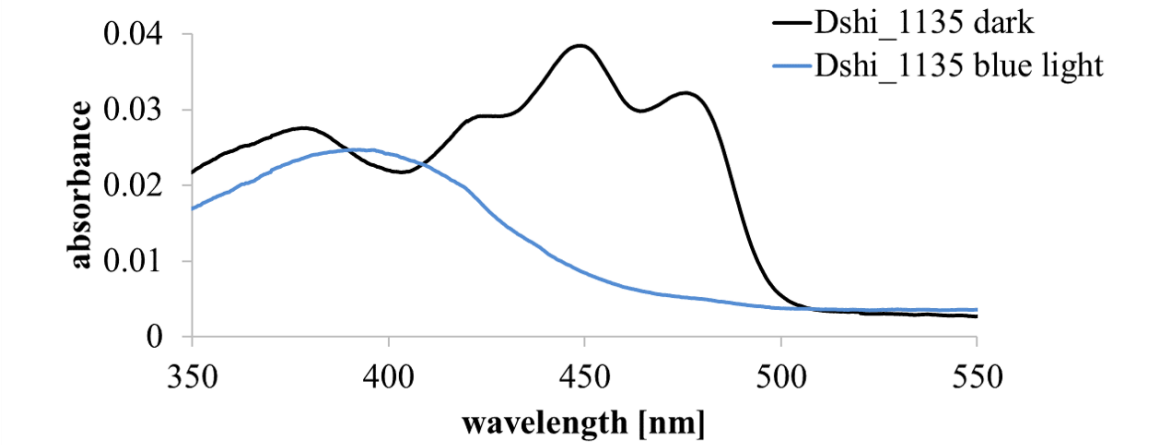

Figure 24: UV/Vis spectra of purified and reconstituted TRX-StrepII-Dshi_1135 under dark and blue light conditions
Ground state absorbance spectra of purified and reconstituted TRX-StrepII-Dshi_1135 protein were recorded under dim red light (black line) and showed absorption maxima at 380 and 450 nm and the vibronic structure at 425 and 475 nm, indicative for the non-covalent binding of the FMN cofactor. The same sample was illuminated with blue light (λ=450 nm) for 5 min and measured again in the UV/Vis spectrophotometer (blue line). An absorbance maximum of 390 nm indicates the conversion of Dshi_1135 into the signaling state.

Under dark conditions the typical ground state absorption spectrum for FMN-binding LOV proteins with maxima at 380 nm and 450 nm and additional vibronic bands at 425 nm and 475 nm was recorded (Figure 24, black line). Illumination of Dshi_1135 with blue light caused a shift of the absorbance maximum to 390 nm (Figure 24 blue line). This clearly indicates the ability of Dshi_1135 to go from the ground state into the signaling state. To test, if Dshi_1135 recovers back into the ground state and thus completes the photocycle reaction, the blue light illuminated sample was stored in complete darkness for 18 h and measured again in the UV/Vis spectrophotometer (data

not shown). The recorded spectrum revealed a decay back into the ground state and thus it was proven that Dshi_1135 is able to undergo a blue light driven photocycle.

Next it was aimed to determine the lifetime and return rate of the Dshi1135 photo adduct. Therefore, purified and reconstituted TRX-StrepII-Dshi_1135 protein was illuminated with blue light (λ=470 nm) for 5 min to convert it into the active signaling state. A time series was then recorded at 450 nm, with absorbance measured every two seconds using the UV/Vis spectrophotometer to create an exponential regression curve. Unfortunately, due to technical difficulties it was not possible to record time series longer than 3 h. Evaluation of the recorded data showed a linear increase of the absorbance at 450 nm during the whole measurement (data not shown). Consequently, the photocycle of Dshi_1135 was not completed after 3 h. Even though no exact return rate could be determined, it can be stated that the lifetime of the Dshi_1135 photo adduct lies between 3-18 h and is therefore considerably long, compared to other known LOV proteins. The fastest known recovery rates of approximately 10 sec were observed for phototropin2 of *A. thaliana* and DsLOV of *D. shibae* (Kasahara *et al.,* 2002; Endres *et al.,* 2015). For the homologous *E. litoralis* protein EL346 a time constant of ~55 min was determined for the photocycle reaction (Rivera-Cancel *et al.,* 2014). It is proposed that the amino acid sequence and the resulting protein conformation characteristics affect the photo adduct lifetime (Christie *et al.,* 2007). Furthermore it was shown in previous studies that the deprotonation of the FMN N5 atom during the decay back into the ground state is a time-defining factor, because the deprotonation is dependent on the accessibility of the active center of the LOV domain (Zoltowski *et al.,* 2009).

4.1.6 Identification of the Photoactive Cysteine

All LOV domains share the same typical α/β PAS fold in which a single FMN molecule is embedded as cofactor. On one of the α-helices within the core domain a conserved GRNCRFLQ motif, containing the photoactive cysteine required for photo adduct formation, is located. In *E. litoralis* EL346 this photoactive cysteine was identified at amino acid position 55. It was shown, that a newly generated EL346 C55A protein mutant fails to form the photo adduct, demonstrating the essential role of this cysteine for covalent flavin binding upon blue light illumination (Rivera-Cancel *et al.,* 2014). Similar observations were made for LOV domains that also lack the active cysteine, such as EL368 from *E. litoralis* (Correa *et al.,* 2013), LovK from *E. litoralis* DSM8509 (Fiebig *et al.,* 2019) or BM-LOV-HK from *Brucella melitensis* (Swartz *et al.,* 2007).

The protein sequence alignment of the Dshi_1135 and the EL346 protein sequences revealed the cysteine at position 61 of Dshi_1135 as potential photoactive residue (Figure 13). In order to prove this hypothesis, the cysteine at this position was exchanged by alanine by site directed mutagenesis of the Dshi_1135 gene, using the pET52b(+)Trx_Dshi1135Full plasmid as template. The successful mutation was verified by sequencing and the newly obtained plasmid pET52b(+)Trx_Dshi1135C61A was transformed into *E. coli* BL21-CodonPlus(DE3)-RIL cells for expression of the TRX-StrepII-Dshi_1135C61A mutant protein. The purified and reconstituted protein was employed for UV/Vis measurements in comparison to the TRX-StrepII-Dshi_1135 wild type protein. First, spectra were recorded under dark conditions. Afterwards, the same protein samples were illuminated with blue light (λ=470 nm) in the cuvette for 5 min for LOV photo adduct formation and spectra were recorded again. For the wild type TRX-StrepII-Dshi_1135 protein, the results after blue light illumination from previous measurements could be reproduced. The obtained absorbance spectra are shown in Figure 25.

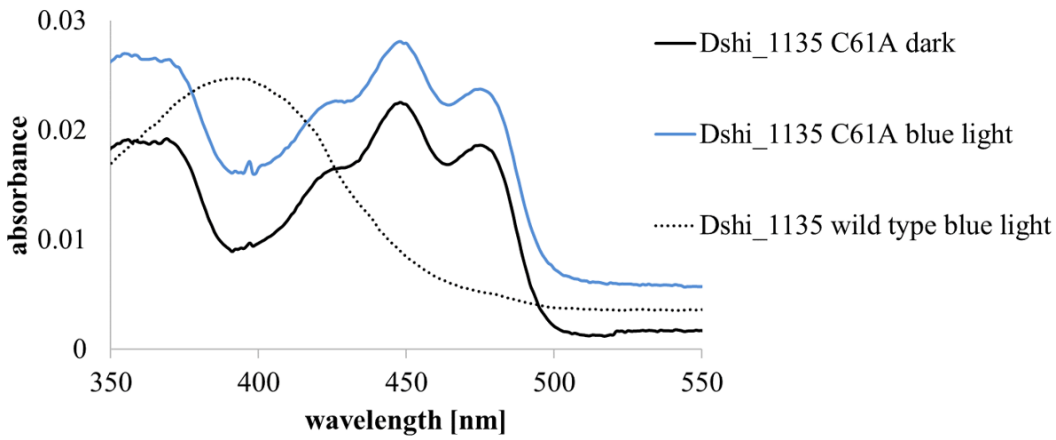

Figure 25: UV/Vis spectra of purified Dshi_1135C61A protein under dark and blue light conditions
An absorbance maximum at 390 nm was detected for the Dshi_1135 wild type protein upon blue light illumination (dotted line) and indicates the conversion of into the signaling state. Ground state absorbance spectra of purified Dshi_1135C61A protein were recorded (black line) and show absorption maxima at 380 and 450 nm and the vibronic structure at 425 and 475 nm, indicative for the non-covalent binding of the FMN cofactor. The same sample was illuminated with blue light (λ=450 nm) for 5 min and measured again in the UV/Vis spectrophotometer (blue line). No change in absorbance was detected, indicating the failed photo adduct formation of the mutant protein.

Under dark conditions a spectrum demonstrating the ground state with major peaks at 380 nm and 450 nm, was recorded for the TRX-StrepII-Dshi_1135 wild type protein, as well as for the TRX-StrepII-Dshi_1135 C61A mutant protein (Figure 24 and Figure 25,

black lines). Also, the vibronic bands with additional peaks at 425 nm and 475 nm were found. These results implicated that the TRX-StrepII-Dshi_1135C61A mutant is still able to non-covalently bind the FMN chromophore comparable to the wild type protein. This kind of absorbance was already observed for other LOV domain proteins with mutations of the photoactive cysteine, indicating that this cysteine is not essential for cofactor coordination in the ground state (Salomon *et al.,* 2000). In contrast to the TRX-StrepII-Dshi_1135 wild type protein, no spectral changes were noticed for the TRX-StrepII-Dshi_1135C61A mutant protein after blue light illumination (Figure 25 blue line). Also, no obvious changes occurred compared to the spectrum of the dark incubated sample. This experiment demonstrated, that the TRX-StrepII-Dshi_1135C61A mutant protein is no longer able to facilitate the photo adduct formation by covalently binding of the FMN cofactor within the LOV domain. These results indicated that the cysteine at position 61 in Dshi_1135 is the photoactive residue and that Dshi_1135 consequently has the photochemical features of a typical LOV protein.

It could already be shown in the past, that the formation of the adduct state is blocked in cysteine-deletion mutants (Diensthuber *et al.,* 2014). For the plant LOV protein AsLOV2 from *Avena sativa* more than 100 different mutant variants were generated and no single mutation was able to entirely eliminate adduct formation, besides for mutations of the photoactive cysteine, clearly indicating the importance of this amino acid at this position (Zayner *et al.,* 2013). Additionally, it also demonstrates, that the light-induced conformational change of LOV proteins does not result from a single mechanism or amino acid. It appears that the partly conserved amino acids around the active center play a role in stability rather than in function. Some mutations are described to positively affect and even enhance the activity of some LOV domains. In *E. litoralis* EL346 the V115A mutation drastically enhanced the autophosphorylation level of the downstream kinase domain, independent of the light quality (Rivera-Cancel *et al.,* 2014). In *Neurospora crassa* VVD, different mutations were shown to either decelerate or accelerate the photo adduct decay of the LOV domain back into the ground state, as the newly introduced amino acids promoted stabilization or destabilization of the FMN-C4(a)-bond, respectively (Zoltowski *et al.,* 2009). In recent studies it was also shown that water molecules that enter the chromophore binding pocket might be directly involved in photocycle chemistry. Water probably serves as the

primary proton acceptor in proton transfer during photocycling. An asparagine side chain close to the chromophore is believed to be involved in coordination of the water molecules and "controls" entry and thus, the adduct state lifetime (Chan & Bogomolni, 2012; Zayner & Sosnick, 2014). Surprisingly, it was also found that some LOV proteins with mutations of the photoactive cysteine, were still able to propagate light-dependent signaling without photo adduct formation and completing a photocycle. Blue light can still initiate the formation of the neutral FMN semiquinone intermediate LOV_{660} (see chapter 1.5.1 and Figure 8) (Kottke *et al.,* 2003; Kay *et al.,* 2003; Yee *et al.,* 2015). This flavin reduction step is still sufficient to initiate the protonation of the FMN N5, but not the covalent bond formation between the C4(a) atom of FMN and the LOV domain. With regard to LOV domain signaling, this protonation of the FMN N5 atom is the key event that causes a series of structural rearrangements, in which a conserved glutamine residue is involved (Kottke *et al.,* 2018). The glutamine amide side chain adjusts the hydrogen-bonding network, which finally leads to alterations of the LOV domain structure and induces activity of the fused output domain (Losi & Gärtner, 2017). One hypothesis why the cysteine in the LOV domain is so highly conserved, even if it is not 100 % essential for activation of LOV domain signaling, is, that LOV domains might evolved from ancestral redox-active flavoproteins that employed the cysteine to be less susceptible to changes in cell redox potential and more effective in light sensing in parallel (Yee *et al.,* 2015).

Therefore, it might be of interest to investigate the influence of different side chains on the activity of Dshi_1135 in the future. Especially, the conserved glutamine residue at position 112 (see Figure 13) should receive attention, as it could be involved in signal propagation.

4.1.7 Analysis of light-dependent Autophosphorylation Activity of Dshi_1135

After it was successfully shown that Dshi_1135 possesses a functional N-terminal LOV domain, it was aimed to investigate the postulated kinase activity of the protein. For other LOV HKs it was demonstrated that they phosphorylate a histidine residue upon blue light activation, before subsequently transferring the phosphate to a conserved aspartate residue within the receiver domain of their cognate RR. As mentioned earlier, Dshi_1135 is missing the conserved histidine residue in the H-box and possesses an arginine residue instead (Figure 13). Therefore, it was of special interest to investigate the kinase activity of Dshi_1135. Kinase activities of EL368 and EL346 were analyses

by autophosphorylation assays under different light conditions, using [γ-^{32}P] ATP as substrate. For EL368 a four-times increased activity was observed after conversion into the active state by blue light illumination (Correa *et al.,* 2013).

To investigate autophosphorylation activity in response to the blue light induced photocycle, the kinase activity of Dshi_1135 under blue light and dark conditions was analysed. The purified and reconstituted TRX-StrepII-Dshi_1135 protein was incubated with [γ-^{32}P] ATP and in the presence and absence of cold ATP under dark and blue light (λ=470 nm) conditions, respectively. After overnight incubation, the reactions were quenched by addition of 2x SDS loading dye and subsequent flash freezing in liquid nitrogen. The samples were denatured for 10 min at 95 °C and separated together with a prestained protein marker on a 12 % SDS gel for 2 h at a constant current. Visualization of successful phosphorylation of TRX-StrepII-Dshi_1135 was performed *via* autoradiography on an X-ray film (Figure 26).

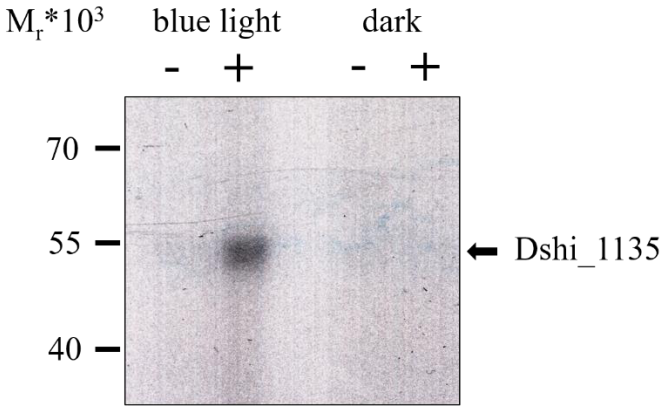

Figure 26: Autophosphorylation assay of Dshi_1135 under blue light and dark conditions
Purified and reconstituted Dshi_1135 protein was incubated with [γ-^{32}P] ATP and with (+) or without (-) additional cold ATP and stored overnight either under dark or blue light conditions. Reactions were quenched by addition of 2x SDS loading dye and flash freezing in liquid nitrogen. All samples were run on 12 % SDS PAGES and the resulting gel was applied to an X-ray film. The film was incubated for 3 days under strict exclusion of light and phosphorylation of Dshi_1135 was visualized by autoradiography. Autophosphorylation of Dshi_1135 was observed under blue light illumination and addition of cold ATP (black arrow), indicating a blue light induced activation of the kinase activity. A prestained molecular mass marker for determination relative molecular masses was used (relative molecular masses (*1'000) are indicated).

A clear band corresponding to a M$_r$ of about 54'000 was detected on the X-ray film for the TRX-StrepII-Dshi_1135 protein sample that was irradiated with blue light and treated with additional cold ATP. In contrast, this band could not be found in any other sample analysed. This finding demonstrates that Dshi_1135 possesses a blue light induced autophosphorylation activity. However, no statement can be made yet which

amino acid residue is involved in this process. Autophosphorylation assays with different Dshi_1135 protein variants, carrying mutations at histidine 218, histidine 258 or arginine 148, could provide information here. If indeed the arginine 148 is involved in autophosphorylation, Dshi_1135 would present a rare case of an arginine kinase in bacteria. The use of a different histidine for autophosphorylation than the conserved residue within the H-box, would also represent an uncommon form of HK.

As an alternative to autophosphorylation assays using [γ-^{32}P] ATP, Phos-tag™ SDS-PAGE was performed to investigate the kinase activity of Dshi_1135. Phos-tag™ is a synthetic and functional molecule that was designed from the catalytic domain of an alkaline phosphatase (Kinoshita *et al.,* 2006). It is able to specifically capture phosphorylated amino acid residues by the help of bound divalent metal ions, like zinc or manganese and builds a non-covalent complex with the phosphorylated protein. When the Phos-tag™ and the respective metal ions are added directly to a conventional SDS gel, it is possible to distinguish between phosphorylated and non-phosphorylated proteins, as the Phos-tag™ - protein complex migrates slower in the gel, than the unbound unphosphorylated proteins. This makes the Phos-tag™ SDS-PAGE a faster and safer method, compared to the use of radioactively labeled [γ-^{32}P] ATP. It was already successfully tested for investigations of different phosphoproteins and represents a reliable method for phosphoprotein analyses (Barbieri & Stock, 2008).

The experimental setup for Phos-tag™ SDS-PAGE was similar to the previous autophosphorylation assay described above. Purified and reconstituted TRX-StrepII-Dshi_1135 protein was mixed with different ATP concentrations (1 µM, 10 µM, 100 µM and 1 mM) and either incubated in the dark or under constant blue light irradiation (λ= 470 nm) overnight. The reactions were stopped by addition of 2x SDS loading dye, but the samples were not heated to 95 °C to prevent dissociation of the phosphorylated protein complex. Samples were subsequently analysed on 10 % SDS gels supplemented with 100 µM Phos-tag™ and $MnCl_2$ ions. Furthermore, unphosphorylated TRX-StrepII-Dshi_1135 protein was analysed in parallel as negative control. As positive control a commercially available mix of phosphorylated and non-phosphorylated α-casein was employed. Additionally, all samples were run on a conventional 12 % SDS-PAGE (Figure 27).

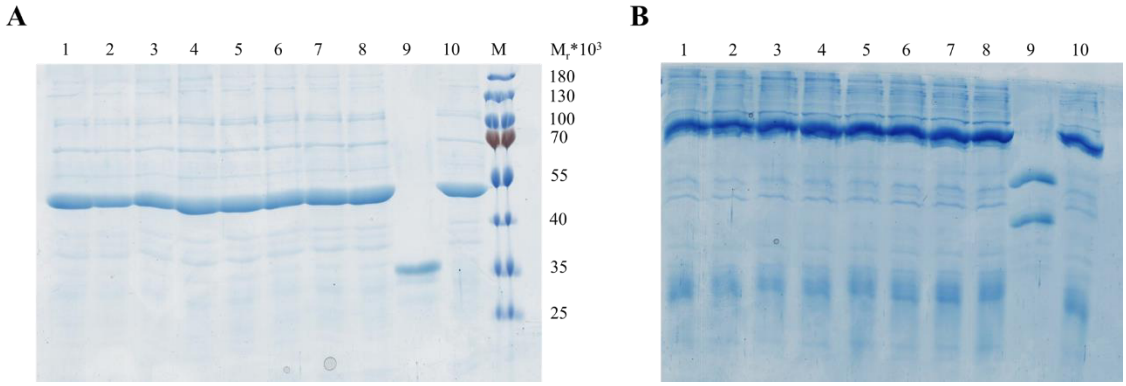

Figure 27: 12 % SDS gel (A) and Phos-tag^{TM} SDS-gel (B) after autophosphorylation assay of TRX-StrepII-Dshi_1135
Purified and reconstituted TRX-StrepII-Dshi_1135 protein was employed for an autophosphorylation assay, using Phos-tag^{TM} SDS-PAGE. Therefore, the protein was mixed with 1 µM, 10 µM, 100 µM or 1 mM ATP, respectively, and incubated overnight in a dark environment or under constant blue light irradiation. Reactions were quenched by addition of 2x SDS loading dye and samples were loaded onto 10 % Phos-tag^{TM} (100 µM) SDS gels. Protein bands were visualized by Coomassie Brilliant Blue staining.
Lane M: prestained molecular mass marker (relative molecular masses (*1'000) are indicated. Lane 1: Dshi_1135+1 µM ATP, blue light. Lane 2: Dshi_1135+10 µM ATP, blue light. Lane 3: Dshi_1135+100 µM ATP, blue light. Lane 4: Dshi_1135+1 mM ATP, blue light. Lane 5: Dshi_1135+1 µM ATP, dark. Lane 6: Dshi_1135+10 µM ATP, dark. Lane 7: Dshi_1135+100 µM ATP, dark. Lane 8: Dshi_1135+1 mM ATP, dark. Lane 9: α-casein, positive control. Lane 10: Dshi_1135 untreated, negative control.

On the 12 % SDS-PAGE in all samples a distinct band with a M_r of 52'000 was identified, indicating that sufficient amounts of TRX-StrepII-Dshi_1135 protein were employed in the assay (Figure 27 A lanes 1-8 and 10). For the α-casein positive control a single band corresponding to a M_r of 35'000 and with an adequate intensity was detected (Figure 27 A lane 9). After running the same amount of TRX-StrepII-Dshi_1135 protein on a Phos-tag^{TM} SDS-PAGE with addition of ATP in concentrations from 1 to 100 µM under dark or blue light conditions, no significant shift of the TRX-StrepII-Dshi_1135 protein could be detected. Thus, there is no indication for the phosphorylation of TRX-StrepII-Dshi_1135 (Figure 27 B lanes 1-8). However, many additional weak bands of impurifying proteins were found in the TRX-StrepII-Dshi_1135 protein samples. All bands were comparable to the band pattern observed for the untreated negative control representing the non-phosphorylated form of Dshi_1135 (Figure 27 B lane 10). In contrast, two distinct and clearly separate bands were found in the positive control, with the lower band representing non-phosphorylated α-casein and with the upper band representing phosphorylated α-casein. For Phos-tag^{TM} SDS-PAGE high-purity protein samples are needed to easily distinguish the specific band shift in the gel due to protein phosphorylation from impurities. In principle the assay worked since

α-casein was detected as a single band after conventional SDS-PAGE (Figure 27 A lane 9) and as double band after Phos-tag™ SDS-PAGE (Figure 27 B lane 9). Unfortunately, autophosphorylation of the Dshi_1135 protein could not be demonstrated. The method of Phos-tag™ SDS-PAGE still leaves room for improvement. Each phosphoprotein behaves differently and optimal concentrations of the employed components, like Phos-tag™ and metal ions, need to be elucidated. It currently remains unclear whether autophosphorylation of Dshi_1135 could not be detected for technical reasons or whether Dshi_1135 is unable to autophosphorylate due to the lack of a histidine residue within the DHpL domain of the protein.

Some flavoproteins are described to be less thermostable in the absence of their respective cofactor (Hefti *et al.,* 2003; Kamerbeek *et al.,* 2007; Caldinelli *et al.,* 2008). The FMN occupancy of affinity chromatography purified TRX-StrepII-Dshi_1135 ranged between 2-30 % and could be increased up to 60 % by reconstitution with FMN. The illustrated autophosphorylation assay in Figure 26 was performed with TRX-StrepII-Dshi_1135 protein, of which an FMN occupancy of 60 % was determined beforehand. This was the highest reached FMN occupancy after reconstitution throughout the entire study and consequently, all other performed assays were carried out with lower occupied TRX-StrepII-Dshi_1135 protein. It is therefore conceivable that a FMN content of at least 60 % is necessary to maintain stability of Dshi_113 and it should be taken into consideration, to enhance the FMN occupancy of the protein already during early steps of production to enhance protein stability. For instance, the addition of either riboflavin or FMN directly into the cultivation medium of the *E. coli* expression culture could be tested.

4.1.8 Potential Response Regulators of Dshi_1135

Bacterial two-component systems are typically comprised of a sensor HK and a cognate RR. In the case of LOV HKs, a blue light stimulus triggers the activation of the LOV domain followed by binding of ATP by the CA and ATPase domain and subsequent autophosphorylation of a conserved histidine residue in the DHp domain with the HK domain. The phosphoryl moiety is then transferred to a conserved aspartate side chain within the receiver domain of the RR. Phosphorylation of the RR modulates downstream effects, which in many cases are altered gene expression levels and changes in cellular physiology (Capra & Laub, 2012; Möglich, 2019).

Since it could be shown that Dshi_1135 is a blue light activated LOV protein with a

potential kinase activity and an identity of 42 % to EL346 of *E. litoralis*, it was of interest to identify potential cognate RR(s). In many two-component systems HK and RR are encoded as neighbours or in the same operon structure and are therefore co-expressed to facilitate an intact signaling pathway. However, in some cases the genes for two-component systems are found without their counterpart in the genome, often referred to as orphans. Also, Dshi_1135 was found to be an orphan HK without a co-localized or anywhere near RR in the genome map. This circumstance made it more difficult to identify potential targets of Dshi_1135. Two strategies were followed and combined to find potential candidates. First, the genome of *D. shibae* was screened for annotated "two-component response regulators", as they all might be potential targets of Dshi_1135. Especially orphan RRs would be interesting candidates for future investigations. Second, the *D. shibae* genome was screened in a protein BLAST search for potential RRs of Dshi_1135 using the amino acid sequences of the known targets PhyR and LovR of *E. litoralis* EL346 as query. Based on the homology between Dshi_1135 and EL346, it seemed reasonable to assume that homologous response regulators also exist in *D. shibae*.

The screening for annotated "two-component response regulators" resulted in 23 hits, which are listed in Table 11. To estimate the role of the identified RRs, it was checked whether mutants of the respective gene loci were part of the *D. shibae* transposon library (Ebert *et al.,* 2013). The total of 23 identified potential RRs of Dshi_1135 were examined with respect to three aspects. First, the genomic neighbourhood of all genes was analyzsd regarding co-localized HKs. As Dshi_1135 was found as a stand-alone LOV HK, orphan RRs would present especially interesting candidates for future experiments. It was found that 18 of the potential RRs possess a directly co-localized HK or one in close proximity in the upstream or downstream region, respectively. Second, the *D. shibae* transposon mutant library was checked for the respective mutant strains of the potential RRs. For 16 of the 23 candidates' transposons mutants were available and were subsequently examined regarding their pigmentation phenotype. It is assumed that the RR(s) of Dshi_1135 participates in the regulation of the PGC in *D. shibae*. Mutation of the Dshi_1135 gene results in a loss of pigmentation as previously described. It must therefore be taken into consideration, that the lack of the cognate RR would also cause a defect in pigment biosynthesis and the respective mutant strain would show an altered pigmentation phenotype. All 16 transposon mutants had a

pink pigmentation, indicative for an intact pigment biosynthesis. Also, three of the identified potential RRs without a co-localized HK (Dshi_1661, Dshi_2820 and Dshi_3485) showed a pink pigmentation. Unfortunately, no transposon mutant strains were available for Dshi_0038 and Dshi_1508. Both were identified as orphan two-component RRs and therefore, the pigmentation of the respective mutant strains would have been interesting. However, RRs with a co-localized HK and/or pink pigmentation do not have to be sorted out directly. In *E. litoralis* it was shown that the RR LovR can be phosphorylated by EL346 and two additional HKs, which is described as the "many to one" relationship and might implicate the functional importance of the RR (Correa *et al.,* 2013). This phenomenon could explain the pink pigmentation, as the respective RR might still be activated by another HK und can participate in regulation of photosynthesis genes. Therefore, it might be possible that one of these RRs still is a target of Dshi_1135. Third, all 23 candidates were checked for their assigned function, using the KEGG genes database (Kanehisa *et al.,* 2016) and the annotated *D. shibae* genome (Wagner-Döbler *et al.,* 2010) (Table 11).

Table 11: Screening of the *D. shibae* genome for annotated "two-component response regulators"

Dshi Nr.	RefSNP (rs) number	Gene name/Description	Notes	Transposon mutant	Pigmentation of the mutant strain
Dshi_0038	DSHI_RS00185	two component transcriptional regulator	-	no	-
Dshi_0212	DSHI_RS01055	two component transcriptional regulator OmpR family, response regulator ChvI	integral membrane sensor signal transduction histidine kinase (Dshi_0211) upstream	yes	pink
Dshi_0449	DSHI_RS02300	two component transcriptional regulator OmpR family, response regulator PrrA	integral membrane sensor signal transduction histidine kinase (Dshi_0448) upstream	yes	pink
Dshi_0465	DSHI_RS02380	*luxR2* two component transcriptional regulator	sensor histidine kinase (Dshi_0467) downstream	yes	pink
Dshi_0513	DSHI_RS21620	transcriptional regulator	histidine kinase (Dshi_0515) downstream	yes	pink
Dshi_0823	DSHI_RS04215	two component, sigma54 specific, transcriptional regulator, repressor protein LuxO	histidine kinase (Dshi_0824) downstream	no	-
Dshi_1081	DSHI_RS05530	two component	integral membrane sensor signal transduction histidine kinase (Dshi_1080) upstream	no	-
Dshi_1196	DSHI_RS06105	two component, sigma54 specific, transcriptional regulator, two-component system	integral membrane sensor signal transduction histidine kinase (Dshi_1197) downstream	yes	pink

Dshi Nr.	RefSNP (rs) number	Gene name/Description	Notes	Transposon mutant	Pigmentation of the mutant strain
Dshi_1406	DSHI_RS07155	response regulator receiver protein	integral membrane sensor signal transduction histidine kinase (Dshi_1408) downstream	no	-
Dshi_1508	DSHI_RS07680	*ctrA* two-component system, cell cycle response regulator CtrA	-	no	-
Dshi_1538	DSHI_RS07830	*phoB* two-component system, OmpR family, phosphate regulon response regulator PhoB	family, phosphate regulon sensor histidine kinase PhoR (Dshi_1532) upstream	no	-
Dshi_1661	DSHI_RS08455	two-component system, response regulator / RNA-binding antiterminator	-	yes	pink
Dshi_1894	DSHI_RS09655	putative response regulator receiver protein	LOV-regulator, Blue-light sensing cell cycle sensor histidine kinase and response regulator CckA (Dshi_1893) upstream	no	-
Dshi_2279	DSHI_RS11585	two component transcriptional regulator two-component system, OmpR family, torCAD operon response regulator TorR	signal transduction histidine kinase (Dshi_2280) downstream	yes	pink

Dshi Nr.	RefSNP (rs) number	Gene name/Description	Notes	Transposon mutant	Pigmentation of the mutant strain
Dshi_2345	DSHI_RS11930	two-component system, NarL family, nitrate/nitrite response regulator NarL	integral membrane sensor signal transduction histidine kinase (Dshi_2344) upstream	yes	pink
Dshi_2497	DSHI_RS12700	two-component system, OmpR family, response regulator	integral membrane sensor signal transduction histidine kinase (Dshi_2498) downstream	yes	pink
Dshi_2674	DSHI_RS13570	two component transcriptional regulator	histidine kinase (Dshi_2676) downstream	yes	pink
Dshi_2820	DSHI_RS14315	response regulator two-component system, cell cycle response regulator	-	yes	pink
Dshi_3430	DSHI_RS17370	*regA* photosynthetic apparatus regulatory protein RegA two-component system, response regulator RegA	sensor histidine kinase RegB (Dshi_3432) downstream	no	-
Dshi_3485	DSHI_RS17640	response regulator phosphoserine phosphatase RsbU/P	-	yes	pink

Dshi Nr.	RefSNP (rs) number	Gene name/Description	Notes	Transposon mutant	Pigmentation of the mutant strain
Dshi_3772	DSHI_RS19040	two component transcriptional regulator two-component system, OmpR family, response regulator	two component integral membrane sensor signal transduction histidine kinase (Dshi_3773) downstream located on pDSHI01	yes	pink
Dshi_3837	DSHI_RS19360	response regulator receiver domain protein	signal transduction histidine kinase (Dshi_3834) upstream located on pDSHI02	yes	pink
Dshi_4048	DSHI_RS20365	two-component system, OmpR family, response regulator	two component integral membrane sensor signal transduction histidine kinase (Dshi_4049) downstream located on pDSHI03	yes	pink

Functions could not be assigned or suspected for all RRs. The gene product of Dshi_0465 or *luxR2*, respectively, belongs to the LuxR family and is probably an AHL (acylated homoserine lactone)-controlled transcriptional regulator in *D. shibae*. Dshi_0823 encodes the LuxO protein. Regulators involved in quorum sensing in *D. shibae* have been identified by genomic analyses and subsequently characterized (Wagner-Döbler *et al.,* 2010; Patzelt *et al.,* 2013). However, Dshi_0465 and Dshi_0823 did not appear in these investigations. Thus, both proteins may represent previously unknown regulators involved in quorum sensing in *D. shibae*. Therefore, it is not assumed, that they have an additional function in the regulation of Bchl *a* biosynthesis.

The Dshi_3430 protein is annotated as RegA and is most likely part of the RegAB two-component system in *D. shibae*. The HK RegB (Dshi_3432) was identified downstream of RegA within the genome. This system is well-studied and known to be involved in the sensing of changes in oxygen tension in *R. capsulatus* (Sganga & Bauer, 1992; Mosley *et al.,* 1994). The homologous system PrrAB also exists in *R. sphaeroides* (Eraso & Kaplan, 1994; Phillips-Jones & Hunter, 1994). Known targets of this system are the *puh*, *puc*, *puf* and *bchC* operon (Elsen *et al.,* 2004) and they are therefore involved in regulation of photosynthesis genes. Dshi_3430 shows more than 80 % identity to RegA and PrrA, respectively, and is considered to be a homologue.

The identified two-component RR Dshi_1508 is encoding the cell cycle regulator CtrA. This protein is known as a master-regulator of cell cycle control, cell division and cell growth in *C. cresentus* and acts together with the HK CckA (Laub *et al.,* 2000; Jacobs *et al.,* 2003). In *D. shibae* it was found that the transcriptional regulator CtrA is part of a phosphorelay system together with the sensor HK CckA (Dshi_1644) and the phosphotransferase ChpT (Dshi_1470). This phosphorelay system controls biosynthesis of signaling molecules and cell differentiation and therefore links both processes in *D. shibae* (Wang & Ziesche *et al.,* 2014). Because CtrA or Dshi_1508 is localized in the genome without its cognate HK, it appeared in the screening for potential RRs even though its function is already known.

In the screening Dshi_1894 was identified as potential RR for Dshi_1135. However, the HK Dshi_1893 is localized as a direct neighbour in the genome. Interestingly, Dshi_1893 was identified as one of three potential LOV proteins in *D. shibae* (Endres *et al.,* 2015). Moreover, it is defined as a CckA HK according to the KEGG genes database. As described above, the CckA HK is part of a phosphorelay system in

D. shibae. However, Dshi_1644 is defined as *D. shibae* CckA in the literature (Wang & Ziesche *et al.,* 2014). Dshi_1644 shows 49 % identity to CckA from *C. cresentus*, whereas Dshi_1893 shows only 30 % identity. It is therefore questionable whether Dshi_1893 is another CckA homolog. Furthermore, the directly adjacent RR Dshi_1894 suggests that Dshi_1893 is its cognate HK. However, if Dshi_1893 actually is a CckA homolog and would be able to phosphorylate CtrA, it would be interesting to investigate the influence of blue light on cell cycle control and cell communication in *D. shibae*.

In a second approach the *D. shibae* genome was screened in a protein BLAST search for potential RRs of Dshi_1135 using the amino acid sequences of the known targets PhyR and LovR from *E. litoralis* EL346 as query. For PhyR the homologous protein Dshi_3837 was found with an identity of 49 %. For LovR, three potential homologues were found. Again, the protein Dshi_3837 with 31 % identity, the protein Dshi_1538 with 29.5 % identity and the protein Dshi_1406 with 26 % identity. The alignments are shown in Figure 28. All three potential RRs also appeared in the first screening for annotated “two-component response regulators” (Table 11). According to the genome annotation of *D. shibae*, Dshi_1538 is defined as PhoB. In other organisms PhoB is part of a two-component system and of the Pho (Phosphate) regulon, which is involved in bacterial inorganic phosphate management (Santos-Beneit, 2015). Dshi_1538 shows 54 % identity to PhoB of *E. coli* and 57 % identity to PhoB of *E. litoralis* and 31 % identity to *E. litoralis* LovR. Since Dshi_1538 has not yet been studied in terms of function, it is not possible to conclude whether it is more likely to be a PhoB or LovR regulator. However, even if Dshi_1538 is acting as a PhoB regulator, it represents an interesting target for Dshi_1135. An interaction of the Pho regulon with other stresses, such as oxidative or osmotic stress was observed in other species (Yuan *et al.,* 2005) and therefore a crosstalk between nutrient stress and general stress might exist. Since the identified RRs of EL346 from *E. litoralis* are postulated to be involved in general stress response, *D. shibae* PhoB might be a target of Dshi_1135. Both, Dshi_3837 and Dshi_1406, have a co-localized sensor HK but no annotated function. At this point it is difficult to make a statement about the function of both proteins in *D. shibae*.

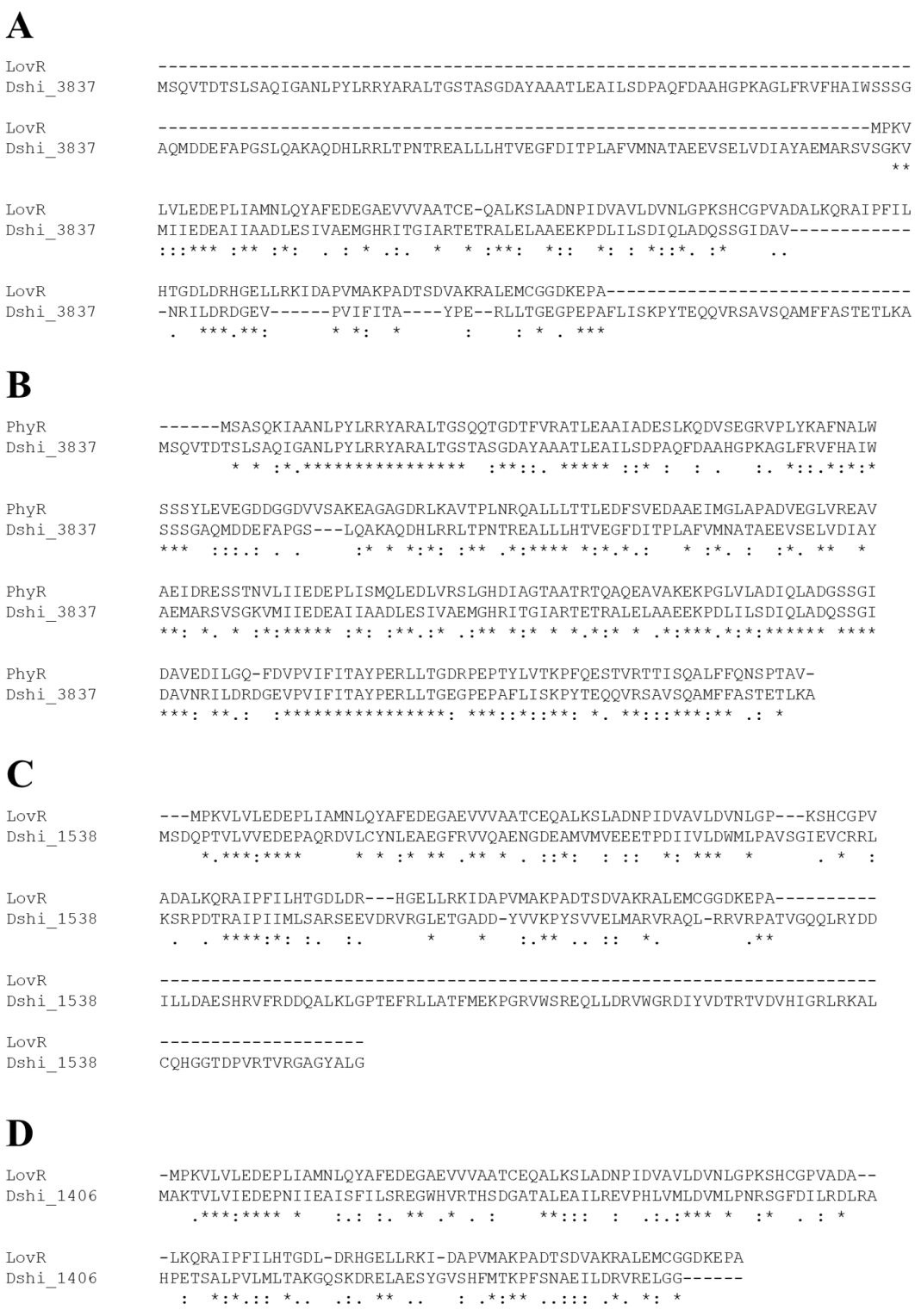

Figure 28: Identified potential response regulators of Dshi_1135 based on a homology screening to *E. litoralis* PhyR and LovR

The *D. shibae* genome was screened in a protein BLAST search for potential RRs, using the *E. litoralis* EL346 RR amino acid sequences of PhyR and LovR, respectively, as queries. Dshi_3837 was identified as homologue for PhyR (A) and LovR (B) with identities of 49 % and 31 %, respectively. The proteins Dshi_1538 (C) and Dshi_1406 (D) were both found as potential homologues of LovR with identities of 29.5 % and 26 %, respectively.

Asterisks indicate identical amino acids; dots indicate homologous amino acids**.** The amino acid alignment was generated using the multiple sequence alignment tool Clustal W (Larkin *et al.,* 2007)**.**

4.1.9 Functional Analysis of potential Response Regulators of the LOV HK Dshi_1135

Since the autophosphorylation experiment with Dshi_1135 could not be properly set up, performing *in vitro* phosphotransfer experiments for the identification of RRs did not seem reasonable. To overcome this problem a heterologous *in vivo* test system in *E. coli* was developed (bachelor thesis Miriam Niewöhner, TU Braunschweig 2019). Here, Dshi_1135 together with the RR Dshi_3837, Dshi_1538 or Dshi_1406, respectively, was produced heterologously in *E. coli* NovaBlue(DE3) cells. To monitor light-dependent gene regulation a *bchF-lacZ* reporter gene fusion was used. The *bchF* gene is the first gene of the larger *bchFNBHL* operon and its promoter is mediating the light-dependent expression. To establish this test system, two different plasmids with compatible origins of replication and an *E. coli* strain deficient in β-galactosidase activity were used. Expression vector pETDuet1, providing two multiple cloning sites (MCS), was used to co-express Dshi_1135, cloned into MCS1, and the genes of the RRs Dshi_3837, Dshi_1538 or Dshi_1406, respectively, inserted into MCS2. Two plasmids, carrying the *bchF-lacZ* reporter gene fusion were generated. Therefore, a 329 bp fragment of the *bchF* promoter region, encoding sequences from -289 to +41 with respect to the translation start of *bchF*, was cloned into the pBBR1MCSLIC-*lacZ* vector and pACYCLIC-*lacZ* vector, respectively. Blue light-dependent activation of the LOV HK Dshi_1135 will initiate autophosphorylation and subsequent transfer of the phosphate to the cognate response regulator. The phosphorylated RR is able to bind to the *bchF* promoter, which leads to ß-galactosidase production. Subsequently, the enzyme activity is determined by a β-galactosidase assay. The enzyme β-galactosidase catalyzes the hydrolytic cleavage of glycosidic bonds of β-galactopyranosides. For instance, it can hydrolyze the artificial substrate X-Gal (5-bromo-4-chloro-3-indolyl-β-D-galactopyranoside) present in an agar plate into galactose and the insoluble blue dye 5,5'-dibromo-4,4'-dichloro-indigo. Therefore, the β-galactosidase activity can be monitored by blue colonies and quantified easily by optical measurements. Determined ß-galactosidase levels finally monitor blue light-dependent signal transduction and promoter activity. In the case of the *in vivo* test system, a higher β-galactosidase activity under blue light that under dark conditions would indicate the activation of the *bchF* promoter by the employed RR and thus prove it as a target of Dshi_1135. A schematic illustration of the *in vivo* test system is depicted in Figure 29.

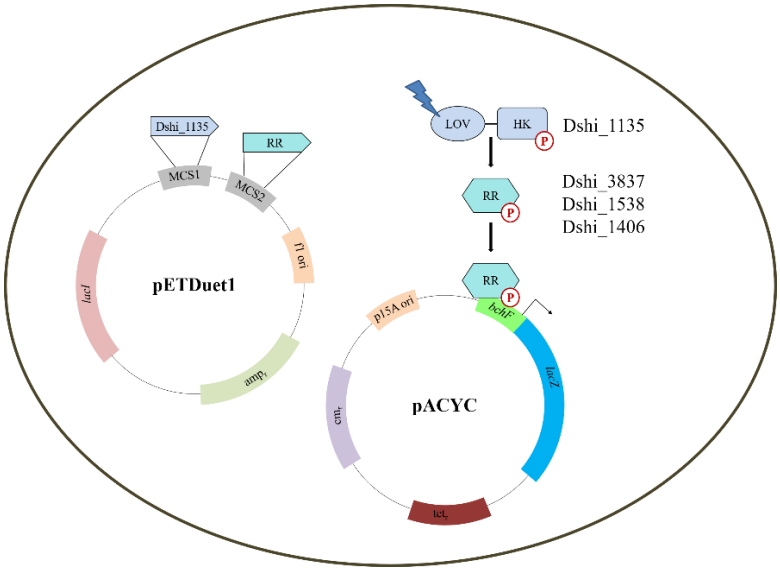

Figure 29: Schematic illustration of the heterologous *in vivo* test system for response regulator identification of Dshi_1135 in *E. coli*
The pETDuet1 vector carries the gene sequence of Dshi_1135 in MCS1 and the gene sequence of Dshi_3837, Dshi_1538 or Dshi_1406 in MCS2, respectively. The pACYC vector carries the *bchF-lacZ* reporter gene fusion. Both vectors are co-transformed into *E. coli* and expression of pETDuet1 encoded proteins is induced by IPTG. It is assumed that under blue light illumination of the cells, the LOV HK Dshi_1135 gets activated and subsequently phosphorylates its potential RR. If this is the case for Dshi_3837, Dshi_1538 and/or Dshi_1406, the regulator binds to the *bchF* promoter and activates expression of the *lacZ*-encoded β-galactosidase.

The generated strains of the *in vivo* test system were incubated on LB agar plates, supplemented with IPTG for induction of protein expression and X-Gal as substrate for β-galactosidase. Blue colonies then indicate β-galactosidase activity. As negative controls, all generated strains and the untransformed *E. coli* NovaBlue(DE3) strain were also incubated on LB agar + X-Gal plates without IPTG. In the absence of IPTG the untransformed cells did not grow as blue colonies, indicating an inactive β-galactosidase (Figure 30 A, -IPTG). Cells that carried only *bchF-lacZ* reporter gene fusion, showed a light blue pigmentation with and without supplemented IPTG (Figure 30 B). This indicated a leaky and not fully repressed *bchF* promoter, which caused a basal expression of β-galactosidase. Surprisingly, the untransformed *E. coli* NovaBlue(DE3) strain showed a noticeable blue color, when IPTG was added (Figure 30 A, +IPTG). Also, the strains carrying the plasmids pACYCLIC_*bchF-lacZ* and pETDuet1_Dshi1135-Dshi_1406, pETDuet1_Dshi1135-Dshi_1538 and pETDuet1_Dshi1135-Dshi_3837, respectively, grew in apparent blue colonies, when IPTG was added (*E. coli* NovaBlue (DE3) + pACYCLIC_*bchF-lacZ* and pETDuet1_Dshi1135-Dshi_1538 are shown exemplary in Figure 30 C, +IPTG).

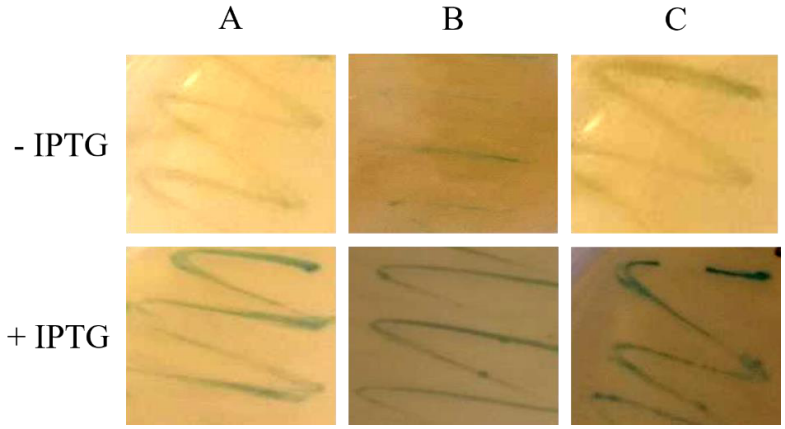

Figure 30: Analysis of the generated *E. coli* NovaBlue(DE3) strains for the *in vivo* test system regarding β-galactosidase activity on LB+X-Gal- agar plates with and without IPTG
The *E. coli* NovaBlue(DE3) strains carrying the plasmids pETDuet1 (A), pACYCLIC_*bchF-lacZ* (B) and pACYCLIC_*bchF-lacZ* and pETDuet1_Dshi1135-Dshi_1538 (C) were streaked out on LB+X-Gal agar plates supplemented with and without IPTG. Plates were incubated overnight at 37 °C and analysed regarding β-galactosidase activity indicated by blue colonies.

Especially the untransformed cells should not be able to hydrolyze the X-Gal substrate with an anticipated inactive β-galactosidase. On closer inspection it became clear, why all strains in the presence of IPTG were able to convert the X-Gal substrate. Due to inaccurate information on the manufacturer's website of the *E. coli* NovaBlue(DE3) cells, it was not clearly evident that the DE3 variant of this strain is not suitable for the selection on basis of β-galactosidase activity. The *E. coli* NovaBlue(DE3) strain carries the *lacZ*ΔM15 mutation, which results in an inactive β-galactosidase. The used variant in this study additionally carries the DE3 lysogenic phage that in turn carries the sequence for the α-peptide of the β-galactosidase, which can complement (α-complementation) the *lacZ*ΔM15 mutation and thus, leads to a functional enzyme. The addition of IPTG induces the β-galactosidase activity and X-Gal can be converted. However, the use of the DE3 system is necessary in order to express the proteins encoded on the pETDuet1 vector *via* the T7 system. Both properties (inactive endogenous β-galactosidase and T7 expression system) that are required for the success of the *in vivo* expression system are therefore not compatible with one another and the approach unfortunately had to be rejected.

To circumvent this problem, an alternative reporter gene system, such as the green fluorescent protein (GFP), should be tested. A corresponding plasmid, pBBR1LIC_*bchF-gfp*, has already been cloned but not tested yet. It could therefore be used directly for test experiments in the heterologous *in vivo* test system. If the *bchF* promoter could be activated in response to blue light by one of the potential RRs tested,

this could be simply measured using the GFP emission signal at 509 nm after excitation at 395 nm.

4.2 Light-Dependent Regulation of Photosynthesis Genes in *D. shibae*

While the light-dependent and anaerobic regulation of the photosynthesis gene expression in *R. sphaeroides* and *R. capsulatus* is quite well understood, only little is known about regulation of the PGC in the aerobic anoxygenic bacterium *D. shibae*. Within the PGC of *D. shibae* gene copies encoding homologs of the PpsR and PpaA regulator proteins were identified (Tomasch *et al.,* 2011). In addition, potential binding sites of the PpsR repressor protein were found upstream of potential operon structures of the PGC. Transcriptome analyses of the transposon mutant strain *ppsR*::Tn revealed a repressor function of PpsR on the PGC, while analysis of the mutant strains *ppaA*::Tn and Dshi_1135::Tn, respectively, indicated an activating function of PpaA and Dshi_1135 (Heyber, 2021). In the first part of this work, it was successfully shown that Dshi_1135 is a blue light activated LOV protein with potential kinase activity. In the second part, the influence of Dshi_1135, PpsR and PpaA on the light-dependent expression of photosynthesis genes in *D. shibae* are be investigated in more detail.

4.2.1 Comparison of the Bchl *a* content in the *D. shibae* DFL12^{T} Wild Type Strain and the Dshi_1135::Tn and *ppsR*::Tn Mutant Strains

All necessary genes, with few exceptions, for biosynthesis of Bchl *a* and spheroidenone in *D. shibae* are encoded in the PGC (Figure 5). The expression of the PGC is highly dependent on the light quality. Exposure of a dark-adapted *D. shibae* cells to high-light conditions lead to a drastic decrease in Bchl *a* content and *vice versa* (Tomasch *et al.,* 2011). These changes can also be observed visually. Dark cultured cells show the typical reddish-pink phenotype, whereas light exposed cultures show no pigmentation anymore.

The Bchl *a* content in the *D. shibae* wild type strain was examined under dark and light conditions. For this purpose, the cells were cultivated in SWM medium at 30 °C under continuous shaking until the stationary growth phase was reached after approximately 24 h. Cultures being irradiated with a light intensity of 100 lux were compared to cells being cultivated in the dark. Dark conditions were facilitated by using shielding black covers (aquila biolabs, Baesweiler, Germany). The dark-cultivated cells showed the typical intensive pink pigmentation, whereas the light-illuminated cells appeared faintly

white to beige, indicating the repression of pigment biosynthesis (Figure 31). Cell amounts of each culture corresponding to an OD_{578}= 2.5 were taken and harvested by centrifugation. For extraction of the pigments, the cells were resuspended in an acetone-methanol-mixture and incubated in the dark for 1 h. Subsequently, the cell debris was removed by centrifugation and the extracted pigments were analysed *via* UV/Vis spectroscopy. Absorbance spectra were recorded from 330 to 800 nm (Figure 31). For the dark-cultivated cells a spectrum with four major peaks was obtained, where the peak at 360 nm can be assigned to the soret band, at 600 nm to the Q_X band, and at 770 nm to the Q_Y of Bchl *a*. The area from 400-550 nm with the fourth maximum at 480 nm indicates the presence of spheroidenone (Figure 31 A). A strongly deviating spectrum was recorded for extracts of cells cultured under light irradiation. Here, only minimal peaks were detected at 360 nm for the soret band, at 770 nm for the Q_Y band resulting from Bchl *a* and around 480 nm for spheroidenone (Figure 31 B).

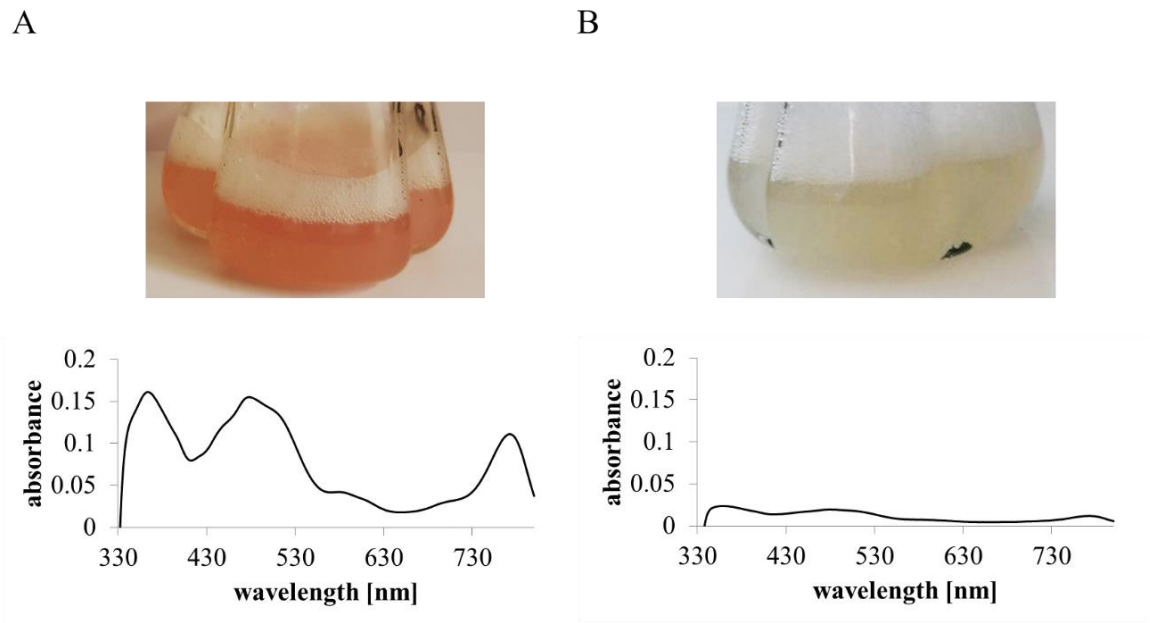

Figure 31: Phenotypes and *in vitro* Bchl *a* spectra of the *D. shibae* DFL12^T wild type strain cultivated in the dark and under light exposure (100 lux)
D. shibae wild type cells were cultivated in SWM medium at 30 °C and 180 rpm under dark conditions (A) or under constant illumination of 100 lux (B) until they reached the stationary growth phase. Cells of each culture corresponding to an OD_{578} of 2.5 were taken and pigments were extracted by acetone-methanol (7:2) treatment. UV/Vis spectra of the obtained extracts were recorded in a wavelength range from 330-800 nm.

In the high-throughput screening of the transposon mutant library the pigmentation phenotypes of the Dshi_1135::Tn and *ppsR*::Tn strains were particularly striking (Figure 6). Therefore, the pigment content in both mutants was determined in detail and

compared to the *D. shibae* wild type strain. The Dshi_1135::Tn and *ppsR*::Tn mutant strains were cultivated in complete darkness and pigments were extracted as described above. The recorded spectra are depicted in Figure 32.

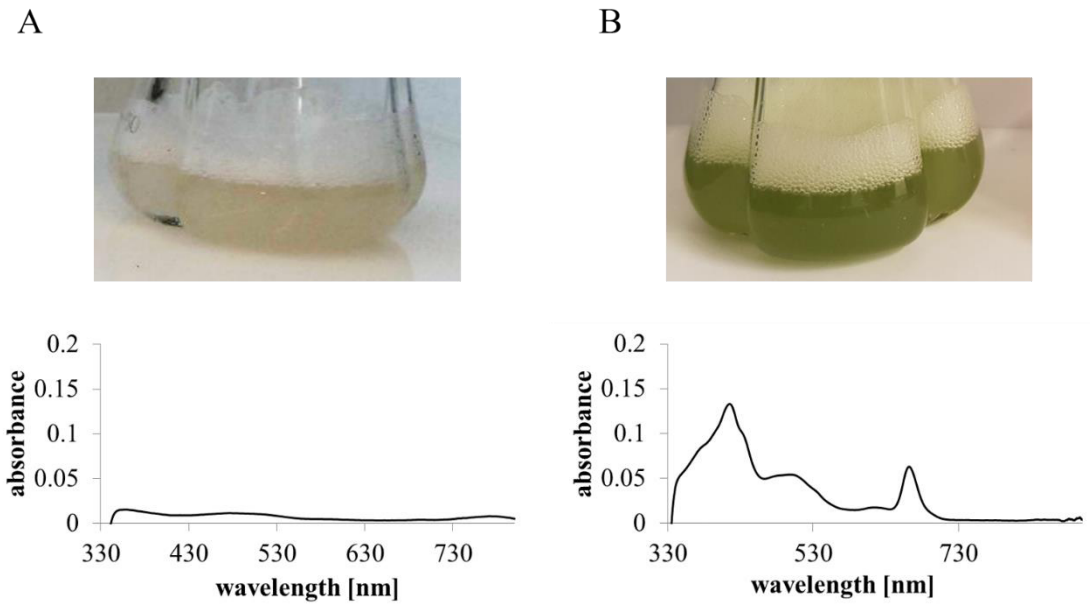

Figure 32: *In vitro* Bchl *a* spectra and phenotypes of the *D. shibae* Dshi_1135::Tn and *ppsR*::Tn mutant strains
The *D. shibae* Dshi_1135::Tn (A) and *ppsR*::Tn mutant (B) strains were cultivated in SWM medium at 30 °C and 180 rpm under dark conditions until they reached the stationary growth phase. Of each culture cells corresponding to an OD_{578} of 2.5 were taken and pigments were extracted by acetone-methanol (7:2) treatment. UV/Vis spectra of the obtained pigments were recorded in a wavelength range from 330-800 nm.

Both mutant strains showed an altered phenotype compared to *D. shibae* wild type cells cultivated in the dark. The Dshi_1135::Tn mutant strain completely lacks pigmentation and appeared colorless. According to this, no specific peaks indicative for Bchl *a* or spheroidenone could be recorded (Figure 32 A). The result obtained for the Dshi_1135::Tn mutant strain indicated that Dshi_1135 plays a major role in the regulation of the pigment biosynthesis in *D. shibae*. Obviously, there is no expression of the PGC in the absence of Dshi_1135. The culture of the *ppsR*::Tn mutant strain possessed a very conspicuous phenotype and appeared in a bright green. The obtained UV/Vis spectrum of the extracted pigments showed three major peaks at 418 nm, 500 nm and 660 nm. Therefore, no Bchl *a* was produced. It assumed that the peaks at 418 nm and 660 nm resulted from BChlide *a*, a late intermediate in Bchl *a* biosynthesis and direct precursor of Bchl *a*. Similar results were obtained in a *R. capsulatus* mutant strain where the genes *bchF* and *bchZ* were disrupted (Bollivar *et al.,* 1994). Pigment

extraction of the mutant strain resulted in a deep green solution, which showed absorption peaks at 433 nm and 665 nm in spectroscopic analysis (Müller *et al.,* 2011). The peak at 500 nm most likely derived from spheroidenone. Since PpsR is the repressor of photosynthesis genes, it would be expected that in the *ppsR*::Tn mutant strain all genes for Bchl *a* and spheroidenone production are derepressed and biosynthesis pathways are fully active. But it seems that certain steps in Bchl *a* biosynthesis are a bottleneck and accumulation of intermediate products finally led to drastically reduced production of Bchl *a.*

4.2.2 Complementation of the *D. shibae* Dshi_1135::Tn Mutant Strain

In order to prove that the inability of Bchl *a* biosynthesis in the *D. shibae* Dshi_1135::Tn mutant strain was actually due to the transposon insertion into the Dshi_1135 gene and not due to secondary effects, the Dshi_1135::Tn mutant strain was complemented. Therefore, the native Dshi_1135 gene was cloned into the pRhokS2 vector, which enables gene expression under the control of the constitutive *aphII* promoter (Katzke *et al.,* 2010). The obtained plasmid pRhokS_Dshi1135 was transformed into the *D. shibae* Dshi_1135::Tn strain *via* diparental mating, using *E. coli* ST18 as donor strain. It was assumed that a successful complementation of the mutant strain would result in a visible recovery of the phenotype. Approximately three weeks after diparental mating, four pink colonies appeared on the agar plates, indicating a successful complementation. All clones were tested positive in colony PCR for the Dshi_1135 gene. Subsequently, one clone was selected and used as inoculum for a liquid culture. After three days, the respective culture grew to a final OD_{578} of approximately 2.2 and showed the typical pink *D. shibae* wild type pigmentation (Figure 33 B). The pink pigmentation of the *D. shibae* Dshi_1135::Tn pRhoKS_Dshi1135 strain already indicated the successful complementation. Next, the Dshi_1135::Tn pRhoKS_Dshi1135 strain was cultivated and pigments were extracted as described above. The absorbance spectrum was recorded from 330-800 nm and analysed with respect to absorption peaks and Bchl *a* content (bachelor thesis Luise Rentz, TU Braunschweig 2020) (Figure 33 C).

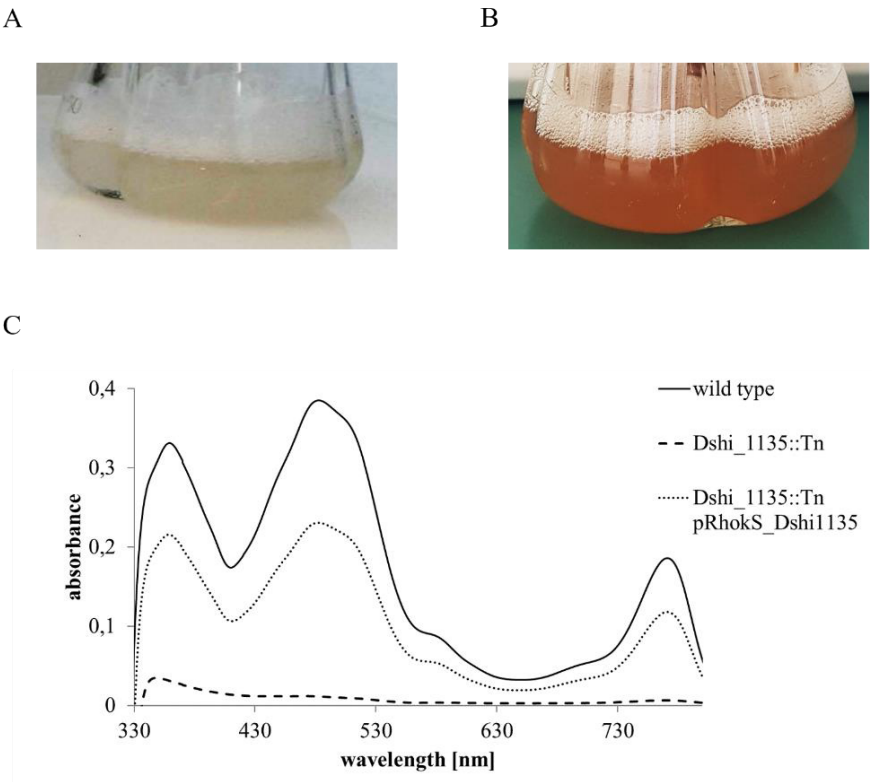

Figure 33: Pigmentation phenotypes and *in vitro* Bchl *a* spectra of the *D. shibae* Dshi_1135::Tn mutant strain and the complemented strain Dshi_1135::Tn pRhoKS_Dshi1135
(A) Pigmentation phenotype of the *D. shibae* Dshi_1135::Tn mutant strain.
(B) Pigmentation phenotype of the *D. shibae* Dshi_1135::Tn pRhokS_Dshi1135 strain.
(C) Comparison of the *in vitro* Bchl *a* absorbance spectra of the *D. shibae* wild type (solid line), the Dshi_1135::Tn transposon mutant (dashed line) and the Dshi_1135::Tn pRhokS_Dshi1135 (dotted line) strains.

The complemented Dshi_1135::Tn mutant strain showed the typical Bchl *a* spectrum with major peaks for the soret band at 360 nm and the Q_Y band at 770 nm as well as a broad peak from 400 nm to 550 nm indicating the production of spheroidenone (Figure 33 B). In the Dshi_1135::Tn pRhoKS_Dshi1135 strain, peaks were slightly lower compared to the wild type strain. Compared to the mutant strain, there was a significant increase in the height of the absorbance peaks. In terms of absorbance at 770 nm, the Bchl *a* concentration was 62 % in the Dshi_1135::Tn pRhoKSDshi_1135 strain compared to the wild type. This difference might appear due to the different promoters under whose control the Dshi_1135 gene is in both strains. The complemented gene is under the control of the constitutive *aphII* promoter, unlike the wild type strain in which the gene is under the control of its native promoter. Possibly, a lower expression level is mediated by the *aphII* promoter, which resulted less mRNA and thus less Dshi_1135 protein.

4.2.3 Expression of a *bchF-lacZ* Reporter Gene Fusion is Light-Dependent

After transcriptome analyses revealed that PGC expression in *D. shibae* is light-dependent (Tomasch *et al.,* 2011), Steffi Heyber pursued the question which light quality influences PGC expression. Especially the influence of blue light was of interest. For transcriptome analyses dark cultivated *D. shibae* wild type cells were shifted to blue light conditions. Samples for preparation of total RNA were taken before and 30 min after the shift. After RNA preparation the transcriptome was analysed using DNA microarrays. It was found that 19.2 % of all protein-coding genes in *D. shibae* were transcribed significantly altered after the shift to blue light conditions. Slightly increased expression was shown for genes of the PGC involved in Bchl *a* and spheroidenone biosynthesis and for their respective regulators. Thus, blue light-dependent regulation of photosynthesis genes in *D. shibae* was determined (Heyber, 2021).

To analyse the effect of different light qualities on the expression of photosynthesis genes in more detail, the *bchF-lacZ* reporter gene fusion was used (see chapter 4.1.9). The plasmid pBBR1LIC_*bchF-lacZ* was transformed into the *D. shibae* wild type strain by diparental mating. After approximately two weeks of incubation, positive clones were selected by colony PCR and subsequently used for the generation of liquid cultures. The newly generated strain DS181 was cultivated in biological triplicates under dark, blue light (λ=467 nm) or white light (100 lux) conditions, respectively, and at 25 °C for 16-18 h until the mid-log growth phase (OD_{578} of 0.5-0.7) was reached. Samples of 0.5 ml of each biological replicate were taken in technical triplicates and β-galactosidase activities were determined. Also, the mean values of all related measurements with the corresponding standard deviations were calculated. (Figure 34). First, it was striking that the *D. shibae* culture grown under blue light showed a similarly weak pigmentation, as the culture grown under white light, while the dark incubated cells showed the typical pink pigmentation. The same observation was also described by Endres *et al*. (2015). In addition to dark, blue light and white light, they already investigated the influence of infrared light (837-864 nm) on pigment synthesis in the wild type. These cells showed the same pink pigmentation as the dark cultured cells. This again indicated that the light quality, for example the wavelength, is relevant with regard to photopigment biosynthesis and that *D. shibae* is quite capable of distinguishing between different light qualities.

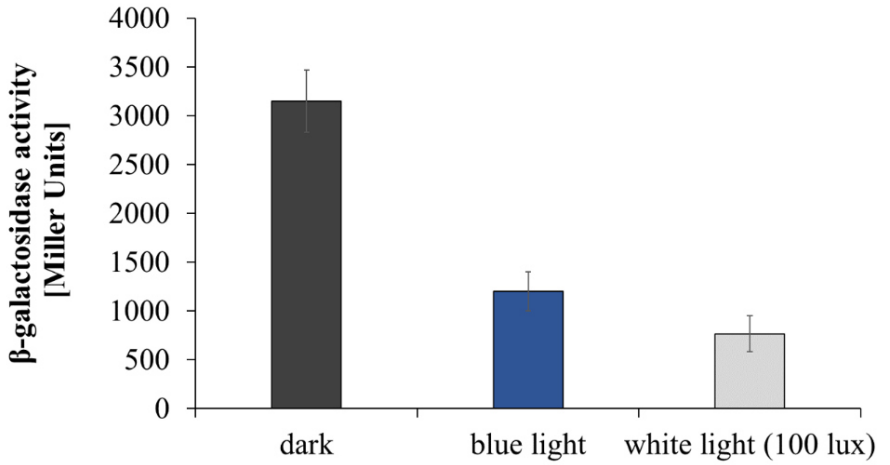

Figure 34: β-galactosidase activities of the *bchF-lacZ* reporter gene fusion in the *D. shibae* wild type strain under different light conditions
The plasmid pBBR1LIC_*bchF-lacZ* was transformed into the *D. shibae* wild type strain by diparental mating, using *E. coli* ST18 as donor strain. The newly generated *D. shibae* strain DS181, carrying the *bchF-lacZ* reporter gene fusion, was grown under dark, blue light (λ=467 nm) and white light (100 lux) conditions in biological triplicates. Samples (0.5 ml) of all cultures were taken in technical triplicates after reaching the mid-log growth phase after 16-18 h of growth at 25 °C and the β-galactosidase activities were determined. Mean values of all related β-galactosidase activity measurements and their corresponding standard deviations are indicated in Miller Units.

In dark cultivated cells a β-galactosidase activity of 3150 Miller Units was calculated. In comparison to cells that were grown under white light conditions, an activity of 765 Miller Units was determined. This showed an approximately 4-fold higher induction of the *lacZ* gene by the *bchF* promoter in the dark than under white light conditions. This finding is in good agreement with the previous results obtained in transcriptome analyses by Tomasch *et al*. (2011). Therefore, this experiment demonstrated that the *bchF* promoter sequence in the *bchF-lacZ* reporter gene fusion was sufficient to mediate light-dependent gene regulation. Also, it was clearly demonstrated that the expression of *bchF-lacZ* is light-dependent. When incubated under blue light, the β-galactosidase activity reached 1200 Miller Units which is only slightly higher compared to white light and 2.6-fold less compared to dark adapted cells. Therefore, even under blue light conditions *bchF-lacZ* expression seemed to be repressed. This result is in good agreement with the observed missing pigmentation of the *D. shibae* wild type strain cultivated under blue light conditions. But it is somewhat surprising with regard to the transcriptome analyses performed under blue light conditions prior to this thesis, where blue light had a slightly positive effect on the expression of photosynthesis genes (Heyber, 2021). These different results can probably be traced back to the varied experimental setup. For transcriptome analyses the cells were initially grown in the dark

until they reached the mid-log growth phase after approximately 16 h. Then the cultures were shifted to blue light conditions for 30 min and subsequently samples for RNA preparation were taken. Taking into account that expression of the PGC was already increased after dark incubation, the shift to blue light conditions for 30 min reflects an additional effect. In contrast, the cultures for the β-galactosidase activity measurements were cultivated from the beginning under constant blue light irradiation. Such long-term exposure to blue light is likely to produce the same response as white light does. It is very likely that the saying "the dose makes the poison" applies here. Brief illumination with blue light is probably a positive signal, whereas permanent illumination could be more harmful. In addition, transcriptome analyses examine the more transient and unstable RNA, whereas β-galactosidase activity assays measure the very stable *lacZ* gene product. Therefore, the results of the shift experiment for transcriptome analysis and the β-galactosidase activity assay cannot directly be compared.

4.2.4 Roles of PpsR, PpaA and Dshi_1135 in Light-Dependent Expression of the *bchF-lacZ* Reporter Gene Fusion

Besides the influence of different light qualities on the expression of the *bchF* reporter gene fusion, the impact of the three regulators Dshi_1135, PpsR and PpaA was investigated. Therefore, the plasmid pBBR1LIC_*bchF-lacZ* was transformed into the respective *D. shibae* transposon mutant strains, resulting in the newly created *D. shibae* strains DS187 (*ppaA*::Tn), DS188 (Dshi_1135::Tn) and DS189 (*ppsR*::Tn). Strains were cultivated under dark, light and blue light conditions and β-galactosidase activities were determined as described in the previous chapter. Obtained results from three independent biological replicates were compared to those measured in the *D. shibae* wild type strain describes above (bachelor thesis Saskia Pucelik, TU Braunschweig 2019) (Figure 35).

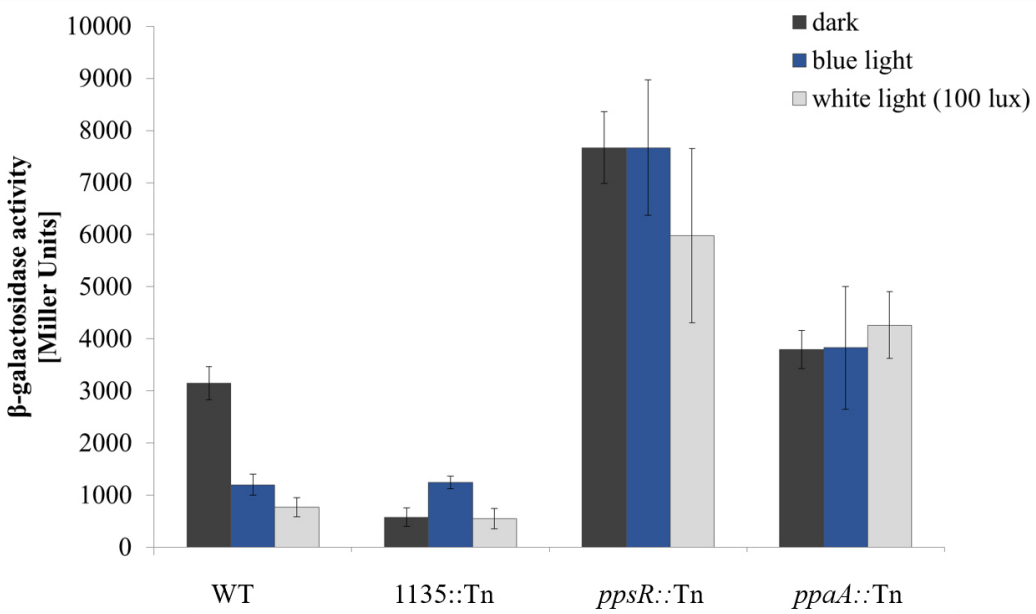

Figure 35: β-galactosidase activities of the *bchF-lacZ* reporter gene fusion in the *D. shibae* wild type strain and the Dshi_1135::Tn, *ppsR*::Tn and *ppaA*::Tn mutant strains under different light conditions

The plasmid pBBR1LIC_*bchF-lacZ* was transformed into the *D. shibae* Dshi_1135::Tn, *ppsR*::Tn and *ppaA*::Tn transposon mutant strains by diparental mating, using *E. coli* ST18 as donor strain. The newly generated *D. shibae* strains DS187, DS188 and DS189, carrying the *bchF-lacZ* reporter gene fusion, were grown under dark, blue light (λ=467 nm) and white light (100 lux) conditions in biological triplicates. Samples (0.5 ml of DS187; 1 ml of DS188 and 0.25 ml of DS189) of all cultures were taken in technical triplicates after reaching the mid-log growth phase after 16-18 h of growth at 25 °C and the β-galactosidase activities were determined and compared to the *D. shibae* wild type strain (DS181). Mean values of
β-galactosidase activities of all related measurements and their corresponding standard deviations are indicated in Miller Units.

In the *D. shibae* Dshi_1135::Tn mutant strain the expression levels of the *bchF-lacZ* reporter gene fusion in the dark only resulted in 575 Miller Units. Compared to the wild type level this reflected a 6-fold lower expression in the dark, indicating a crucial role of Dshi_1135 for *bchF*-lacZ activation or derepression under dark conditions. In contrast, ß-galactosidase activities under blue light and light conditions of 1200 and 550 Miller Units, respectively, were comparable to the expression in the wild type strain. The *D. shibae ppsR*::Tn mutant strain showed a very strong expression of the *bchF-lacZ* fusion under dark and blue light conditions at 7700 Miller Units, expression under white light was only slightly weaker at 6000 Miller Units. Compared to the wild type strain, the expression of *bchF-lacZ* in the *D. shibae ppsR*::Tn mutant strain was about 8-fold stronger under white light and about 6-fold stronger under blue light conditions. Even under dark conditions a 2.5-fold higher expression was determined. These results clearly indicated a repressor function of the PpsR regulator in *D. shibae*. For the

ppaA::Tn transposon mutant strain an expression level of about 3800 Miller Units was determined in the dark and also under blue light conditions. Only a slightly higher activity of 4200 Miller Units was measured under white light conditions. When comparing these values with the wild type, these results reflect a derepression or anti-repressor function of the PpaA protein. This conclusion is in good agreement to the anti-repressor function of the homologous PpaA proteins in *R. capsulatus* and *R. sphaeroides*.

For the PpsR regulator it was proposed that under white and blue light conditions it acts as a repressor of the *bchF-lacZ* reporter gene fusion. Here, it is striking that even in the dark the *bchF-lacZ* expression in the *ppsR*::Tn mutant strain is more that 2-fold higher compared to the expression in the wild type strain. This may implicate that under the applied dark conditions PpsR is not completely inactive in the wild type and that consequently genes are not fully derepressed. Otherwise, dark expression in the *D. shibae* wild type and the *ppsR*::Tn mutant strain should have been on similar levels. Beyond that, derepression in the *ppsR*::Tn mutant strain may enable an activating function by another regulator, as for example Dshi_1135 and a cognate RR. This assumption may explain the low expression of *bchF-lacZ* under dark conditions in the Dshi_1135::Tn mutant strain. On the other hand, Dshi_1135 could also be involved as an anti-repressor of PpsR. PpsR is a well-studied master regulator of photosynthesis genes in purple bacteria (Kovács *et al.,* 2005). It is involved in the redox-dependent regulation of photosynthesis genes in *R. sphaeroides* and *R. capsulatus* and uses intramolecular disulfide bonds and a heme cofactor to sense the presence of oxygen (Cheng *et al.,* 2012; Yin *et al.,* 2012). As mentioned earlier, regulation of photosynthesis genes in *D. shibae* is not dependent on the oxygen level. For *D. shibae* PpsR it remains elusive how the repressor function is regulated.

For *R. sphaeroides* and *R. capsulatus* anti-repressors for PpsR have already been described. In *R. sphaeroides*, the two regulatory proteins AppA and PpaA are present and both independently form a complex with PpsR in a redox-dependent manner, which alters the binding affinity to target promoters (Masuda & Bauer, 2002; Winkler *et al.,* 2013; Fang & Bauer, 2017). In *R. capsulatus*, however, the AppA regulator is completely missing and the PpaA homologue AerR is the major antagonist of PpsR. A similar situation was found in *D. shibae* as the genome only encodes the PpaA but not the AppA protein. Additionally, the *ppaA* gene is located upstream of the *ppsR* gene

within the PGC and both are supposed to be transcribed as an operon. This operon structure was also found to be conserved in other purple bacteria (Cheng *et al.,* 2014). Transcriptome analyses showed that under dark conditions the PGC was significantly repressed in the *ppaA*::Tn mutant strain (Heyber, 2021). This indicated the importance of PpaA for the activation of the PGC presumably by acting as an anti-repressor of PpsR. In this study, expression of *bchF-lacZ* did not vary under the tested light conditions and this might indicate that PpaA in *D. shibae* is involved in light-dependent regulation of the PGC. Surprisingly, the measured β-galactosidase activities of the *bchF-lacZ* fusion in the *ppaA::Tn* mutant strain did not explicitly show the function of PpaA as major anti-repressor of PpsR in *D. shibae*. If this were the case, only little or no expression of the *bchF-lacZ* fusion should have been observed due to the permanent binding and of the PpsR repressor. Instead, the result implicated that PpaA can only partly reduce the PpsR activity. Thus, the results of the transcriptome analyses and the β-galactosidase activity measurements are contradictory to each other. In addition the *ppaA::Tn* mutant strain still shows the typical reddish-pink pigmentation like the *D. shibae* wild type strain. If PpaA was of major importance, a lack of pigmentation would have been expected due to the missing antagonist of PpsR. However, this is not consistent with the results made for a *R. capsulatus aerR* deletion mutant. There, the mutation resulted in a complete loss of pigmentation, indicating the importance of the regulator (Cheng *et al.,* 2014). The *D. shibae ppaA*::Tn mutant looks more similar to the *R. sphaeroides ppaA* deletion mutant that also still shows pigmentation (Vermeulen & Bauer, 2015). In *R. sphaeroides* AppA is the major anti-repressor of PpsR and PpaA only plays a minor role. Thus, a loss of PpaA is not as dramatic as in *R. capsulatus*. However, as mentioned before, *D. shibae* does not possess an AppA homologue. AppA of *R. sphaeroides* is a BLUF domain containing blue light responsive photoreceptor (Masuda & Bauer, 2002) and its conformational change after blue light illumination is proposed to weaken the DNA binding affinity of the AppA-$PpsR_2$ complex. Thus, photosynthesis gene expression is partly dependent on blue light in this organism. Since the activity of PpsR in *D. shibae* was also found to be somehow blue light-dependent, this may be due to a so far unknown anti-repressor of PpsR that contains a photoreceptor. From the results obtained from the expression study in the Dshi_1135::Tn mutant strain, Dshi_1135 qualifies for this job.

It was demonstrated that Dshi_1135 is essential for the activation of the photosynthesis

genes in the absence of light. Therefore, it was hypothesized that the dark state of Dshi_1135 is the regulatory relevant state and that the protein promotes expression of photosynthesis genes strictly under dark conditions. Thus, Dshi_1135 would represent a rare case where a LOV protein mediates activation of a gene in the dark, rather than in blue light or light. Possible functions that could be assigned to Dshi_1135 include an activating role together with a until now unknown RR that binds to the promoter in the absence of PpsR or independently of an RR by acting directly as an anti-repressor of PpsR. To further investigate these hypotheses, a Δ*ppaA*-ΔDshi_1135 double mutant would need to be generated and examined using the *bchF-lacZ* reporter gene fusion. The results regarding the role of Dshi_1135 deviated from the original assumption, that Dshi_1135 is promotes the activation of photosynthesis genes under blue light-dependent conditions (Heyber, 2021). But with these recent findings it is more likely that Dshi_1135 is involved in activation of photosynthesis genes under dark conditions. In contrast to other wavelength' of the visible spectrum, blue light can penetrate the water column the deepest with up to 30 meters. Therefore, blue light provides one of the most sensitive environmental factors for *D. shibae*. In *R. sphaeroides* and *R. capsulatus* photosynthesis is exclusively performed under (semi)anaerobic conditions to prevent the encounter of Bchl *a*, oxygen and light, as this would result in the formation of toxic ROS. *D. shibae* is an AAP bacterium and there is no regulation of photosynthesis genes based on redox-level. Therefore, it is likely that a stronger regulation on light-level has to be ensured, to prevent ROS formation. Blue light and blue light-sensitive photoreceptors, like Dshi_1135, could play a crucial role here and the possibility, that Dshi_1135 acts as a dark-operating transcription factor of photosynthesis genes should be observed closer. Here, it becomes clearly evident that besides the missing information about the detailed mode of signaling and action during photosynthesis gene regulation, that photopigment biosynthesis is controlled differently than in other related species, even though homologues regulators are partly present.

4.2.5 Mutation of the Potential PpsR Binding Sites in the *bchF* Promoter

Expression analyses using the *bchF-lacZ* reporter gene fusion in the *D. shibae* wild type and *ppsR*::Tn mutant strain revealed that PpsR acts as a repressor of the *bchF* gene and therefore most likely also for other operons of the PGC. Activation of the *bchF-lacZ* gene fusion is facilitated by derepression that is probably mediated by PpaA. In addition, Dshi_1135 is needed for activation under dark conditions. Whether it acts *via*

a cognate RR as an activator in the absence of PpsR, or by acting as an additional anti-repressor is not clear. To study the role of Dshi_1135 independent of PpsR, PpsR binding sites within the *bchF* promoter were mutated and fused to the *lacZ* reporter gene. Moreover, the *bchF* promoter fragment was shortened and again fused to *lacZ*. All newly created *lacZ* reporter gene fusions were then analysed in the *D. shibae* wild type and the *ppsR::Tn* and Dshi_1135::Tn mutant strains.

The *bchF* promoter region spans 257 bp between the divergently arranged *bchF* and *ppaA* genes (Figure 36 A). Within this intergenic region of *ppaA* and *ppsR* five potential PpsR binding motifs have been found, comprising the palindromic sequence 5'-TGT-N_{12}-ACA-3' (Figure 36 B and C).

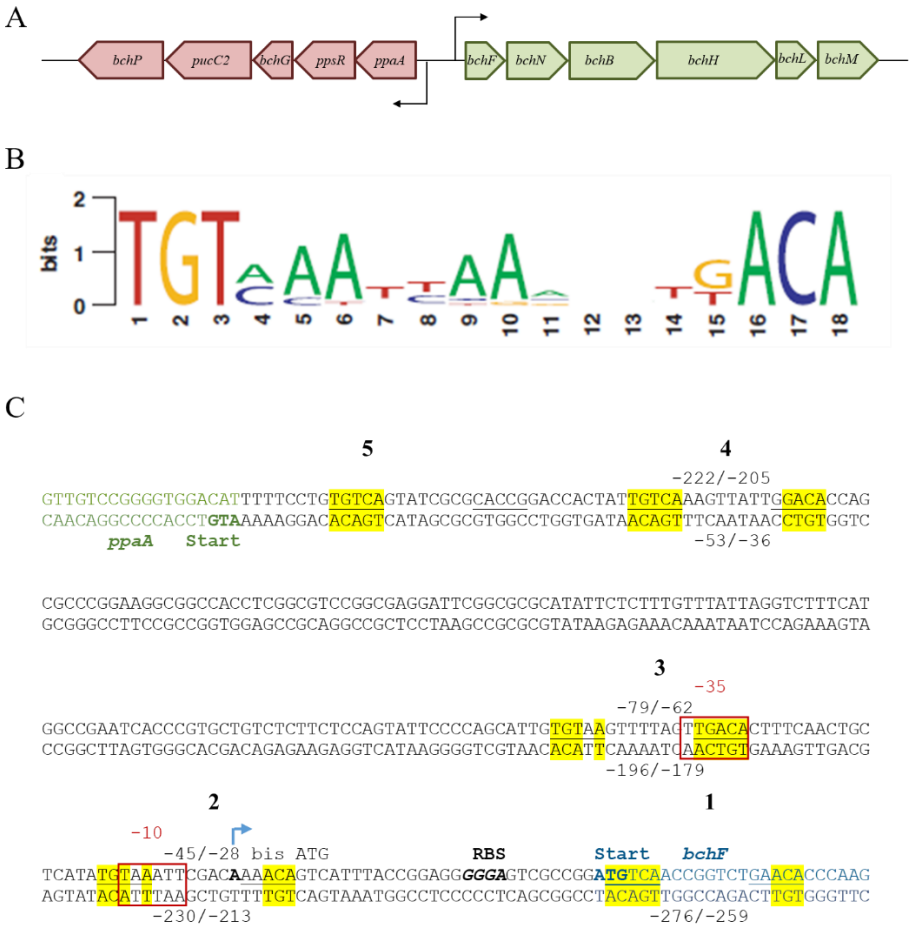

Figure 36: Potential PpsR binding sites in the intergenic region of *ppaA* and *bchF*
(A) Schematic diagram of the *bchFNBHLM* operon and the divergent *ppaA*-operon. Arrows indicate the potential transcription starts.
(B) Sequence logo showing the postulated consensus sequence of the potential 5'-TGT-N_{12}-ACA-3' binding motif of the PpsR regulator in *D. shibae* (Tomasch *et al.,* 2011).
(C) Promoter region of the *bchF* gene with a length of 257 bp. Potential PpsR binding sites are marked in yellow and numbered from 1 to 5, red boxes indicate the -35 and -10 region of the *bchF* gene for RNA polymerase binding, green marked base pairs indicate the sequence of the *ppaA* gene, blue marked base pairs indicate the sequence of the *bchF* gene, RBS indicates the ribosome binding site.

Since not all potential PpsR binding sites correspond exactly to the postulated palindromic sequence, only those base pairs that are in agreement with this sequence were highlighted (Figure 36 C). Of the five binding motifs that were identified, two are closer to the transcription start of the *ppaA* gene (motif 5 and 4) and two are closer to the transcription start of the *bchF* gene (motif 2 and 3). The fifth binding site, motif 1, was found to be overlapping with the translational start of *bchF*. This binding site was not included in the mutagenesis approach. The *bchF-lacZ* reporter gene fusion includes the native *bchF* promoter region from position -289 to +41 with respect to the translation start of *bchF*. In addition, the required LIC sequences for ligation independent cloning are contained at both sides of the fragment, which resulted in a total length of 363 bp. All five potential PpsR binding sites are included in this construct (Figure 37).

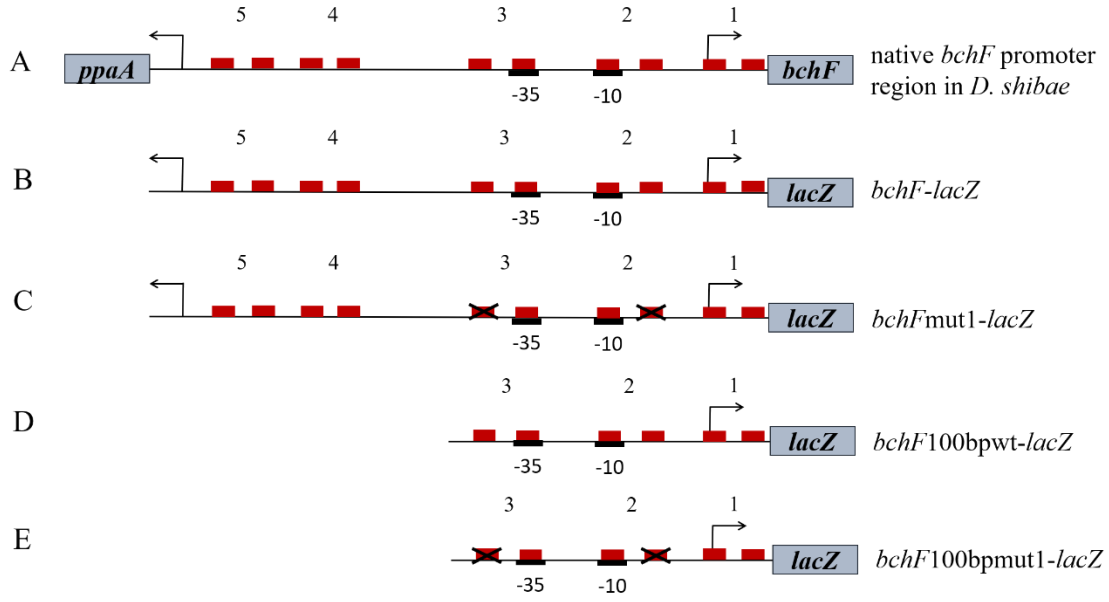

Figure 37: Scheme of all *bchF-lacZ* reporter gene fusions with positions of the potential PpsR binding sites
(A) Native *bchF* promoter region with the divergently arranged genes *bchF* and *ppaA*.
(B) Full length and unmutated *bchF-lacZ* reporter gene fusion, containing the 289 bp sequence upstream of the *bchF* transcription start. Total length 363 bp.
(C) Full length *bchF-lacZ* reporter gene fusion, containing the 289 bp sequence upstream of the *bchF* transcription start and mutations in the PpsR binding motifs 2 and 3. Total length 363 bp.
(D) Shortened and unmutated *bchF-lacZ* reporter gene fusion containing the first 100 bp of the *bchF* promoter sequence with respect to the transcription start. Total length 174 bp.
(E) Shortened *bchF-lacZ* reporter gene fusion containing the first 100 bp of the *bchF* promoter sequence with respect to the *bchF* transcription start and mutations in the PpsR binding motifs 2 and 3. Total length 174 bp.
The red boxes indicate the potential PpsR binding motifs 1-5. In the black the -35 and -10 region is marked for RNA polymerase binding. The arrows indicate the transcription starts of *ppaA* and *bchF*.

As a first modified variant the *bchF*mut1-*lacZ* reporter gene fusion was generated. The desired mutated fragment was cloned into the pBBR1MCSLIC-*lacZ* vector by ligation independent cloning. The newly obtained *bchF*mut1-*lacZ* reporter gene fusion is identical to *bchF-lacZ* with respect to length, but contains mutations in the PpsR binding motifs 2 and 3 (Figure 37 C). Because both motifs are partly localized within the predicted -35 and -10 region of the *bchF* promoter, only half sites of the binding motif were mutated. A mutation of the -35 and -10 region would impair binding of the RNA polymerase to the *bchF* promoter and thus also the expression of the downstream gene. Therefore, it would not be possible to distinguish lack of expression due to impaired PpsR or RNA polymerase binding. In binding motif 1 the sequence ACA was mutated to TTG and in motif 2 the TGT sequence was exchanged against CCA. If these binding motifs were essential for PpsR binding, a strong expression under dark conditions in the *D. shibae* wild type strain is expected.

In order to check whether the length of the *bchF* promoter region and the binding motifs 4 and 5, which are closer to the transcription start of the *ppaA* gene, play a role in PpsR-dependent repression on the *bchF* gene, two different *bchF-lacZ* reporter gene fusions were created. The two fragments containing the sequences from position -100 to +41 with respect to the translation start site of the wild-type and mutated *bchF* promoter, respectively, were cloned into the pBBR1MCSLIC-*lacZ* vector, resulting in the constructs *bchF*100bpwt-*lacZ* and *bchF*100bpmut1-*lacZ*, respectively. Both constructs are shortened and PpsR binding motifs 4 and 5 are no longer contained (Figure 37 D and E). With these shortened *bchF-lacZ* variants it was investigated, whether the first 100 bp of the *bchF* promoter with respect to the translational start site are sufficient for PpsR binding and light-dependent regulation. Moreover, it could be tested whether an PpsR-independent regulation mediated by Dshi_1135 is present.

All three newly generated *bchF-lacZ* variants were transformed into the *D. shibae* wild type and the Dshi_1135::Tn mutant strain, respectively, by diparentel mating. Positive clones were identified by colony PCR. The expression of the reporter gene fusions was analysed under dark, blue light and white light conditions by measuring the β-galactosidase activities. For better comparison, the calculated ß-galactosidase activities are depicted in Figure 38 together with the previously obtained values of the *bchF-lacZ* construct in the *D. shibae* wild type, Dshi_1135::Tn and the *ppsR::*Tn strains.

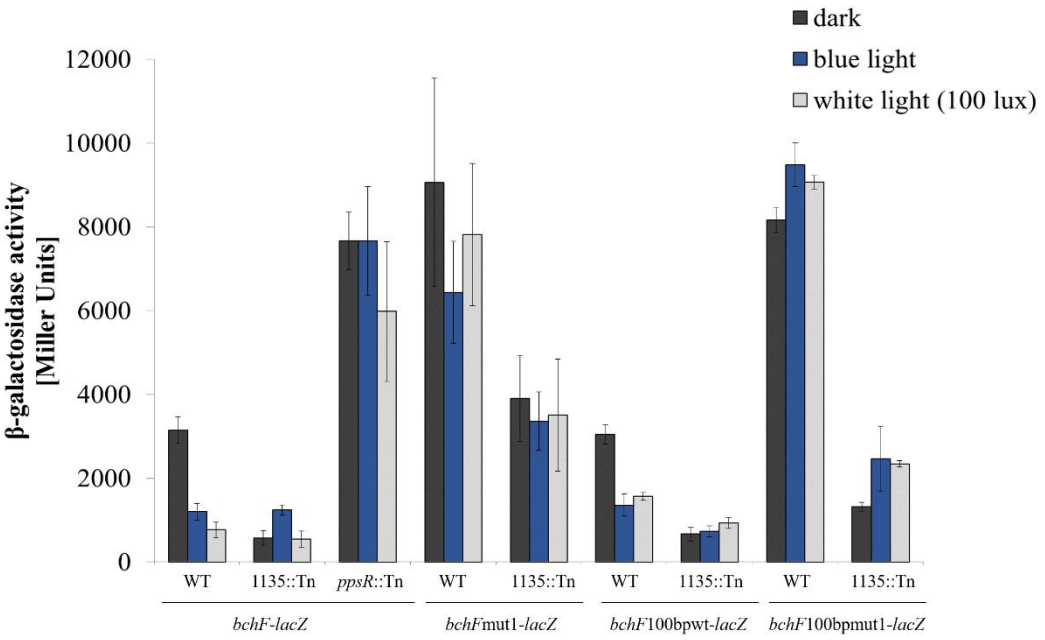

Figure 38: β-galactosidase activities of *bchF*mut1-*lacZ*, *bchF*100bpwt-*lacZ* and *bchF*100bpmut1-*lacZ* reporter gene fusions in the *D. shibae* wild type and the Dshi_1135::Tn mutant strain under different light conditions

The plasmids pBBR1LIC_*bchF*mut1-*lacZ*, pBBR1LIC_*bchF*100bpwt-*lacZ* and pBBR1LIC_*bchF*100bpmut1-*lacZ* were transformed into the *D. shibae* wild type and Dshi_1135::Tn transposon mutant strains by diparental mating, using *E. coli* ST18 as donor strain. The newly generated *D. shibae* strains DS190, DS191, DS192, DS193, DS194 and DS195, carrying the different *bchF-lacZ* reporter gene fusions, were grown under dark, blue light (λ=467 nm) and white light (100 lux) conditions in biological triplicates. Samples (1 ml of DS194; 0.5 ml of DS190, DS191, DS193 and 0.25 ml of DS192, DS195) of all cultures were taken in technical triplicates after reaching the mid-log growth phase after 16-18 h of growth at 25 °C and the β-galactosidase activities were determined and compared to the *D. shibae* wild type strain (DS181), the *D. shibae* Dshi_1135::Tn mutant strain (DS188) and the *ppsR*::Tn mutant strain (DS189), all carrying the full length and unmutated *bchF-lacZ* reporter gene fusion. β-galactosidase activities of all related measurements and their corresponding standard deviations are indicated in Miller Units.

In the *D. shibae* wild type strain *bchF*mut1-*lacZ* expression levels of about 9000 Miller Units in the dark, 6500 Miller Units under blue light and 7800 Miller Units under white light conditions have been determined. These values are comparable to the expression level of the *bchF-lacZ* fusion in the *ppsR*::Tn mutant strain. This indicated that the introduced mutations within the *bchF* promoter abolished binding of PpsR and thereby leading to derepression (Figure 38). In the *D. shibae* Dshi_1135::Tn mutant strain the β-galactosidase assay of the *bchF*mut1-*lacZ* reporter gene fusion resulted in activity levels of 3900 Miller Units in in the dark, 3350 Miller Units under blue light and 3500 Miller Units under white light conditions. Compared to the expression of the *bchF-lacZ* fusion in the Dshi_1135::Tn mutant strain a significant increase was determined. This might be explained by the impaired binding of the PpsR repressor. But the determined values did not reach the expression levels of the *bchF-lacZ* fusion in the *ppsR*::Tn mutant strain.

The only difference between these two strains is the missing of Dshi_1135, suggesting that Dshi_1135 has an activating function that is required for higher expression of the *bchF*mut1-*lacZ* reporter gene fusion (Figure 38).

Shortening of the *bchF* promoter region to 100 bp in the reporter gene fusion *bchF*100bpwt-*lacZ* led to expression levels of 3050 Miller Units in the dark, 1350 Miller Units under blue light and 1600 Miller Units under white light conditions. These values are comparable to those obtained with *bchF-lacZ* fusion in the wild type strain. This result showed that the *bchF* promoter sequence from base pair position -100 to +41 is sufficient to mediate the observed light-dependent gene expression. The PpsR binding sequences 4 and 5 are not involved in the repression of *bchF* gene expression by PpsR. Most likely, the motifs 4 and 5 are necessary for the regulation of the divergent *ppaA* promoter by PpsR. Expression analyses of the *bchF*100bpwt-*lacZ* construct in the Dshi_1135::Tn mutant strain resulted in β-galactosidase activity levels of 650 Miller Units in the dark, 700 Miller Units under blue light and 900 Miller Units under white light conditions. These values are comparable to the *bchF-lacZ* expression in Dshi_1135::Tn, except for the blue light value which is about half as much (Figure 38). Finally, the expression levels of the shortened promoter including the mutated PpsR binding sites, *bchF*100bpmut1-*lacZ*, obtained for the *D. shibae* wild type strain ranged from 8100-9500 Miller Units under all light conditions. These values are comparable to those measured with the *bchF*mut1-*lacZ* fusion in *D. shibae* wild type cells, indicating derepression of the promoter. In the *D. shibae* Dshi_1135::Tn mutant strain, *bchF*100bpmut1-*lacZ* activity levels of 1300 Miller Units in the dark, 2500 Miller Units under blue light and 2300 Miller Units under white light conditions were determined. These values are higher compared to *bchF-lacZ* in Dshi_1135::Tn, but lower with respect to the values obtained with the *bchF*mut1-*lacZ* construct in Dshi_1135::Tn (Figure 38).

In summary, these expression analyses of the various constructs clearly demonstrated that the postulated binding motifs 2 and 3 are actually PpsR binding sites and that they are mediating repression of the *bchF* gene expression. Furthermore, it could be proven that the mutation of half sites of the palindromic sequences is sufficient to hinder the PpsR repressor function. Obviously, the inserted mutations prevented PpsR binding to the *bchF* promoter sequence and thus the employment of the *bchF*mut1-*lacZ* reporter gene fusion could mimic the *ppsR*::Tn mutant strain in terms of *bchF* expression.

Additionally, it became evident that PpsR seems to repress *bchF* expression mainly under light and blue light conditions, whereas the higher expression of *bchF-lacZ* in the dark is due to inactivation of PpsR, most likely by the postulated anti-repressor PpaA. Transcriptome analyses already indicated that the PGC is no longer transcribed under dark conditions in a *ppaA*::Tn mutant strain (Heyber, 2021). But until now a light-dependent anti-repressor function for PpaA was not shown. Results obtained from the expression of the various *bchF* reporter gene fusions in the Dshi_1135::Tn mutant strain indicated an activating function of Dshi_1135. Expression in the Dshi_1135::Tn was always lower compared to the wild type strain. These results match nicely with the transcriptome results observed previously. Here, transcript levels of the PGC in the dark is drastically reduced compared to the wild type levels. Moreover, it was shown in this thesis, that Dshi_1135 possesses a blue light activated LOV domain and thereby is able to detect light and dark conditions. An activating function of Dshi_1135 might be obtained by activating the *bchF* promoter *via* a cognate RR. This would require an autokinase activity of Dshi_1135 and the transfer of the phosphate to a so far unknown RR. In addition, the binding site of the postulated RR has to be located within the 100 bp upstream of the translational start site. Alternatively, Dshi_1135 may act as a light-dependent anti-repressor interacting with PpsR under dark conditions. This function would resemble the function of the AppA protein in *R. sphaeroides*. Here, the action of PpsR is modulated by the anti-repressor AppA. The two proteins form a complex *in vitro* and *in vivo*, enabling light- and oxygen-dependent regulation of gene expression (Gomelsky & Kaplan, 1997; Masuda & Bauer, 2002). Both hypotheses assume an active state of Dshi_1135 under dark conditions.

On the basis of previous results gained from transcriptome analyses and the newly acquired results from reporter gene fusion expression analyses, a model was developed integrating the role of the PpsR repressor, the PpaA anti-repressor and Dshi_1135 for light-dependent regulation of photosynthesis genes in *D. shibae* (Figure 39).

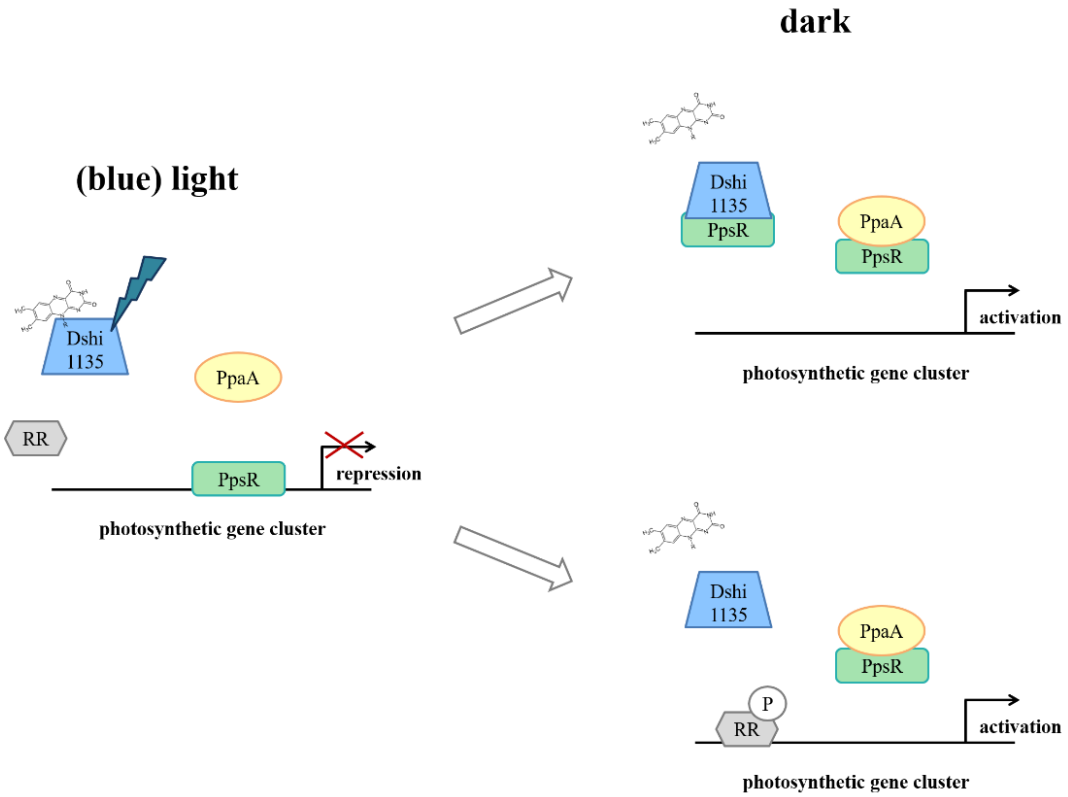

Figure 39: Model of the regulation of the photosynthesis gene cluster by the regulators Dshi_1135, PpsR and PpaA in dependence on light
Based on the current and present data, it is assumed that upon blue light illumination, the LOV protein Dshi_1135 covalently binds its cofactor FMN, followed by a reversible photocycle reaction. In this state, Dshi_1135 is not actively involved in regulation of the PGC. The potential RR of Dshi_1135 cannot be phosphorylated and thus activated. Thus, it is not involved in the regulation of the PGC under (blue) light conditions. Also, the PpaA regulator, which is supposedly an anti-repressor of PpsR, is inactive. This enables unhindered binding of the PpsR repressor to its target promoter(s), causing a strong repression of photosynthesis genes. Under dark conditions, two scenarios are possible based on the obtained data. First, it is possible that the anti-repressor PpaA binds PpsR, preventing PGC repression. The LOV protein Dshi_1135 is active in its dark state, where it binds FMN noncovalently, and can also bind PpsR as an anti-repressor. This leads to derepression and thus activation of the PGC. In the second possible case, PpaA again acts as an anti-repressor of PpsR. In addition, it is possible that Dshi_1135 acts as an activator in the dark state *via* an RR. Potential autokinase activity of Dshi_1135 phosphorylates its RR, which is then able to activate photosynthesis gene expression by binding to the target promoter.

In this study the promoter of the *bchF* gene was used as a representative for promoters activating genes and operons of the PGC of *D. shibae*. In almost all promoters PpsR binding motifs were found (Tomasch *et al.,* 2011). This led to the conclusion that PpsR is the main regulator of the PGC in *D. shibae* and represses expression under (blue) light conditions. This finding is supported by the transcriptome analysis, where in the *ppsR*::Tn mutant strain substantial lower amounts of transcripts with fold changes up to seven compared to wild type expression were determined (Heyber, 2021). Additionally, the assays indicated that the LOV protein Dshi_1135, maybe in interplay with a RR or as an anti-repressor, acts as an activator of photosynthesis genes in the absence of PpsR

in a light-dependent manner. It became evident, that the regulation of photosynthesis genes in *D. shibae* is quite complex and even though, many homologous regulators to the closely related Rhodobacter species were identified, it is hard to draw fundamental similarities between both regulatory mechanisms. While PpsR and PpaA in *R. capsulatus* and *R. sphaeroides* are involved in redox-dependent activation of photosynthetic genes under anaerobic conditions, they play a regulatory role independent of redox control in *D. shibae*. *R. sphaeroides* does possess AppA, which contains a blue light sensing BLUF domain and acts as an anti-repressor of PpsR in the dark (Masuda & Bauer, 2002). AppA tightly binds to PpsR and inhibits the binding of PpsR to target DNA sequences. However, when illuminated with blue light, AppA is unable to bind to PpsR. Thus, PpsR again is able to bind to its cognate binding sites and represses gene transcription. Moreover, Endres *et al*. (2015) identified the protein DsLOV in *D. shibae* to be a short LOV protein that seems to be somehow involved in light-dependent photopigment biosynthesis. During the high-throughput screening for the identification of potential regulators of photosynthesis genes in *D. shibae*, the *clpX*::Tn mutant strain was found, showing no pigmentation at all (Heyber, 2021). In addition, Steffi Heyber demonstrated that ClpX influences gene expression of the PGC, since transcriptional activation of the PGC under dark conditions was drastically reduced in the *clpX::Tn* mutant strain compared to the wild type. Therefore, the missing ClpX protease seems to be involved in regulation of PGC expression. One explanation could be that ClpX specifically degrades a repressor protein under dark growth conditions. Such a regulation mechanism for photosynthesis genes, that involves a protease, has not been described so far for other photoheterotrophic bacteria. This illustrates that, that *D. shibae* uses a different and complex regulatory network to control photosynthesis gene expression. Undoubtedly, this regulation is highly dependent and responsive to light and many mechanisms and characteristics were elucidated in this work.

The remaining question still is why the photosynthesis genes are expressed in the dark and expression is inhibited under light conditions. This phenomenon is often discussed in context to oxidative stress that occurs under high light conditions which causes an over-excitation of the photosystem. Accordingly, the process of photosynthesis is restricted only to low light conditions and high doses of blue light lead to repression of photosynthetic gene expression.

5 Summary

The potential LOV histidine kinase Dshi_1135 was found in a high-throughput screening of the *D. shibae* transposon mutant library for identification of unknow regulators of photosynthesis genes in the marine model bacterium *D. shibae*. First experiments indicated a role in the light-dependent regulation of these genes. This study focused on the biochemical characterization of Dshi_1135 and on its role in light-dependent regulation of photosynthesis genes. Furthermore, the function of the transcription regulator PpsR in photosynthesis gene expression was investigated.

Soluble Dshi_1135 was recombinantly produced using a thioredoxin tag and the *E. coli* Lemo21(DE3) expression strain. Purification of the Dshi_1135 protein was performed by affinity chromatography using Strep Tactin® Superflow matrix. UV/Vis spectroscopy revealed that Dshi_1135 possesses a FMN cofactor. Dshi_1135 covalently binds FMN under blue light conditions but loses it in the dark. A reversible photocycle was observed for Dshi_1135 and a photoactive cysteine residue at position 61 was identified by site-directed mutagenesis. Phosphotransfer experiments showed an autophosphorylation of Dshi_1135 upon blue light irradiation. It was therefore clearly proven that Dshi_1135 is a blue light activated LOV protein.

Analyses of a *bchF-lacZ* reporter gene fusion revealed, that the expression of photosynthesis gene cluster is induced under dark conditions, but not under light and blue light conditions. All collected data regarding the role of Dshi_1135 in regulation of photosynthesis genes indicate, that this protein acts as a blue light sensor but is active under dark conditions, which would be rare exception among the LOV proteins studied to date. Finally, PpsR was shown to be a strong repressor of *bchF* expression under blue and white light and also slightly in the dark. Additionally, the palindromic sequence TGT-N_{12}-ACA was identified as the respective PpsR binding motif.

Overall, the LOV domain protein Dshi_1135 was identified and functionally characterized as a novel blue light sensor and regulator of photosynthesis gene expression in the marine model bacterium *D. shibae*.

6 Outlook

The following investigations and aspects should be considered for the design of future experiments:

- Optimization of the production and purification protocol for Dshi_1135 to obtain stable recombinant purified protein.
- GPC experiments for the determination of the oligomeric state of Dshi_1135 under different light conditions.
- Refinement of the autophosphorylation assay and further development of the protocol towards phosphotransfer experiments for the identification of RRs of Dshi_1135.
- Optimization of the heterologous test system in *E. coli* for response regulator identification.
- Identification of the phospho-accepting amino acid residue in Dshi_1135 by site-directed mutagenesis to prove kinase activity of the protein.
- Investigation of the dark-sensor function of Dshi_1135.
- Creation of a ΔDshi_1135-Δ*ppaA* double deletion mutant to investigate the possible role of Dshi_1135 as an anti-repressor of PpsR.
- Interaction studies of PpsR and PpaA and of PpsR and Dshi_1135.
- Investigation of the roles of ClpX and DsLOV in the regulation of photosynthesis genes in *D. shibae*.

7 References

Ahmad, M. & Cashmore, A. R. (1993). HY4 gene of *A. thaliana* encodes a protein with characteristics of a blue-light photoreceptor. *Nature* **366**, 162–166.

Allgaier, M., **Uphoff, H.**, **Felske, A. & Wagner-Döbler, I. (2003).** Aerobic anoxygenic photosynthesis in Roseobacter clade bacteria from diverse marine habitats. *Applied and Environmental Microbiology* **69**, 5051–5059.

Altschul, S. F., **Gish, W.**, **Miller, W.**, **Myers, E. W. & Lipman, D. J. (1990).** Basic local alignment search tool. *Journal of Molecular Biology* **215**, 403–410.

Anna Staroń **&** Thorsten Mascher **(2010).** General stress response in α-proteobacteria: PhyR and beyond. *Molecular Microbiology* **78**, 271–277.

Arendt, W., **Groenewold, M. K.**, **Hebecker, S.**, **Dickschat, J. S. & Moser, J. (2013).** Identification and characterization of a periplasmic aminoacyl-phosphatidylglycerol hydrolase responsible for *Pseudomonas aeruginosa* lipid homeostasis. *The Journal of Biological Chemistry* **288**, 24717–24730.

Baker, T. A. & Sauer, R. T. (2012). ClpXP, an ATP-powered unfolding and protein-degradation machine. *Biochimica et Biophysica Acta* **1823**, 15–28.

Banerjee, R. & Ragsdale, S. W. (2003). The many faces of vitamin B12: catalysis by cobalamin-dependent enzymes. *Annual Review of Biochemistry* **72**, 209–247.

Barbieri, C. M. & Stock, A. M. (2008). Universally applicable methods for monitoring response regulator aspartate phosphorylation both *in vitro* and *in vivo* using Phos-tag-based reagents. *Analytical Biochemistry* **376**, 73–82.

Battersby, A. R. (2000). Tetrapyrroles: the pigments of life. *Natural Product Reports* **17**, 507–526.

Bauer, C., **Rabl, C.-R.**, **Heberle, J. & Kottke, T. (2011).** Indication for a radical intermediate preceding the signaling state in the LOV domain photocycle. *Photochemistry and Photobiology* **87**, 548–553.

Beale, S. I. & Castelfranco, P. A. (1973). ^{14}C incorporation from exogenous compounds into δ-aminolevulinic acid by greening cucumber cotyledons. *Biochemical and Biophysical Research Communications* **52**, 143–149.

Beatty, J. T. (2002). On the natural selection and evolution of the aerobic phototrophic bacteria. *Photosynthesis Research* **73**, 109–114.

Biebl, H., **Allgaier, M.**, **Tindall, B. J.**, **Koblizek, M.**, **Lünsdorf, H.**, **Pukall, R. & Wagner-Döbler, I. (2005).** *Dinoroseobacter shibae* gen. nov., sp. nov., a new aerobic phototrophic bacterium isolated from dinoflagellates. *International Journal of Systematic and Evolutionary Microbiology* **55**, 1089–1096.

Blankenship, R. E. (2010). Early evolution of photosynthesis. *Plant Physiology* **154**, 434–438.

Bollivar, D. W. (2006). Recent advances in chlorophyll biosynthesis. *Photosynthesis Research* **90**, 173–194.

Bollivar, D. W., **Suzuki, J. Y.**, **Beatty, J. T.**, **Dobrowolski, J. M. & Bauer, C. E. (1994).** Directed mutational analysis of bacteriochlorophyll a biosynthesis in *Rhodobacter capsulatus*. *Journal of Molecular Biology* **237**, 622–640.

Botella, E., **Fogg, M.**, **Jules, M.**, **Piersma, S.**, **Doherty, G.**, **Hansen, A.**, **Denham, E. L.**, **Le Chat, L. & Veiga, P. & other authors (2010).** pBaSysBioII: an integrative plasmid generating gfp transcriptional fusions for high-throughput analysis of gene expression in *Bacillus subtilis*. *Microbiology (Reading, England)* **156**, 1600–1608.

Boynton, T. O., **Daugherty, L. E.**, **Dailey, T. A. & Dailey, H. A. (2009).** Identification of *Escherichia coli* HemG as a novel, menadione-dependent flavodoxin with protoporphyrinogen oxidase activity. *Biochemistry* **48**, 6705–6711.

Braatsch, S., **Moskvin, O. V.**, **Klug, G. & Gomelsky, M. (2004).** Responses of the *Rhodobacter sphaeroides* transcriptome to blue light under semiaerobic conditions. *Journal of Bacteriology* **186**, 7726–7735.

Bradford, M. M. (1976). A rapid and sensitive method for the quantitation of microgram quantities of protein utilizing the principle of protein-dye binding. *Analytical Biochemistry* **72**, 248–254.

Bragg, J., **Rajkovic, A.**, **Anderson, C.**, **Curtis, R.**, **van Houten, J.**, **Begres, B.**, **Naples, C.**, **Snider, M.**, **Fraga, D. & Singer, M. (2012).** Identification and characterization of a putative arginine kinase homolog from *Myxococcus xanthus* required for fruiting body formation and cell differentiation. *Journal of Bacteriology* **194**, 2668–2676.

Brinkhoff, T., **Giebel, H.-A. & Simon, M. (2008).** Diversity, ecology, and genomics of the Roseobacter clade: a short overview. *Archives of Microbiology* **189**, 531–539.

Brinkmann, H., **Göker, M.**, **Koblížek, M.**, **Wagner-Döbler, I. & Petersen, J. (2018).** Horizontal operon transfer, plasmids, and the evolution of photosynthesis in Rhodobacteraceae. *The ISME Journal* **12**, 1994–2010.

Brinkmeyer, R., **Knittel, K.**, **Jürgens, J.**, **Weyland, H.**, **Amann, R. & Helmke, E. (2003).** Diversity and structure of bacterial communities in Arctic versus Antarctic pack ice. *Applied and Environmental Microbiology* **69**, 6610–6619.

Bryant, D. A., **Hunter, C. N. & Warren, M. J. (2020).** Biosynthesis of the modified tetrapyrroles-the pigments of life. *The Journal of Biological Chemistry* **295**, 6888–6925.

Buchan, A., **González, J. M. & Moran, M. A. (2005).** Overview of the marine roseobacter lineage. *Applied and Environmental Microbiology* **71**, 5665–5677.

Caldinelli, L., **Iametti, S.**, **Barbiroli, A.**, **Fessas, D.**, **Bonomi, F.**, **Piubelli, L.**, **Molla, G. & Pollegioni, L. (2008).** Relevance of the flavin binding to the stability and folding of engineered cholesterol oxidase containing noncovalently bound FAD. *Protein Science: a publication of the Protein Society* **17**, 409–419.

Capra, E. J. & Laub, M. T. (2012). Evolution of two-component signal transduction systems. *Annual Review of Microbiology* **66**, 325–347.

Chan, R. H. & Bogomolni, R. A. (2012). Structural water cluster as a possible proton acceptor in the adduct decay reaction of oat phototropin 1 LOV2 domain. *The Journal of Physical Chemistry. B* **116**, 10609–10616.

Chen, M. (2014). Chlorophyll modifications and their spectral extension in oxygenic photosynthesis. *Annual Review of Biochemistry* **83**, 317–340.

Cheng, Z., **Li, K.**, **Hammad, L. A.**, **Karty, J. A. & Bauer, C. E. (2014).** Vitamin B12 regulates photosystem gene expression via the CrtJ antirepressor AerR in *Rhodobacter capsulatus*. *Molecular Microbiology* **91**, 649–664.

Cheng, Z., **Wu, J.**, **Setterdahl, A.**, **Reddie, K.**, **Carroll, K.**, **Hammad, L. A.**, **Karty, J. A. & Bauer, C. E. (2012).** Activity of the tetrapyrrole regulator CrtJ is controlled by oxidation of a redox active cysteine located in the DNA binding domain. *Molecular Microbiology* **85**, 734–746.

Chew, A. G. M. & Bryant, D. A. (2007a). Characterization of a plant-like protochlorophyllide a divinyl reductase in green sulfur bacteria. *The Journal of Biological Chemistry* **282**, 2967–2975.

Chew, A. G. M. & Bryant, D. A. (2007b). Chlorophyll biosynthesis in bacteria: the origins of structural and functional diversity. *Annual Review of Microbiology* **61**, 113–129.

Christie, J. M., **Corchnoy, S. B.**, **Swartz, T. E.**, **Hokenson, M.**, **Han, I.-S.**, **Briggs, W. R. & Bogomolni, R. A. (2007).** Steric interactions stabilize the signaling state of the LOV2 domain of phototropin 1. *Biochemistry* **46**, 9310–9319.

Christie, J. M., **Reymond, P.**, **Powell, G. K.**, **Bernasconi, P.**, **Raibekas, A. A.**, **Liscum, E. & Briggs, W. R. (1998).** Arabidopsis NPH1: a flavoprotein with the properties of a photoreceptor for phototropism. *Science (New York, N.Y.)* **282**, 1698–1701.

Christie, J. M., **Salomon, M.**, **Nozue, K.**, **Wada, M. & Briggs, W. R. (1999).** LOV (light, oxygen, or voltage) domains of the blue-light photoreceptor phototropin (*nph1*): binding sites for the chromophore flavin mononucleotide. *Proceedings of the National Academy of Sciences of the United States of America* **96**, 8779–8783.

Christie-Oleza, J. A. & Armengaud, J. (2015). Proteomics of the Roseobacter clade, a window to the marine microbiology landscape. *Proteomics* **15**, 3928–3942.

Cohen-Bazire, G., **Sistrom, W. R. & Stanier, R. Y. (1957).** Kinetic studies of pigment synthesis by non-sulfur purple bacteria. *Journal of Cellular and Comparative Physiology* **49**, 25–68.

Conrad, K. S., **Manahan, C. C. & Crane, B. R. (2014).** Photochemistry of flavoprotein light sensors. *Nature Chemical Biology* **10**, 801–809.

Coomber, S. A. & Hunter, C. N. (1989). Construction of a physical map of the 45 kb photosynthetic gene cluster of *Rhodobacter sphaeroides*. *Arch. Microbiol.* **151**, 454–458.

Correa, F., **Ko, W.-H.**, **Ocasio, V.**, **Bogomolni, R. A. & Gardner, K. H. (2013).** Blue light regulated two-component systems: enzymatic and functional analyses of light-oxygen-voltage (LOV)-histidine kinases and downstream response regulators. *Biochemistry* **52**, 4656–4666.

Costa, S., **Almeida, A.**, **Castro, A. & Domingues, L. (2014).** Fusion tags for protein solubility, purification and immunogenicity in *Escherichia coli*: the novel Fh8 system. *Frontiers in Microbiology* **5**.

Cottrell, M. T., **Mannino, A. & Kirchman, D. L. (2006).** Aerobic anoxygenic phototrophic bacteria in the Mid-Atlantic Bight and the North Pacific Gyre. *Applied and Environmental Microbiology* **72**, 557–564.

Crosson, S. & Moffat, K. (2001). Structure of a flavin-binding plant photoreceptor domain: insights into light-mediated signal transduction. *Proceedings of the National Academy of Sciences of the United States of America* **98**, 2995–3000.

Crosson, S. & Moffat, K. (2002). Photoexcited structure of a plant photoreceptor domain reveals a light-driven molecular switch. *The Plant Cell* **14**, 1067–1075.

Csotonyi, J. T., **Swiderski, J.**, **Stackebrandt, E. & Yurkov, V. (2010).** A new environment for aerobic anoxygenic phototrophic bacteria: biological soil crusts. *Environmental Microbiology Reports* **2**, 651–656.

Csotonyi, J. T., **Swiderski, J.**, **Stackebrandt, E. & Yurkov, V. V. (2008).** Novel halophilic aerobic anoxygenic phototrophs from a Canadian hypersaline spring system. *Extremophiles: Life Under Extreme Conditions* **12**, 529–539.

Davis, S. J., **Vener, A. V. & Vierstra, R. D. (1999).** Bacteriophytochromes: phytochrome-like photoreceptors from nonphotosynthetic eubacteria. *Science (New York, N.Y.)* **286**, 2517–2520.

Diensthuber, R. P., **Engelhard, C.**, **Lemke, N.**, **Gleichmann, T.**, **Ohlendorf, R.**, **Bittl, R. & Möglich, A. (2014).** Biophysical, mutational, and functional investigation of the chromophore-binding pocket of light-oxygen-voltage photoreceptors. *ACS Synthetic Biology* **3**, 811–819.

Dikiy, I., **Edupuganti, U. R.**, **Abzalimov, R. R.**, **Borbat, P. P.**, **Srivastava, M.**, **Freed, J. H. & Gardner, K. H. (2019).** Insights into histidine kinase activation mechanisms from the monomeric blue light sensor EL346. *Proceedings of the National Academy of Sciences of the United States of America* **116**, 4963–4972.

Dong, C., **Elsen, S.**, **Swem, L. R. & Bauer, C. E. (2002).** AerR, a second aerobic repressor of photosynthesis gene expression in *Rhodobacter capsulatus*. *Journal of Bacteriology* **184**, 2805–2814.

Ebert, M., **Laaß, S.**, **Burghartz, M.**, **Petersen, J.**, **Koßmehl, S.**, **Wöhlbrand, L.**, **Rabus, R.**, **Wittmann, C.**, **Tielen, P. & Jahn, D. (2013).** Transposon mutagenesis identified chromosomal and plasmid genes essential for adaptation of the marine bacterium *Dinoroseobacter shibae* to anaerobic conditions. *Journal of Bacteriology* **195**, 4769–4777.

Ebert, M., **Laaß, S.**, **Thürmer, A.**, **Roselius, L.**, **Eckweiler, D.**, **Daniel, R.**, **Härtig, E. & Jahn, D. (2017).** FnrL and Three Dnr Regulators Are Used for the Metabolic Adaptation to Low Oxygen Tension in *Dinoroseobacter shibae*. *Frontiers in Microbiology* **8**, 642.

Elsen, S., **Jaubert, M.**, **Pignol, D. & Giraud, E. (2005).** PpsR: a multifaceted regulator of photosynthesis gene expression in purple bacteria. *Molecular Microbiology* **57**, 17–26.

Elsen, S., **Swem, L. R.**, **Swem, D. L. & Bauer, C. E. (2004).** RegB/RegA, a highly conserved redox-responding global two-component regulatory system. *Microbiology and Molecular Biology Reviews* **68**, 263–279.

Endres, S., **Granzin, J.**, **Circolone, F.**, **Stadler, A.**, **Krauss, U.**, **Drepper, T.**, **Svensson, V.**, **Knieps-Grünhagen, E. & Wirtz, A. & other authors (2015).** Structure and function of a short LOV protein from the marine phototrophic bacterium *Dinoroseobacter shibae*. *BMC Microbiology* **15**, 30.

Eraso, J. M. & Kaplan, S. (1994). PrrA, a putative response regulator involved in oxygen regulation of photosynthesis gene expression in *Rhodobacter sphaeroides*. *Journal of Bacteriology* **176**, 32–43.

Falkowski, P. G., **Fenchel, T. & Delong, E. F. (2008).** The microbial engines that drive Earth's biogeochemical cycles. *Science (New York, N.Y.)* **320**, 1034–1039.

Fang, M. & Bauer, C. E. (2017). The Vitamin B12-Dependent Photoreceptor AerR Relieves Photosystem Gene Repression by Extending the Interaction of CrtJ with Photosystem Promoters. *mBio* **8**.

Fiebig, A., **Varesio, L. M.**, **Alejandro Navarreto, X. & Crosson, S. (2019).** Regulation of the *Erythrobacter litoralis* DSM 8509 general stress response by visible light. *Molecular Microbiology* **112**, 442–460.

Foreman, R., **Fiebig, A. & Crosson, S. (2012).** The LovK-LovR two-component

system is a regulator of the general stress pathway in *Caulobacter crescentus*. *Journal of Bacteriology* **194**, 3038–3049.

Frädrich, C., **March, A.**, **Fiege, K.**, **Hartmann, A.**, **Jahn, D. & Härtig, E. (2012).** The transcription factor AlsR binds and regulates the promoter of the *alsSD* operon responsible for acetoin formation in *Bacillus subtilis*. *Journal of Bacteriology* **194**, 1100–1112.

Fraikin, G. Y., **Strakhovskaya, M. G. & Rubin, A. B. (2013).** Biological photoreceptors of light-dependent regulatory processes. *Biochemistry Moscow* **78**, 1238–1253.

Fuerst, J. A., **Hawkins, J. A.**, **Holmes, A.**, **Sly, L. I.**, **Moore, C. J. & Stackebrandt, E. (1993).** *Porphyrobacter neustonensis* gen. nov., sp. nov., an aerobic bacteriochlorophyll-synthesizing budding bacterium from fresh water. *International Journal of Systematic Bacteriology* **43**, 125–134.

Gaidenko, T. A., **Kim, T.-J.**, **Weigel, A. L.**, **Brody, M. S. & Price, C. W. (2006).** The blue-light receptor YtvA acts in the environmental stress signaling pathway of *Bacillus subtilis*. *Journal of Bacteriology* **188**, 6387–6395.

Gauden, M., **Yeremenko, S.**, **Laan, W.**, **van Stokkum, I. H. M.**, **Ihalainen, J. A.**, **van Grondelle, R.**, **Hellingwerf, K. J. & Kennis, J. T. M. (2005).** Photocycle of the flavin-binding photoreceptor AppA, a bacterial transcriptional antirepressor of photosynthesis genes. *Biochemistry* **44**, 3653–3662.

Gich, F. & Overmann, J. (2006). *Sandarakinorhabdus limnophila* gen. nov., sp. nov., a novel bacteriochlorophyll a-containing, obligately aerobic bacterium isolated from freshwater lakes. *International Journal of Systematic and Evolutionary Microbiology* **56**, 847–854.

Gomelsky, L., **Sram, J.**, **Moskvin, O. V.**, **Horne, I. M.**, **Dodd, H. N.**, **Pemberton, J. M.**, **McEwan, A. G.**, **Kaplan, S. & Gomelsky, M. (2003).** Identification and *in vivo* characterization of PpaA, a regulator of photosystem formation in *Rhodobacter sphaeroides*. *Microbiology (Reading, England)* **149**, 377–388.

Gomelsky, M. & Hoff, W. D. (2011). Light helps bacteria make important lifestyle decisions. *Trends in Microbiology* **19**, 441–448.

Gomelsky, M., **Horne, I. M.**, **Lee, H. J.**, **Pemberton, J. M.**, **McEwan, A. G. &**

Kaplan, S. (2000). Domain structure, oligomeric state, and mutational analysis of PpsR, the *Rhodobacter sphaeroides* repressor of photosystem gene expression. *Journal of Bacteriology* **182**, 2253–2261.

Gomelsky, M. & Kaplan, S. (1995a). *appA*, a novel gene encoding a trans-acting factor involved in the regulation of photosynthesis gene expression in *Rhodobacter sphaeroides* 2.4.1. *Journal of Bacteriology* **177**, 4609–4618.

Gomelsky, M. & Kaplan, S. (1995b). Genetic evidence that PpsR from *Rhodobacter sphaeroides* 2.4.1 functions as a repressor of *puc* and *bchF* expression. *Journal of Bacteriology* **177**, 1634–1637.

Gomelsky, M. & Kaplan, S. (1997). Molecular genetic analysis suggesting interactions between AppA and PpsR in regulation of photosynthesis gene expression in *Rhodobacter sphaeroides* 2.4.1. *Journal of Bacteriology* **179**, 128–134.

Gomelsky, M. & Kaplan, S. (1998). AppA, a redox regulator of photosystem formation in *Rhodobacter sphaeroides* 2.4.1, is a flavoprotein. Identification of a novel fad binding domain. *The Journal of Biological Chemistry* **273**, 35319–35325.

Gough, S. P., **Petersen, B. O. & Duus, J. O. (2000).** Anaerobic chlorophyll isocyclic ring formation in *Rhodobacter capsulatus* requires a cobalamin cofactor. *Proceedings of the National Academy of Sciences of the United States of America* **97**, 6908–6913.

Grebe, T. W. & Stock, J. B. (1999). The Histidine Protein Kinase Superfamily. In, pp. 139–227: Elsevier.

Han, Y., **Meyer, M. H. F.**, **Keusgen, M. & Klug, G. (2007).** A haem cofactor is required for redox and light signalling by the AppA protein of *Rhodobacter sphaeroides*. *Molecular Microbiology* **64**, 1090–1104.

Harper, S. & Speicher, D. W. (2011). Purification of proteins fused to glutathione S-transferase. *Methods in Molecular Biology (Clifton, N.J.)* **681**, 259–280.

Hecker, M. & Völker, U. (2001). General stress response of *Bacillus subtilis* and other bacteria. In, pp. 35–91: Elsevier.

Hefti, M. H., **Vervoort, J. & van Berkel, W. J. H. (2003).** Deflavination and reconstitution of flavoproteins. *European Journal of Biochemistry* **270**, 4227–4242.

Heinemann, I. U., **Jahn, M. & Jahn, D. (2008).** The biochemistry of heme

biosynthesis. *Archives of Biochemistry and Biophysics* **474**, 238–251.

Herrou, J. & Crosson, S. (2011). Function, structure and mechanism of bacterial photosensory LOV proteins. *Nat Rev Microbiol* **9**, 713–723.

Heyber, S. S. (2021). (Dissertation) Lichtabhängige Bakteriochlorophyllbiosynthese des marinen Bakteriums *Dinoroseobacter shibae*. Technische Universität Carolo Wilhelmina, TU Braunschweig. Institut für Mikrobiologie.

Hirose, S., **Nagashima, K. V. P.**, **Matsuura, K. & Haruta, S. (2012).** Diversity of purple phototrophic bacteria, inferred from *pufM* gene, within epilithic biofilm in Tama River, Japan. *Microbes and Environments* **27**, 327–329.

Holtzhauer, M. (1996). *Methoden in der Proteinanalytik*. Berlin, Heidelberg: Springer Berlin Heidelberg.

Huala, E., **Oeller, P. W.**, **Liscum, E.**, **Han, I. S.**, **Larsen, E. & Briggs, W. R. (1997).** Arabidopsis NPH1: a protein kinase with a putative redox-sensing domain. *Science (New York, N.Y.)* **278**, 2120–2123.

Huang, D. D., **Wang, W. Y.**, **Gough, S. P. & Kannangara, C. G. (1984).** delta-Aminolevulinic acid-synthesizing enzymes need an RNA moiety for activity. *Science (New York, N.Y.)* **225**, 1482–1484.

Jacob-Dubuisson, F., **Mechaly, A.**, **Betton, J.-M. & Antoine, R. (2018).** Structural insights into the signalling mechanisms of two-component systems. *Nature Reviews. Microbiology* **16**, 585–593.

Jacobs, C., **Ausmees, N.**, **Cordwell, S. J.**, **Shapiro, L. & Laub, M. T. (2003).** Functions of the CckA histidine kinase in Caulobacter cell cycle control. *Molecular Microbiology* **47**, 1279–1290.

Jahn, D., **Moser, J.**, **Schubert, W.-D. & Heinz, D. W. (2006).** Transfer RNA-Dependent Aminolevulinic Acid Formation: Structure and Function of Glutamyl-tRNA Synthetase, Reductase and Glutamate-1-Semialdehyde-2,1-Aminomutase. In *Chlorophylls and Bacteriochlorophylls*, pp. 159–171. Edited by B. Grimm, R. J. Porra, W. Rüdiger & H. Scheer. Dordrecht: Springer Netherlands.

Jahn, D., **Verkamp, E. & Söll, D. (1992).** Glutamyl-transfer RNA: a precursor of heme and chlorophyll biosynthesis. *Trends in Biochemical Sciences* **17**, 215–218.

Jardillier, L., **Zubkov, M. V.**, **Pearman, J. & Scanlan, D. J. (2010).** Significant CO_2 fixation by small prymnesiophytes in the subtropical and tropical northeast Atlantic Ocean. *The ISME Journal* **4**, 1180–1192.

Jiao, N., **Zhang, F. & Hong, N. (2010).** Significant roles of bacteriochlorophyll *a* supplemental to chlorophyll a in the ocean. *The ISME Journal* **4**, 595–597.

Jiao, N., **Zhang, Y.**, **Zeng, Y.**, **Hong, N.**, **Liu, R.**, **Chen, F. & Wang, P. (2007).** Distinct distribution pattern of abundance and diversity of aerobic anoxygenic phototrophic bacteria in the global ocean. *Environmental Microbiology* **9**, 3091–3099.

Jurk, M., **Schramm, P. & Schmieder, P. (2013).** The blue-light receptor YtvA from *Bacillus subtilis* is permanently incorporated into the stressosome independent of the illumination state. *Biochemical and Biophysical Research Communications* **432**, 499–503.

Kalhoefer, D., **Thole, S.**, **Voget, S.**, **Lehmann, R.**, **Liesegang, H.**, **Wollher, A.**, **Daniel, R.**, **Simon, M. & Brinkhoff, T. (2011).** Comparative genome analysis and genome-guided physiological analysis of *Roseobacter litoralis*. *BMC Genomics* **12**, 324.

Kamerbeek, N. M., **van Zwieten, R.**, **Boer, M.** de, **Morren, G.**, **Vuil, H.**, **Bannink, N.**, **Lincke, C.**, **Dolman, K. M. & Becker, K. & other authors (2007).** Molecular basis of glutathione reductase deficiency in human blood cells. *Blood* **109**, 3560–3566.

Kanehisa, M., **Sato, Y.**, **Kawashima, M.**, **Furumichi, M. & Tanabe, M. (2016).** KEGG as a reference resource for gene and protein annotation. *Nucleic Acids Research* **44**, D457-62.

Kasahara, M., **Swartz, T. E.**, **Olney, M. A.**, **Onodera, A.**, **Mochizuki, N.**, **Fukuzawa, H.**, **Asamizu, E.**, **Tabata, S. & Kanegae, H. & other authors (2002).** Photochemical properties of the flavin mononucleotide-binding domains of the phototropins from Arabidopsis, rice, and *Chlamydomonas reinhardtii*. *Plant Physiology* **129**, 762–773.

Katzke, N., **Arvani, S.**, **Bergmann, R.**, **Circolone, F.**, **Markert, A.**, **Svensson, V.**, **Jaeger, K.-E.**, **Heck, A. & Drepper, T. (2010).** A novel T7 RNA polymerase dependent expression system for high-level protein production in the phototrophic bacterium *Rhodobacter capsulatus*. *Protein Expression and Purification* **69**, 137–146.

Kay, C. W. M., **Schleicher, E.**, **Kuppig, A.**, **Hofner, H.**, **Rüdiger, W.**, **Schleicher,**

M., **Fischer, M.**, **Bacher, A.**, **Weber, S. & Richter, G. (2003).** Blue light perception in plants. Detection and characterization of a light-induced neutral flavin radical in a C450A mutant of phototropin. *The Journal of Biological Chemistry* **278**, 10973–10982.

Kim, H.-S., **Willett, J. W.**, **Jain-Gupta, N.**, **Fiebig, A. & Crosson, S. (2014).** The *Brucella abortus* virulence regulator, LovhK, is a sensor kinase in the general stress response signalling pathway. *Molecular Microbiology* **94**, 913–925.

Kinoshita, E., **Kinoshita-Kikuta, E.**, **Takiyama, K. & Koike, T. (2006).** Phosphate-binding tag, a new tool to visualize phosphorylated proteins. *Molecular & Cellular Proteomics: MCP* **5**, 749–757.

Kirchman, D. L. & Hanson, T. E. (2013). Bioenergetics of photoheterotrophic bacteria in the oceans. *Environmental Microbiology Reports* **5**, 188–199.

Koblížek, M. (2015). Ecology of aerobic anoxygenic phototrophs in aquatic environments. *FEMS Microbiology Reviews* **39**, 854–870.

Koblížek, M., **Zeng, Y.**, **Horák, A. & Oborník, M. (2013).** Regressive Evolution of Photosynthesis in the Roseobacter Clade. In *Genome Evolution of Photosynthetic Bacteria*, pp. 385–405. Edited by J. T. Beatty, 1st edn. Amsterdam: Elsevier.

Koh, E. Y., **Phua, W. & Ryan, K. G. (2011).** Aerobic anoxygenic phototrophic bacteria in Antarctic sea ice and seawater. *Environmental Microbiology Reports* **3**, 710–716.

Kolber, Z. S., **Plumley, F. G.**, **Lang, A. S.**, **Beatty, J. T.**, **Blankenship, R. E.**, **VanDover, C. L.**, **Vetriani, C.**, **Koblizek, M.**, **Rathgeber, C. & Falkowski, P. G. (2001).** Contribution of aerobic photoheterotrophic bacteria to the carbon cycle in the ocean. *Science (New York, N.Y.)* **292**, 2492–2495.

Kolber, Z. S., **van Dover, C. L.**, **Niederman, R. A. & Falkowski, P. G. (2000).** Bacterial photosynthesis in surface waters of the open ocean. *Nature* **407**, 177–179.

Kottke, T., **Heberle, J.**, **Hehn, D.**, **Dick, B. & Hegemann, P. (2003).** Phot-LOV1: Photocycle of a Blue-Light Receptor Domain from the Green Alga *Chlamydomonas reinhardtii*. *Biophysical Journal* **84**, 1192–1201.

Kottke, T., **Xie, A.**, **Larsen, D. S. & Hoff, W. D. (2018).** Photoreceptors Take Charge: Emerging Principles for Light Sensing. *Annual Review of Biophysics* **47**, 291–313.

Kovach, M. E., **Elzer, P. H.**, **Steven Hill, D.**, **Robertson, G. T.**, **Farris, M. A.**, **Roop, R. & Peterson, K. M. (1995).** Four new derivatives of the broad-host-range cloning vector pBBR1MCS, carrying different antibiotic-resistance cassettes. *Gene* **166**, 175–176.

Kovács, A. T., **Rákhely, G. & Kovács, K. L. (2005).** The PpsR regulator family. *Research in Microbiology* **156**, 619–625.

Kraiselburd, I., **Moyano, L.**, **Carrau, A.**, **Tano, J. & Orellano, E. G. (2017).** Bacterial Photosensory Proteins and Their Role in Plant-pathogen Interactions. *Photochemistry and Photobiology* **93**, 666–674.

Kram, K. E. & Finkel, S. E. (2015). Rich Medium Composition Affects *Escherichia coli* Survival, Glycation, and Mutation Frequency during Long-Term Batch Culture. *Applied and Environmental Microbiology* **81**, 4442–4450.

Kramer, R. M., **Shende, V. R.**, **Motl, N.**, **Pace, C. N. & Scholtz, J. M. (2012).** Toward a molecular understanding of protein solubility: increased negative surface charge correlates with increased solubility. *Biophysical Journal* **102**, 1907–1915.

Krauss, U., **Minh, B. Q.**, **Losi, A.**, **Gärtner, W.**, **Eggert, T.**, **Haeseler, A. von & Jaeger, K.-E. (2009).** Distribution and phylogeny of light-oxygen-voltage-blue-light-signaling proteins in the three kingdoms of life. *Journal of Bacteriology* **191**, 7234–7242.

Kutta, R. J., **Magerl, K.**, **Kensy, U. & Dick, B. (2015).** A search for radical intermediates in the photocycle of LOV domains. *Photochemical & photobiological sciences: Official journal of the European Photochemistry Association and the European Society for Photobiology* **14**, 288–299.

Laass, S., **Kleist, S.**, **Bill, N.**, **Drüppel, K.**, **Kossmehl, S.**, **Wöhlbrand, L.**, **Rabus, R.**, **Klein, J. & Rohde, M. & other authors (2014).** Gene regulatory and metabolic adaptation processes of *Dinoroseobacter shibae* DFL12T during oxygen depletion. *The Journal of Biological Chemistry* **289**, 13219–13231.

Laemmli, U. K. (1970). Cleavage of structural proteins during the assembly of the head of bacteriophage T4. *Nature* **227**, 680–685.

Lami, R., **Cottrell, M. T.**, **Ras, J.**, **Ulloa, O.**, **Obernosterer, I.**, **Claustre, H.**, **Kirchman, D. L. & Lebaron, P. (2007).** High abundances of aerobic anoxygenic

photosynthetic bacteria in the South Pacific Ocean. *Applied and Environmental Microbiology* **73**, 4198–4205.

Larkin, M. A., **Blackshields, G.**, **Brown, N. P.**, **Chenna, R.**, **McGettigan, P. A.**, **McWilliam, H.**, **Valentin, F.**, **Wallace, I. M. & Wilm, A. & other authors (2007).** Clustal W and Clustal X version 2.0. *Bioinformatics (Oxford, England)* **23**, 2947–2948.

Laub, M. T., **McAdams, H. H.**, **Feldblyum, T.**, **Fraser, C. M. & Shapiro, L. (2000).** Global analysis of the genetic network controlling a bacterial cell cycle. *Science (New York, N.Y.)* **290**, 2144–2148.

LaVallie, E. R., **DiBlasio, E. A.**, **Kovacic, S.**, **Grant, K. L.**, **Schendel, P. F. & McCoy, J. M. (1993).** A thioredoxin gene fusion expression system that circumvents inclusion body formation in the *E. coli* cytoplasm. *Bio/technology (Nature Publishing Company)* **11**, 187–193.

Layer, G., **Jahn, D.**, **Deery, E.**, **Lawrence, A. D. & Warren, M. J. (2010).** Biosynthesis of Heme and Vitamin B12. In *Comprehensive Natural Products II. Chemistry and Biology*, pp. 445–499. Edited by L. Mander. Amsterdam: Elsevier.

Lee, H. H., **Ostrov, N.**, **Wong, B. G.**, **Gold, M. A.**, **Khalil, A. S. & Church, G. M. (2019).** Functional genomics of the rapidly replicating bacterium *Vibrio natriegens* by CRISPRi. *Nature Microbiology* **4**, 1105–1113.

Liotenberg, S., **Steunou, A.-S.**, **Picaud, M.**, **Reiss-Husson, F.**, **Astier, C. & Ouchane, S. (2008).** Organization and expression of photosynthesis genes and operons in anoxygenic photosynthetic proteobacteria. *Environmental Microbiology* **10**, 2267–2276.

Liu, Y., **Zheng, Q.**, **Lin, W. & Jiao, N. (2019).** Characteristics and Evolutionary Analysis of Photosynthetic Gene Clusters on Extrachromosomal Replicons: from Streamlined Plasmids to Chromids. *mSystems* **4**.

Losi, A. (2004). The bacterial counterparts of plant phototropins. *Photochemical & photobiological sciences: Official journal of the European Photochemistry Association and the European Society for Photobiology* **3**, 566–574.

Losi, A. (2007). Flavin-based Blue-Light photosensors: a photobiophysics update. *Photochemistry and Photobiology* **83**, 1283–1300.

Losi, A. (2013). LOV Proteins: Photobiophysics. In *Encyclopedia of Biophysics*,

pp. 1312–1316: Springer, Berlin, Heidelberg.

Losi, A. & Gärtner, W. (2008). Bacterial bilin- and flavin-binding photoreceptors. *Photochemical & photobiological sciences: Official journal of the European Photochemistry Association and the European Society for Photobiology* **7**, 1168–1178.

Losi, A. & Gärtner, W. (2012). The evolution of flavin-binding photoreceptors: an ancient chromophore serving trendy blue-light sensors. *Annual Review of Plant Biology* **63**, 49–72.

Losi, A. & Gärtner, W. (2017). Solving Blue Light Riddles: New Lessons from Flavin-binding LOV Photoreceptors. *Photochemistry and Photobiology* **93**, 141–158.

Losi, A., **Mandalari, C. & Gärtner, W. (2014).** From Plant Infectivity to Growth Patterns: The Role of Blue-Light Sensing in the Prokaryotic World. *Plants (Basel, Switzerland)* **3**, 70–94.

Losi, A., **Mandalari, C. & Gärtner, W. (2015).** The Evolution and Functional Role of Flavin-based Prokaryotic Photoreceptors. *Photochemistry and Photobiology* **91**, 1021–1031.

Losi, A., **Polverini, E.**, **Quest, B. & Gärtner, W. (2002).** First Evidence for Phototropin-Related Blue-Light Receptors in Prokaryotes. *Biophysical Journal* **82**, 2627–2634.

Marles-Wright, J. & Lewis, R. J. (2008). The *Bacillus subtilis* stressosome: A signal integration and transduction hub. *Communicative & Integrative Biology* **1**, 182–184.

Martínez-García, S. & Pinhassi, J. (2019). Adaptations of Microorganisms to Low Nutrient Environments: Managing Life in the Oligotrophic Ocean. In *Reference Module in Life Sciences:* Elsevier.

Masuda, S. & Bauer, C. E. (2002). AppA Is a Blue Light Photoreceptor that Antirepresses Photosynthesis Gene Expression in *Rhodobacter sphaeroides*. *Cell* **110**, 613–623.

Masuda, S. & Bauer, C. E. (2005). The Antirepressor AppA Uses the Novel Flavin-Binding BLUF Domain as a Blue-Light-Absorbing Photoreceptor to Control Photosystem Synthesis. In *Handbook of Photosensory Receptors*, pp. 433–445. Edited by J. L. Spudich & W. R. Briggs. Weinheim: Wiley-VCH.

Masuda, S., **Dong, C.**, **Swem, D.**, **Setterdahl, A. T.**, **Knaff, D. B. & Bauer, C. E. (2002).** Repression of photosynthesis gene expression by formation of a disulfide bond in CrtJ. *Proceedings of the National Academy of Sciences of the United States of America* **99**, 7078–7083.

McGoldrick, H. M., **Roessner, C. A.**, **Raux, E.**, **Lawrence, A. D.**, **McLean, K. J.**, **Munro, A. W.**, **Santabarbara, S.**, **Rigby, S. E. J. & Heathcote, P. & other authors (2005).** Identification and characterization of a novel vitamin B12 (cobalamin) biosynthetic enzyme (CobZ) from *Rhodobacter capsulatus*, containing flavin, heme, and Fe-S cofactors. *The Journal of Biological Chemistry* **280**, 1086–1094.

Miller, J. H. (1992). *Experiments in molecular genetics*, 11th edn. Cold Spring Harbor, NY: Cold Spring Harbor Laboratory.

Möbius, K., **Arias-Cartin, R.**, **Breckau, D.**, **Hännig, A.-L.**, **Riedmann, K.**, **Biedendieck, R.**, **Schröder, S.**, **Becher, D. & Magalon, A. & other authors (2010).** Heme biosynthesis is coupled to electron transport chains for energy generation. *Proc Natl Acad Sci USA* **107**, 10436–10441.

Möglich, A. (2019). Signal transduction in photoreceptor histidine kinases. *Protein science: a publication of the Protein Society* **28**, 1923–1946.

Möglich, A., **Ayers, R. A. & Moffat, K. (2009).** Structure and signaling mechanism of Per-ARNT-Sim domains. *Structure (London, England: 1993)* **17**, 1282–1294.

Moskvin, O. V., **Gilles-Gonzalez, M.-A. & Gomelsky, M. (2010).** The PpaA/AerR regulators of photosynthesis gene expression from anoxygenic phototrophic proteobacteria contain heme-binding SCHIC domains. *Journal of Bacteriology* **192**, 5253–5256.

Moskvin, O. V., **Gomelsky, L. & Gomelsky, M. (2005).** Transcriptome analysis of the *Rhodobacter sphaeroides* PpsR regulon: PpsR as a master regulator of photosystem development. *Journal of Bacteriology* **187**, 2148–2156.

Mosley, C. S., **Suzuki, J. Y. & Bauer, C. E. (1994).** Identification and molecular genetic characterization of a sensor kinase responsible for coordinately regulating light harvesting and reaction center gene expression in response to anaerobiosis. *Journal of Bacteriology* **176**, 7566–7573.

Müller, A. H., **Gough, S. P.**, **Bollivar, D. W.**, **Meldal, M.**, **Willows, R. D. &**

Hansson, M. (2011). Methods for the preparation of chlorophyllide a: an intermediate of the chlorophyll biosynthetic pathway. *Analytical Biochemistry* **419**, 271–276.

Nagashima, S. & Nagashima, K. V. (2013). Comparison of Photosynthesis Gene Clusters Retrieved from Total Genome Sequences of Purple Bacteria. In *Genome Evolution of Photosynthetic Bacteria*, pp. 151–178. Edited by J. T. Beatty, 1st edn. Amsterdam: Elsevier.

Nash, A. I., **Ko, W.-H.**, **Harper, S. M. & Gardner, K. H. (2008).** A Conserved Glutamine Plays a Central Role in LOV Domain Signal Transmission and Its Duration. *Biochemistry* **47**, 13842–13849.

Newton, R. J., **Griffin, L. E.**, **Bowles, K. M.**, **Meile, C.**, **Gifford, S.**, **Givens, C. E.**, **Howard, E. C.**, **King, E. & Oakley, C. A. & other authors (2010).** Genome characteristics of a generalist marine bacterial lineage. *The ISME Journal* **4**, 784–798.

Niesen, F. H., **Berglund, H. & Vedadi, M. (2007).** The use of differential scanning fluorimetry to detect ligand interactions that promote protein stability. *Nature Protocols* **2**, 2212–2221.

Niewöhner, Miriam (2019). Etablierung eines heterologen Systems zur Identifizierung eines Antwortregulators der LOV-Histidinkinase Dshi_1135 aus *Dinoroseobacter shibae.* Bachelor Thesis. Technische Universität Carolo Wilhelmina, TU Braunschweig. Institut für Mikrobiologie.

Nowicka, B. & Kruk, J. (2016). Powered by light: Phototrophy and photosynthesis in prokaryotes and its evolution. *Microbiological Research* **186-187**, 99–118.

Parkinson, J. S. & Kofoid, E. C. (1992). Communication modules in bacterial signaling proteins. *Annual Review of Genetics* **26**, 71–112.

Patzelt, D., **Wang, H.**, **Buchholz, I.**, **Rohde, M.**, **Gröbe, L.**, **Pradella, S.**, **Neumann, A.**, **Schulz, S. & Heyber, S. & other authors (2013).** You are what you talk: quorum sensing induces individual morphologies and cell division modes in Dinoroseobacter shibae. *The ISME Journal* **7**, 2274–2286.

Payne, W. J. (1958). Studies on bacterial utilization of uronic acids. III. Induction of oxidative enzymes in a marine isolate. *Journal of Bacteriology* **76**, 301–307.

Petersen, J., **Brinkmann, H.**, **Bunk, B.**, **Michael, V.**, **Päuker, O. & Pradella, S.**

(2012). Think pink: photosynthesis, plasmids and the Roseobacter clade. *Environmental Microbiology* **14**, 2661–2672.

Petersen, J., **Frank, O.**, **Göker, M. & Pradella, S. (2013).** Extrachromosomal, extraordinary and essential-the plasmids of the Roseobacter clade. *Applied Microbiology and Biotechnology* **97**, 2805–2815.

Petersen, J. & Wagner-Döbler, I. (2017). Plasmid Transfer in the Ocean - A Case Study from the Roseobacter Group. *Frontiers in Microbiology* **8**, 1350.

Phillips-Jones, M. K. & Hunter, C. N. (1994). Cloning and nucleotide sequence of RegA, a putative response regulator gene of *Rhodobacter sphaeroides*. *FEMS Microbiology Letters* **116**, 269–275.

Piwosz, K., **Kaftan, D.**, **Dean, J.**, **Šetlík, J. & Koblížek, M. (2018).** Nonlinear effect of irradiance on photoheterotrophic activity and growth of the aerobic anoxygenic phototrophic bacterium *Dinoroseobacter shibae*. *Environmental Microbiology* **20**, 724–733.

Ponnampalam, S. N. & Bauer, C. E. (1997). DNA binding characteristics of CrtJ. A redox-responding repressor of bacteriochlorophyll, carotenoid, and light harvesting-II gene expression in *Rhodobacter capsulatus*. *The Journal of Biological Chemistry* **272**, 18391–18396.

Ponnampalam, S. N., **Buggy, J. J. & Bauer, C. E. (1995).** Characterization of an aerobic repressor that coordinately regulates bacteriochlorophyll, carotenoid, and light harvesting-II expression in *Rhodobacter capsulatus*. *Journal of Bacteriology* **177**, 2990–2997.

Porra, R. J., **Schäfer, W.**, **Gad'on, N.**, **Katheder, I.**, **Drews, G. & Scheer, H. (1996).** Origin of the two carbonyl oxygens of bacteriochlorophyll a. Demonstration of two different pathways for the formation of ring E in *Rhodobacter sphaeroides* and *Roseobacter denitrificans*, and a common hydratase mechanism for 3-acetyl group formation. *European Journal of Biochemistry* **239**, 85–92.

Pradella, S., **Päuker, O. & Petersen, J. (2010).** Genome organisation of the marine Roseobacter clade member *Marinovum algicola*. *Arch. Microbiol.* **192**, 115–126.

Pucelik, Saskia (2019). Klonierung von *bchF*-Promotor-*lacZ* Reportergenfusionen und lichtabhängige Genexpressionsanalysen in *Dinoroseobacter shibae*. Bachelor Thesis.

Technische Universität Carolo Wilhelmina, TU Braunschweig. Institut für Mikrobiologie.

Purcell, E. B. & Crosson, S. (2008). Photoregulation in prokaryotes. *Current Opinion in Microbiology* **11**, 168–178.

Purcell, E. B., **Siegal-Gaskins, D.**, **Rawling, D. C.**, **Fiebig, A. & Crosson, S. (2007).** A photosensory two-component system regulates bacterial cell attachment. *Proceedings of the National Academy of Sciences of the United States of America* **104**, 18241–18246.

Rentz, Luise (2020). Mutagenese und funktionelle Analyse der potentiellen LOV-Histidinkinase Dshi_1135 aus *Dinoroseobacter shibae*. Bachelor Thesis. Technische Universität Carolo Wilhelmina, TU Braunschweig. Institut für Mikrobiologie.

Riès-kautt, M. & Ducruix, A. (1997). Inferences drawn from physicochemical studies of crystallogenesis and precrystalline state. In *Methods in Enzymology: Macromolecular Crystallography Part A*, pp. 23–59: Academic Press.

Righetti, P. G. (1990). Recent developments in electrophoretic methods. *Journal of Chromatography A* **516**, 3–22.

Rivera-Cancel, G., **Ko, W.-H.**, **Tomchick, D. R.**, **Correa, F. & Gardner, K. H. (2014).** Full-length structure of a monomeric histidine kinase reveals basis for sensory regulation. *Proc Natl Acad Sci USA* **111**, 17839–17844.

Salomon, M., **Christie, J. M.**, **Knieb, E.**, **Lempert, U. & Briggs, W. R. (2000).** Photochemical and mutational analysis of the FMN-binding domains of the plant blue light receptor, phototropin. *Biochemistry* **39**, 9401–9410.

Sambrook, J. & Russell, D. W. (2001). *Molecular cloning. A laboratory manual*, 3rd edn. Cold Spring Harbor, N.Y: Cold Spring Harbor Laboratory Press.

Samuelson, J. C. (2011). Recent developments in difficult protein expression: a guide to *E. coli* strains, promoters, and relevant host mutations. *Methods in Molecular Biology (Clifton, N.J.)* **705**, 195–209.

Sanger, F., **Nicklen, S. & Coulson, A. R. (1977).** DNA sequencing with chain-terminating inhibitors. *Proceedings of the National Academy of Sciences of the United States of America* **74**, 5463–5467.

Santos-Beneit, F. (2015). The Pho regulon: a huge regulatory network in bacteria.

Frontiers in Microbiology **6**, 402.

Sawers, R. G., **Zehelein, E. & Böck, A. (1988).** Two-dimensional gel electrophoretic analysis of *Escherichia coli* proteins: influence of various anaerobic growth conditions and the fnr gene product on cellular protein composition. *Arch. Microbiol.* **149**, 240–244.

Schwalbach, M. S. & Fuhrman, J. A. (2005). Wide-ranging abundances of aerobic anoxygenic phototrophic bacteria in the world ocean revealed by epifluorescence microscopy and quantitative PCR. *Limnol. Oceanogr.* **50**, 620–628.

Sean Crosson (2005). LOV-Domain Structure, Dynamics, and Diversity. In *Handbook of Photosensory Receptors*, pp. 323–336: John Wiley & Sons, Ltd.

Senge, M. O. & Smith, K. M. (1995). Biosynthesis and Structures of the Bacteriochlorophylls. In *Anoxygenic Photosynthetic Bacteria*, pp. 137–151. Edited by R. E. Blankenship. Dordrecht: Kluwer Acad. Publ.

Sganga, M. W. & Bauer, C. E. (1992). Regulatory factors controlling photosynthetic reaction center and light-harvesting gene expression in *Rhodobacter capsulatus*. *Cell* **68**, 945–954.

Shemin, D. & Russell, C. S. (1953). δ-Aminolevulinic Acid, its role in the biosynthesis of porphyrins and purines. *J. Am. Chem. Soc.* **75**, 4873–4874.

Shiba, T. (1991). *Roseobacter litoralis* gen. nov., sp. nov., and *Roseobacter denitrificans* sp. nov., Aerobic Pink-Pigmented Bacteria which Contain Bacteriochlorophyll *a*. *Systematic and Applied Microbiology* **14**, 140–145.

Shiba, T., **Shioi, Y.**, **Takamiya, K.**, **Sutton, D. C. & Wilkinson, C. R. (1991).** Distribution and physiology of aerobic bacteria containing bacteriochlorophyll *a* on the East and west coasts of australia. *Applied and Environmental Microbiology* **57**, 295–300.

Shiba, T., **Simidu, U. & Taga, N. (1979).** Distribution of aerobic bacteria which contain bacteriochlorophyll *a*. *Applied and Environmental Microbiology* **38**, 43–45.

Shimada, I. a. T. (1992). Blue-Light Irradiation Reduces the Expression of *puf* and *puc* Operons in *Rhodobacter sphaeroides* under Semi-Aerobic Conditons. *Plant and Cell Physiology*.

Simon, M., **Scheuner, C.**, **Meier-Kolthoff, J. P.**, **Brinkhoff, T.**, **Wagner-Döbler, I.**, **Ulbrich, M.**, **Klenk, H.-P.**, **Schomburg, D.**, **Petersen, J. & Göker, M. (2017).** Phylogenomics of Rhodobacteraceae reveals evolutionary adaptation to marine and non-marine habitats. *The ISME Journal* **11**, 1483–1499.

Smart, J. L., **Willett, J. W. & Bauer, C. E. (2004).** Regulation of **hem** gene expression in *Rhodobacter capsulatus* by redox and photosystem regulators RegA, CrtJ, FnrL, and AerR. *Journal of Molecular Biology* **342**, 1171–1186.

Smith, D. B. & Johnson, K. S. (1988). Single-step purification of polypeptides expressed in *Escherichia coli* as fusions with glutathione S-transferase. *Gene* **67**, 31–40.

Soora, M. & Cypionka, H. (2013). Light enhances survival of *Dinoroseobacter shibae* during long-term starvation. *PloS one* **8**, e83960.

Spiro, S. (1994). The FNR family of transcriptional regulators. *Antonie van Leeuwenhoek* **66**, 23–36.

Stock, A., **Chen, T.**, **Welsh, D. & Stock, J. (1988).** CheA protein, a central regulator of bacterial chemotaxis, belongs to a family of proteins that control gene expression in response to changing environmental conditions. *Proceedings of the National Academy of Sciences of the United States of America* **85**, 1403–1407.

Stock, J. B., **Surette, M. G.**, **Levit, M. & Park, P. (1995).** Two-Component Signal Transduction Systems: Structure-Function Relationships and Mechanisms of Catalysis. In *Two-Component Signal Transduction*, pp. 25–51. Edited by J. A. Hoch & T. J. Silhavy. Washington, DC, USA: ASM Press.

Studier, F. W. (2005). Protein production by auto-induction in high density shaking cultures. *Protein Expression and Purification* **41**, 207–234.

Suzuki, J. Y. & Bauer, C. E. (1995). Altered monovinyl and divinyl protochlorophyllide pools in *bchJ* mutants of *Rhodobacter capsulatus*. Possible monovinyl substrate discrimination of light-independent protochlorophyllide reductase. *The Journal of Biological Chemistry* **270**, 3732–3740.

Swartz, T. E. & Bogomolni, R. A. (2005). LOV-Domain Photochemistry. In *Handbook of Photosensory Receptors*, pp. 305–321: John Wiley & Sons, Ltd.

Swartz, T. E., **Corchnoy, S. B.**, **Christie, J. M.**, **Lewis, J. W.**, **Szundi, I.**, **Briggs, W.**

R. & Bogomolni, R. A. (2001). The photocycle of a flavin-binding domain of the blue light photoreceptor phototropin. *The Journal of Biological Chemistry* **276**, 36493–36500.

Swartz, T. E., **Tseng, T.-S.**, **Frederickson, M. A.**, **Paris, G.**, **Comerci, D. J.**, **Rajashekara, G.**, **Kim, J.-G.**, **Mudgett, M. B. & Splitter, G. A. & other authors (2007).** Blue-light-activated histidine kinases: two-component sensors in bacteria. *Science (New York, N.Y.)* **317**, 1090–1093.

Tartoff, K. D. & Hobbs, C. A. (1987). *Improved media for growing plasmid and cosmid clones*.

Taylor, D. P., **Cohen, S. N.**, **Clark, W. G. & Marrs, B. L. (1983).** Alignment of genetic and restriction maps of the photosynthesis region of the *Rhodopseudomonas capsulata* chromosome by a conjugation-mediated marker rescue technique. *Journal of Bacteriology* **154**, 580–590.

Taylor, M. W., **Schupp, P. J.**, **Dahllöf, I.**, **Kjelleberg, S. & Steinberg, P. D. (2004).** Host specificity in marine sponge-associated bacteria, and potential implications for marine microbial diversity. *Environmental Microbiology* **6**, 121–130.

Thoma, S. & Schobert, M. (2009). An improved *Escherichia coli* donor strain for diparental mating. *FEMS microbiology letters* **294**, 127–132.

Tomasch, J., **Gohl, R.**, **Bunk, B.**, **Diez, M. S. & Wagner-Döbler, I. (2011).** Transcriptional response of the photoheterotrophic marine bacterium *Dinoroseobacter shibae* to changing light regimes. *The ISME Journal* **5**, 1957–1968.

Vagenende, V., **Yap, M. G. S. & Trout, B. L. (2009).** Mechanisms of protein stabilization and prevention of protein aggregation by glycerol. *Biochemistry* **48**, 11084–11096.

Vermeulen, A. J. & Bauer, C. E. (2015). Members of the PpaA/AerR Antirepressor Family Bind Cobalamin. *Journal of Bacteriology* **197**, 2694–2703.

Wagner-Döbler, I., **Ballhausen, B.**, **Berger, M.**, **Brinkhoff, T.**, **Buchholz, I.**, **Bunk, B.**, **Cypionka, H.**, **Daniel, R. & Drepper, T. & other authors (2010).** The complete genome sequence of the algal symbiont *Dinoroseobacter shibae*: a hitchhiker's guide to life in the sea. *The ISME Journal* **4**, 61–77.

Wagner-Döbler, I. & Biebl, H. (2006). Environmental biology of the marine Roseobacter lineage. *Annual Review of Microbiology* **60**, 255–280.

Walker, C. J., **Mansfield, K. E.**, **Smith, K. M. & Castelfranco, P. A. (1989).** Incorporation of atmospheric oxygen into the carbonyl functionality of the protochlorophyllide isocyclic ring. *The Biochemical Journal* **257**, 599–602.

Wang, H., **Tomasch, J.**, **Jarek, M. & Wagner-Döbler, I. (2014).** A dual-species co-cultivation system to study the interactions between Roseobacters and dinoflagellates. *Frontiers in Microbiology* **5**, 311.

Wang, H., **Tomasch, J.**, **Michael, V.**, **Bhuju, S.**, **Jarek, M.**, **Petersen, J. & Wagner-Döbler, I. (2015).** Identification of Genetic Modules Mediating the Jekyll and Hyde Interaction of *Dinoroseobacter shibae* with the Dinoflagellate *Prorocentrum minimum*. *Frontiers in Microbiology* **6**, 1262.

Wang, H., **Ziesche, L.**, **Frank, O.**, **Michael, V.**, **Martin, M.**, **Petersen, J.**, **Schulz, S.**, **Wagner-Döbler, I. & Tomasch, J. (2014).** The CtrA phosphorelay integrates differentiation and communication in the marine alphaproteobacterium *Dinoroseobacter shibae*. *BMC Genomics* **15**, 130.

Warren, M. J., **Cooper, J. B.**, **Wood, S. P. & Shoolingin-Jordan, P. M. (1998).** Lead poisoning, haem synthesis and 5-aminolaevulinic acid dehydratase. *Trends in Biochemical Sciences* **23**, 217–221.

Webster, N. S., **Negri, A. P.**, **Munro, M. M. H. G. & Battershill, C. N. (2004).** Diverse microbial communities inhabit Antarctic sponges. *Environmental Microbiology* **6**, 288–300.

Weidner, S., **Arnold, W.**, **Stackebrandt, E. & Pühler, A. (2000).** Phylogenetic Analysis of Bacterial Communities Associated with Leaves of the Seagrass *Halophila stipulacea* by a Culture-Independent Small-Subunit rRNA Gene Approach. *Microbial Ecology* **39**, 22–31.

Weinstock, M. T., **Hesek, E. D.**, **Wilson, C. M. & Gibson, D. G. (2016).** *Vibrio natriegens* as a fast-growing host for molecular biology. *Nature Methods* **13**, 849–851.

Whitman, W. B., **Coleman, D. C. & Wiebe, W. J. (1998).** Prokaryotes: the unseen majority. *Proceedings of the National Academy of Sciences of the United States of America* **95**, 6578–6583.

Willows, R. D. (2003). Biosynthesis of chlorophylls from protoporphyrin IX. *Natural Product Reports* **20**, 327–341.

Willows, R. D. & Kriegel, A. M. (2009). Biosynthesis of Bacteriochlorophylls in Purple Bacteria. In *The Purple Phototrophic Bacteria*, pp. 57–79. Edited by C. N. Hunter & F. Daldal. Dordrecht: Springer.

Winkler, A., **Heintz, U.**, **Lindner, R.**, **Reinstein, J.**, **Shoeman, R. L. & Schlichting, I. (2013).** A ternary AppA-PpsR-DNA complex mediates light regulation of photosynthesis-related gene expression. *Nature Structural & Molecular Biology* **20**, 859–867.

Wolanin, P. M., **Thomason, P. A. & Stock, J. B. (2002).** Histidine protein kinases: key signal transducers outside the animal kingdom. *Genome Biol* **3**.

Wu, J., **Ohta, N.**, **Zhao, J. & Newton, A. (1999).** A novel bacterial tyrosine kinase essential for cell division and differentiation. *Proceedings of the National Academy of Sciences of the United States of America* **23**, 13068-13073.

Xiong, J. & Bauer, C. E. (2002). Complex evolution of photosynthesis. *Annual Review of Plant Biology* **53**, 503–521.

Xiong, J., **Fischer, W. M.**, **Inoue, K.**, **Nakahara, M. & Bauer, C. E. (2000).** Molecular evidence for the early evolution of photosynthesis. *Science (New York, N.Y.)* **289**, 1724–1730.

Yamamoto, H., **Fang, M.**, **Dragnea, V. & Bauer, C. E. (2018).** Differing isoforms of the cobalamin binding photoreceptor AerR oppositely regulate photosystem expression. *eLife* **7**.

Yang, Z., **Zhang, L.**, **Zhang, Y.**, **Zhang, T.**, **Feng, Y.**, **Lu, X.**, **Lan, W.**, **Wang, J. & Wu, H. & other authors (2011).** Highly Efficient Production of Soluble Proteins from Insoluble Inclusion Bodies by a Two-Step-Denaturing and Refolding Method. *PloS One* **6**, e22981.

Yee, E. F., **Diensthuber, R. P.**, **Vaidya, A. T.**, **Borbat, P. P.**, **Engelhard, C.**, **Freed, J. H.**, **Bittl, R.**, **Möglich, A. & Crane, B. R. (2015).** Signal transduction in light-oxygen-voltage receptors lacking the adduct-forming cysteine residue. *Nat Commun* **6**, 10079.

Yen, H. C. & Marrs, B. (1976). Map of genes for carotenoid and bacteriochlorophyll

biosynthesis in *Rhodopseudomonas capsulata*. *Journal of Bacteriology* **126**, 619–629.

Yin, L. & Bauer, C. E. (2013). Controlling the delicate balance of tetrapyrrole biosynthesis. *Philosophical Transactions of the Royal Society B: Biological Sciences* **368**, 20120262.

Yin, L., **Dragnea, V. & Bauer, C. E. (2012).** PpsR, a regulator of heme and bacteriochlorophyll biosynthesis, is a heme-sensing protein. *The Journal of Biological Chemistry* **287**, 13850–13858.

Yuan, Z.-C., **Zaheer, R. & Finan, T. M. (2005).** Phosphate limitation induces catalase expression in *Sinorhizobium meliloti*, *Pseudomonas aeruginosa* and *Agrobacterium tumefaciens*. *Molecular Microbiology* **58**, 877–894.

Yurkov, V. & Csotonyi, J. T. (2009). New Light on Aerobic Anoxygenic Phototrophs. In *The Purple Phototrophic Bacteria*, pp. 31–55. Edited by C. N. Hunter & F. Daldal. Dordrecht: Springer.

Yurkov, V. V. & Beatty, J. T. (1998). Aerobic anoxygenic phototrophic bacteria. *Microbiology and Molecular Biology Reviews* **62**, 695–724.

Zayner, J. P., **Antoniou, C.**, **French, A. R.**, **Hause, R. J. & Sosnick, T. R. (2013).** Investigating models of protein function and allostery with a widespread mutational analysis of a light-activated protein. *Biophysical Journal* **105**, 1027–1036.

Zayner, J. P. & Sosnick, T. R. (2014). Factors that control the chemistry of the LOV domain photocycle. *PloS one* **9**, e87074.

Zheng, Q., **Zhang, R.**, **Koblížek, M.**, **Boldareva, E. N.**, **Yurkov, V.**, **Yan, S. & Jiao, N. (2011).** Diverse arrangement of photosynthetic gene clusters in aerobic anoxygenic phototrophic bacteria. *PloS one* **6**, e25050.

Zoltowski, B. D., **Vaccaro, B. & Crane, B. R. (2009).** Mechanism-based tuning of a LOV domain photoreceptor. *Nature Chemical Biology* **5**, 827–834.

Zschiedrich, C. P., **Keidel, V. & Szurmant, H. (2016).** Molecular mechanisms of two-component signal transduction. *Journal of Molecular Biology* **428**, 3752–3775.

8 Appendix

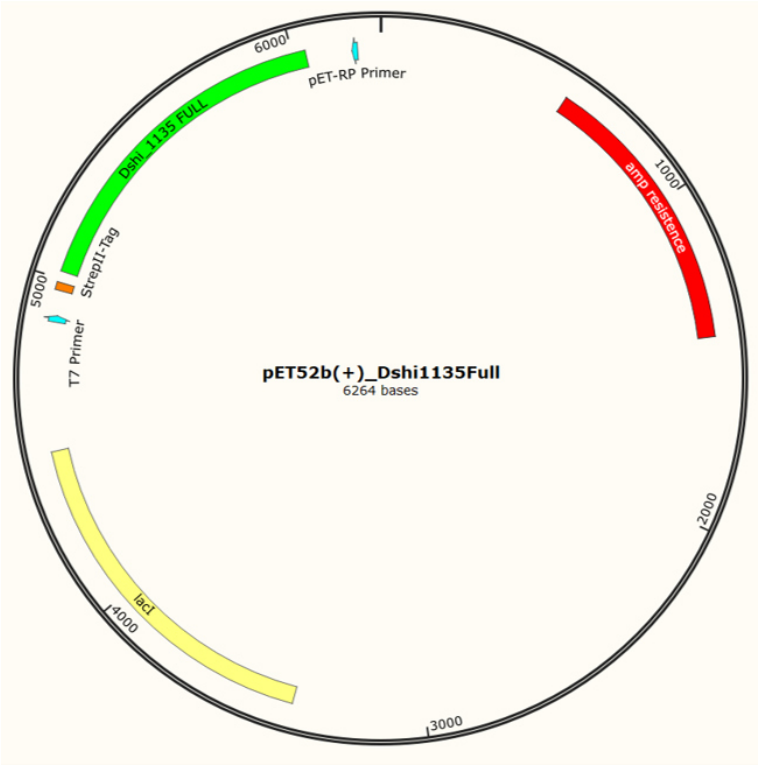

Figure 40: Vector map of pET52b(+)_Dshi1135Full

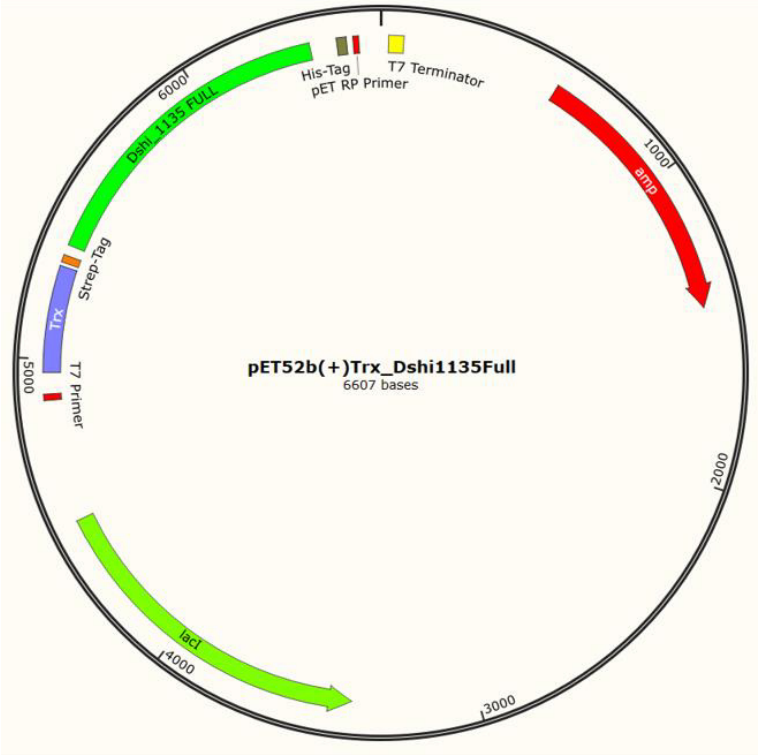

Figure 41: Vector map of pET52b(+)Trx_Dshi1135Full

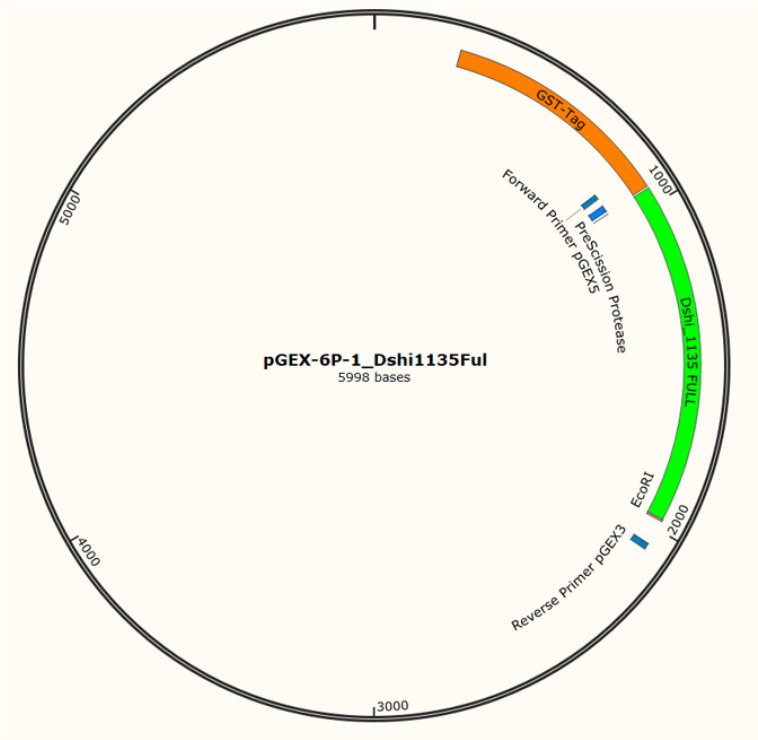

Figure 42: Vector map of pGEX-6P-1_Dshi1135Full

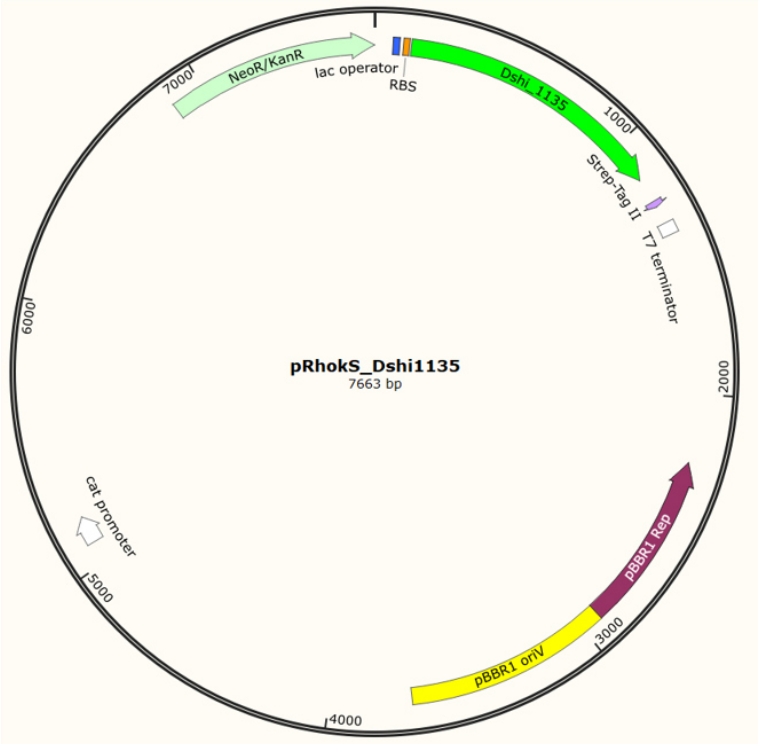

Figure 43: Vector map of pRhokS_Dshi1135

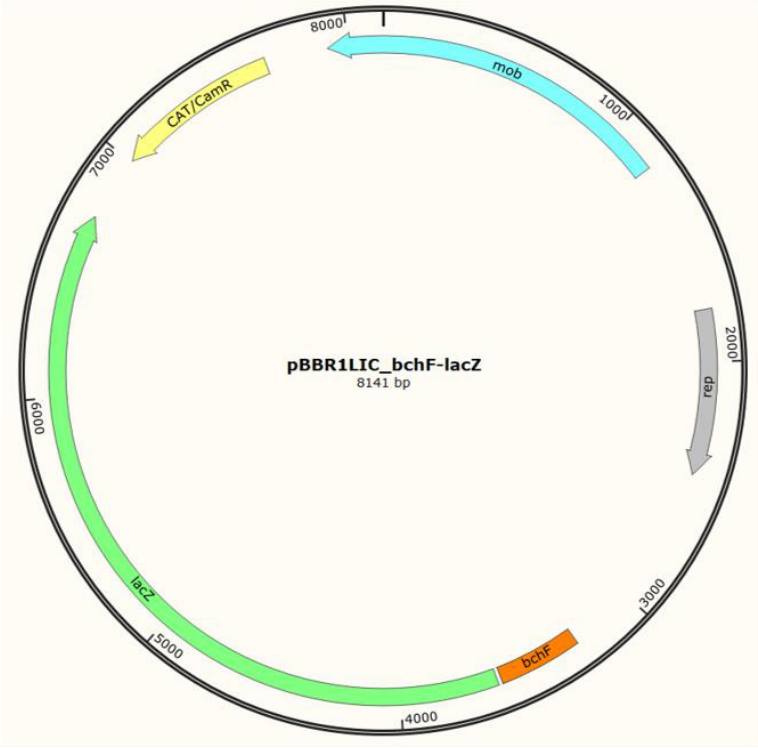

Figure 44: Vector map of pBBR1LIC_*bchF-lacZ*

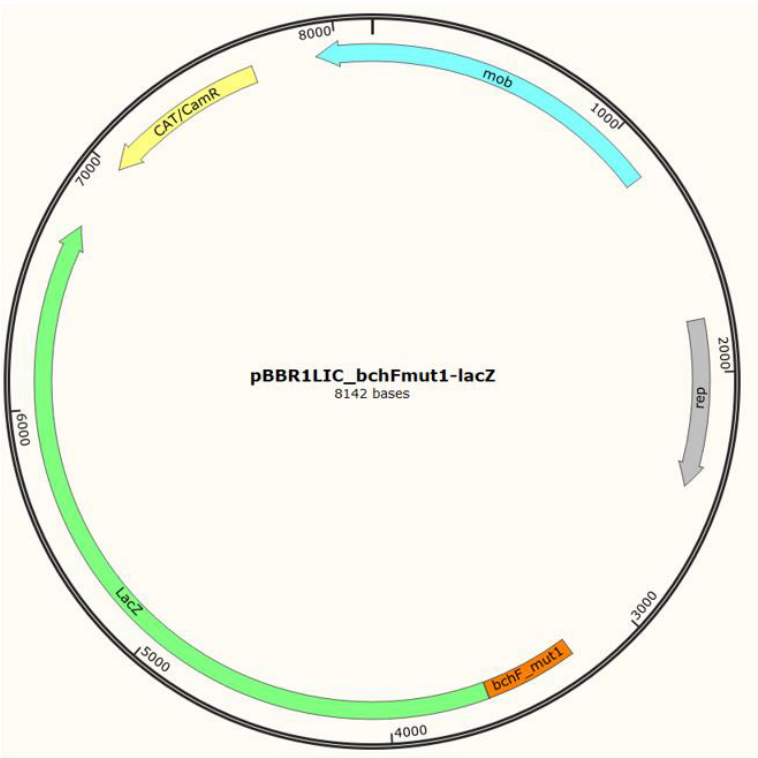

Figure 45: Vector map of pBBR1LIC_*bchF*mut1-*lacZ*

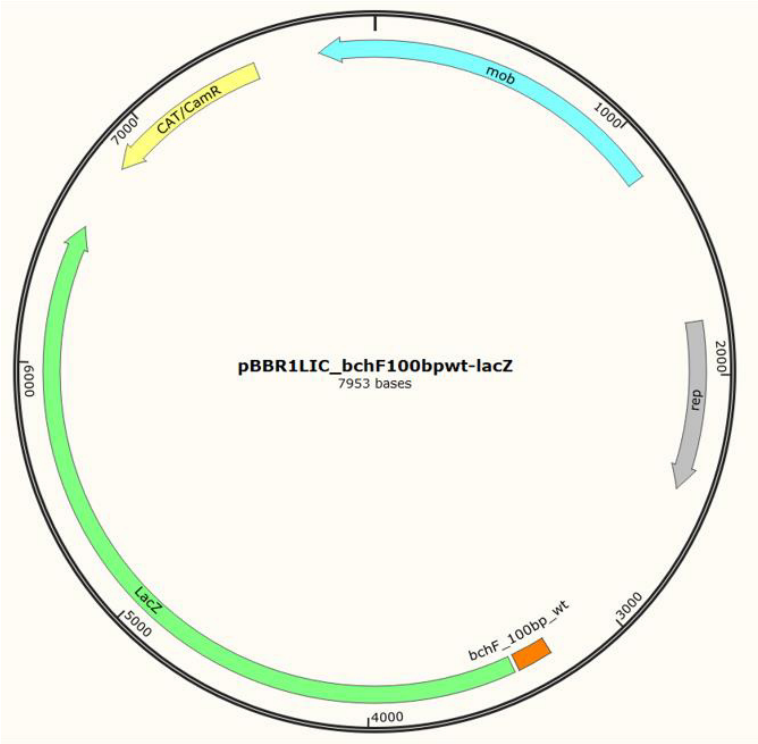

Figure 46: Vector map of pBBR1LIC_*bchF*100bpwt-*lacZ*

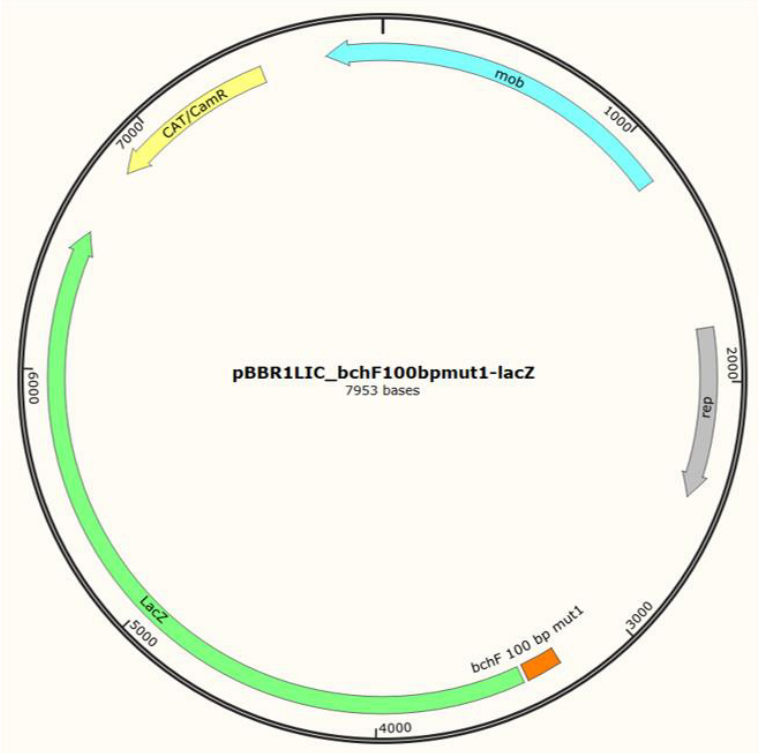

Figure 47: Vector map of pBBR1LIC_*bchF*100bpmut1-*lacZ*

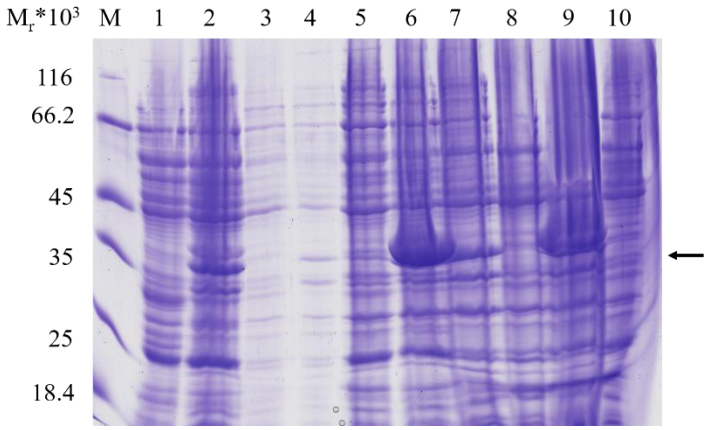

Figure 48: Test of TB and self-inducing medium for soluble expression of Strep-Dshi_1135
For test expression in TB medium 50 µM of IPTG were used for induction and cells were grown at 17 °C and 180 rpm for 18 h. For test expressions in self-inducing medium cells were grown at 17 °C and 180 rpm for 18 h. Samples in duplicates were taken of the used pre-culture and after cultivation of the main cultures. One replicate of each sample was fractionated by lysozyme digestion and subsequent centrifugation. The other replicate was fractionated by French Press disruption and high-speed centrifugation. The resulting soluble and insoluble protein fractions were mixed with 2x SDS loading dye and denatured at 95 °C for 10 min. Equal amounts of protein (corresponding to the OD_{578}) were analysed on 12 % SDS gels and visualized *via* Coomassie Brilliant Blue staining.
Lane M: molecular mass marker (relative molecular masses (*1'000) are indicated. Lane 1: pre-culture (soluble fraction), Lane 2: pre-culture (insoluble fraction), Lane 3: self-inducing medium (lysozyme digestion, soluble fraction), Lane 4: self-inducing medium (lysozyme digestion, insoluble fraction), Lane 5: TB medium (lysozyme digestion, soluble fraction), Lane 6: TB medium (lysozyme digestion, insoluble fraction),), Lane 7: self-inducing medium (French Press disruption, soluble fraction), Lane 8: self-inducing medium (French Press disruption, insoluble fraction), Lane 9: TB medium (French Press disruption, soluble fraction), Lane 10: TB medium (French Press disruption, insoluble fraction).
The arrow highlights the protein band corresponding to StrepII-Dshi_1135 with an approximate relative molecular weight of 40'000.

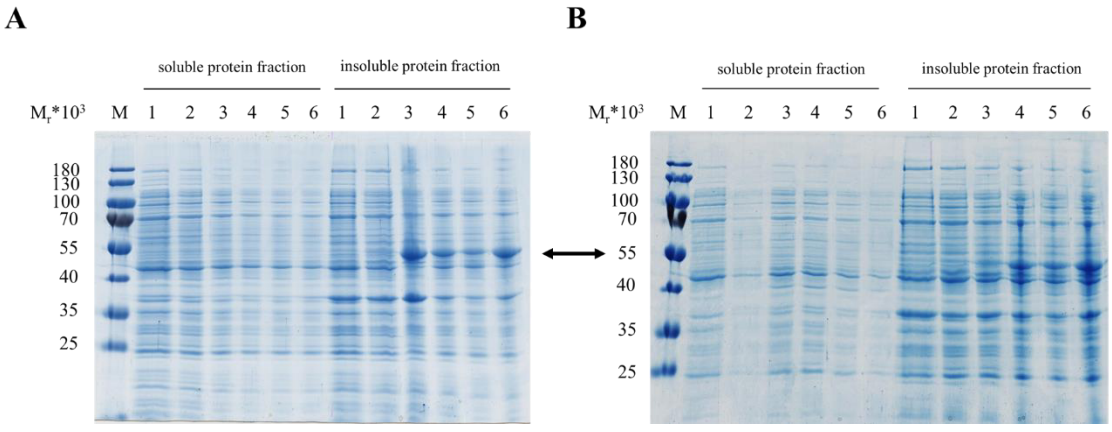

Figure 49: Determination of expression efficiency of TRX-StrepII-Dshi_1135 fusion protein dependent on cultivation temperature and IPTG concentration
Dshi1135 produced as TRX-StrepII-Dshi_1135 from plasmid pET52b(+)Trx_Dshi1135Full in *E. coli* BL21-CodonPlus(DE) after induction with 50 µM of IPTG and cultivation at 17 °C (A) and 30 °C (B), respectively. Samples were taken 0 h, 1 h, 2 h, 3 h, 4 h and 18 h after induction and fractionated by lysozyme digestion and subsequent centrifugation. The resulting soluble and insoluble protein fractions were mixed with 2x SDS loading dye and denatured at 95 °C for 10 min. Equal amounts of protein (corresponding to the OD_{578}) were analysed on 12 % SDS gels and visualized *via* Coomassie Brilliant Blue staining.
Lane M: prestained molecular mass marker (relative molecular masses (*1'000) are indicated. Lane 1: 0 h

after induction, Lane 2: 1 h after induction, Lane 3: 2 h after induction, Lane 4: 3 h after induction, Lane 5: 4 h after induction, Lane 6: 18 h after induction.
The arrow highlights the protein band corresponding to TRX-StrepII-Dshi_1135 with an approximate relative molecular weight of 52'000.

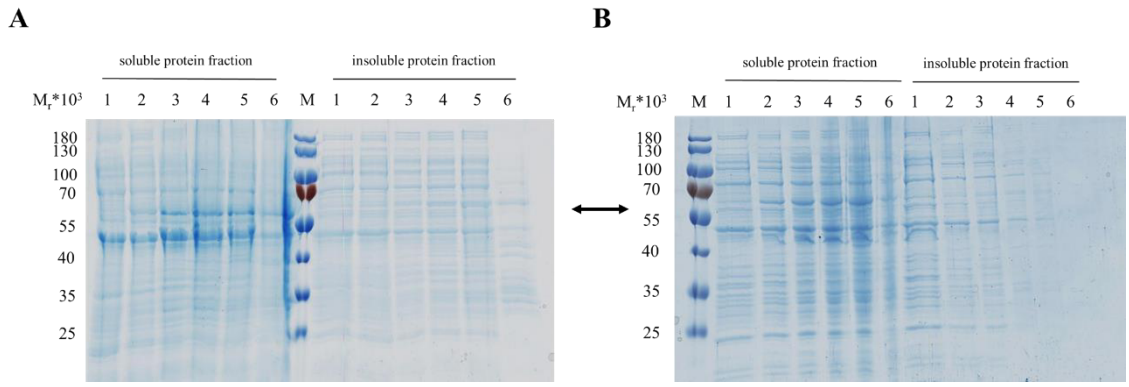

Figure 50: Determination of expression efficiency and localization of GST-Dshi_1135 fusion protein in Vmax™ Express cells dependent on IPTG concentration
Dshi1135 produced as GST-Dshi_1135 from plasmid pGEX6P-1_Dshi1135Full in Vmax™ Express cells after induction with 500 µM (A) and 1 mM of IPTG (B) and cultivation at 30 °C. Samples were taken 0 h, 1 h, 2 h, 3 h, 4 h and 18 h after induction and fractionated by lysozyme digestion and subsequent centrifugation. The resulting soluble and insoluble protein fractions were mixed with 2x SDS loading dye and denatured at 95 °C for 10 min. Equal amounts of protein (corresponding to the OD_{578}) were analysed on 12 % SDS gels and visualized *via* Coomassie Brilliant Blue staining.
Lane M: prestained molecular mass marker (relative molecular masses (*1'000) are indicated. Lane 1: 0 h after induction. Lane 2: 1 h after induction, Lane 3: 2 h after induction, Lane 4: 3 h after induction, Lane 5: 4 h after induction, Lane 6: 18 h after induction.
The arrow highlights the protein band corresponding to GST-Dshi_1135 with an approximate relative molecular weight of 64'000.

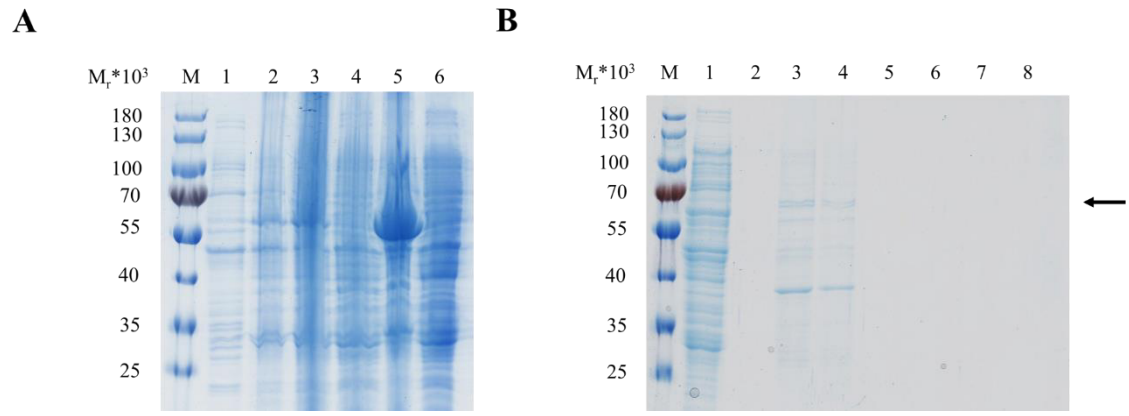

Figure 51: Purification of GST-Dshi_1135 produced in Vmax™ Express cells
The GST-Dshi_1135 fusion protein was recombinantly expressed in Vmax™ Express cells after induction with 1 mM IPTG and cultivation at 30 °C. Produced protein was subsequently purified *via* affinity chromatography using the Protino® Glutathione Agarose 4 B resin. All samples were mixed with 2x SDS-loading dye, denatured at 95 °C for 10 min, subsequently analysed on 12 % SDS gels and visualized *via* Coomassie Brilliant Blue staining.
Lane M: prestained molecular mass marker (relative molecular masses (*1'000) are indicated.
(A) Lane 1: before induction. Lane 2: 18 h after induction. Lane 3: disrupted cells. Lane 4: cell free extracts. Lane 5: pellet fraction. Lane 6: flow-through fraction.

(B) Lane 1: washing step I. Lane 2: washing step II. Lane 3: elution fraction I. Lane 4: elution fraction II. Lane 5: elution fraction III. Lane 6: elution fraction IV. Lane 7: elution fraction V. Lane 8: elution fraction VI.
The arrow highlights the protein band corresponding to GST-Dshi_1135 with an approximate relative molecular weight of 64'000.

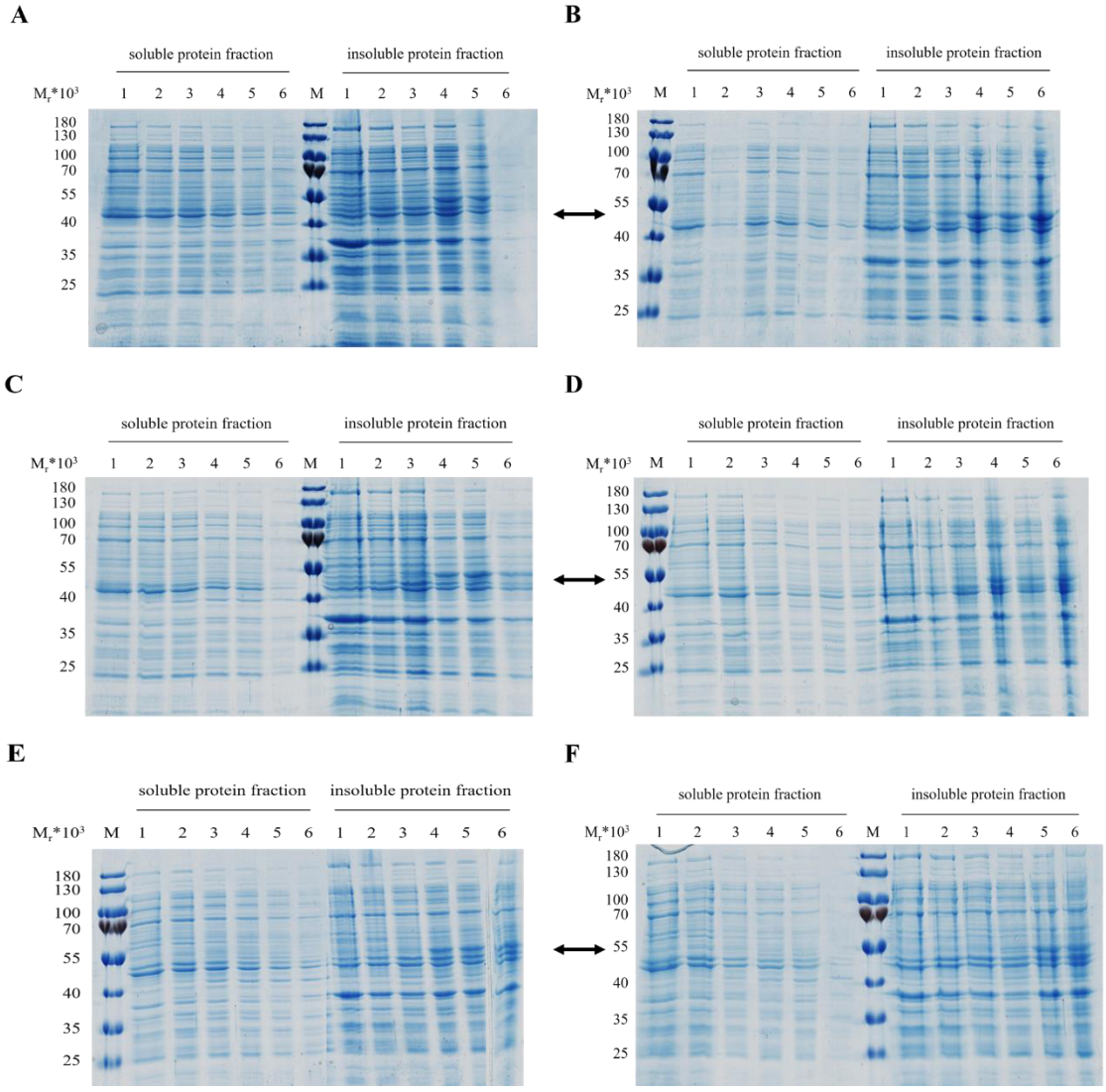

Figure 52: Determination of expression efficiency, optimal L-rhamnose concentration and localization of TRX-StrepII-Dshi_1135 fusion protein in *E. coli* Lemo21(DE3) cells
Dshi1135 produced as TRX-StrepII-Dshi_1135 from plasmid pET52b(+)Trx_Dshi1135Full in *E. coli* Lemo21(DE3) cells after induction with 400 µM and 100 µM L-rhamnose (A), 250 µM L-rhamnose (B), 500 µM L-rhamnose (C), 750 µM L-rhamnose (D), 1 mM L-rhamnose or 2 mM L-rhamnose, respectively. Cells were cultivated at 17 °C and 180 rpm. Samples were taken 0 h, 1 h, 2 h, 3 h, 4 h and 18 h after induction and fractionated by lysozyme digestion and subsequent centrifugation. The resulting soluble and insoluble protein fractions were mixed with 2x SDS loading dye and denatured at 95 °C for 10 min. Equal amounts of protein (corresponding to the OD578) were analysed on 12 % SDS gels and visualized via Coomassie Brilliant Blue staining.
Lane M: prestained molecular mass marker (relative molecular masses (*1'000) are indicated. Lane 1: 0 h after induction. Lane 2: 1 h after induction, Lane 3: 2 h after induction, Lane 4: 3 h after induction, Lane 5: 4 h after induction, Lane 6: 18 h after induction.
The arrow highlights the protein band corresponding to TRX-StrepII-Dshi_1135 with an approximate relative molecular weight of 52'000.

Danksagung

An dieser Stelle möchte ich mich bei all denen bedanken, die mich auf unterschiedlichste Weise unterstützt und somit zum Gelingen dieser Arbeit beigetragen haben.

Zuallererst möchte ich mich bei meinem Mentor Prof. Dr. Dieter Jahn bedanken. Danke für die Aufnahme in Deinen Arbeitskreis und dass ich dadurch für eine Weile in die Welt der Wissenschaft eintauchen durfte. Vielen Dank auch dafür, dass Du Dir immer Zeit genommen hast und mit Rat und Tat zur Seite standest, wenn mal wieder ein Knoten im Kopf gelöst werden wollte. Gerade zum Ende meiner Arbeit habe ich Deine Unterstützung sehr zu schätzen gewusst!

Bei Prof. Dr. Michael Hust möchte ich mich sehr herzlich für die Übernahme des Korreferats bedanken.

Prof. Dr. Simone Bergmann danke ich sehr für die freundliche Übernahme des Prüfungsvorsitzes.

Einen besonders großen Dank möchte ich Dr. Elisabeth Härtig - oder einfach Elli - aussprechen. Vielen Dank, dass Du mich so herzlich in Deine Arbeitsgruppe aufgenommen hast und für all den Spaß, den wir im Labor oder auch außerhalb zusammen hatten. Danke für Dein Vertrauen, Deine Motivation, Deine Unterstützung, die unzähligen Pferdegeschichten, die Escape Room Abenteuer, die lustigen Mixer-Abende auf der VAAM und nicht zu vergessen für die besten Käsespätzle der Welt. Ich hatte eine tolle Zeit bei Dir in der Mibi und werde mich immer gerne daran erinnern!

Bei Lisa Plötzky, Maren Behringer, Alina Rommerskirch, Anja Hartmann und Mathias Ebert möchte ich mich für die tolle Atmosphäre innerhalb der Arbeitsgruppe bedanken. Ohne Euch hätte der Laboralltag nur halb so viel Spaß gemacht. Besonders möchte ich Euch - Lisa und Maren - danken. Für Eure Freundschaft, Eure Hilfsbereitschaft, die unglaublich lustigen Momente in der Denkzelle und die vielen dadurch entstandenen Insider, das Teilen von Zimmern auf Konferenzen, die schöne Zeit auch außerhalb des Labors und dafür, dass ich mich immer auf Euch verlassen konnte. Danke!

Meinen Bachelorstudenten Konstanze Luckhardt, Saskia Pucelik, Emelie Rieneck, sowie Miriam Niewöhner möchte ich Danke sagen für ihre gute Arbeit im Labor und die tollen Ergebnisse, die auch Teil dieser Doktorarbeit geworden sind.

Bei der gesamten Mibi möchte ich mich für die tolle Atmosphäre, die Hilfsbereitschaft, die unterhaltsamen Mittagspausen und die vielen lustigen Feiern bedanken. Besonders hervorheben und bedanken möchte ich mich bei Christina Nitzsche und Gunhild Voss für all die Hilfe bei Fragen, die nichts mit dem Labor zu tun hatten. Danke an Daniela Schnobel, die stets unsere Finanzen im Blick hatte und die ein oder andere Bestellung gerettet hat. Barbara Cwiklinski und Dagmar Rose möchte ich Danke sagen, dafür, dass sie den Laden am Laufen halten und für den unermüdlichen Einsatz in der Spülküche - vor allem mit den Dino-Kolben.

Meinen Freunden Viktoria Schreiber, Marius Klangwart, Inga Conrad-Kanofsky, Konstantin Kanofsky und Anne Niemeyer möchte ich für all die schönen Jahre zusammen während des Studiums und auch danach danken. Wer von uns hätte vor über 10 Jahren, als wir als kleine Erstis zusammen im Mathevorkurs saßen, gedacht, dass wir mal so weit kommen? Ich hätte wahrscheinlich dagegen gewettet. Umso schöner ist es, dass wir alle unseren Weg gemacht haben und uns dabei nie aus den Augen verloren haben. Auf die nächsten tollen Jahre mit der Browntown Gang!

Zu guter Letzt möchte ich mich bei den wichtigsten Menschen bedanken - meiner Familie. Mama und Papa - danke, dass ihr immer da wart und mich bei allem unterstützt habt, was mir im Leben so in den Sinn gekommen ist. Ihr habt mich in den richtigen Momenten motiviert und gefordert, aber auch aufgefangen und aufgebaut, wenn ich es brauchte. Auch meine beiden großen Brüder Thorben und Stefan, mein Onkel Willi, meine Großeltern, die diesen Moment leider nicht mehr miterleben dürfen, meine Schwägerin Astrid und mein Schwager Timm und meine Nichte Cristina und mein Neffe Niklas sollen nicht unerwähnt bleiben. Ihr habt alle auf Eure Weise zum Gelingen dieser Arbeit beigetragen. Ich bin sehr froh, dass es Euch gibt!